

Control and Identification in Activated Sludge Processes

Leo Lukasse

Promotor: Prof. dr. ir. G. van Straten
hoogleraar in de meet-, regel- en systeemtechniek

Co-promotoren: Dr. ir. K.J. Keesman
universitair hoofddocent, leerstoelgroep Meet-, regel- en systeemtechniek

Dr. ir. A. Klapwijk
universitair hoofddocent, leerstoelgroep Milieutechnologie

11/12/1998 10:52

Leo Lukasse

Control and Identification in Activated Sludge Processes

Regeling en Identifikatie in Aktief-Slib Processen

PROEFSCHRIFT

ter verkrijging van de graad van doctor
op gezag van de rector magnificus
van de Landbouwniversiteit Wageningen,
dr. C.M. Karssen,
in het openbaar te verdedigen
op woensdag 13 januari 1999
des namiddags te half twee in de Aula

11/12/1998 10:52

CIP-Data Koninklijke Bibliotheek, DEN HAAG

Lukasse L.J.S.

Control and Identification in Activated Sludge Processes / L.J.S. Lukasse

[S.I. : s.n.]

Thesis Wageningen Agricultural University. - With ref. - With summary in Dutch

ISBN 90-5485-956-3

This dissertation has been completed in partial fulfillment of the requirements of the Dutch Institute of Systems and Control DISC for graduate studies.

BIBLIOTHEEK
LANDBOUWUNIVERSITEIT
WAGENINGEN

Stellingen

1. De term 'tijdsvariant systeem' vloeit voort uit een verkeerd begrip van de werkelijkheid. Er wordt een 'tijdsvariant model' van een 'tijdsinvariant systeem' mee bedoeld. De modellenbouwer heeft, al of niet bewust, niet alle dynamica van het systeem gemodelleerd; daarom geeft het model een betere beschrijving van de werkelijkheid als een deel van het model als tijdsvariant wordt beschouwd.
2. De zeer aannemelijke hypothese, dat meer onderbrekingen in de beluchting van een C-verwijderend Actief Slib Proces een hoger effluent Chemisch Zuurstof Verbruik geeft, wordt in Neiva *et al.* (1996) niet bevestigd door de waarnemingen. De daaraan verbonden conclusie dat de hypothese onjuist is, is echter incorrect. De strijdigheid tussen hypothese en waarnemingen zegt veeleer iets over het experimentontwerp.
Neiva M.R., Galdino L.A., Catunda P.F.C., Haandel A. van (1996). Reduction of operational costs by planned interruptions of aeration in activated sludge plants. *Wat. Sci. Tech.*, **33**, pp. 17-27.
3. De conclusie in Puznava *et al.* (1998) dat hun feedforward regelaar superieur is aan hun feedback regelaar, vloeit voort uit onvoldoende waardering voor het principe van feedback. De grote verdienste van feedback-regelaars is nl. het vermogen om procesuitgangen gewenste waardes op te leggen ondanks onzekerheid in dat proces. Puznava N., Zeghal S. and Reddet E. (1998). Simple control strategies of methanol dosing for post-denitrification. *Wat. Sci. Tech.*, **38**(3), 1998, pp. 291-297.
4. De bewijskracht van ervaring wordt door veel wiskundigen onvoldoende gewaardeerd.
5. De meeste wetenschappers besteden veel te weinig tijd aan de vraag *welk* probleem zij moeten oplossen. Zij houden zich liever bezig met de vraag *hoe* ze een probleem moeten oplossen.
6. Alle goede wetenschappelijke publikaties hebben één conclusie gemeen: er is verder onderzoek vereist.
7. Het is schrijnend dat veel, zgn. onbevooroordeelde, wetenschappers de talrijke verslagen over wonderlijke gebeurtenissen na het aanroepen der goden glashard ontkennen. Op dit specifieke terrein mag de *waarneming* kennelijk, hoe dan ook, niet gedaan worden.

8. Evolutie gedreven door natuurlijke selectie zou uiteindelijk de hele natuur zwart kleuren. De meest efficiënte plant benut nl. al het licht voor fotosynthese en is daarom zwart. Dieren zullen daarna allemaal zwart als schutkleur aannemen, 24 uur per dag functioneel. Hopelijk maak ik dit stadium der evolutie niet meer mee.
9. 'Eerlijke (de)regulering' is een contradictio in terminis.
10. Een goed functionerende regelaar beheerst het te besturen proces. Een slecht functionerende regelaar beheerst het leven van zijn ontwerper.
11. De beste graadmeter voor de inzet van een onderzoeker is het aantal malen dat hij thuis het verwijt krijgt: 'Houd nu eens op aan je werk te denken, we zitten nu gezellig aan de koffie', gedeeld door het aantal malen dat hij daarop reageert.

Stellingen behorend bij het proefschrift 'Control and Identification in Activated Sludge Processes' van Leo Lukasse, Wageningen, 13 januari 1999.

Dankwoord

Graag benut ik de mogelijkheid om aan dit proefschrift een dankwoord toe te voegen en daarin de mensen te bedanken, die me de afgelopen vier jaar tot bijzondere steun zijn geweest.

In de eerste plaats wil ik mijn dagelijkse begeleider en co-promotor Dr. Karel Keesman bedanken. Karel, toen ik vier jaar geleden begon kende ik je niet. Ik mocht je leren kennen als een fantastisch persoon en wetenschapper. Je hebt me de ruimte gegeven andere keuzes te maken dan jij voor ogen had. De reizen die we samen maakten waren gaaf. Onze Japanse badhuizen, campings, de lifts over 'the roof of Kyushu' en je vruchtentheeceremonies zijn kostbare herinneringen.

Mijn collega's in het Agrotechnion, en van de sectie meet-, regel- en systeemtechniek in het bijzonder, wil ik bedanken voor de goede werksfeer. My room mates Frank and Tien proved valuable comrades. Both Frank's and Tien's attitude with respect to religion intrigued me. Frank, het was gezellig en de som van al je hulp bij mijn computerprobleempjes is groot, daarom: met dank aan Frank. En dan die Ilse, sociaal hoogtepunt in onze mannencultuur. Bedankt voor alle gezellige momenten.

Michiel, zonder jou was dit proefschrift veel dunner geweest. Je hebt de proefopstelling tweeënhalve jaar draaiend gehouden, zelfs de ammonium en nitraat analyzers. De experimenten moest je keer op keer herhalen. En ondanks dat alles ken ik je enkel vrolijk!

Van de maandelijksse discussiebijeenkomsten met promotor Prof. dr. Gerrit van Straten, Karel, Michiel, co-promotor Bram Klapwijk, Harry en Henri heb ik veel graantjes meegepikt. Niet alleen vakinhoudelijk. Ik leerde er zowel commentaar leveren als krijgen. Gerrit's kritische oog voor zowel details als grote lijnen, en zijn vermogen om discussies te starten. De rijke water-ervaring van Bram, met zijn nuchtere evenwichtigheid. Het aanstekelijk enthousiasme van Harry. Henri's diepzinnige beschouwingen over de betekenis van een ogenschijnlijk simpel woord. Van dat alles leerde ik. En uhm, wat is ook weer het verschil tussen actuele -, instantane -, endogene -, en maximale respiratie snelheid?

Last but not least wil ik mijn familie, gezin en schoonfamilie bedanken voor alle steun tijdens de afgelopen vier jaar. In het bijzonder tijdens het moeilijke voorjaar van 1998 werd me duidelijk hoe waardevol jullie zijn voor mij. Het door pa en ma bijgebrachte plichtsbesef, de van pa geërfd nuchterheid en het van ma meegekregen perfectionisme: het bleken hele nuttige eigenschappen in mijn promotie-onderzoek. Petra, schoonpa en broer Jan leerden me om perfectionisme tegen produktiviteit af te wegen.

Petra, Marnix, Jorinde wat fijn dat ik van jullie mag zijn. Tijdens de laatste periode heb ik veel van jullie gevergd. Terwijl ik tot steeds later het toetsenbord klopte, zaten jullie vaak op me te wachten. Hopelijk kan ik het een beetje goedmaken door dit proefschrift aan jullie op te dragen. De overgeslagen vakantie? We halen hem echt in.

Wageningen, 15-9-'98
Leo

Voor Petra, Marnix en Jorinde

Contents

1	General introduction	1
1.1	The Activated Sludge Process and its new challenge: total-N removal	1
1.2	Control and identification of Activated Sludge Processes	2
1.2.1	General topics in Activated Sludge Process control	2
1.2.2	Adaptive Receding Horizon Optimal Control	3
1.3	Control of N-removal in alternating Activated Sludge Processes	4
1.3.1	Control schemes	5
1.3.2	Problems	6
1.4	The use of DO-sensors and respirometers	7
1.4.1	State of the art	7
1.4.2	Problems	8
1.5	Pilot scale ASP	8
1.6	Aims of this thesis	9
1.7	Thesis outline	10
1.7.1	PART I, N-removal in alternating activated sludge processes	10
1.7.2	PART II, identification on the basis of DO-measurements and respirometry	12
1.8	References	13

PART I, N-removal in alternating activated sludge processes

2	Identification for model predictive control of biotechnological processes, case study: nitrogen removal in an activated sludge process	19
2.1	Abstract	19
2.2	Introduction	19
2.3	Modelling approach	20
2.3.1	Prior knowledge and presumptions	20
2.3.2	Model identification	20
2.3.3	Parameter uncertainty	21
2.4	Identification of ammonium/nitrate dynamics	22
2.4.1	Prior knowledge	22
2.4.2	Experiments	22
2.4.3	Output error model identification	23
2.4.4	Effect of prediction horizon on model parameters	25
2.5	Discussion	26
2.6	Conclusions	26
2.7	References	27
2.8	Appendix 1, covariance for multi-output model parameter estimates minimizing the (weighted) sum of squared 1, 2, ..., H -step ahead prediction errors.	27

3	A recursively identified model for short-term predictions of NH_4/NO_3-concentrations in alternating activated sludge processes	31
3.1	Abstract	31
3.2	Introduction	31
3.3	Process model	32
3.4	Recursive parameter estimation	34
3.5	Application to real measurements	36
3.6	Results & Discussion	38
3.7	Simulation study	40
3.8	Conclusions	42
3.9	References	42
3.10	App. 1, stability characteristics of the Kalman filter applied to unobservable systems.	44
4	Optimal control of N-removal in ASP's	47
4.1	Abstract	47
4.2	Introduction	47
4.3	Optimal control of nitrogen removal according to ASM no. 1	48
4.4	Receding horizon optimal control implementation	49
4.5	Pilot plant results	53
4.6	Discussion	54
4.7	Conclusions	54
4.8	References	55
4.9	Appendix 1, list of symbols	55
5	Adaptive receding horizon optimal control of N-removing activated sludge processes	57
5.1	Abstract	57
5.2	Nomenclature	57
5.3	Introduction	58
5.4	RHOC scheme	58
5.5	Recursive identification scheme	60
5.6	Adaptive RHOC	61
5.7	Simulation results	62
5.8	Pilot plant results	63
5.9	Discussion	64
5.10	Conclusions	65
5.11	References	65
6	L_1-Norm optimal control of N-removal in an activated sludge process	67
6.1	Abstract	67
6.2	Introduction	67
6.3	The L_1 -norm optimal state feedback law	68
6.4	Application to N-removal in activated sludge processes	72
6.5	Conclusions	75
6.6	References	76
6.7	Appendix 1, list of symbols	76
6.8	Appendix 2, counter example	77

7	A comparison of NH_4/NO_3 control strategies for alternating activated sludge processes	79
7.1	Abstract	79
7.2	Introduction	79
7.3	Methodology	80
7.3.1	Plant model	80
7.3.2	Influent scenario	80
7.3.3	Evaluation criteria	81
7.4	Controllers to be compared	81
7.5	Best feasible results	83
7.6	Sensitivity analysis	85
7.7	Discussion	87
7.8	Conclusions	87
7.9	References	88

8	Optimised operation and design of alternating activated sludge processes for N-removal	89
8.1	Abstract	89
8.2	Introduction	89
8.3	Currently available operation strategies	90
8.4	Simulation methodology	91
8.4.1	The 2-reactors alternating process model	91
8.4.2	Influent scenario	91
8.4.3	Evaluation criteria	92
8.5	Receding horizon optimal control of the alternating process	92
8.6	RHOC results	95
8.7	Simple controllers imitating RHOC	97
8.8	Discussion	98
8.9	Conclusions	100
8.10	References	101

PART II, identification on the basis of DO-measurements and respirometry

9	Grey-box identification of dissolved oxygen dynamics in activated sludge processes	103
9.1	Abstract	103
9.2	Introduction	103
9.3	Modelling approach	104
9.3.1	Prior knowledge and preassumptions	104
9.3.2	Identification of model structure and parameters	104
9.4	Application	105
9.4.1	Prior knowledge	106
9.4.2	Experiment design	106
9.4.3	Identification of model structure and parameters	106
9.5	Conclusions	109
9.6	References	110
9.7	Appendix 1, list of symbols	110
9.8	Appendix 2, parameter uncertainties in eqns. 7, 10 - 12	111

10	Estimation of BOD_{st}, respiration rate and kinetics of activated sludge	113
10.1	Abstract	113
10.2	Nomenclature	113
10.3	Introduction	114
10.4	Measurement strategy	115
10.5	Respirometer model	116
10.6	Estimation procedure	118
10.6.1	step 1 Estimation of q and Δ	118
10.6.2	step 2 Estimation of k_s	119
10.7	Results	120
10.8	Estimation of the actual respiration rate in the aeration tank	121
10.9	Proposals for improved measurement strategy	121
10.10	Conclusions	123
10.11	References	124
11	Diagnosis and identification by excitation of the dynamics in continuous flow respirometers	125
11.1	Abstract	125
11.2	Introduction	125
11.3	Dynamic respirometer model	127
11.4	Identification of respirometer model parameters D , r_e , τ and Δ	127
11.5	Identification of sludge kinetics and S_{in}	129
11.6	Measurement strategy	130
11.7	Experimental results	131
11.8	Discussion	134
11.9	Conclusions	136
11.10	Nomenclature	137
11.11	References	137
12	Conclusions and suggestions	139
12.1	Conclusions for the practitioner	139
12.2	Increased NH ₄ concentration to meet total-N standards	140
12.3	Control in view of time-averaged effluent standards	141
12.4	pH-based auto-tuning of timers for N-removal	143
12.5	Dynamic simulations: the future	144
12.6	References	145
	Summary	147
	Samenvatting	151
	Curriculum vitae	155

1 General introduction

1.1 The Activated Sludge Process and its new challenge: total-N removal

The activated sludge process (ASP) is a widely used system for biological wastewater treatment. Traditionally the ASP mainly served to remove organics and ammonium from the wastewater. The basic design of an ASP plant is depicted in Fig. 1. In the reactor the organics in the influent flow (q_m) are transformed into settleable biomass (activated sludge flocs) by biomass growth. In the next step the sludge settles at the bottom of the

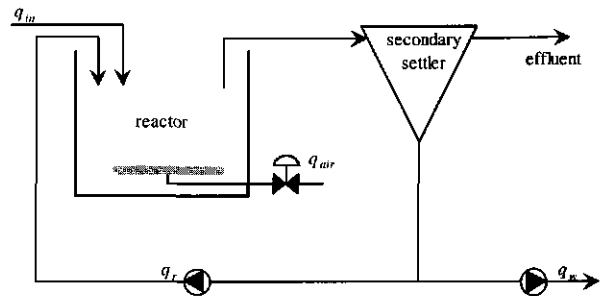


Fig. 1, basic activated sludge process.

The treated effluent of the plant flows over the weirs at the top of the settler, while the settled sludge is withdrawn from the bottom. The major part of it is recycled to the reactor (q_r), and a small part is wasted (q_w). Sludge recycling prevents the washout of biomass by decoupling the sludge residence time from the hydraulic residence time in the plant. The main control handles are the rates (l/h) of return flow q_r , wastage flow q_w and air flow q_{air} .

During the last decade the interest in total-N removal from wastewater has risen due to increasing attention for the problem of eutrophication in the aquatic environment. In the Netherlands, and many other regions in the EU, in 1991 this resulted in a new guideline for the stepwise introduction of total-N removal (EU-directive 91/271/EEC). In the Netherlands this EU-directive is implemented in the "Lozingenbesluit Wvo stedelijk afvalwater" (Staatsblad 140, 1996). Before only an effluent standard of 20 mg/l Kjeldahl-N in the summer period was applied. According to the new law every Dutch wastewater treatment plant has to comply with new effluent N-total standards by the end of 1998, with the possibility to postpone this deadline as far as 31-12-2005 for specific plants. The new standards are a yearly averaged effluent N-total of 10 mg/l for plants with a design capacity over 20,000 p.e. (population equivalents) and 15 mg/l for plants with a design capacity less than 20,000 p.e.. For plants over 100,000 p.e. the standard applies to the flow-proportional average, otherwise the time-proportional average suffices.

Total-N removal requires two biological processes: nitrification and denitrification. Nitrification is a two steps process described by



Nitrite (NO_2^-) only is an intermediate with usually low concentration, and therefore is usually grouped together with nitrate (NO_3^-) as NO_x . The nitrifiers *Nitrosomonas* and *Nitrobacter* both are

autotrophic organisms. Autotrophic organisms are able to build up their biomass from inorganic carbon and H₂O by reduction processes. Nitrification takes place when the autotrophs meet NH₄ under aerobic conditions.

Denitrification is described by



Most heterotrophic species present in ASP reactors are able to denitrify. Denitrifiers (heterotrophic organisms that are able to denitrify) preferably use DO as electron acceptor, but switch to NO_x instead if no DO is available. The denitrification process only takes place when denitrifiers meet RBOS (Readily Biodegradable Organic Substrate) in an anoxic environment (presence of NO_x, absence of DO). Under those conditions denitrifiers consume organics, using nitrate and nitrite as oxidiser.

Both amongst scientists and practitioners a reasonable consensus exists upon the statement that the Activated Sludge Model no. 1 (ASM no. 1) by Henze *et al.* (1987) is the most popular mathematical description of the biochemical processes in ASP reactors for N removal. The most popular model for the settling process probably is the double exponential model (Takács, 1991).

1.2 Control and identification of Activated Sludge Processes

This thesis focuses on control and identification of ASP's. Over the last decades there has been a large and ongoing interest in (nonlinear) system identification (*e.g.* Young, 1984; Ljung, 1987) and its application to activated sludge processes (*e.g.* Busby and Andrews, 1975; Farkas *et al.*, 1991; Vanrolleghem, 1994; Côté *et al.*, 1995; Jeppsson, 1996; Tenno and Uronen, 1996; Julien *et al.*, 1997). The objective of identification is to reduce the uncertainty about process dynamics, such that designs of processes and controllers can be improved. Good control can improve the utilization of the reactor volume and reduce the required over-dimensioning of plant designs.

1.2.1 General topics in Activated Sludge Process control

The main challenge in control of the activated sludge process is disturbance attenuation in the complex non-linear multivariable ASP, whose stiff dynamics contain a considerable uncertainty and are subject to large seasonal variations. To get a comprehensive overview of the problems involved see Andrews (1974), Marsili-Libelli (1989), Olsson *et al.* (1989) and van Leeuwen (1990).

The traditional ASP control objective is disturbance attenuation (Andrews *et al.*, 1976; Dold *et al.*, 1984; Kabouris and Georgakakos, 1991; Olsson, 1992). Disturbance attenuation is just a means to achieve the higher level objectives of minimizing costs (*e.g.* avoid excessive aeration) and maximizing the conversion rates of biological processes in the reactor (*e.g.* reducing substrate limitation during the low loaded part of the day). The main source of disturbance is the influent. Large diurnal variations occur both in influent flow and composition, as a result of the characteristic life pattern of the connected households. Fortunately the large hydraulic residence time (typically > 10 h) largely dampens this diurnal cycle just by dilution, especially in continuously mixed reactors (Jenkins and Garrison, 1968). Yet there remains a significant task for active control to further dampen diurnal variations.

Rain events incidentally cause very high flow rates and changes in influent composition. Especially hydraulic shock loads due to storm events may cause serious overloading incidents in the secondary clarifier, resulting in loss of biomass in the effluent (Aspegren *et al.*, 1996). This contributes to very high effluent BOD during the incident, and reduced process rates in the aftermath of the incident.

The uncertainty in dynamics of ASP's make the use of *feedback* control indispensable (Fig. 2). The uncertainty is caused by unpredictable changes in sludge activity and composition, especially due to seasonal variations in temperature and rainfall. *E.g.* the rates of nitrification and denitrification respectively decrease by about 60% and 50% if the temperature drops from 20 °C to 10 °C (Metcalf and Eddy, 1979). Seasonal variations in rainfall affect the influent flow and composition. That in turn has a long-term effect on the sludge inventory.

Solving the overall multivariable control problem of an ASP is a utopia. To keep the problem solvable it needs to be decomposed. Decomposition is possible by decoupling the control of fast and slow processes (*e.g.* Hiraoka and Tsumara, 1989). The main dynamic processes in ASP reactors

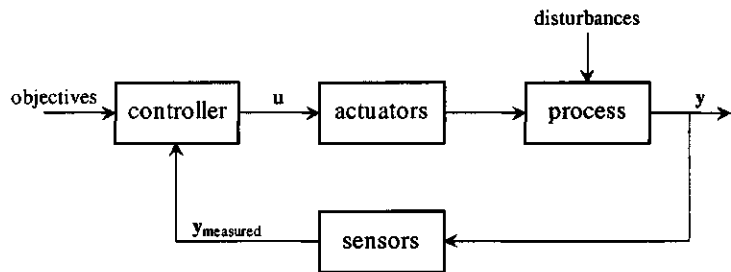


Fig. 2, general feedback control loop.

can be separated into three timescales: fast DO dynamics, slower substrate (amongst others N) dynamics and slow biomass (sludge) dynamics. The characteristic time constants of these three timescales are respectively minutes, hours and weeks. Substrate plays the keyrole as it is directly related to effluent quality. DO - and biomass control just serve to create an environment for efficient substrate removal, where the word efficient stands for an optimized balance between effluent quality and operational costs. Viewed in that light it is natural that a substrate controller dictates the setpoints for both DO and sludge controllers, if necessary taking into account the realizability of these setpoints.

1.2.2 Adaptive Receding Horizon Optimal Control

Optimal control solves an objective functional subject to the modelled system dynamics and possible constraints on the model states, inputs and outputs (*e.g.* Lewis, 1986). As its solution is an *open-loop* optimal control strategy it is unsuitable for practical implementation. Its use mainly comes from the increased insight when applied in simulations. Several optimal control simulation studies of the activated sludge process have been reported (Sincic and Bailey, 1978; Yeung *et al.*, 1980; Stehfest, 1985; Kabouris and Georgakakos, 1990; Kabouris *et al.*, 1992).

Receding Horizon Optimal Control (RHOC) is the way to implement the theory of optimal control on-line, introducing feedback from the process (Fig. 2). The general digital RHOC algorithm solves at each sampling instant $k \in \{0, 1, 2, \dots\}$ the optimization problem

$$\min_{\mathbf{u}_k \dots \mathbf{u}_{k+H-1}} J(\mathbf{u}) = G(\mathbf{x}(k+H)) + \sum_{i=k+1}^{k+H} F(\mathbf{x}(i), \mathbf{u}(i)) \quad (3)$$

subject to the modelled system dynamics

$$\begin{aligned} \mathbf{x}_{k+1} &= f(\mathbf{x}_k, \mathbf{u}_k, \mathbf{d}_k, \boldsymbol{\theta}) & \mathbf{x}_k &= \hat{\mathbf{x}}_k \\ \mathbf{y}_k &= g(\mathbf{x}_k, \mathbf{u}_k, \boldsymbol{\theta}) \end{aligned} \quad (4)$$

with control interval T , prediction horizon H , vector of control inputs $\mathbf{u} \in \mathbb{R}^m$, state vector $\mathbf{x} \in \mathbb{R}^n$, output vector $\mathbf{y} \in \mathbb{R}^q$, vector of disturbance inputs $\mathbf{d} \in \mathbb{R}^s$, parameter vector $\boldsymbol{\theta} \in \mathbb{R}^p$. The term $G(\mathbf{x}(k+H))$ in $J(\mathbf{u})$ allocates a (possibly negative) value to the state of the process at the end of the prediction horizon, while the term $F(\mathbf{x}(i), \mathbf{u}(i))$ allocates (possibly negative) values to the states \mathbf{x} and controls \mathbf{u} on the time interval $[kT, (k+H)T]$. The RHOC algorithm can be made adaptive by recursive estimation of parameter vector $\boldsymbol{\theta}$ (see *e.g.* Ljung and Söderström, 1983).

Many theoretical papers on RHOC are available now (Chen and Shaw, 1982; Mayne and Michalska, 1990; Genceli and Nikolaou, 1993; Michalska and Mayne, 1993; Yang and Polak, 1993; Nicolao *et al.*, 1996; Ohtsuka and Fujii, 1997). Also a number of practical applications has been published (*e.g.* Shinar and Glizer, 1995; Afonso *et al.*, 1996; Chalabi *et al.*, 1996; de Madrid *et al.*, 1996; Tap *et al.*, 1996; Camacho and Berenguel, 1997; Miller and Pachter, 1997; Becerra *et al.*, 1998). Although no applications in wastewater treatment have been published, the interest in adaptive RHOC for ASP's exists. This is illustrated in *e.g.* Dupont and Sinkjær (1993) and Thornberg and Thomsen (1994). After identifying the process dynamics and disturbance characteristics from the data they used the current state as initial condition to evaluate the effect of different near-future control input scenario's in simulation. Selection of the most suitable control inputs is left to the operator. Already in Olsson *et al.* (1989) this procedure was indicated as a future trend.

RHOC is the way to implement the above described procedure on-line, moreover it automatically selects the most suitable control input trajectory, *i.e.* the control input trajectory that minimizes the formulated objective functional (eqn. 3). In the ideal case the dynamic model (eqn. 4) equals the true system dynamics and the knowledge with respect to future disturbance inputs is perfect. In that ideal scenario eqn. 3 should merely express the economy of the process.

The main hindrance for the on-line implementation of RHOC has always been the large computational demand for solving the RHOC's non-linear optimization problem. The fast evolution of computing power rapidly invalidates this argument. Yet some problems for RHOC in general remain:

1. The risk of getting stuck at local minima when solving nonlinear optimization problems.
2. Models usually have serious shortcomings, that need to be accounted for by adding penalty terms to eqn. 3.
3. On-line solving of the overall dynamic optimization problem for a plant is impossible for systems with unobservable states, like the ASP.
4. Information with respect to future disturbance inputs is usually incomplete.

1.3 Control of N-removal in alternating Activated Sludge Processes

The introduction of denitrification and improved nitrification in ASP's is accompanied by some new control problems, in addition to the existing more general problems discussed in section 1.2.1. As

mentioned in the preceding section nitrification requires the combination of three factors: NH_4 , aerobic conditions and autotrophs. NH_4 is the main source of total-N in the influent wastewater. It will just remain in the wastewater until it meets autotrophs under aerobic conditions. Aerobic conditions are created by applying a sufficient air flow rate (Fig. 1) to the reactor or a part of it. The limiting factor in nitrification is the low maximum growth rate of the autotrophic nitrifiers (eqn. 1), especially during winter. In operation this requires a long sludge residence time (= sludge age) to prevent washout of autotrophs. Typically, for nitrification the sludge age should be over 20 days.

The denitrification process has the attractive potential to remove organics from wastewater without aeration and at a reduced sludge production due to the lower anoxic yield factor. As mentioned before denitrification requires the presence of three factors: denitrifying heterotrophs, anoxic conditions and RBOS. Denitrifiers are abundantly available in any ASP for total-N removal, and hence do not deserve special attention. Two different approaches exist for introducing anoxic conditions. One is to use anoxic zones (e.g. Spies and Seyfried, 1988; Londong, 1992; Nowak and Svardal, 1996; Meyer and Hanke, 1997). This requires plug-flow-like hydraulics, i.e. the presence of a spacial distribution in the reactor, or multiple reactors in series. The other approach applies intermittent aeration in the reactors to create anoxic periods (e.g. Sasaki *et al.*, 1993). Under anoxic conditions the denitrification rate is mostly RBOS-limited, therefore the RBOS-rich influent is usually fed to the location where conditions are anoxic. To enable the feeding of all influent to locations with anoxic conditions the anoxic periods approach is often implemented in a plant design with two parallel reactors ran in counterphase (e.g. Thornberg *et al.*, 1993), or combined with a small anoxic zone preceding the alternating reactor (Wouters-Wasiak *et al.*, 1994; Carucci *et al.*, 1997). NO_x accumulates under aerobic conditions (eqn. 1). Hence in case of applying anoxic zones a large internal recirculation flow is required to bring NO_x from the end of the aerobic zone to the beginning of the anoxic zone. Applying anoxic periods brings the anoxic conditions to the NO_x .

1.3.1 Control schemes

Three control handles are available in the nitrification process: waste flow rate q_w , hydraulic residence time in aerobic zones or periods, and air flow rate q_{air} in the aerobic phase (Fig. 1). Waste flow rate q_w affects the sludge residence time, and hence the concentration of autotrophs. Settler design and risk avoidance put fierce constraints to the freedom to manipulate q_w . Moreover the response time of the sludge inventory to changes in q_w is very long (months). Hence q_w is unsuitable for active control of the nitrification process (Vaccari and Christodoulatos, 1989). A common active control handle for the nitrification process is the hydraulic residence time in aerobic zones or periods, i.e. the size of aerobic zones or the length of aerobic periods. It is very general to manipulate q_{air} in the aerobic phase with the objective to control the measured Dissolved Oxygen (DO) concentration around a fixed setpoint DO_R . Usually $DO_R = 2 \text{ mg/l}$, a sufficient value to prevent DO-limitation of nitrification. However some cases are reported where the aeration costs are reduced by introducing controlled DO-limitation in the aerobic zone (Sekine *et al.*, 1985; Isaacs, 1996).

In principle the anoxic zones approach for denitrification introduces two new control handles, these are the internal recirculation flow rate and the size of the anoxic zone. In the anoxic periods approach two new control handles occur, being the length of the anoxic periods and, if multiple hydraulically connected reactors are used, the flow schedule through the reactors (Andrews *et al.*, 1980; Zhao *et al.*, 1994; Zhao *et al.*, 1995; Isaacs, 1996; Thomsen *et al.*, 1997).

The anoxic *periods* approach for alternating nitrification/denitrification offers two principal advantages over the anoxic *zones* approach. Firstly, it does not require the large internal recirculation flow rate with its inherent pumping costs and continuous transport of oxygen to the anoxic phase. Secondly, excitation of dynamics is inherent to the anoxic *periods* approach. This offers an ideal setting for (recursive) identification of process dynamics, especially the rates of nitrification/denitrification can easily be estimated (*e.g.* Carstensen *et al.*, 1995).

In both the anoxic *zones* and the anoxic *periods* approach an external carbon source, usually ethanol, may be added to the anoxic phase to speed up denitrification (Sekoulov *et al.*, 1990; Tam *et al.*, 1992; Isaacs *et al.*, 1995; Lindberg, 1997). This is an effective, but expensive, approach. Adding an external carbon source should be the last option as there are additional costs related to the carbon source addition itself, it causes extra sludge production and it does not exploit the possibility to reduce aeration costs by denitrification.

Feedback control requires the use of sensors to measure the plant's state (Fig. 2). There is a widespread reluctance to use the expensive, maintenance intensive, and failure sensitive measurement devices for NH_4 and NO_x . This is the driving force behind the use of indirect, incomplete, or even no, measurements in control of nitrification/denitrification. The most common indirect measurement is ORP (Oxidation Reduction Potential) (Sekine *et al.*, 1985; Charpentier *et al.*, 1989; Ménardière *et al.*, 1991; Wouters-Wasiak *et al.*, 1994). Also pH is used as an indirect measurement, though still scantily (Al-Ghusain *et al.*, 1994; Carucci *et al.*, 1997; Wett *et al.*, 1997). Recently it was demonstrated that OUR can be used as well (Surmacs-Gorska *et al.*, 1995; Klapwijk *et al.*, 1998). Incomplete measurements are used when alternating the aeration on the basis of measurements of solely NH_4 (*e.g.* Spies and Seyfried, 1988) or solely NO_x (*e.g.* Kayser and Ermel, 1985; van Dalen, 1993). No measurements are used when alternating the aeration in the anoxic *periods* approach on the basis of timeclocks. Its open loop nature makes it cheap but also increases the risk of gross failures. Obviously the best controller performance can be achieved if both NH_4 and NO_x are measured.

1.3.2 Problems

Different strategies for controlling the alternating aeration have evolved. The amazing thing is that all the alternative control-schemes just coexist. What is missing is a profound comparison between the different control-schemes, and a comparison with the best feasible result. Only when the performance loss of the simpler control schemes is known, a balanced trade-off between costs of instrumentation (purchase, maintenance) and loss of performance is possible. A mutual comparison can easily be carried out in simulation. Drawback of simulations is that the dynamics of both the sensors and the process need to be modelled. And even the best model of the ASP is nothing but a poor resemblance of the real process. However, a fair experimental *comparison* of multiple controllers is impossible, not only for financial reasons. Simultaneous experimental testing would require the availability of multiple identical plants in parallel. Sequential testing on one plant would disrupt the results by changes in process conditions and influent, disabling a mutual comparison. Hence simulation is the best way to compare different control-schemes.

To enable comparison with the best feasible result, the best feasible result needs to be known. At the moment it is largely unknown. The best feasible result can be approximated by applying Receding Horizon Optimal Control. As mentioned before, RHOC has not yet been applied in waste-

water treatment. RHOC requires the availability of a simple internal process model, which should yield accurate predictions over the control horizon H . Such a model is not yet available for N-removal in ASP's. For a complicated system like the ASP a simple model is only possible by neglecting large parts of the process dynamics. Large simplifications of dynamics result in time-varying models. Recursive identification of (some of) the model parameters is required to preserve accurate predictions from a time-varying model in an on-line situation.

As mentioned before, the anoxic *periods* approach offers an ideal setting for (recursive) identification of the rates of nitrification/denitrification. Up to now no reports are available on the use of NH_4 and NO_x sensors for on-line recursive identification of the rates of nitrification and denitrification. The only known exploitation of this kind of process conditions for estimating process rates is the use of DO sensors to estimate the respiration rate (= oxygen uptake rate) (e.g. Suescun *et al.*, 1998).

In particular monitoring of the nitrification rate could be useful in controlling the autotrophic biomass inventory. Nowadays this control is done in an open loop manner, by just aiming at a large sludge age and hoping that this suffices to maintain sufficient autotrophs. Due to the lack of knowledge with respect to the concentration of autotrophs it is often reasoned that effluent NH_4 should be very low. In that way the concentration of autotrophs is maximized. In this operation strategy possible significant improvements in operational costs and effluent quality remain unutilized.

1.4 The use of DO-sensors and respirometers

The DO-sensor undoubtedly is the most widespread sensor in ASP's. It is generally used in a DO feedback control loop with a DO-setpoint DO_R of usually 2 mg/l. Manipulating the air flow rate such that DO remains at its setpoint contributes to important costs savings as compared to the historical situation of just using a constant large air flow rate (Flanagan *et al.*, 1977; Corder and Lee, 1984; Evans and Laughton, 1994; Neiva *et al.*, 1996).

1.4.1 State of the art

The problem of just controlling DO in aerated reactors at its setpoint has been solved (Marsili-Libelli *et al.*, 1985; Olsson *et al.*, 1985; Rundqwist, 1988; Haarsma and Keesman, 1995; Lindberg and Carlsson, 1996b). Nowadays the research challenges with respect to the use of DO-sensors concern the control and estimation of variables deduced from DO readings (Olsson and Andrews, 1978; Tanuma *et al.*, 1985; Chandra *et al.*, 1987; Vargas-Lopez *et al.*, 1989; Brouwer *et al.*, 1998). An important example is estimation of the respiration rate (Holmberg, 1982; Marsili-Libelli, 1984; Holmberg *et al.*, 1989), possibly in conjunction with oxygen transfer rate k_{La} (Bocken *et al.*, 1988; Carlsson and Wigren 1993; Lindberg and Carlsson, 1996a) from DO-sensor readings only. DO-sensors also occur in respirometers (e.g. Spanjers, 1993; Spanjers *et al.*, 1998). Even more complex setups are built around the respirometer to identify sludge kinetics and concentrations of individual influent components from DO-sensor readings (Vanrolleghem and Verstraete, 1993; Spanjers and Vanrolleghem, 1994; Reid *et al.*, 1995; Vanrolleghem and Coen, 1995; Wentzel *et al.*, 1995; Brouwer *et al.*, 1998).

Also identification of the DO-sensor dynamics itself has been applied. This is useful in monitoring the well-functioning of the sensor and reverse filtering of measurements before estimating the respi-

ration rate from measured DO-transients (Spanjers and Olsson, 1992; Lindberg and Carlsson, 1996a; Suescun *et al.*, 1998).

Spanjers *et al.* (1994) presented an estimation method for Short Term Biochemical Oxygen Demand (BOD_{st}) using a continuous flow respirometer. It estimates BOD_{st} at a 15 minutes sampling interval with a 15 minutes time-delay. This method is potentially interesting for control purposes. After all BOD_{st} is defined as the rapidly degradable part of BOD_5 . Effluent BOD_5 is a sludge independent measure of the total amount of DO required to oxidize the effluent organics and NH_4 in the receiving surface water. Active feedback control of BOD_5 is impossible because of the 5-days time delay inherent to its measurement. When reliable estimates of BOD_{st} are available these may be used explicitly in feedback control loops, as BOD_{st} reflects the controllable part of BOD_5 .

1.4.2 Problems

Improvement of methods for experimental identification of the non-linear function $k_{La}(q_{air})$, *i.e.* the relationship between k_{La} and q_{air} (Fig. 1), will always remain relevant. It is especially valuable in experimentally evaluating the relationship between $k_{La}(q_{air})$ and the design of (newly developed) aeration equipment, between $k_{La}(q_{air})$ and the use of specific carrier materials in aerated reactors (*e.g.* Morper, 1994), or between $k_{La}(q_{air})$ and the presence of certain detergents in the influent. After all a higher k_{La} at a given q_{air} results in a higher efficiency of energy usage for aeration, and hence identification of $k_{La}(q_{air})$ for newly developed equipment can yield important sales arguments.

Identification of influent components and sludge kinetics from in-sensor experiments with continuous flow respirometers has received considerable attention in recent years. Moreover, in view of the increased attention for respirometry in the IAWQ context (Spanjers *et al.*, 1998), it is to be expected that new approaches for further exploitation of continuous flow respirometers will emerge in the near future. What deserves more attention is the need to assure the well-functioning of the device itself.

Spanjers *et al.* (1994) presented an estimation procedure for BOD_{st} using a continuous flow respirometer. The possible benefit of a rapid measurement strategy for BOD_{st} is clear, but their estimation procedure lacks accuracy. It looks though as if some modifications on their procedure can improve the accuracy of their estimates.

1.5 Pilot scale ASP

A large part of this thesis is based on experimental results. All experiments have been carried out at a pilot scale ASP, belonging to the Environmental Engineering group in our department. The pilot plant is schematically depicted in Fig. 3. It consists of a 475 l aerated continuously-mixed reactor (reactor 2), preceded by a 40 l anoxic continuously-mixed reactor for predenitrification (reactor 1). Application of the anoxic *periods* approach to reactor 2 by switching the air flow rate q_{air} on/off is studied in-depth. Preceding the alternating reactor 2 by the anoxic reactor 1 enables the feeding of all influent to locations with anoxic conditions. It combines the anoxic *periods* approach with the anoxic *zones* approach, like in Wouters-Wasiak *et al.* (1994) and Carucci *et al.* (1997). This pilot plant is a simple representation of a carousel with anoxic predenitrification zone. The main simpli-

fication is the absence of a spacial distribution in reactor 2, while in carrousel a clear DO-gradient may occur and in many cases anoxic zones may be imposed on-purpose.

All on-line measurements are conducted in reactor 2. *DO* is measured with a WTW DO-sensor EO90. The respiration rate r (Oxygen Uptake Rate) is measured using an RA1000 respirometer

(Maontherm B.V., Holland).

NH_4 and NO_x are measured using SKALAR auto-analysers type SA 9000. The continuous flow sludge sample fed to the analysers is preconditioned by crossflow membrane filtration. In this way clogging inside the analyzers is prevented. The Mixed Liquor Suspended Solids (sludge) concentration *MLSS* is measured using a SOLITAX-probe (Dr. Lange). It has experimentally been observed that the effect of air bubbles due to aeration on the *MLSS*-readings is at most 0.2 g/l. *pH* is measured (and controlled in some experiments) by the Liquesys CPM 240 (Endress & Hauser). The temperature T is measured by a PT 100.

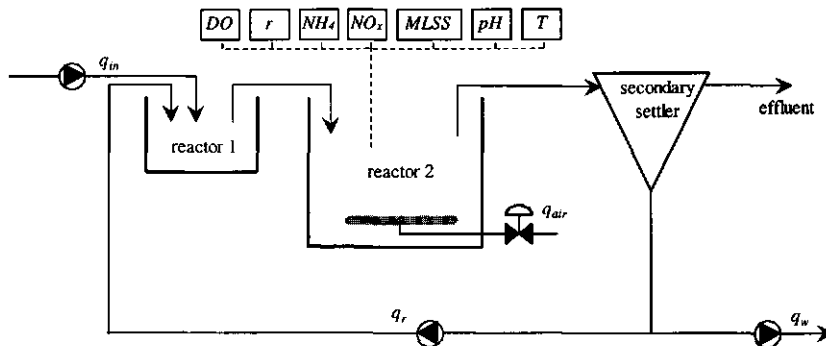


Fig. 3, pilot scale activated sludge process.

Presettled municipal influent is drawn off the adjacent fullscale wastewater treatment plant (WWTP) of the town of Bennekom and fed to the anoxic reactor 1. The influent flow rate q_{in} is freely adjustable. In many experiments q_{in} is just a downscaled version of the on-line measured influent flow rate at the adjacent fullscale WWTP. The return sludge flow rate q_r is freely manipulable as well, in most experiments it is equal to the average influent flow rate q_{in} . The waste flow rate q_w is manually adjusted such that the measured sludge concentration *MLSS* in reactor 2 remains about 3.5 g/l. The airflow rate q_{air} (bubble aeration) in reactor 2 is manipulable between 0 and 6 m³/h. In most experiments reactor 2 is intermittently aerated. During the aerobic periods *DO* is controlled to a setpoint of 2 mg/l by the controller presented in Haarsma and Keesman (1995).

1.6 Aims of this thesis

This thesis is separated in two parts. In part I the main objective is to reduce the lack of knowledge with respect to (sub)optimality of N-control strategies in alternating reactors. This is done by

1. Developing an on-line implementable close-to-optimal controller for alternating processes using measurements of NH_4 and NO_x . The controller will be tested by means of pilot-plant experiments.
2. The performance of this best feasible controller will then be compared with the most common existing control strategies. This comparison is conducted in simulation, as that is the only way to exclude erroneous conclusions due to arbitrary events.

3. Application of the above procedure will be repeated to a plant design with two hydraulically connected reactors in parallel. In this case the optimal plant design is no longer obvious. Hence the different operation strategies are simulated to a range of different plant designs within the above described class. The objective is to find the optimal *combination* of process design and operation.

Part II of the thesis concerns identification on the basis of DO-measurements and respirometry. The objectives are

4. The development of an identification procedure for the DO-dynamics in ASP reactors. This identification procedure must amongst others yield estimates of $k_L a$.
5. The development of an estimation procedure for BOD_{st} and sludge kinetics from in-sensor experiments in continuous flow respirometers. The final scope is to use the estimates in ASP-control.
6. Improvement of the operation of continuous flow respirometers by applying diagnosis and identification to the DO-sensor readings collected from special-purpose in-sensor experiments. The benefit of such procedures is the reduced need for maintenance and the improved accuracy of the measured respiration rate by the device.

1.7 Thesis outline

All chapters in this thesis have been, or will be, published independently (except for chapter 12). Consequently they can be read independently, the inherent drawback is that some repetition is unavoidable. As a side-effect exact chronological ordering of the steps made during the research is impossible in the thesis.

The chapters in this thesis are divided in two parts. Part I (chapter 2 - 8) deals with the development of the best feasible, close-to-optimal adaptive receding horizon optimal controller (RHOC) for N-removal in a continuously mixed alternating activated sludge process reactor. Subsequently this controller and the most common existing controllers are mutually compared by means of simulations. In addition the application of the close-to-optimal RHOC controller to a system of two hydraulically connected alternating reactors is simulated for a range of plant designs within this class. In this way the combination of design and operation is optimized.

Part II (chapter 9 - 11) concerns identification on the basis of DO-measurements and respirometry. First the DO-dynamics in a continuously mixed ASP reactor are identified, including the non-linear relation between $k_L a$ and q_{air} . Subsequently the dynamics of a (DO-sensor based) continuous flow respirometer are identified by exciting its dynamics.

1.7.1 PART I, N-removal in alternating activated sludge processes

Chapters 2 till 5 present the design procedure for the adaptive RHOC for control of NH_4 and NO_x . The first step is presented in chapter 4, where it is concluded from an optimal control study that alternating nitrification/denitrification may be optimal, as opposed to simultaneous nitrification/denitrification at limiting DO-levels.

In chapter 2 a model for N-removal in alternating ASP's is identified. Limitation to the case of *alternating* operation is justified by the above-mentioned conclusion in chapter 4. The model should be computationally efficient, as the model will serve as the internal model (eqn. 4) of the adaptive RHOC controller to be developed in chapter 5. Model simplicity is achieved by capturing the slower process dynamics in time-varying model parameters. It is taken into account that the model structure must be suited for recursive identification of the time-varying model parameters. RHOC, like any model predictive controller, computes the current controls on the basis of model predictions upto horizon H . Hence the sum of squared 1, 2, ..., H -step ahead prediction errors is a natural identification criterion. This idea is applied to NH_4/NO_x measurements collected from reactor 2 in the pilot scale ASP of Fig. 3. Prediction horizon H appears to affect the parameter estimates significantly, supporting the idea that use of this new identification criterion will improve MPC performance in general.

RHOC with this simple model is applied to the pilot plant's alternating reactor in chapter 4. It appeared that the performance of this controller is suboptimal due to inaccurate model predictions. This was to be expected, as the simplicity of the N-removal model in chapter 2 has been achieved by capturing the slower process dynamics in the model parameters, while in this stage they are not recursively estimated. The results of chapter 4 illustrate that recursive identification of (some of the) model parameters is required to keep the model uptodate.

Chapter 3 presents the algorithm for recursive identification of those model parameters. The Kalman filter is used, because it has the attractive feature that the filter gain accompanying non-identifiable parameters (*e.g.* the nitrification rate during anoxic periods) increases linearly in time. It is proven that this increase of the filter gain will not cause instability during normal process operation. The method performs excellently on real data. The recursively identified model will serve as the internal model of the adaptive RHOC controller developed in chapter 5. A practically relevant spin-off is the on-line recursive estimation of the rates of nitrification and denitrification from NH_4 and NO_x measurements.

In chapter 4 optimal control theory is applied to the ASM no.1 model (Henze *et al.*, 1987). It appears that, from an N-removal point of view, both alternating nitrification/denitrification and simultaneous nitrification/denitrification at limiting DO-levels might be optimal. Hence, in view of the risk of sludge bulking at limiting DO-levels, an alternating strategy is favoured. Subsequently an RHOC controller for N-removal in alternating reactors is derived, using the model identified in chapter 2. The controller successfully passed several tests both in simulation and in pilot plant experiments, but it also appeared that the performance of this controller is suboptimal due to inaccurate model predictions.

Therefore adaptive RHOC is introduced in chapter 5, being the combination of the recursively identified model in chapter 3 and the RHOC controller in chapter 4. Proofs with respect to the stability of the resulting control algorithm can not be given, but only one instability scenario was encountered throughout many experiments. This scenario is easy to prevent and does not occur under normal operating conditions.

Chapter 6 presents an l_1 -norm optimal state feedback controller for 2-dimensional linear time invariant (LTI) systems with decoupled dynamics and a single control input. The process of N-removal in a continuously mixed reactor can be approximated by such a system description, pro-

vided that the aeration is alternated and the process rates are not NH_4/NO_x -limited. The motivation for this research comes from the unusual observation in chapter 4 that the RHOC performance is nearly invariant to its prediction horizon.

In chapter 7 the three most common control strategies for N-removal in alternating reactors and the close-to-optimal controller of chapter 5 are mutually compared by means of simulation. It appears that three totally different controllers (timer-based, NH_4 -bounds based and adaptive RHOC) can achieve a more or less equal performance, if tuned optimally. Adaptive RHOC turns out to be superior in terms of sensitivity to suboptimal tuning. The timer-based approach is attractive for its simplicity, but very sensitive to suboptimal tuning.

Chapter 8 describes a simulation study with the scope to optimise the plant design and operation strategy of alternating activated sludge processes for N-removal with two hydraulically connected reactors. The methodology is to simulate the application of RHOC to a range of different plant designs within this class of systems. The RHOC algorithm is obtained by reformulating the controller of chapter 4 for a 2-reactors system. It appears that in the optimal process design the two reactors are placed in series, while the first reactor is about four times as large as the second one. A conceptually simple feedback controller straightforwardly implements the improved operation strategy.

1.7.2 PART II, identification on the basis of DO-measurements and respirometry

Chapter 9 presents a grey-box modelling approach for the identification of the nonlinear DO dynamics. Herein, singular value decomposition of the locally available Jacobian matrix, or equivalently eigenvalue decomposition of the parameter covariance matrix, as well as parameter transformation are essential techniques. The use of respiration rate measurements greatly simplifies the modelling procedure. The approach is amongst others capable of identifying the non-linear function $k_{LA}(q_{air})$, i.e. the relationship between the oxygen transfer rate k_{LA} and the aeration input signal q_{air} .

Chapters 10 and 11 both deal with excitation of the respiration chamber dynamics in a continuous flow respirometer with the objective to extract additional information from its dissolved oxygen (DO) sensor readings. In chapter 10 an effort is made to improve the accuracy of the BOD_{st} -estimation technique developed by Spanjers *et al.* (1994). Contrary to expectation, the estimates still suffer from unacceptable inaccuracy due to large parameter correlation. However, a slight modification in the measurement strategy is proposed which is expected to enable more accurate estimation.

The results of experiments with this modified measurement strategy are reported in chapter 11. The estimation results convincingly discourage further efforts to identify sludge kinetics and BOD_{st} from this type of experiments, in which the respiration chamber dynamics are excited by alternating the continuous inflow between loaded and endogenous sludge.

The two other objectives of chapter 11 are the identification of the DO-sensor dynamics and the dilution rate in a continuous flow respirometer by excitation of the respiration chamber dynamics. Two separate simple procedures are presented. Both procedures consist of on-purpose in-sensor experiments succeeded by an ordinary least squares estimation step. The feasibility of both objectives is experimentally verified. Large experimental data sets are presented, which strongly advocate the on-line in-

corporation of both procedures in the everyday operation of the respirometer as tools for autocalibration and monitoring of the device's well-functioning.

In chapter 12 those conclusions drawn in the individual chapters which are of direct relevance to practitioners are summarized. Moreover some remaining ideas, which I believe are novel and likely to be successful, are shortly expounded in chapter 12 as well. The ideas concern: 1) Meeting N-total effluent standards by permitting elevated effluent NH_4 ; 2) Control explicitly aiming at meeting *yearly averaged* effluent standards; 3) The use of pH-measurements for continuous on-line tuning of timers in a timer-based operation strategy for alternating N-removal in a continuously mixed ASP reactor.

1.8 References

- Afonso P., Oliveira N.M.C. and Castro J.A.A.M. (1996). Model predictive control of a pilot plant reactor with a simulated exothermic reaction. *Computers and Chemical Engineering*, **20**, pp. 769-774.
- Al-Ghusain I.A., Huang J., Hao O.J. and Lim, B.S. (1994) Using pH as a real-time control parameter for waste water treatment and sludge digestion processes. *Wat. Sci. Tech.*, **30**(4), pp. 159-168.
- Andrews J.F. (1974). Dynamic models and control strategies for wastewater treatment processes. *Water Research*, **8**, pp. 261-289.
- Andrews J.F. (1977). Specific oxygen utilization rate for control of the activated sludge process. *Prog. Wat. Tech.*, **8**(6), pp. 451-460.
- Andrews J.F., Sørensen P.E. and Garrett M.T. (1980). Control of nitrification in the oxygen activated sludge process. *Prog. Wat. Tech.*, **12**(5), pp. 497-519.
- Andrews J.F., Stenstrom M.K. and Buhr H.O. (1976). Control systems for the reduction of effluent variability from the activated sludge process. *Prog. Wat. Tech.*, **8**(1), pp. 41-68.
- Aspegren H., Nyberg U. and Andersson B. (1996). Introduction of a RTC system for stormwater management in the practical operation of the Klagshamn wastewater system. *Med. Fac. Landbouww. Univ. Gent*, **61**(4a), Proc. 10th FAB, Gent, Belgium, pp. 1693-1700.
- Becerra V.M., Roberts P.D. and Griffiths G.W. (1998). Novel developments in process optimisation using predictive control. *Journal of Process Control*, **8**(2), pp. 117-138.
- Bocken S.M., Braae M. and Dold P.L. (1989). Dissolved oxygen control and oxygen utilisation rate estimation: extension of the Holmberg/Olsson method. *Wat. Sci. Tech.*, **21**, pp. 1197-1208.
- Brouwer H., Bloemen M., Klapwijk A. and Spanjers H. (1998). Feedforward control by manipulating the aerobic nitrification volume in ASP's. *Preprints of 19th Biennial IAWQ World Congress*, **2**, pp. 380-387 (to appear in *Wat. Sci. Tech.*).
- Brouwer H., Klapwijk A. and Keesman K.J. (1998). Identification of activated sludge and wastewater characteristics using respirometric batch-experiments. *Water Research*, **32**(4), pp. 1240-1254.
- Busby J.B. and Andrews J.F. (1975). Dynamic modeling and control strategies for the activated sludge process. *J. of Wat. Pollution Control Fed.*, **47**(5), pp. 1055-1080.
- Camacho E.F. and Berenguel M. (1997). Robust adaptive model predictive control of a solar plant with bounded uncertainties. *Int.'l J. of Adaptive Control and Signal Processing*, **11**(4), pp. 311-325.

- Carlsson B. and Wigren T. (1993). On-line identification of the dissolved oxygen dynamics in an activated sludge process. *Proc. 12th IFAC World congress*, 7, pp. 421-426.
- Carlsson B., Lindberg C.F., Hasselblad S. and Xu S. (1994). On-line estimation of the respiration rate and the oxygen transfer rate at Kunsängen wastewater plant in Uppsala. *Wat. Sci. Tech.*, 30(4), pp. 255-263.
- Carstensen J., Harreroës P. and Madsen H. (1995). Statistical identification of Monod-kinetic parameters from on-line measurements. *Wat. Sci. Tech.*, 31(2), pp. 125-133.
- Carucci A., Rolle E. and Smurra P. (1997). Experiences of on-line control at a wastewater treatment plant for nitrogen removal. *Preprints of 7th int.'l workshop on instrumentation, automation and control of water and wastewater treatment and transport systems*. IAWQ, Brighton, pp. 459-465 (to appear in *Wat. Sci. Tech.*).
- Chalabi Z.S., Bailey B.J. and Wilkinson D.J. (1996). A real-time optimal control algorithm for greenhouse heating. *Comput. Electron. Agric.*, 15(1), pp. 1-13.
- Chandra S., Mines R.O. and Sherrard J.H. (1987). Evaluation of oxygen uptake rate as an activated sludge process control parameter. *J. of Water Pollution Control Fed.*, 59(12), pp. 1009-1016.
- Charpentier J., Godart H., Martin G. and Mogno Y. (1989). Oxidation-Reduction Potential (ORP) regulation as a way to optimize aeration and C, N and P-removal: Experimental basis and various full-scale examples. *Wat. Sci. Tech.*, 21, pp. 1209-1223.
- Chen C.C. and Shaw L. (1982). On receding horizon feedback control. *Automatica*, 18(3), pp. 349-352.
- Corder G.D. and Lee P.L. (1986). Feedforward control of a wastewater plant. *Water Research*, 20(3), pp. 301-309.
- Côté M., Grandjean B.P.A., Lessard P. and Thibault J. (1995). Dynamic modelling of the activated sludge process: improved prediction using neural networks. *Water Research*, 29(4), pp. 995-1004.
- Dalen R. van (1993). Nitrate measurement and control at WWTP Hattem. *Proc. of NVA-congress on 'Far reaching nutrient removal, measuring and controlling in a different way?'*, Amsterdam (in Dutch).
- Dold P.L., Buhr H.O. and Marais G.v.R. (1984). An equalization control strategy for activated sludge process control. *Wat. Sci. Tech.*, 17, pp. 221-234.
- Dupont R. and Sinkjær O. (1993). Optimisation of wastewater treatment plants by means of computer models. *Wat. Sci. Tech.*, 30(4), pp. 181-190.
- Evans B. and Laughton P. (1994). Emerging trends in electrical energy usage at Canadian (Ontario) municipal wastewater treatment facilities and strategies for improving energy efficiency. *Wat. Sci. Tech.*, 30(4), pp. 17-23.
- Farkas J., Kralik M., Derco J. and Farkasova P. (1991). Dynamic modelling of activated sludge processes - IV. Multivariable statistical model. *Chem. papers*, 45(6), pp. 757-768.
- Flanagan M.J., Bracken B.D. and Roesler J.F. (1977). Automatic Dissolved Oxygen Control. *J. of the Environmental Engineering Division*, 103(EE4), pp. 707-721.
- Genceli, H. and Nikolaou M. (1993). Robust stability analysis of constrained l_1 -norm model predictive control. *AIChE Journal*, 39(12), pp. 1954-1965.
- Haarsma G.J. and Keesman K.J. (1995). Robust model predictive dissolved oxygen control. *Med. Fac. Landbouww. Univ. Gent*, 60(4b), Proc. 9th FAB, Gent, Belgium, pp. 2415-2426.
- Henze M., Grady jr. C.P.L., Gujer W., Marais G.v.R. and Matsuo T. (1987). Activated sludge model no. 1. *IAWQ Scientific and Technical Report no. 1*, IAWQ, London, U.K.

- Hiraoka M. and Tsumara K. (1989). System identification and control of the activated sludge process by use of a statistical model. *Wat. Sci. Tech.*, **21**, pp. 1161-1172.
- Holmberg A. (1982). A microprocessor-based estimation and control system for the activated sludge process. *Proc. of 1st IFAC workshop on modelling and control of biotechnological processes*, Pergamon, Oxford, U.K., pp. 111-119.
- Holmberg U., Olsson G. and Andersson B. (1989). Simultaneous DO control and respiration estimation. *Wat. Sci. Tech.*, **21**, pp. 1185-1195.
- Isaacs S. (1996). Short horizon control strategies for an alternating activated sludge process. *Wat. Sci. Tech.*, **34**(1-2), pp. 203-212.
- Isaacs S., Henze M. and Kümmel M. (1995). An adaptive algorithm for external carbon addition to an alternating activated sludge process for nutrient removal from waste water. *Chemical Engineering Science*, **50**(4), pp. 617-629.
- Jenkins D. and Garrison W.E. (1968). Control of activated sludge by mean cell residence time. *J. of Water Pollution Control Federation*, **40**(11), part 1.
- Jeppsson U. (1996). *Modelling aspects of wastewater treatment processes*. PhD-thesis.
- Julien S., Babary J.P. and Lessard P. (1997). Theoretical and practical identifiability of a reduced order model in an activated sludge process doing nitrification and denitrification. *Preprints of 7th int. l workshop on instrumentation, control and automation of water and wastewater treatment and transport systems*. IAWQ, Brighton, UK, pp. 393-400. (to appear in *Wat. Sci. Tech.*)
- Kabouris J.C. and Georgakakos A.P. (1990). Optimal control of the activated sludge process. *Water Research*, **24**(10), pp. 1197-1208.
- Kabouris J.C. and Georgakakos A.P. (1991). Stochastic control of the activated sludge process. *Wat. Sci. Tech.*, **24**(6), pp. 249-255.
- Kabouris J.C., Georgakakos A.P. and Camara A. (1992). Optimal control of the activated sludge process: Effect of sludge storage. *Water Research*, **26**(4), pp. 507-517.
- Kayser R. and Ermel G. (1985). Control of simultaneous nitrification-denitrification. *proc. of 4th IAWPRC workshop on Instrum. Control water wastewater treat. transp. syst.*, Pergamon, New York, pp. 481-488.
- Klapwijk A., Brouwer H., Vrolijk E. and Kujawa K. (1998). Control of intermittently aerated nitrogen removal plants by detection endpoints of nitrification and denitrification using respirometry only. *Water Research*, **32**(5), pp. 1700-1703.
- Leeuwen, J. van(1990). Review of oxidative control of bulking in activated sludge wastewater treatment to improve sedimentation. *South African journal of Chemical Engineering*, **2**(1), pp. 27-40.
- Lewis F.L. (1986). *Optimal Control*. John Wiley & Sons, New York.
- Lindberg C.F. (1997). *Control and estimation strategies applied to the activated sludge process*. PhD-thesis.
- Lindberg C.F. and Carlsson B. (1996a). Estimation of the respiration rate and oxygen transfer function utilizing a slow DO sensor. *Wat. Sci. Tech.*, **33**(1), pp. 325-333.
- Lindberg C.F. and Carlsson B. (1996b). Nonlinear and set-point control of the dissolved oxygen concentration in an activated sludge process. *Wat. Sci. Tech.*, **34**(3-4), pp. 135-142.
- Ljung L. (1987). *System Identification: Theory for the User*. Prentice Hall, New Jersey.
- Ljung L. and Söderström T. (1983). *Theory and Practice of recursive identification*. MIT Press, Cambridge, Mass.
- Londong J. (1992). Strategies for optimized nitrate reduction with primary denitrification. *Wat. Sci. Tech.*, **26**(5-6), pp. 1087-1096.

- Madrid A.P. de, Dormido S., Morilla F. and Grau L. (1996). Dynamic programming predictive control. *Proc. 13th IFAC World Congress*, San Francisco, G, pp. 279-284.
- Marsili-Libelli S. (1984). Activated sludge process control using dissolved oxygen measurements. *Wat. Sci. Tech.*, **16**, pp. 613-620.
- Marsili-Libelli S., Giardi R. and Lasagni M. (1985). Self-tuning control of the activated sludge process. *Environmental Technology Letters*, **6**, pp. 576-583.
- Mayne D.Q. and Michalska H. (1990). Receding horizon control of nonlinear systems. *IEEE Transactions on Automatic Control*, **35**(7), pp. 814-824.
- Ménardiére M. de la, Charpentier J., Vachon A. and Martin G. (1991). ORP as control parameter in a single sludge biological nitrogen and phosphorus removal activated sludge system. *Water SA*, **17**(2), 123-132.
- Metcalf and Eddy, Inc. (1979). *Wastewater engineering: treatment/disposal/reuse*. 2nd edition, McGrawhill, New York.
- Meyer H.G. and Hanke R. (1997). Reduction of nitrogen and phosphorus discharges from Bayer's Dormagen production site. *European J. of Water Pollution Control*, **7**(1), pp. 8-16.
- Michalska H. and Mayne D.Q. (1993). Robust receding horizon control of constrained nonlinear systems. *IEEE Transactions on Automatic Control*, **38**(11), pp. 1623-1633.
- Miller R.B. and Pachter M. (1997). Maneuvering flight control with actuator constraints. *Journal of Guidance Control and Dynamics*, **20**(4), pp. 729-734.
- Morper M.R. (1994). Upgrading of activated sludge systems for nitrogen removal by application of the LINPOR@-CN process. *Wat. Sci. Tech.*, **29**(12), pp. 167-176.
- Neiva R.M., Galdino jr. L.A., Catunda P.F.C. and Haandel A. van (1996). Reduction of operational costs by planned interruptions of aeration in activated sludge plants. *Wat. Sci. Tech.*, **33**(3), pp. 17-27.
- Nicolao G. de, Magni L. and Scattolini R. (1996). On the robustness of receding-horizon control with terminal constraints. *IEEE Transactions on Automatic Control*, **41**(3), pp. 451-453.
- Nowak O. and Svardal K. (1996). Denitrification via nitrite - long-term experience with pretreatment of rendering plant effluent. *Med. Fac. Landbouww. Univ. Gent*, **61**(4b), Proc. 10th FAB, Gent, Belgium, pp. 2009-2016.
- Ohtsuka T. and Fujii H. (1997). real-time optimization algorithm for nonlinear receding-horizon optimal control. *Automatica*, **33**(6), pp. 1147-1154.
- Olsson G. and Andrews J.F. (1978). The dissolved oxygen profile - a valuable tool for control of the activated sludge process. *Water Research*, **12**, pp. 985-1004.
- Olsson G., Andersson B., Hellström B.H., Holmström H., Reinius L.G. and Vopatek P. (1989). Measurements, data analysis and control methods in wastewater treatment plants - state of the art and future trends. *Wat. Sci. Tech.*, **21**(10-11), pp. 1197-1208.
- Olsson G., Rundqwist L., Eriksson L. and Hall L. (1985). Self tuning control of the dissolved oxygen concentration in activated sludge systems. *Proc. of 4th IAWPRC workshop on instrum. control water wastewater treat. transp. syst.*, Pergamon, New York, pp. 473-480
- Olsson, G. (1992). Control of wastewater treatment systems. *ISA Transactions*, **31**(1), pp. 87-96.
- Potter T.G., Tseng C.C. and Koopman B. (1998). Nitrogen removal in a partial nitrification complete denitrification process. *Water Environment Research*, **70**(3), pp. 334-342.
- Reid J.M.C., Nason R.B. and Fisher J.T. (1995). On-line monitoring of sewage for the detection of toxicity and measurement of short-term BOD. *J. CIWEM*, **9**(2), pp. 186-191.
- Rundqwist L. (1988). Experiences of self-tuning control of an activated sludge process, *Proc. of IFAC congress on adaptive control of chemical systems*, **6**, Copenhagen, Denmark, pp. 177-182.

- Sasaki K., Yamamoto Y., Tsumura K., Hatsumata S. and Tatewaki M. (1993). Simultaneous removal of nitrogen and phosphorus in intermittently aerated 2-tank activated sludge process using DO and ORP-bending-point control. *Wat. Sci. Tech.*, **28**(11-12), pp. 513-521.
- Sekine T., Iwahori K., Fujimoto E. and Inamori Y. (1985). Advanced control strategies for the activated sludge process., *Proc. of 4th IAWPRC workshop on instrum. control water wastewater treat. transp. syst.*, Pergamon, New York, pp. 269-276.
- Sekoulov I., Addicks R. and Oles J. (1990). Post-denitrification with controlled feeding of activated sludge as H donator. *Wat. Sci. Tech.*, **22**(7-8), pp. 161-170.
- Shinar J. and Glizer V.J. (1995). Application of receding horizon control strategy to pursuit-evasion problems. *Optimal Control Appl. Methods*, **16**(2), pp. 127-141.
- Sincic D. and Bailey J.E. (1978). Optimal periodic control of activated sludge processes - I. Results for the base case with Monod/decay kinetics. *Water Research*, **12**, pp. 47-53.
- Spanjers H. (1993). *Respirometry in activated sludge*. PhD-thesis.
- Spanjers H. and Olsson G. (1992). Modeling of the dissolved oxygen probe response in the improvement of the performance of a continuous respiration meter. *Water Research*, **26**, pp. 945-954.
- Spanjers H., Olsson G. and Klapwijk A. (1994). Determining short-term biochemical oxygen demand and respiration rate in an aeration tank by using respirometry and estimation. *Water Research*, **28**, pp. 1571-1583.
- Spanjers H. and Vanrolleghem P. (1994). Respirometry as a tool for rapid characterization of wastewater and activated sludge. *Wat. Sci. Tech.*, **31**(2), pp. 105-114.
- Spanjers H., Vanrolleghem P.A., Olsson G., Dold P.L. (1998). Respirometry in control of the activated sludge process: principles. *IAWQ Scientific and Technical Report no. 7*.
- Spies P.J. and Seyfried C.F. (1988). Ammonia controlled activated sludge process for nitrification-denitrification. *Wat. Sci. Tech.*, **20**(4-5), pp. 29-36.
- Stehfest H. (1985). Optimal periodic control of a steep-feed activated sludge plant. *Environmental Technology Letters*, **6**, pp. 556-565.
- Suescun J., Irizar I., Ostolaza X. and Ayesa E. (1998). Dissolved oxygen control and simultaneous estimation of oxygen uptake rate in activated-sludge plants. *Wat. Env. Res.*, **70**(3), pp. 316-322.
- Surmacz-Gorska J., Gernaey K., Demuynck C., Vanrolleghem P. and Verstraete W. (1995). Nitrification process control in activated sludge using oxygen uptake rate measurements. *Environmental Technology*, **16**, 569-577.
- Takács I., Patry G.G. and Nolasco D. (1991). A dynamic model of the clarification-thickening process. *Water Research*, **25**(10), pp. 1263-1271.
- Tam N.F.Y., Wong Y.S. and Leung G. (1992). Effect of exogenous carbon sources on removal of inorganic nutrient by the nitrification-denitrification process. *Water Research*, **26**(9), pp. 1229-1236.
- Tanuma R., Sasaki K. and Matsunaga I. (1985). Gain maximising dissolved oxygen control in the activated sludge process. *Proc. of 4th IAWPRC workshop on instrum. control water wastewater treat. transp. syst.*, Pergamon, New York, pp. 261-268.
- Tap R.F., Willigenburg L.G. van, Straten G. van (1996). Experimental results of receding horizon optimal control of greenhouse climate. *Acta Horticulturae*, **406**, pp. 229-238.
- Tenno R. and Uronen P. (1996). State estimation for a large-scale wastewater treatment system. *Automatica*, **32**(3), pp. 305-317.
- Thomsen H.A., Nielsen M.K., Nielsen E.H. and Hansen N.P. (1998). Load dependent control of BNR-WWTP by dynamic changes of aeration volumes. *Wat.Sci. Tech.*, **37**(12), pp. 157-164.

- Thornberg D.E. and Thomsen H.A. (1994). Interaction between computer simulations and control using on-line nitrogen measurements. *Wat. Sci. Tech.*, **30**(4), pp. 199-206.
- Thornberg D.E., Nielsen M.K. and Andersen K.L. (1993). Nutrient removal: on-line measurements and control strategies. *Wat. Sci. Tech.*, **28**(11-12), pp. 549-560.
- Tseng C.C., Potter T.G. and Koopman B. (1998). Effect of influent chemical oxygen demand to nitrogen ratio on a partial nitrification complete denitrification process. *Water Research*, **32**(1), pp. 165-173.
- Vaccari D.A. and Christodoulatos C. (1989). A comparison of several control algorithms for activated sludge waste rate. *Wat. Sci. Tech.*, **21**, pp. 1249-1260.
- Vanrolleghem P. (1994). *On-line modelling of activated sludge processes: development of an adaptive sensor*. PhD-thesis.
- Vanrolleghem P. and Coen F. (1995). Optimal design of in-sensor-experiments for on-line modelling of nitrogen removal processes. *Wat. Sci. Tech.*, **31**(2), pp. 149-160.
- Vanrolleghem P. and Verstraete W. (1993). Simultaneous biokinetic characterization of heterotrophic and nitrifying populations of activated sludge with an on-line respirographic biosensor. *Wat. Sci. Tech.*, **28**(11-12), pp. 377-387.
- Vargas-Lopez C.E., Stentiford E.I. and Mara D.D. (1989). Discussion of 'Evaluation of oxygen uptake rate as an activated sludge process control parameter' by Chandra *et al.* *J. of Water Pollution Control Fed.*, **61**(1), pp. 99-102.
- Wentzel M.C., Mbewe A. and Ekama G.A. (1995). Batch test for measurement of readily biodegradable COD and active organism concentrations in municipal waste waters. *Water SA*, **21**(2), pp. 117-124.
- Wett B., Rostek R., Rauch W. and Ingerle K. (1998). pH-controlled reject-water-treatment. *Wat. Sci. Tech.*, **37**(12), pp. 165-172.
- Wouters-Wasiak K., Héduit A., Audic J.M. and Lefèvre F. (1994). Real-time control of nitrogen removal at full-scale using oxidation reduction potential. *Wat. Sci. Tech.*, **30**(4), pp. 207-210.
- Yang T.H. and Polak E. (1993). Moving horizon control of nonlinear systems with input saturations, disturbances and plant uncertainty. *Int. J. of Control*, **58**(4), pp. 875-903.
- Yeung S.Y.S., Sincic D. and Bailey J.E. (1980). Optimal periodic control of activated sludge processes: II. comparison with conventional control for structured sludge kinetics. *Water Research*, **14**, pp. 77-83.
- Young, P. (1984). *Recursive estimation and time-series analysis, an introduction*. Springer-Verlag, Berlin.
- Zhao H., Isaacs S.H., Sørensen H., Kümmel M. (1994). Nonlinear optimal control of an alternating activated sludge process. *Journal of Process Control*, **4**(1), pp. 33-43.
- Zhao H., Isaacs S.H., Sørensen H. and Kümmel M. (1995). An analysis of nitrogen removal and control strategies in an alternating activate sludge process. *Water Research*, **29**(2), pp. 535-544.

PART I, N-removal in alternating activated sludge processes

2 Identification for model predictive control of biotechnological processes, case study: nitrogen removal in an activated sludge process[†]

2.1 Abstract

Identification for control focuses on the 1-step ahead prediction errors. Model predictive controllers (MPC) with prediction horizon H compute the current controls using the 1, 2, ..., H -step ahead model predictions. Therefore in identification for MPC the (weighted) sum of squared 1, 2, ..., H -step ahead prediction errors is a natural identification criterion. To illustrate this idea the ammonium/nitrate dynamics in a pilot scale activated sludge process are identified for different H -values, using real measurements. H appears to affect the parameter estimates significantly, supporting the idea that use of this new identification criterion will improve MPC performance.

Keywords: identification criterion, prediction error, k-step ahead prediction, parameter uncertainty, predictive control, eigenvalue decomposition, non-linear, biotechnology, wastewater, nitrogen removal

2.2 Introduction

Usually, identification for control focuses on minimising the sum of squared 1-step ahead prediction errors. In case of model predictive control (MPC) with prediction horizon H the (weighted) sum of squared 1, 2, ..., H -step ahead prediction errors is a more reasonable identification criterion. In this paper the effect of H on the identified model will be investigated.

In the vast majority of MPC applications linear models and quadratic cost criteria are used, allowing for computationally efficient analytical solutions, thus enabling the control of fast processes (Soeterboek, 1990; Bitmead et al., 1990). In case of biotechnological processes, with time constants ranging from minutes to days, the motive of limited computation time is less relevant. Therefore, in these applications, important process non-linearities can be included in the model, such that the MPC will explicitly account for them.

Controlling the concentrations of ammonium (NH_4) and nitrate (NO_3) is a hot item in current days waste water treatment due to tightening government legislation on nitrogen removal aiming at protection of aquatic ecosystems. As an application this paper presents the identification of the non-linear NH_4 and NO_3 dynamics in an activated sludge pilot plant from DO setpoint (DO_R) and measured NH_4 and NO_3 concentrations, using the sequence of 1, 2, ..., H -step ahead prediction errors as

[†] Published by Lukasse L.J.S., Keesman K.J. and Straten G. van (1997) in *Proc. 11th IFAC symp. on Syst. Ident.*, 3, Fukuoka, Japan, pp. 1525-1530 (without appendix).

optimisation criterion. In further research the resulting non-linear model will be used in a model predictive controller (MPC).

2.3 Modelling approach

2.3.1 Prior knowledge and presumptions

The prior knowledge of continuously stirred, continuously fed biotechnological processes will generally be available in the form of a mass balance for the states ($\mathbf{x} \in \mathbb{R}^n$) of the process,

$$\frac{d\mathbf{x}}{dt} = \mathbf{K}(\boldsymbol{\theta})\boldsymbol{\varphi}(\mathbf{x}, \mathbf{u}, \boldsymbol{\theta}) - \frac{q}{V} \cdot \mathbf{x} + \frac{q}{V} \cdot \mathbf{x}^{\text{in}} \quad (1)$$

where $\mathbf{K}(\boldsymbol{\theta}) \in \mathbb{R}^{n \times r}$ is a matrix of yield coefficients, $\boldsymbol{\varphi}(\mathbf{x}, \mathbf{u}, \boldsymbol{\theta}) \in \mathbb{R}^r$ is a vector of reaction rates, $\mathbf{x}^{\text{in}} \in \mathbb{R}^n$ is the concentration of \mathbf{x} in the inflow, $\boldsymbol{\theta} \in \mathbb{R}^p$ is the vector of model parameters, V is the reactor volume and the flow rate q often is an element of the vector of control inputs ($\mathbf{u} \in \mathbb{R}^s$). The general sampled-data measurement equation relates the states to the measured outputs $\mathbf{y}(k) \in \mathbb{R}^m$:

$$\mathbf{y}(k) = \mathbf{g}(\mathbf{x}(kT), \mathbf{u}(kT), kT; \boldsymbol{\theta}) + \mathbf{e}(k) \quad (2)$$

in which $\mathbf{e}(\cdot) \in \mathbb{R}^m$ is the so-called "output-error" containing errors from both the modelling and measurement process.

2.3.2 Model identification

Using the available *a priori* knowledge an open-loop identification experiment is designed and carried out. Subsequently the parameter vector $\boldsymbol{\theta}$, belonging to the prior set \mathcal{D} , is estimated from the $N+1$ measurement points in the identification data set, using the (weighted) sum of squared 1, 2, ..., H -step ahead prediction errors as identification criterion:

$$\hat{\boldsymbol{\theta}} = \arg \min_{\boldsymbol{\theta} \in \mathcal{D}} J(\boldsymbol{\theta}) = \arg \min_{\boldsymbol{\theta} \in \mathcal{D}} \sum_{i=1}^H \sum_{k=i}^{N-H+i} \boldsymbol{\varepsilon}(k | k-i, \boldsymbol{\theta})^T \mathbf{W}_i \boldsymbol{\varepsilon}(k | k-i, \boldsymbol{\theta}) \quad (3)$$

where the prediction error $\boldsymbol{\varepsilon}(k | k-i, \cdot)$ is defined as

$$\boldsymbol{\varepsilon}(k | k-i, \boldsymbol{\theta}) = \mathbf{y}(k) - \hat{\mathbf{y}}(k | k-i, \boldsymbol{\theta}) \quad (4)$$

The positive definite weighting matrices $\mathbf{W}_i \in \mathbb{R}^{m \times m}$ enable mutual weighting of the model outputs, depending on i .

Optimising $\hat{\boldsymbol{\theta}}$ over N successive data points with prediction horizon H requires model integration over I sampling intervals for each evaluation of the identification criterion, with I given by

$$I = -H^2 + HN + H \quad 1 \leq H \leq N \quad (5)$$

It is easily shown that I has its maximum $\frac{N^2}{4} + 1$ for $H = N/2$ and its minimum $I = N$ for H either 1 or N . Note that $H = 1$ amounts to minimising the one-step ahead prediction error, and $H = N$ amounts to running the model from time 0 over the entire length of the data set without updates from measurements (output error minimisation). Integrating once over N time steps is computationally more efficient than integrating N times over one time step, therefore initially an acceptable model with prediction horizon $H = N$ will be determined.

Acceptance of a model is based on the trade-off between goodness of fit, parameter uncertainty and model complexity. If necessary, the model structure is modified within the admissible class of model structures M . As a measure for goodness of fit the (weighted) mean squared error (M) is used:

$$M = \frac{1}{-H^2 + HN + H} \cdot \sum_{i=1}^H \sum_{k=i}^{N-H+i} \boldsymbol{\varepsilon}(k | k-i, \boldsymbol{\theta})^T \mathbf{W}_i \boldsymbol{\varepsilon}(k | k-i, \boldsymbol{\theta}) \quad (6)$$

Once a model is accepted, a suitable prediction horizon H^* for MPC is selected based on the accepted model and knowledge about process disturbances to be controlled by the MPC. Subsequently, the parameters of the accepted model are estimated again using the new prediction horizon H^* in eqn. 3. Finally, the model with this new parameter vector will be used in MPC.

2.3.3 Parameter uncertainty

Uncertainties in parameters estimated from the weighted sum of squared 1, 2, ..., H -step ahead prediction errors of non-linear models with m -dimensional output vectors can be locally approximated around $\hat{\boldsymbol{\theta}}$ by the covariance matrix of the estimates, defined by (see appendix)

$$\boldsymbol{\Sigma}_{\hat{\boldsymbol{\theta}}} = \left(\sum_{i=1}^H \sum_{k=i}^{N-H+i} \mathbf{X}_k^i T \mathbf{W}_i \mathbf{X}_k^i \right)^{-1} \cdot \left(\sum_{i=1}^H \sum_{j=1}^H \sum_{k=\max(i,j)}^{N-H+\min(i,j)} \mathbf{X}_k^i T \mathbf{W}_i \boldsymbol{\Sigma}_{\boldsymbol{\varepsilon}} \mathbf{W}_j \mathbf{X}_k^j \right) \cdot \left(\sum_{i=1}^H \sum_{k=i}^{N-H+i} \mathbf{X}_k^i T \mathbf{W}_i \mathbf{X}_k^i \right)^{-1} \quad (7)$$

where $\mathbf{X}_k^i \in \mathbb{R}^{m \times p}$ is the locally available Jacobian matrix

$$\mathbf{X}_k^i = \frac{\partial \hat{\mathbf{y}}(k | k-i; \boldsymbol{\theta})}{\partial \boldsymbol{\theta}} \quad (8)$$

Notice that in eqn. 7 $\boldsymbol{\Sigma}_{\boldsymbol{\varepsilon}} \in \mathbb{R}^{m \times m}$ is a diagonal matrix with diagonal elements

$$\boldsymbol{\Sigma}_{\boldsymbol{\varepsilon}}(j, j) = \frac{1}{-H^2 + HN + H - p} \cdot \sum_{i=1}^H \sum_{k=i}^{N-H+i} \boldsymbol{\varepsilon}_j(k | k-i, \boldsymbol{\theta})^2 \quad (9)$$

which are used as approximations of the true variance $\sigma_{\boldsymbol{\varepsilon}_j}^2$, assuming that N is large enough and that the residuals $\boldsymbol{\varepsilon}(k; \cdot)$ are independent. The correctness of this last assumption can be checked by a correlation analysis. In practice $\boldsymbol{\varepsilon}(k; \cdot)$ will never be fully independent, and so $\boldsymbol{\Sigma}_{\boldsymbol{\varepsilon}}(j, j)$ will always deviate from $\sigma_{\boldsymbol{\varepsilon}_j}^2$. However, it is still valid to use $\boldsymbol{\Sigma}_{\hat{\boldsymbol{\theta}}}$ as a tool for mutual comparison of parameter accuracies, although $\boldsymbol{\Sigma}_{\hat{\boldsymbol{\theta}}}$ is no longer the true parameter covariance.

Before mutually comparing the elements of $\boldsymbol{\Sigma}_{\hat{\boldsymbol{\theta}}} \in \mathbb{R}^{p \times p}$ they are made relative, *i.e.* $\boldsymbol{\Sigma}_{\hat{\boldsymbol{\theta}}}$ is scaled such that it represents the uncertainty for $\hat{\boldsymbol{\theta}}$ with all elements equal to 1. This is achieved by using the fact that

$$\boldsymbol{\Sigma}_{\mathbf{K}\hat{\boldsymbol{\theta}}} = \mathbf{K} \boldsymbol{\Sigma}_{\hat{\boldsymbol{\theta}}} \mathbf{K}^T \quad (10)$$

for any $\mathbf{K} \in \mathbb{R}^{k \times p}$, with $k \in \mathbb{N}$. By defining \mathbf{K} as a diagonal matrix with diagonal elements $\mathbf{K}_{i,i} = 1/\hat{\boldsymbol{\theta}}_i$, the covariance matrix $\boldsymbol{\Sigma}_{\mathbf{K}\hat{\boldsymbol{\theta}}} \in \mathbb{R}^{p \times p}$ is obtained for all elements of $\hat{\boldsymbol{\theta}}$ scaled to one. Dominant parameter directions can easily be found by eigenvalue decomposition of $\boldsymbol{\Sigma}_{\mathbf{K}\hat{\boldsymbol{\theta}}}$ (Bard, 1974), that is

$$\mathbf{E}^T \boldsymbol{\Sigma}_{\mathbf{K}\hat{\boldsymbol{\theta}}} \mathbf{E} = \boldsymbol{\Lambda} \quad (11)$$

where \mathbf{E} is an orthogonal matrix of eigenvectors and Λ is a diagonal matrix of eigenvalues. A relatively large value of the j -th eigenvalue $\Lambda_{j,j}$ indicates a relatively large uncertainty in the direction spanned by the j -th column of \mathbf{E} . If element $\mathbf{E}_{i,j}$ is relatively large as compared to the other elements in the j -th column of \mathbf{E} , parameter $\hat{\theta}_i$ is the most uncertain and so the first candidate for parameter reduction (Lukasse, 1996; Schneider & Munack, 1995). In the same way a combination of relatively small $\Lambda_{j,j}$ and relatively large $\mathbf{E}_{i,j}$ indicates that $\hat{\theta}_i$ is the most certain parameter.

2.4 Identification of ammonium/nitrate dynamics

2.4.1 Prior knowledge

The IAWQ model no. 1 (Henze *et al.*, 1987) is a generally accepted model for activated sludge processes. With some simplifications of this general model the following state space model can be formulated for NH_4/NO_3 :

$$\frac{d}{dt} \begin{bmatrix} NH_4 \\ NO_3 \end{bmatrix} = \begin{bmatrix} 1 & -1 & 0 \\ 0 & 1 & -1 \end{bmatrix} \begin{bmatrix} P_{NH} \\ C_{NH} \\ C_{NO} \end{bmatrix} - \begin{bmatrix} (q^{in} + q^r) NH_4 \\ (q^{in} + q^r) NO_3 \end{bmatrix} + \begin{bmatrix} \frac{q^{in}}{V} NH_4^{in} \\ \frac{q^r}{V} NO_3^r \end{bmatrix} \quad (12)$$

$$\mathbf{y}(k) = \begin{bmatrix} NH_4(kT) \\ NO_3(kT) \end{bmatrix} + \begin{bmatrix} e_1(k) \\ e_2(k) \end{bmatrix} \quad (13)$$

$$P_{NH} = f(\text{hydrolysis, ammonification})$$

$$C_{NH} = \frac{DO_R}{DO_R + k_{DO,a}} \cdot \frac{NH_4}{NH_4 + k_{NH}} \cdot \mu_{max,a} \cdot X_{B,a} / 4.33 \quad (14)$$

$$C_{NO} = \frac{k_{DO,h}}{DO_R + k_{DO,h}} \cdot \frac{NO_3}{NO_3 + k_{NO}} \cdot \frac{S_S}{k_S + S_S} \cdot \mu_{max,h} \cdot \eta \cdot X_{B,h} / 2.86 \quad (15)$$

with as control inputs q^{in} and DO_R . V and q^r are known constants, and NH_4^{in} , NO_3^r and S_S are unmeasured disturbances. From earlier measurements NH_4^{in} is known to exhibit an irregular diurnal cycle with an average of roughly 75 mg/l, extremes of 40 and 100 mg/l, and hardly any high frequency components. All remaining variables (Table 1) can be regarded as time-varying parameters, where an important part of the time variance is caused by seasonal effects.

2.4.2 Experiments

The open loop identification experiment with Dissolved Oxygen setpoint DO_R and influent flow q^{in} as inputs was carried out on an activated sludge pilot plant with a 475 l reactor fed with presettled domestic waste water. DO is maintained at DO_R by a well-

Table 1, nominal values of model parameters.

variable	value
η	0.8
$X_{B,a}$ (mg COD/l)	90
$X_{B,h}$ (mg COD/l)	1450
$\mu_{max,a}$ (day ⁻¹)	0.50
$\mu_{max,h}$ (day ⁻¹)	8.0
$k_{DO,a}$ (mg/l)	1.3
$k_{DO,h}$ (mg/l)	0.1
k_{NH} (mg/l)	1.0
k_{NO} (mg/l)	0.15

performing slave MPC (Haarsma & Keesman, 1995). A series of steps of changing magnitudes is put on DO_R and q^{in} in order to excite the non-linear NH_4/NO_3 dynamics (eqn. 12 and Figs. 1, 2). The choices of magnitudes and duration of the steps are based on *a priori* knowledge.

It is known from the literature that simultaneous consumption of NH_4 and NO_3 at limiting DO levels only occurs under very specific circumstances (Münch et al., 1996). All practical continuously mixed plants apply alternately nitrification at non-limiting DO levels and denitrification at DO equal to zero (e.g. Zhao et al., 1995). Therefore in this stage no effort is made to identify the notoriously difficult DO-limiting range and DO_R is only switched between zero and high DO levels (DO 1.5-2 mg/l), *i.e.* the experimental design focuses on identification for a control strategy with alternating aeration.

NH_4 and NO_3 are measured with a sampling interval of 1 min. During the experiment the ammonium and nitrate-analysers performed some auto-calibrations, which caused gaps in the data set (Figs. 1, 2). This complicates the identification, but is very realistic indeed as many advanced measurement devices exhibit this behaviour.

2.4.3 Output error model identification

In the prior model (eqns. 12 - 15) the non-linear production and consumption terms contain the main uncertainties. Both the terms P_{NH} and C_{NH} (eqn. 12) are known to be positively correlated with DO_R , while the relatively small term P_{NH} is not measurable. Therefore P_{NH} will be set to zero, which is expected to result in an underestimation of C_{NH} . To account for this effect an additional parameter (θ_4) is introduced in the matrix of yield coefficients, allowing for a systematic deviation between NH_4 consumption and NO_3 production. As also S_S is not measurable, but known to be positively correlated with q^{in} , the term $\frac{S_S}{k_S + S_S}$ in eqn. 15 is replaced by q^{in} . Parameter products in C_{NH} and C_{NO} are

lumped together (θ_1 and θ_3), since they are known to be structurally non-identifiable. θ_2 accounts for deviations between the true NH_4^{in} and the model constant NH_4^{in} .

The Monod kinetic function for DO_R in eqn. 14 is replaced by a Blackman (1/0) kinetic model, which linearizes the dynamic model for $DO_R \leq DO_{max}$, the range of future application. From the measurements it is clear that k_{NH} in the term $\frac{NH_4}{NH_4 + k_{NH}}$ (eqn. 14) is very small, as its expected slowing

effect on $\frac{dNH_4}{dt}$ during decreasing NH_4 cannot be seen in the data (Figs. 1, 2 around $t = 9$ h and $t = 18$ h), the same holds for k_{NO} . The experimental design is such that $k_{DO,h}$ cannot be identified from these data. So the data contain insufficient information for estimation of k_{NH} , k_{NO} and $k_{DO,h}$ and therefore they are fixed at reasonably small values.

In the second state equation (eqn. 12) there are the terms $q^r NO_3^r / V$ and $-q^r NO_3^r / V$ originating from the presence of the sludge recycle flow q^r . NO_3^r varies in an unknown way, but on average it is more or less equal to NO_3 . The combined effect of the two terms is relatively small when compared to C_{NH} and C_{NO} , so only a small error is introduced by omitting both terms.

From prior knowledge DO_{max} is known to have a value around 2.0 mg/l. The identification experiment was not designed to identify DO_{max} exactly, but to get an indication. The fit on the cross validation data, discussed below, improves by reducing DO_{max} from 2.0 to 1.5 mg/l, while the fit on the identification data is invariant under this change, so DO_{max} is fixed at a value of 1.5 mg/l.

A time delay (Δ) is observed between inputs and outputs (Fig. 1 at $t = 5$ h and Fig. 2 at $t = 15$ h). It is known to be caused mainly by the measurement devices and so Δ is introduced in the output equation. It has been found that the two analysers produce more or less equal time delays, hence only one time delay is introduced in the measurement equations.

Concluding, with the modifications outlined above the final model for identification is

$$\frac{d}{dt} \begin{bmatrix} NH_4 \\ NO_3 \end{bmatrix} = \begin{bmatrix} -1 & 0 \\ \theta_4 & -1 \end{bmatrix} \begin{bmatrix} C_{NH} \\ C_{NO} \end{bmatrix} - \begin{bmatrix} \frac{(q^{in} + q^r)}{V} NH_4 \\ \frac{q^{in}}{V} NO_3 \end{bmatrix} + \begin{bmatrix} \theta_2 \frac{q^{in}}{V} NH_4^{in} \\ 0 \end{bmatrix} \quad (16)$$

$$C_{NH} = \theta_1 \cdot \frac{NH_4}{NH_4 + k_{NH}} \cdot \begin{cases} 1 & DO_R(t) > DO_{max} \\ DO_R(t)/DO_{max} & DO_R(t) \leq DO_{max} \end{cases} \quad (17)$$

$$C_{NO} = \theta_3 \cdot \frac{k_{DO,h}}{DO_R + k_{DO,h}} \cdot \frac{NO_3}{NO_3 + k_{NO}} \cdot q_{in} \quad (18)$$

$$\begin{bmatrix} y_1(k) \\ y_2(k) \end{bmatrix} = \begin{bmatrix} NH_4(kT - \Delta) \\ NO_3(kT - \Delta) \end{bmatrix} + \begin{bmatrix} e_1(k) \\ e_2(k) \end{bmatrix} \quad (19)$$

with the constants given in Table 2.

The output error estimation results are given by:

$$M = 0.6751 \text{ (mg/l)}^2$$

$$\hat{\theta} = [0.0778 \quad 0.6656 \quad 0.0757 \quad 1.4040]^T$$

$$\Sigma_{\hat{\theta}} = 1.0e-004 \cdot$$

$$\begin{bmatrix} 0.0022 & 0.0039 & 0.0000 & -0.0253 \\ 0.0039 & 0.0156 & 0 & -0.0530 \\ 0.0000 & 0 & 0.0033 & 0.0001 \\ -0.0253 & -0.0530 & 0.0001 & 0.5706 \end{bmatrix}$$

$$E =$$

$$\begin{bmatrix} 0.6310 & -0.7555 & -0.1746 & -0.0237 \\ 0.0676 & -0.1706 & 0.9830 & -0.0053 \\ -0.0014 & 0.0303 & -0.0001 & -0.9995 \\ 0.7729 & 0.6318 & 0.0566 & 0.0181 \end{bmatrix}$$

$$\text{diag}(\Lambda) = 1.0e-004 \cdot [0.0957 \quad 0.5814 \quad 0.0184 \quad 0.5702]$$

The diagonal elements of Λ and M found for this model structure are both small. So a good model fit (Fig. 1) is combined with accurate parameter estimates. The third element of $\text{diag}(\Lambda)$ is the

Table 2, model constants.

variable	value
NH_4^{in} (mg/l)	75
V (l)	475
q^r (l/min)	0.7
Δ (min)	25
k_{NH} (mg/l)	0.0685
k_{NO} (mg/l)	0.08
$k_{DO,h}$ (mg/l)	0.09
DO_{max} (mg/l)	1.5

smallest, consequently the third column of E contains the dominant direction in the parameter space. Clearly this direction is highly dominated by θ_2 , hence θ_2 dominates the model behaviour.

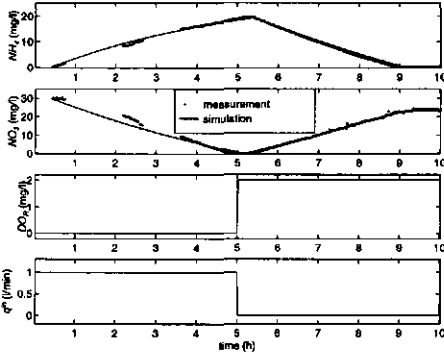


Fig. 1, model fit to identification data set.

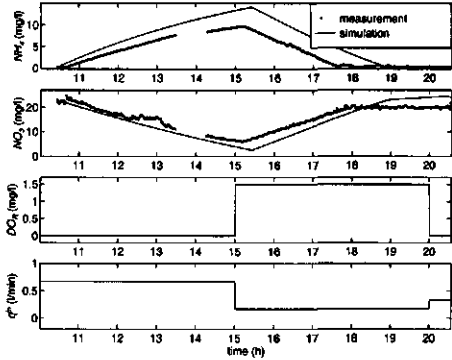


Fig. 2, model fit to cross validation data set.

In a cross validation test the fit is distinctly worse (compare Figs. 1 and 2). It is likely that this is caused by a decrease in disturbance input NH_4^{in} , resulting in the faster increase of simulated NH_4 than measured NH_4 in the first five hours of the cross validation data set. From this observation it is clear that the fit to the cross validation data can be largely improved by reducing θ_2 (eqn. 16). Obviously, it would be preferable to measure the actual input NH_4^{in} which would eliminate the highly sensitive θ_2 entirely, unfortunately this was technically infeasible during the experiments. This, together with the reasonable model structure from a mechanistic point of view, makes the model acceptable.

2.4.4 Effect of prediction horizon on model parameters

In order to investigate the effect of H on the parameter estimates for the model structure given in eqns. 16-19, $\hat{\theta}$ has been estimated for H ranging from 1 to 600 min with all weighting matrices W_i equal to I (Figs. 3, 4). In Fig. 3 $\hat{\theta}$ is only plotted for H up to 250, as larger H does not show much change. Fig. 3 is highly interesting as it shows that the current model structure is suitable when using a prediction horizon from about 10 minutes on, while for $H < 10$ especially $\hat{\theta}_3$ and $\hat{\theta}_4$ contain a large uncertainty and so one should look for a better model structure. The most obvious step would be to check the noise correlation

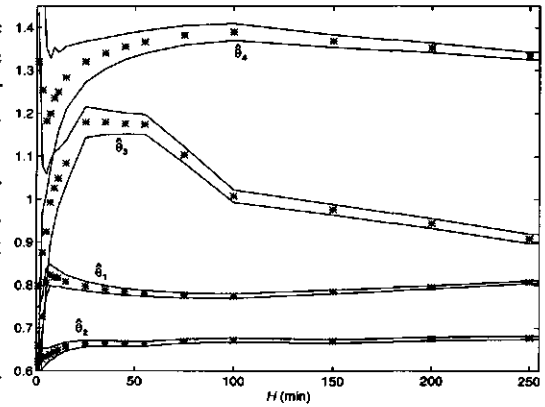


Fig. 3, nominal $\hat{\theta}$ with 2σ -bounds as function of H . All elements of $\hat{\theta}$ depend significantly on H , so for this example it is relevant to use as identification criterion the sum of squared 1, 2, ..., H -step ahead prediction errors (eqn. 3) instead of just the 1-step ahead prediction error.

The mean squared error M is plotted in Fig. 4. Notice the rapid increase of M in case more-step-ahead predictions are made with the optimal $\hat{\theta}$ for $H=1$. The positive trend in Fig. 4 is obvious: the further into the future a prediction is made the larger the prediction error. It can be shown that the decreases for both $H \in [200, 300]$ and $H \in [450, 550]$ are effects of the gaps in the data set.

2.5 Discussion

Biotechnological processes characteristically exhibit time-varying dynamics. An obvious way to tackle this in an MPC context is updating the model by means of on-line recursive identification. However minimising the sum of squared 1, 2, ..., H -step ahead prediction errors (eqn. 3) for non-linear models can be computationally very involving due to the large number of integrations required in each iteration of the optimisation routine. A gradient based optimisation algorithm, which for non-linear models always has to determine the gradient numerically, needs to integrate the model over $(p+1)(H^2+HN+H)$ sampling intervals per iteration, with p the dimension of θ . Therefore in an on-line realisation the combination of p , H and the number of optimisation iterations at each time step is largely limited by the available computation time per sampling interval.

Although not used in this paper the weights W_i enable mutual weighting of the i -step ahead predictions for $i \in [1, \dots, H]$. It has been argued that in MPC the current control input $u(k)$ is computed on the basis of the prediction sequence $\hat{y}(k+1|k,.)$, ..., $\hat{y}(k+H|k,.)$. However, it is reasonable to expect that $u(k)$ depends stronger on $\hat{y}(k+1|k,.)$ than on $\hat{y}(k+H|k,.)$, which can be expressed in the identification phase by applying a series of decreasing weighting matrices W_i . This weighting is likely to have a positive effect on the final MPC performance. The question of how to choose the series of weighting matrices W_i remains.

2.6 Conclusions

It was argued that in model identification for MPC with prediction horizon H the sum of squared 1, 2, ..., H -step ahead prediction errors (eqn. 3) is a better identification criterion than the 1-step ahead prediction error, because the 1, 2, ..., H -step ahead predictions of the model are used to compute the current controls. In the example of ammonium/nitrate dynamics in an activated sludge process the value of H significantly affects the parameter estimate $\hat{\theta}$. Hence, it is reasonable to expect that the use of the (weighted) sum of squared 1, 2, ..., H -step ahead prediction errors as identification criterion improves MPC performance. Whether this improvement is worth the extra effort depends on many factors and will vary from case to case.

Acknowledgements: The experimental work was done by M. Bloemen. This research was supported by the Technology Foundation (STW) under grant no. WBI44.3275.

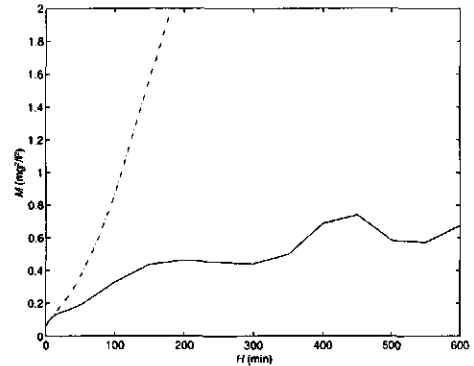


Fig. 4. mean squared error M for θ estimated with $H = 1$ (-) and minimal M (-) as a function of H .

2.7 References

- Bard, Y. (1974). *Nonlinear parameter estimation*. pp. 173, Academic Press, London.
- Bitmead, R.R., M. Gevers, V. Wertz (1990). *Adaptive Optimal Control: the thinking man's GPC.*, Prentice Hall, Brunswick, Victoria, Australia.
- Haarsma, G.J., K.J. Keesman (1995). Robust model predictive dissolved oxygen control. Forum for Applied Biotechnology, 9th, *MFLRBER 60(4b)*, pp. 2415-2426.
- Henze M., Grady jr. C.P.L., Gujer W., Marais G.v.R. and Matsuo T. (1987). Activated sludge model no. 1. *IAWQ Scientific and Technical Report no. 1*, IAWQ, London, U.K.
- Lukasse, L.J.S., K.J. Keesman and G. van Straten (1996). Grey-box identification of dissolved oxygen dynamics in activated sludge processes. *proc. 13th IFAC World Congress*, San Francisco.
- Münch, E.V., P. Lant, J. Keller (1996). Simultaneous nitrification and Denitrification in bench-scale sequencing batch reactors. *Water Research*, **30(2)**, pp. 277-284.
- Schneider, R., A. Munack (1995). Improvements in the on-line parameter identification of bioprocesses. *proc. 6th Int. Conf. on Computer Applications in Biotechnology*. Garmisch-Partenkirchen, Germany.
- Soeterboek, R. (1990). *Predictive Control - a unified approach*. PhD-thesis.
- Zhao, H., S.H. Isaacs, H. Søbereg, M. Kümmel (1995). An analysis of nitrogen removal and control strategies in an alternating alternating activated sludge process. *Water Research*, **29(2)**, pp. 535-544.

2.8 Appendix 1, covariance for multi-output model parameter estimates minimizing the (weighted) sum of squared 1, 2, ..., H-step ahead prediction errors.

The general non-linear weighted least squares estimation problem can be locally linearized around the estimate $\hat{\theta}$ to obtain

$$\min_{\theta} J(\theta) = \epsilon(k; \theta)^T \mathbf{R} \epsilon(k; \theta) \quad (\text{A.1})$$

subject to

$$\epsilon(k; \theta) = \mathbf{y}(k) - \hat{\mathbf{y}}(k; \theta) \quad (\text{A.2})$$

$$\hat{\mathbf{y}}(k; \theta) = \mathbf{X}(k)\theta \quad (\text{A.3})$$

where \mathbf{X} is the locally available matrix of regression variables and \mathbf{R} is a positive definite symmetric weighting matrix. The covariance matrix related to the weighted least squares parameter estimate is given by (Eykhoff, 1974)

$$\Sigma_{\hat{\theta}} = (\mathbf{X}^T \mathbf{R} \mathbf{X})^{-1} \mathbf{X}^T \mathbf{R} \mathbf{N} \mathbf{R} \mathbf{X} (\mathbf{X}^T \mathbf{R} \mathbf{X})^{-1} \quad (\text{A.4})$$

where \mathbf{N} is the noise covariance matrix

$$\mathbf{N} = E\{\mathbf{e}(k) \cdot \mathbf{e}(k)^T\} \quad (\text{A.5})$$

By proper definition of \mathbf{X} and \mathbf{y} the expression for the covariance matrix (eqn. A.4) can be extended to this paper's case of minimization of the (weighted) sum of squared 1, 2, ..., H -step ahead prediction errors from a data set containing N measurement points from an m -dimensional output system. Define

$$\mathbf{y} = \begin{bmatrix} \mathbf{y}(1) \\ \mathbf{y}(2) \\ \mathbf{y}(3) \\ \mathbf{y}(2) \\ \mathbf{y}(3) \\ \mathbf{y}(4) \end{bmatrix} \quad \mathbf{N} = \begin{bmatrix} \Sigma_e & \mathbf{0} & \mathbf{0} & \mathbf{0} & \mathbf{0} & \mathbf{0} \\ \mathbf{0} & \Sigma_e & \mathbf{0} & \Sigma_e & \mathbf{0} & \mathbf{0} \\ \mathbf{0} & \mathbf{0} & \Sigma_e & \mathbf{0} & \Sigma_e & \mathbf{0} \\ \mathbf{0} & \Sigma_e & \mathbf{0} & \Sigma_e & \mathbf{0} & \mathbf{0} \\ \mathbf{0} & \mathbf{0} & \Sigma_e & \mathbf{0} & \Sigma_e & \mathbf{0} \\ \mathbf{0} & \mathbf{0} & \mathbf{0} & \mathbf{0} & \mathbf{0} & \Sigma_e \end{bmatrix} \quad (\text{A.11})$$

Because \mathbf{R} and \mathbf{N} are sparse matrices the computation of $\mathbf{X}^T \mathbf{R} \mathbf{N} \mathbf{R} \mathbf{X}$ can be made more efficient by summation over the submatrix-products. It requires just some ordinary matrix manipulations to show that

$$\mathbf{X}^T \mathbf{R} \mathbf{N} \mathbf{R} \mathbf{X} = \sum_{i=1}^H \sum_{j=1}^H \sum_{k=\max(i,j)}^{N-H+\min(i,j)} \mathbf{X}_k^i T \mathbf{W}_i \Sigma_e \mathbf{W}_j \mathbf{X}_k^j \quad (\text{A.12})$$

Substituting eqns. A.8 and A.12 into eqn. A.4 yields

$$\Sigma_{\hat{\theta}} = \left(\sum_{i=1}^H \sum_{k=i}^{N-H+i} \mathbf{X}_k^i T \mathbf{W}_i \mathbf{X}_k^i \right)^{-1} \left(\sum_{i=1}^H \sum_{j=1}^H \sum_{k=\max(i,j)}^{N-H+\min(i,j)} \mathbf{X}_k^i T \mathbf{W}_i \Sigma_e \mathbf{W}_j \mathbf{X}_k^j \right) \left(\sum_{i=1}^H \sum_{k=i}^{N-H+i} \mathbf{X}_k^i T \mathbf{W}_i \mathbf{X}_k^i \right)^{-1} \quad (\text{A.13})$$

So this is the expression for parameter covariance in case the estimated parameter vector minimizes the (weighted) sum of squared 1, 2, ..., H -step ahead prediction errors.

3 A recursively identified model for short-term predictions of NH_4/NO_3 -concentrations in alternating activated sludge processes[†]

3.1 Abstract

One of the stumbling blocks in the operation of alternatingly aerated activated sludge processes (ASP's) for nitrogen removal is the limited knowledge of both the varying influent composition and the complex dynamics of the biological process. This paper presents a simple physical N-removal model for alternatingly aerated, continuously mixed ASP's. The simplicity is achieved by capturing the slower process dynamics in recursively estimated time-varying model parameters. Both seasonal and diurnal parameter variations are tracked. Also the influent ammonium concentration is treated as a recursively estimated model parameter. The method performs excellently on real data collected from an alternatingly aerated pilot scale ASP fed with municipal wastewater. Simulation of the resulting time-varying model yields accurate and computationally cheap predictions of ammonium and nitrate concentrations in the specific plant under operation over the next hours. Simulation for different control input scenario's can be used to optimize process performance, either manually by operators or automatically by model based optimizing controllers. Another possible application is optimization of the sludge (biomass) concentration, as the estimated parameters contain information regarding process load and concentrations and activities of the N-removing biomass. From this information it can be computed whether there is an excess/shortage of sludge in the reactor.

Keywords: activated sludge process, alternating aeration, control, Kalman filter, model, nitrogen removal, nonlinear, optimization, recursive estimation, stability.

3.2 Introduction

In the Netherlands, a law (Lozingenbesluit Wvo stedelijk afvalwater, 1996) enforces the introduction of nitrogen removal, with both nitrification and denitrification, in all municipal waste water treatment plants. The same applies to many other areas in the European Union (EU-directive 91/271/EEG) and other parts of the world. Operation strategies for ASP's with both nitrification and denitrification are still evolving¹⁻². One of the stumbling blocks is the limited process knowledge. Strong diurnal and seasonal variations occur both in influent flow, influent composition and in process dynamics. Important causes of these variations are the characteristic life pattern of the connected households, rainfall and temperature variations³. Besides these variations in one plant, all plants differ from each other. Each individual plant contains a unique influent characteristic and micro-organism population. What can give an important contribution to the optimization of process

[†] published by L.J.S. Lukasse, K.J. Keesman and G. van Straten in *Journal of Process Control*, 9, 1998, pp. 87-100.

operation is a simple model, capable of yielding accurate predictions of the ammonium (NH_4) and nitrate (NO_3) concentrations during the next hours. Simulation of such a model for different control input scenarios can be used to determine the most suitable control input. Selection of the most suitable control input can be done either manually by operators or automatically by model based optimizing controllers⁴⁻⁵.

The objective of this study is to develop a simple physical model for accurate predictions of the NH_4/NO_3 -concentrations in one alternately aerated, continuously mixed ASP during the next hours. In many cases N-removal takes place in this alternating type of process⁶⁻⁹. A simple physical model is possible by replacing the complex, relatively slow and uncertain dynamics of the sludge inventory by time-varying model parameters. The alternating operation guarantees cyclical variations of ammonium (NH_4) and nitrate (NO_3) and hence excitation of process dynamics. This is a good setting for recursive estimation of model parameters. The recursive estimator must provide up to date estimates of the time-varying model parameters: influent NH_4 (NH_4^in), maximum nitrification rate ($C_{NH,max}$) and maximum denitrification rate ($C_{NO,max}$).

There is a number of papers available on the estimation of $C_{NH,max}$ from in-sensor experiments. Most of them are respirometry-based¹⁰⁻¹³, but also other measurement principles have been proposed¹⁴. The major drawbacks of these approaches are 1) the large number of pitfalls in the translation from sensor readings to estimates of $C_{NH,max}$ in the reactor, and 2) the use of complicated measurement devices, that have hardly found acceptance outside the academic world. In the literature there is only one report on recursive estimation of $C_{NH,max}/C_{NO,max}$ from NH_4/NO_3 measurements¹⁵. It concerns the decoupled estimation of $C_{NH,max}$ from parts of the NH_4 measurements and $C_{NO,max}$ from parts of the NO_3 measurements in the unusual ASP layout of two alternating tanks in parallel. That method cannot be applied to the common one tank ASP system, because it mainly uses data from one tank in periods that its influent flow is zero, which is an unusual situation in the common one tank ASP system. Hence, the method of this paper offers a new possibility for the common one tank ASP system. It uses one combined recursive estimator for all three parameters, including NH_4^in , and it utilizes all measurements from standard NH_4/NO_3 -sensors.

3.3 Process model

In earlier work¹⁶ identification experiments were conducted on the alternating reactor of a pilot scale ASP. In the alternating reactor the airflow is manipulated by a dissolved oxygen (DO) controller, that receives its alternating setpoint (DOR) from a higher level N-controller (Fig. 1). In these experiments it was found that the major part of the NH_4/NO_3 -dynamics in alternating ASP's on the time scale of interest (hours) can be explained by only three processes: the reactor's influent load, nitrification and denitrification. Nitrification is the transformation of NH_4 into NO_3 under aerobic conditions. Denitrification is the transformation of NO_3 into N_2 -gas under anoxic conditions. Hence, the combined NH_4/NO_3 -balances in alternately aerated reactors can be modeled as

$$\begin{bmatrix} \dot{NH}_4 \\ \dot{NO}_3 \end{bmatrix} = \frac{-q^in}{V} \begin{bmatrix} NH_4 \\ NO_3 \end{bmatrix} + \begin{bmatrix} -C_{NH} \\ C_{NH} + C_{NO} \end{bmatrix} u + \begin{bmatrix} \frac{q^in}{V} NH_4^in \\ -C_{NO} \end{bmatrix} \quad (1)$$

$$C_{NH} = \begin{cases} C_{NH,max} & \text{if } NH_4 > 0 \\ \frac{q^{in}}{V} NH_4^{in} & \text{if } NH_4 = 0 \end{cases} \quad (2)$$

$$C_{NO} = \begin{cases} C_{NO,max} & \text{if } NO_3 > 0 \\ 0 & \text{if } NO_3 = 0 \end{cases} \quad (3)$$

$$\begin{bmatrix} y_1(k) \\ y_2(k) \end{bmatrix} = \begin{bmatrix} NH_4(k-d) \\ NO_3(k-d) \end{bmatrix} + \begin{bmatrix} e_1(k) \\ e_2(k) \end{bmatrix} \quad (4)$$

with

e_1, e_2 = noise on measurements of respectively NH_4 and NO_3 .

$u \in \{0, 1\}$ i.e. {anoxic (dissolved oxygen setpoint $DO_R = 0$ mg/l), aerobic ($DO_R = 3$ mg/l)}

V = reactor volume (475 l)

d = measurement time delay rounded off at whole sampling intervals (4 sampling intervals).

q^{in} = influent flow, on some plants control input, on other plants disturbance input (l/min).

NH_4^{in} = influent NH_4 concentration (mg/l).

$C_{NH,max}$ = max. consumption rate of NH_4 (mg/l.min).

$C_{NO,max}$ = max. consumption rate of NO_3 (mg/l.min).

In eqn. 1 the term $q^{in}NH_4^{in}$ represents the reactor's influent load, $C_{NH}u$ represents nitrification and $C_{NO}(1-u)$ represents denitrification. The model is extremely simple in comparison to the generally accepted ASM no. 1 model¹⁷. The simplification is justified as basically only four time-varying slopes determine the system behaviour (Fig. 4). Due to the alternating process operation simultaneous nitrification/denitrification will only occur during the transient from aerobic to anoxic phases and *vice versa*. These transients typically take a couple of minutes, while one phase lasts at least 20 minutes. So the transients are negligible and it is justified to assume $DO = DO_R$ instead of modelling the region of DO-limited process rates ($0 < DO < 3$ mg/l). It was also observed that the region of substrate limited process rates is very small. Consequently, the process is hardly operated in this region. Therefore the generally used Monod kinetics can be replaced by hard switching functions, i.e. nitrification is maximal if $NH_4 > 0$ and equal to the influent load if $NH_4 = 0$ (eqn. 2), and denitrification is maximal if $NO_3 > 0$ and zero if $NO_3 = 0$ (eqn. 3). The remaining simplifications are the slower or less significant process mechanisms related to growth of biomass. These changes are accounted for by recursive estimation of the model parameters $C_{NH,max}$ and $C_{NO,max}$. Also NH_4^{in} is known to exhibit strong variations. Hence, the parameter vector for recursive identification is defined as

$$\theta := [NH_4^{in} \ C_{NH,max} \ C_{NO,max}]^T$$

Since most recursive parameter estimation techniques are based on discrete-time models, the N-removal model is discretized. The Equivalent Discrete time System¹⁸ of the continuous time nitrogen removal model (eqns. 1 - 4), after elimination of the state variables NH_4 and NO_3 , is given by

$$\begin{bmatrix} y_1(k+1) \\ y_2(k+1) \end{bmatrix} = e^{-\frac{q^{in}(k-d)\tau}{V}} \begin{bmatrix} y_1(k) \\ y_2(k) \end{bmatrix} + \mathbf{X}(k)\theta(k) \quad (5)$$

with the Jacobian

$$\mathbf{X}(k) = \frac{\partial \hat{\mathbf{y}}(k+1|k)}{\partial \boldsymbol{\theta}} = \frac{1 - e^{-\frac{q^n(k-d)T}{V}}}{\frac{q^n(k-d)}{V}} \begin{bmatrix} X_{11}(k) & X_{12}(k) & X_{13}(k) \\ X_{21}(k) & X_{22}(k) & X_{23}(k) \end{bmatrix} \quad (6)$$

where T is the sampling interval (5 min). The elements $X_{11}(k)$, ..., $X_{23}(k)$ in eqn. 6 are defined in Table 1.

Table 1. X_{11}, \dots, X_{23} in Jacobian \mathbf{X} (eqn. 6) in all possible operating modes.

	$X_{11}(k)$	$X_{12}(k)$	$X_{13}(k)$	$X_{21}(k)$	$X_{22}(k)$	$X_{23}(k)$
$\{y_1(k+1), y_1(k)\} > 0$	$\frac{q^n(k-d)}{V}$	$-u(k-d)$	0	0	$u(k-d)$	$u(k-d)-1$
$\{y_1(k+1), y_1(k)\} = 0$	0	0	0	$\frac{q^n(k-d)}{V}$	0	$u(k-d)-1$
$\{y_2(k+1), y_2(k)\} = 0$	$\frac{q^n(k-d)}{V}$	$-u(k-d)$	0	0	0	0

3.4 Recursive parameter estimation

The parameter time-variance is modeled as a random walk, such that by including eqn. 5 the complete state-space model for this application becomes

$$\begin{aligned} \boldsymbol{\theta}(k+1) &= \boldsymbol{\theta}(k) + \mathbf{w}(k) \\ \mathbf{y}(k+1) - e^{-\frac{q^n(k-d)T}{V}} \mathbf{y}(k) &= \mathbf{X}(k)\boldsymbol{\theta}(k) + \mathbf{v}(k) \end{aligned} \quad (7)$$

where $\boldsymbol{\theta} \in \mathbb{R}^p$, $\mathbf{y} \in \mathbb{R}^n$, $\mathbf{w} \in \mathbb{R}^p$ and $\mathbf{v} \in \mathbb{R}^n$, in this application $p = 3$ and $n = 2$. The vectors $\mathbf{w}(k)$ and $\mathbf{v}(k)$ are independent Gaussian distributed white noise sequences. The random walk assumption is a common choice when prior knowledge about the nature of parameter changes is poor. The well-known Kalman filter¹⁹ is chosen to recursively estimate the time-varying parameter vector $\boldsymbol{\theta}$. This filter has the attractive property that the filter gain varies as a function of the Jacobian \mathbf{X} , which is directly related to the parameter observability. Moreover it directly takes into account the uncertainties in the state and observation equations, reflected by \mathbf{w} and \mathbf{v} . The Kalman filter is given by

$$\begin{aligned} \hat{\boldsymbol{\theta}}(k) &= \hat{\boldsymbol{\theta}}(k-1) + \mathbf{L}(k)\boldsymbol{\varepsilon}(k, \hat{\boldsymbol{\theta}}(k-1)) \\ \mathbf{L}(k) &= \mathbf{P}(k-1)\mathbf{X}^T(k)\{\mathbf{R}(k) + \mathbf{X}(k)\mathbf{P}(k-1)\mathbf{X}^T(k)\}^{-1} \end{aligned} \quad (8)$$

$$\mathbf{P}(k) = \mathbf{P}(k-1) + \mathbf{Q}(k) - \mathbf{P}(k-1)\mathbf{X}^T(k)\{\mathbf{R}(k) + \mathbf{X}(k)\mathbf{P}(k-1)\mathbf{X}^T(k)\}^{-1}\mathbf{X}(k)\mathbf{P}(k-1)$$

with the prediction error

$$\boldsymbol{\varepsilon}(k, \hat{\boldsymbol{\theta}}(k-1)) = \mathbf{y}(k) - \hat{\mathbf{y}}(k|k-1) \quad (9)$$

and the predicted output

$$\hat{\mathbf{y}}(k|k-1) = e^{-\frac{q^n(k-d)T}{V}} \mathbf{y}(k-1) + \mathbf{X}(k-1)\hat{\boldsymbol{\theta}}(k-1) \quad (10)$$

The Kalman filter has three positive definite matrices which need to be initialized: $\mathbf{P}(0)$, \mathbf{Q} and \mathbf{R} . Theoretically $\mathbf{Q} = \mathbf{E}\{\mathbf{w}(k)\mathbf{w}(k)^T\} \in \mathbb{R}^{p \times p}$ is the parameter random walk covariance matrix, and $\mathbf{R} = \mathbf{E}\{\mathbf{v}(k)\mathbf{v}(k)^T\} \in \mathbb{R}^{n \times n}$ is the measurement noise covariance matrix in eqn. 7. With this tuning the Kalman filter would yield the maximum likelihood estimate of $\boldsymbol{\theta}(k)$, if the model structure in eqn. 7 is correct. However, in practice this last condition is usually not met and therefore \mathbf{Q} and \mathbf{R} lose their theoretical meaning and are treated as ordinary tuning matrices.

Typically $\mathbf{P}(0)$, \mathbf{Q} and \mathbf{R} are diagonal matrices, unless one has prior knowledge about parameter or measurement error correlations. $\mathbf{P}(0)$ is usually set at $\mathbf{I} * 10^6$, with \mathbf{I} the unity matrix, a very large value allowing for fast initial convergence and making an accurate initial guess $\hat{\boldsymbol{\theta}}(0)$ redundant²⁰. A reasonable value for \mathbf{R} can be obtained by evaluating the noise on the measurement signals. In this study the measurement noise is very small for both outputs (Fig. 3, 4), so \mathbf{R} is a diagonal matrix whose diagonal elements get very small values. Most heuristics are involved in setting \mathbf{Q} . Its elements are set in proportion to each other, using prior knowledge of the variability of the elements of $\boldsymbol{\theta}$, but also in proportion to the elements of \mathbf{R} . Typically, increasing element Q_{ii} improves the tracking of θ_i , but also increases the measurement noise sensitivity of $\hat{\boldsymbol{\theta}}_i$.

As can be seen from Table 1 the Jacobian $\mathbf{X}(k)$ can take four forms as the system can switch between four different modes: $\{y(k+1), y(k)\} > 0$ under either aerobic or anoxic conditions, $\{y_1(k+1), y_1(k)\} = 0$ under aerobic conditions and $\{y_2(k+1), y_2(k)\} = 0$ under anoxic conditions. So the non-linear system in this study can be regarded as a system alternating between four different linear systems. For this application the system in eqn. 7 is unobservable in all four linear modes, as it is observable if and only if $\text{rank}([\mathbf{X} \mid \mathbf{X}\mathbf{I} \mid \dots \mid \mathbf{X}\mathbf{I}^{p-1}]^T) = p$, where \mathbf{X} is the Jacobian defined in eqn. 6. A detailed study unravelled that in each of the four linear modes the elements of \mathbf{P} corresponding to the unobservable elements of $\boldsymbol{\theta}$ will increase linearly (Appendix 1). Obviously this will cause a linear increase in some of the elements of \mathbf{L} as well (eqn. 8b). This increase makes the Kalman filter superior to a recursive estimator with fixed gain, as it correctly reflects the decreasing confidence in the estimate of a time-varying parameter if no new information is collected from which its estimate may be updated. In eqn. 8c the linear increase in \mathbf{P} is counteracted by a quadratic decrease if $\boldsymbol{\theta}$ is observable. Due to the facts that each individual parameter in this paper's application is observable in at least one of the four modes and that the system regularly switches between these modes, all elements of \mathbf{P} and \mathbf{L} will remain reasonably small. It is shown in Appendix 1 that the system must remain in one single mode for at least a year before elements of \mathbf{P} reach the value 10^6 . As the system typically remains in one mode for at most a couple of hours, this value will never be reached.

To evaluate the stability properties of the recursive estimator, substitute eqns. 7b, 9 and 10 into eqn. 8a. This yields the difference equation describing the parameter estimate evolution:

$$\hat{\boldsymbol{\theta}}(k) = (\mathbf{I} - \mathbf{L}(k)\mathbf{X}(k-1))\hat{\boldsymbol{\theta}}(k-1) + \mathbf{L}(k)\mathbf{X}(k-1)\boldsymbol{\theta}(k-1) + \mathbf{L}(k)\mathbf{v}(k-1) \quad (11)$$

Subtract eqn. 11 from eqn. 7a to get the difference equation describing the estimation error evolution:

$$\mathbf{e}(k) = \boldsymbol{\theta}(k) - \hat{\boldsymbol{\theta}}(k) = (\mathbf{I} - \mathbf{L}(k)\mathbf{X}(k-1))\mathbf{e}(k-1) + \mathbf{w}(k-1) - \mathbf{L}(k)\mathbf{v}(k-1) \quad (12)$$

The following theorem applies to the two preceding equations.

Theorem²¹: A sufficient condition for convergence of the Kalman filter to a steady-state gain $\bar{\mathbf{L}}$ that stabilises eqns. 11 and 12 is that the system to which it is applied (eqn. 7) is controllable and observable.

The system in eqn. 7 is controllable, as $\text{rank}([\mathbf{I} \mid \mathbf{I}^1\mathbf{I} \mid \dots \mid \mathbf{I}^{p-1}\mathbf{I}]) = p$. Unfortunately, it is unobservable in all four linear modes, as mentioned before. So the theorem guarantees no stability of eqns. 11 and 12. Therefore a more detailed study of the stability characteristics is required.

In Appendix 1 it is shown that the system in eqn. 7 can always be written in the form

$$\mathbf{X}(k) = [\mathbf{X}_1(k) \quad \mathbf{0}] \quad \text{and} \quad \mathbf{L}(k) = \begin{bmatrix} \mathbf{L}_1(k) \\ \mathbf{0} \end{bmatrix}$$

with $\mathbf{X}_1(k)$ the full rank Jacobian of the observable subsystem in eqn. 7 and $\mathbf{0}$ the Jacobian of the unobservable subsystem. As a result

$$\mathbf{L}(k)\mathbf{X}(k-1) = \begin{bmatrix} \mathbf{L}_1(k)\mathbf{X}_1(k-1) & \mathbf{0} \\ \mathbf{0} & \mathbf{0} \end{bmatrix} \quad (13)$$

Stability of eqns. 11 and 12 requires the eigenvalues of the matrix $\mathbf{I}-\mathbf{L}(k)\mathbf{X}(k-1)$ to have absolute values less than one (the edge of stability for discrete time systems), *i.e.*

$$|\lambda(\mathbf{I}-\mathbf{L}(k)\mathbf{X}(k-1))| < 1 \quad (14)$$

where $\lambda(\cdot) \in \mathbb{R}^p$ denotes the set of eigenvalues of the matrix $\mathbf{I}-\mathbf{L}(k)\mathbf{X}(k-1)$. By substituting eqn. 13 in the equation above the eigenvalues of eqns. 11 and 12 are given by

$$\lambda(\mathbf{I}-\mathbf{L}(k)\mathbf{X}(k-1)) = \lambda \left(\begin{bmatrix} \mathbf{I}_1 & \mathbf{0} \\ \mathbf{0} & \mathbf{I}_2 \end{bmatrix} - \begin{bmatrix} \mathbf{L}_1(k)\mathbf{X}_1(k-1) & \mathbf{0} \\ \mathbf{0} & \mathbf{0} \end{bmatrix} \right) = \lambda(\mathbf{I}_1 - \mathbf{L}_1(k)\mathbf{X}_1(k-1)) \cup \lambda(\mathbf{I}_2) \quad (15)$$

Clearly, the eigenvalues are a union of the eigenvalues of the observable and the unobservable subsystems. The Kalman filter stabilises the observable subsystem due to the theorem. The eigenvalues of the unobservable subsystem take the value 1, which makes it unstable. The unstable modes in eqn. 11 remain constant as both $\mathbf{X}_2(k)$ and $\mathbf{L}_2(k)$ are $\mathbf{0}$, meaning that if a parameter is not observable then its estimate remains constant. The accompanying unstable modes in $\mathbf{e}(k)$ (eqn. 12) are driven by $\mathbf{w}(k)$, as $\mathbf{L}_2(k) = \mathbf{0}$ (eqn. 7). So changes in the unstable modes of $\mathbf{e}(k)$ originate from changes in $\boldsymbol{\theta}(k)$. From physical knowledge $\boldsymbol{\theta}(k)$ is known to be bounded, so $\mathbf{e}(k)$ is bounded. Summarising, the asymptotic instability of eqns. 11 and 12 originates from constant elements of $\hat{\boldsymbol{\theta}}(k)$ in phases where these elements are unobservable, while $\boldsymbol{\theta}$ varies. Clearly, this type of instability is totally acceptable for this application.

3.5 Application to real measurements

Experimental data were collected from an alternatingly aerated pilot scale ASP (Fig. 1) with continuously mixed aeration tank ($V = 475$ l, MLSS = 3.5 g/l), continuously fed with presettled municipal waste water. NH_4 and NO_3 in the aeration tank are measured by means of SKALAR auto-analyzers type SA 9000. DO is is

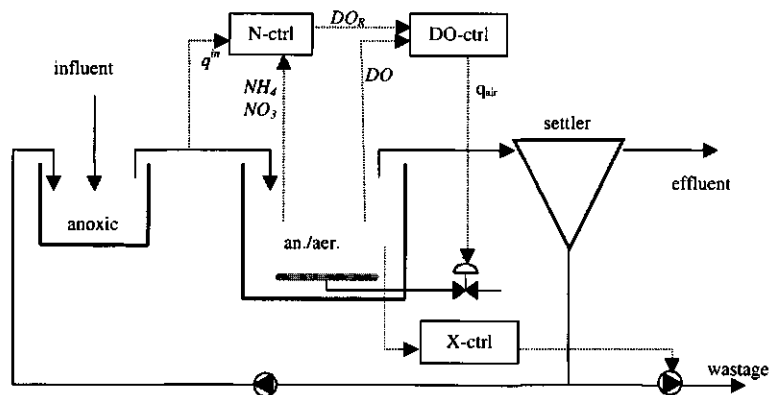


Fig. 1, scheme of ASP pilot plant with cascaded controllers for N and DO.

tightly controlled at a setpoint alternating between 0 and 3 mg/l using the airflow as manipulated variable. The data resulting from two of the experiments are shown in Figs. 2 - 4. During both experiments pH remained rather constant at a value of 7. In the first data set (Figs. 2, 3) q^{in} is a

downscaled version of the measured influent flow at the adjacent full-scale wastewater treatment plant. The large jumps in q^{in} (Fig. 2) are due to the on/off switching of pumps at the full-scale wastewater treatment plant. In the second data set (Fig. 4) q^{in} is kept constant at 48 l/h. In both experiments an N-controller was used to keep NH_4 low, but above zero. Clearly, this controller did not perform as expected during the second experiment (Fig. 4), but the data set is interesting from a recursive identification point of view. The time axes in Figs. 2 - 4 are such that multiples of 24 h coincide with midnight.

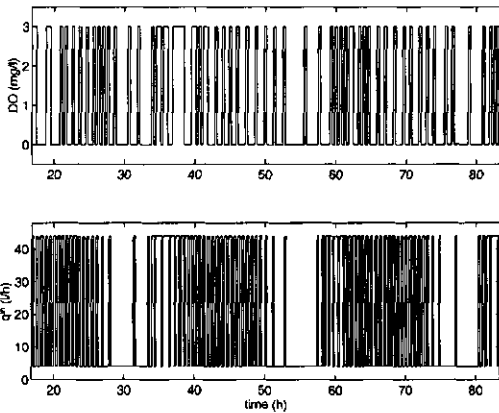


Fig. 2, input signals applied during experiment 1.

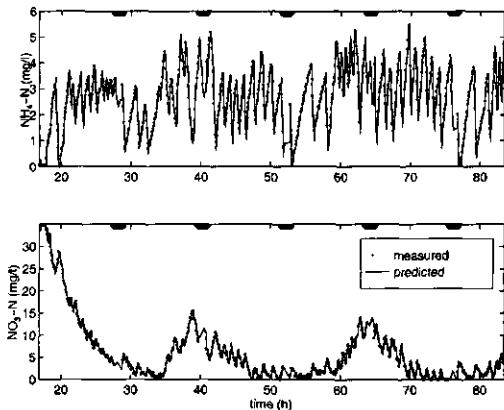


Fig. 3, prediction results for experiment 1 (calibration phases indicated by fat overbar).

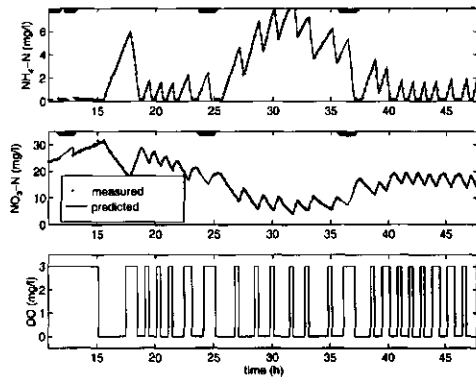


Fig. 4, prediction results for experiment 2 ($q^{in} = 48$ l/h, calibration phases indicated by fat overbar).

The validity of the data is first tested before they are used in the recursive estimation scheme to prevent the recursive estimator from poor results due to the use of unreliable measurements. There are three cases in which measurement $y_i(k)$, $i \in \{1, 2\}$, is judged invalid:

1. During analyzer auto-calibration:

$$y_i(k) \in C = \{y_i(k) \in \mathbb{R} \mid k \text{ in calibration period}\}$$

2. When NH_4 or NO_3 is depleted (i.e. close to zero), and analyzer is not in calibration (in this situation it is likely that $y_i(k)$ actually is 0, but due to a little offset the analyzer gives a signal non-equal to 0):

$$y_i(k) \in D = \{y_i(k) \in \mathbb{R} \mid y_i(k) \notin C; y(k) < \begin{bmatrix} 0.5 \\ 0.3 \end{bmatrix}; |y(k) - y(k-1)| < \begin{bmatrix} 0.5 \\ 7.0 \end{bmatrix} \cdot 10^{-3}\} \quad (16)$$

For the rare cases that depletion starts somewhere in the sampling interval, *i.e.* $\{y_i(k-1) > 0, y_i(k) = 0\}$, $\mathbf{X}(k-1)$ is set to zero as it is unknown when depletion started and hence $\hat{\theta}$ should remain unchanged.

3. When a measurement is far off from its expected value it is unreliable, *i.e.* an outlier:

$$y_i(k) \in O = \{y_i(k) \in \mathbb{R} \mid y_i(k), y_i(k-1) \notin C; y_i(k) \notin \hat{y}_i(k|k-1) + \bar{\varepsilon}_i(k) \pm \beta(k) \cdot \sigma_i(k)\} \quad (17)$$

In the outlier test the terms $\bar{\varepsilon}(k)$, $\beta(k)$ and $\sigma(k)$ are the outputs of an outlier detection filter¹⁹, given by

$$\bar{\varepsilon}(k) = (1 - \alpha)\bar{\varepsilon}(k-1) + \alpha\varepsilon(k) \quad (18)$$

$$\sigma^2(k) = (1 - \alpha)\sigma^2(k-1) + \alpha \cdot \text{diag}((\varepsilon(k) - \bar{\varepsilon}(k))(\varepsilon(k) - \bar{\varepsilon}(k))^T) \quad (19)$$

$$\beta(k) = (1 - \alpha)\beta(k-1) + \alpha\beta(\infty) \quad (20)$$

with forgetting factor $\alpha \in [0, 1]$. The difference equation for β is used to enable startup, characteristically $\beta(0) > \beta(\infty) > 2$. In this study the values $\alpha = 0.1$, $\beta(0) = 15$ and $\beta(\infty) = 3$ proved satisfactory.

Table 2 contains a schematic presentation of the way unreliable measurements are handled. Notice that increasing R_{ii} results in an increased covariance $\mathbf{P}(k)$ (eqn. 8), reflecting the decreased reliability of $\hat{\theta}(k-1)$.

Table 2, special actions in unusual situations.

situation	action
$y_i(k) \in C$	$\varepsilon_i(k k-1) = 0, R_{ii} = 1 \cdot 10^6$
$y_i(k) \in D$	$\hat{y}_i(k k-1) = 0$
$y_i(k) \in O$	$\varepsilon_i(k k-1) = 0$ (in eqn. 8, not in eqns. 18-20), $R_{ii} = 1 \cdot 10^6$
$y_i(k-1) \in C$	$y_i(k-1) = \hat{y}_i(k-1 k-2), \varepsilon_i(k k-1) = 0, R_{ii} = 1 \cdot 10^6$
$y_i(k-1) \in O$	$y_i(k-1) = \hat{y}_i(k-1 k-2), \varepsilon_i(k k-1) = 0, R_{ii} = 1 \cdot 10^6$
$y_i(k-1) \in D, y_i(k) \notin D$	$\mathbf{X}(k-1) = 0, \mathbf{R} = \Gamma 10^6$
$y_i(k-1) \notin D, y_i(k) \in D$	$\mathbf{X}(k-1) = 0, \mathbf{R} = \Gamma 10^6$
$\{y_i(k), y_i(k-1)\} \in C$	evolution of outlier testing filter (eqns. 18-20) halted
$\hat{y}_i(k k-1) < 0$	$\hat{y}_i(k k-1) = 0$

3.6 Results & Discussion

The Kalman filter tuning matrices $\mathbf{P}(0)$, \mathbf{Q} and \mathbf{R} are set according to the earlier discussed strategy, using data set 1 (Figs. 2, 3). The tuning of \mathbf{Q} is based on the knowledge that NH_4^m usually exhibits

diurnal variations. $C_{NO,max}$ is related to the Readily Biodegradable Organic Substrate (RBOS) concentration in the reactor, which is likely to be subject to diurnal variations as well. So the influent related θ_1 and the RBOS related θ_3 will usually fluctuate a lot faster than the sludge related θ_2 . Therefore Q_{11} and Q_{33} are given a distinctly larger value than Q_{22} . Obviously, this choice effects the frequency content of the parameter estimates. The diagonals of the three resulting diagonal matrices are set to

$$\text{diag}(\mathbf{Q}) = [10 \ 5 \cdot 10^{-7} \ 1 \ 10^{-5}], \text{diag}(\mathbf{R}) = [0.1 \ 0.1], \text{diag}(\mathbf{P}(0)) = [1 \ 1 \ 1]10^6$$

Contrary to expectation, the influent related parameter NH_4^m does not show much diurnal variation (Figs. 5 and 6). This is probably due to the attenuation of diurnal influent cycli in an over-dimensioned presettler, which is usually not present at full-scale plants.

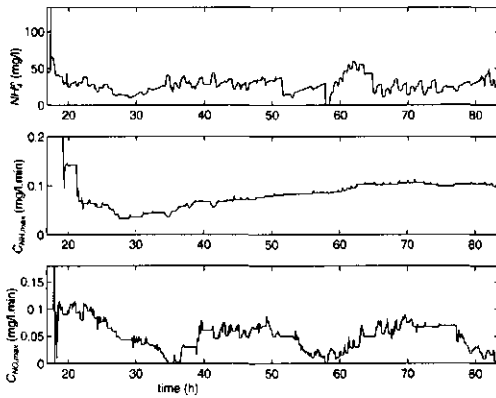


Fig. 5, parameter estimates for data set 1.

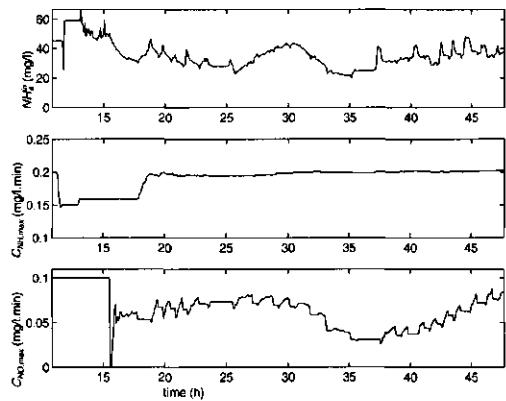


Fig. 6, parameter estimates for data set 2.

As expected, the estimated $C_{NH,max}$ shows little variation on a short time scale (Figs. 5 and 6), but a clear change is observed on a larger time scale: $\hat{C}_{NH,max}$ estimated from data set 1 is distinctly smaller than from data set 2 (compare Figs. 5 and 6). This demonstrates a lower concentration and/or activity of nitrifying biomass during the first experiment, which had been carried out one year before the second experiment.

A diurnal variation is observable in $C_{NO,max}$ in both data sets, it consistently reaches its minimum at about noon, just after the end of the low loaded part of the day. Candidate explanations for this phenomenon have to use quantities that show equal diurnal cycles during *both* experiments. Only two such signals have been observed: both the percentage of aerobic time is low and the diurnal NO_3 -cycle reaches its minimum during the hours preceding the lowest $\hat{C}_{NO,max}$. Limitation due to low NO_3 is unlikely, as NO_3 remains above 4 mg/l in data set 2, and it would contradict with the earlier identification experiments¹⁶ if the availability of NO_3 limits the denitrification rate at these values. So the little aerobic time is the only plausible explanation for the reduced $C_{NO,max}$. It is known that the anoxic hydrolysis rate is lower than the aerobic one. As a consequence, a period with little aerobic time results in reduced RBOS in the reactor, and this induces a lower $C_{NO,max}$. However, be aware that this explanation is a hypothesis, and it is beyond the scope of this study to verify/falsify it.

The good model predictions for both data sets (Fig. 3, 4), are especially clear during calibrations (Fig. 7). During those periods it becomes apparent that even more-step-ahead predictions (up to 1 h) contain reasonably small errors. Strictly speaking these nice results only demonstrate that the method works well for the main reactor of the pilot scale ASP in Fig. 1. Yet the method is believed to be applicable to any alternating reactor, regardless where its influent comes from, as long as it is more or less continuously mixed. It is irrelevant what type of N- and DO-controllers are used, the only prerequisite is that DO_R switches between zero and oxygen abundance (2 mg/l or more) and that the DO-controller manages to control DO tightly.

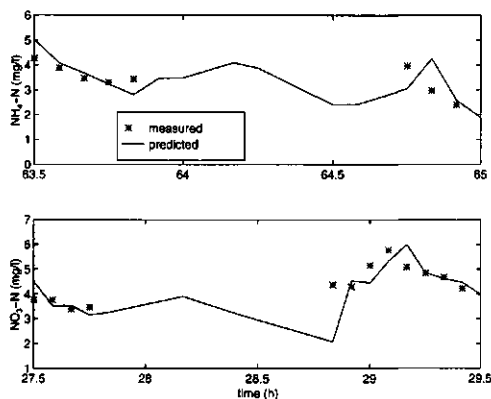


Fig. 7, close up of two different calibration phases in data set 1.

3.7 Simulation study

The results of the preceding section seem to be good, but there are no true parameter values to compare with. Therefore a simulation study is carried out to investigate the capability to track diurnal variations in NH_4^{in} and $C_{NO,max}$. First the continuous time model (eqns. 1-4) is simulated over one day with DO_R alternating between 0 and 3 mg/l in 50 min cycles (20 min aerobic and 30 min anoxic), $q^{in} = 45$ l/h, $C_{NH,max} = 0.2$ mg/l.min and sinusoidal cycles for NH_4^{in} and $C_{NO,max}$ (Fig. 9) given by

$$NH_4^{in}(t) = 45 + 20 \cdot \sin\left(\frac{2\pi(t-5)}{24}\right) \quad (\text{mg/l}) \quad (21)$$

$$C_{NO,max}(t) = 0.1 + 0.02 \cdot \sin\left(\frac{2\pi(t-2)}{24}\right) \quad (\text{mg/l.min}) \quad (22)$$

with t the time of the day (h). To make the simulation more acceptable, the model's switching functions for C_{NH} and C_{NO} (eqns. 2, 3) were replaced by the generally accepted Monod kinetic terms

$$C_{NH} = C_{NH,max} \frac{NH_4}{NH_4 + k_{NH}} \quad \text{and} \quad C_{NO} = C_{NO,max} \frac{NO_3}{NO_3 + k_{NO}} \quad (23)$$

with the half saturation constants $k_{NH} = k_{NO} = 0.01$ mg/l. This very small value is in correspondence with observations at our pilot plant during the earlier identification experiments¹⁶.

The recursive estimation scheme is applied to the data generated by this simulation (Fig. 8). The estimated trajectories of NH_4^{in} and $C_{NO,max}$ follow the true trajectories quite well (Fig. 9), apart from a slight phase shift appearing as a time delay (from which 20 min are caused by the analysers' measurement time delay). The phase shift could be reduced by increasing the elements of \mathbf{Q} (eqn. 8), but this will increase the noise sensitivity of $\hat{\theta}$ as well. As the current tuning of the Kalman filter is based on a trade-off between tracking capacity and noise sensitivity for the real data set 1, it was decided not to change \mathbf{Q} .

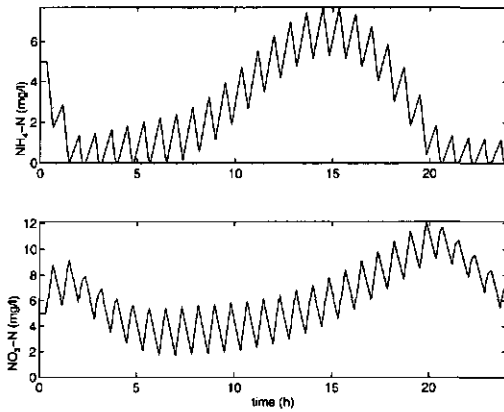


Fig. 8, data generated by simulation.

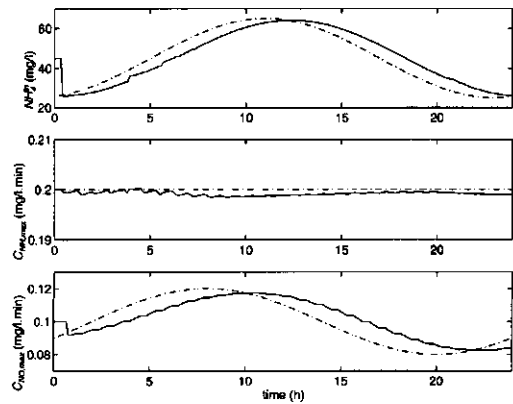


Fig. 9, true (-) and estimated (-) parameters for data generated by simulation of a continuously loaded plant.

The observed slight bias between $\hat{C}_{NH,max}$ and

$C_{NH,max}$ (Fig. 9) is caused by the Monod kinetic term $C_{NH,max} * NH_4 / (NH_4 + k_{NH})$ in the simulation model, according to which some degree of substrate inhibition occurs at any substrate concentration. In fact $\hat{C}_{NH,max}$ is the estimate of $C_{NH,max} * NH_4 / (NH_4 + k_{NH})$ instead of $C_{NH,max}$. On average $NH_4 = 4$ mg/l in the simulation data (Fig. 8) and hence $C_{NH,max} * NH_4 / (NH_4 + k_{NH})$ is around 0.1995 mg/l.min, the value to which $\hat{C}_{NH,max}$ converges. Obviously, the bias between $\hat{C}_{NH,max}$ and $C_{NH,max}$ contributes to improved model predictions.

To illustrate the improved model predictions due to recursive identification the mean squared 1-step-ahead (= 5 minutes ahead) prediction error M (mg/l)² is computed for the above described case with recursively estimated parameters and for the case the model predicts with fixed, but unbiased parameters: $[NH_4^in, C_{NH,max}, C_{NO,max}] = [45 \ 0.2 \ 0.1]$. This results in

$$[M_{NH} \ M_{NO}] = [1.2 \ 1.0] \cdot 10^{-3} \quad \text{for recursively estimated parameters}$$

$$[M_{NH} \ M_{NO}] = [11.1 \ 4.4] \cdot 10^{-3} \quad \text{for constant parameters}$$

So even in case of only diurnal parameter variations the model predictions are largely improved by using the recursive estimation scheme. In reality there are also large parameter variations on a longer time scale, e.g. seasonal variations. This will cause the constant parameters to become biased, and further deteriorate the predictive capacity of a model with constant parameters.

Tracking of diurnal changes in the sludge-related $C_{NH,max}$ is not interesting, because such fast changes are not expected to occur in reality, however there will occur changes on a longer time scale. Moreover, the data used in the preceding section and the above simulation concern plants with constant q^{in} , while in many full scale plants influent is supplied during the anoxic phases only. To study the tracking of gradual changes in $C_{NH,max}$ and the estimator's behaviour in case of alternating feeding a new simulation is carried out where $C_{NH,max}$ has a slight trend and q^{in} alternates between 0 during aerobic phases and 75 l/h during anoxic phases. As expected the tracking of NH_4^in and $C_{NO,max}$ does not differ much from that obtained with continuous feeding (compare Figs. 9 and

10). Moreover, slow changes in $C_{NH,max}$ can be tracked as well with the current settings of Q , albeit with a larger phase shift than NH_4^i and $C_{NO,max}$ (Fig. 10).

3.8 Conclusions

A simple physical model for N-removal in alternately aerated, continuously mixed activated sludge processes suffices to accurately predict NH_4 and NO_3 trajectories over the next hours. This is only possible by replacing the complex, relatively slow and uncertain dynamics of the sludge inventory by recursively estimated time-varying model parameters. A Kalman filter based recursive estimator has been designed for these parameters. This estimator showed good performance on different experimental data sets with one and the same tuning. The model with recursively estimated parameters provides accurate predictions of NH_4 and NO_3 concentrations during the next hour (Fig. 7). The only quantities that need to be measured are NH_4 , NO_3 , q^i and DO . The applicability of the recursive estimator to both alternately and continuously fed plants was verified by simulation studies. This enhances the applicability of the method, as both alternating and continuous feeding occurs in practice.

Due to the combination of simplicity and accurate predictions this recursively identified model is a suitable tool for optimizing plant operation, as it allows fast and accurate simulation of different control input scenario's over the next hours. Evaluation of the different control input scenario's can be done both directly in model based optimizing controllers⁵ and in decision support systems for plant operators.

Another possible application is the use of the parameter estimates on a higher level. The recursively estimated parameters contain information with respect to the influent N-load ($q^i \cdot NH_4^i$), maximum nitrification rate ($C_{NH,max}$) and maximum denitrification rate ($C_{NO,max}$). This information is usually not available in current practice, and least of all closely monitored. From this enhanced process knowledge it can be deduced to what extent the process is over/underloaded, and hence whether the sludge concentration should be increased/decreased. Another application is the detection of toxic effects when $C_{NH,max}/C_{NO,max}$ drop too low.

Acknowledgements: We are very grateful to the editor and reviewers for the constructive reviewing process, to M. Bloemen, who carried out the experiments, and to the Dutch Technology Foundation (STW), which financially supported this research under grant no. WBI44.3275.

3.9 References

- 1 Leeuw, E.J. and Oever E. van 't: Process selection, design and operation of the Ede WWTP. *Water Science and Technology* 1996, 33(12), 57-63

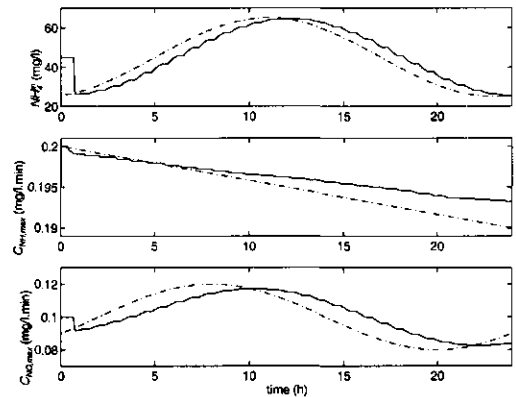


Fig. 10, true (---) and estimated (—) parameters for data generated by simulation of an alternately loaded plant.

- 2 Münch, E.V., Lant, P. and Keller, J.: Simultaneous nitrification and denitrification in bench-scale sequencing batch reactors. *Water Research* 1996, 30(2), 277-284
- 3 Metcalf & Eddy, Inc. 'Wastewater engineering: treatment/disposal/reuse.' 2nd edition, McGrawhill, New York, 1979
- 4 Isaacs, S.: Short horizon control strategies for an alternating activated sludge process. *Water Science and Technology* 1996, 34(1/2), 203-212
- 5 Lukasse, L.J.S., Keesman, K.J., Klapwijk, A. and Straten, G. van: Adaptive receding horizon optimal control of N-removing activated sludge processes. *Med. Fac. Landbouww. Univ. Gent, proc. 11th FAB* 1997, Gent, Belgium, 62(4b), 1665-1672
- 6 Al-Ghusain, I.A., Huang, J., Hao, O.J. and Lim, B.S.: Using pH as a real-time control parameter for waste water treatment and sludge digestion processes. *Water Science and Technology* 1994, 30(4), 159-168
- 7 Einfeldt, J.: The implementation of biological P and N removal with the bio-denitro process on a 265.000 pe treatment plant. *Water Science and Technology* 1992, 25(4/5), 161-168
- 8 Ménardiére, M. de la, Charpentier, J., Vachon, A. and Martin, G.: ORP as control parameter in a single sludge biological nitrogen and phosphorus removal activated sludge system. *Water SA* 1991, 17(2), 123-132.
- 9 Surmacz-Gorska, J., Gernaey, K., Demuynck, C., Vanrolleghem, P. and Verstraete, W.: Nitrification process control in activated sludge using oxygen uptake rate measurements. *Environmental Technology* 1995, 16, 569-577
- 10 Brouwer, H., Klapwijk, A. and Keesman, K.J.: Modelling and control of activated sludge plants on the basis of respirometry. *Water Science and Technology* 1994, 30(4), 265-274.
- 11 Kappeler, J. and Gujer, W.: Estimation of kinetic parameters of heterotrophic biomass under aerobic conditions and characterisation of wastewater for activated sludge modelling. *Water Science and Technology* 1992, 25(6), 125-139.
- 12 Spanjers, H. and Keesman, K.J.: Identification of wastewater biodegradation kinetics. *Proc. 3rd IEEE Conf. on Control Appl.* 1994, Glasgow, UK, 1011-1016.
- 13 Spanjers, H. and Vanrolleghem, P.: Respirometry as a tool for rapid characterisation of wastewater and activated sludge. *Water Science and Technology* 1995, 31(2), 105-114.
- 14 Gernaey, K., Vanrolleghem, P. and Verstraete, W.: On-line estimation of *Nitrosomonas* kinetic parameters in activated sludge samples using titration in-sensor-experiments. *Water Research* 1998, 32(1), 71-80.
- 15 Zhao, H., Isaacs, S.H., Sjøberg, H. and Kümmel, M.: Nonlinear optimal control of an alternating activated sludge process in a pilot plant. *J. Proc. Cont.* 1994, 4(1), 33-43.
- 16 Lukasse, L.J.S., Keesman, K.J., Straten, G. van.: Identification for model predictive control of biotechnological processes, case study: nitrogen removal in an activated sludge process. *Proc. 11th IFAC symposium on System Identification*, Fukuoka, Japan, 1997, 3, 1525-1530
- 17 Henze, M., Grady jr., C.P.L., Gujer, W., Marais, G.v.R., Matsuo, T. IAWQ Scientific and Technical Report no. 1, IAWQ, London, UK, 1987
- 18 Lewis, F.L. 'Optimal Control.' John Wiley & Sons, New York, 1986, pp. 64
- 19 Ljung, L., Söderström, T. 'Theory and Practice of recursive identification.' MIT Press, Cambridge, Mass., 1983
- 20 Young, P. 'Recursive estimation and time-series analysis, an introduction.' Springer-Verlag, Berlin, 1984
- 21 Kwakernaak, H., Sivan, R. 'Linear optimal control systems.' John Wiley & Sons, New York, 1972, pp. 367.

3.10 Appendix 1, stability characteristics of the Kalman filter applied to unobservable systems.

Any system of the form

$$\mathbf{y}(k+1) = \mathbf{A}\mathbf{y}(k) + \mathbf{X}'(k)\boldsymbol{\theta}'(k) \quad (\text{A.1})$$

with $\mathbf{X}'(k)$ not full column rank, is equivalent to

$$\mathbf{y}(k+1) = \mathbf{A}\mathbf{y}(k) + \mathbf{X}(k)\boldsymbol{\theta}(k) \quad (\text{A.2})$$

with

$$\mathbf{X}(k) = [\mathbf{X}_1(k) \quad \mathbf{0}] \quad (\text{A.3})$$

where $\mathbf{X}_1(k) \in \mathbb{R}^{n \times q}$ has full column rank. $\mathbf{X}(k)\boldsymbol{\theta}(k)$ follows from $\mathbf{X}'(k)\boldsymbol{\theta}'(k)$ by singular value decomposition of $\mathbf{X}'(k)$:

$$\mathbf{X}'(k) = \mathbf{U}(k)\boldsymbol{\Sigma}(k)\mathbf{V}^T(k) \quad (\text{A.4})$$

Substitute this in $\mathbf{X}'(k)\boldsymbol{\theta}'(k)$ to get

$$\mathbf{X}'(k)\boldsymbol{\theta}'(k) = \mathbf{U}(k)\boldsymbol{\Sigma}(k)\mathbf{V}^T(k)\boldsymbol{\theta}'(k) \quad (\text{A.5})$$

and define

$$\mathbf{X}(k) := \mathbf{U}(k)\boldsymbol{\Sigma}(k) = [\mathbf{X}_1(k) \quad \mathbf{0}] \quad (\text{A.6})$$

and

$$\boldsymbol{\theta}(k) := \mathbf{V}^T(k)\boldsymbol{\theta}'(k) \quad (\text{A.7})$$

By partitioning the Jacobian \mathbf{X} according to eqn. A.3 the parameter random walk model in eqn. 7 can be divided in an observable subsystem with Jacobian \mathbf{X}_1 and an unobservable subsystem with Jacobian $\mathbf{0}$. Due to the equivalence of $\mathbf{X}(k)\boldsymbol{\theta}(k)$ and $\mathbf{X}'(k)\boldsymbol{\theta}'(k)$, everything that applies to the system in eqn. A.2 applies to all systems with non-full column rank Jacobians.

The Kalman filter based estimator has the form

$$\begin{aligned} \hat{\boldsymbol{\theta}}(k) &= \hat{\boldsymbol{\theta}}(k-1) + \mathbf{L}(k)\boldsymbol{\varepsilon}(k, \hat{\boldsymbol{\theta}}(k-1)) \\ \mathbf{L}(k) &= \mathbf{P}(k-1)\mathbf{X}^T(k)\{\mathbf{R}(k) + \mathbf{X}(k)\mathbf{P}(k-1)\mathbf{X}^T(k)\}^{-1} \\ \mathbf{P}(k) &= \mathbf{P}(k-1) + \mathbf{Q}(k) - \mathbf{P}(k-1)\mathbf{X}^T(k)\{\mathbf{R}(k) + \mathbf{X}(k)\mathbf{P}(k-1)\mathbf{X}^T(k)\}^{-1}\mathbf{X}(k)\mathbf{P}(k-1) \end{aligned} \quad (\text{A.8})$$

In the sequel the time arguments do not change, hence they are omitted for brevity. Let

$$\mathbf{E} = \{\mathbf{R} + \mathbf{X}\mathbf{P}\mathbf{X}^T\}^{-1}$$

By partitioning the Jacobian \mathbf{X} according to eqn. A.3 \mathbf{E} can be written as

$$\mathbf{E} = \{\mathbf{R} + [\mathbf{X}_1 \quad \mathbf{0}] \begin{bmatrix} \mathbf{P}_{11} & \mathbf{P}_{12} \\ \mathbf{P}_{21} & \mathbf{P}_{22} \end{bmatrix} \begin{bmatrix} \mathbf{X}_1^T \\ \mathbf{0} \end{bmatrix}\}^{-1} = \{\mathbf{R} + \mathbf{X}_1\mathbf{P}_{11}\mathbf{X}_1^T\}^{-1}$$

Consequently the gain matrix $\mathbf{L}(k)$ is given by

$$\mathbf{L} = \mathbf{P}\mathbf{X}^T\mathbf{E} = \begin{bmatrix} \mathbf{P}_{11} & \mathbf{P}_{12} \\ \mathbf{P}_{21} & \mathbf{P}_{22} \end{bmatrix} \begin{bmatrix} \mathbf{X}_1^T \\ \mathbf{0} \end{bmatrix} \mathbf{E} = \begin{bmatrix} \mathbf{P}_{11}\mathbf{X}_1^T \\ \mathbf{P}_{21}\mathbf{X}_1^T \end{bmatrix} \{\mathbf{R} + \mathbf{X}_1\mathbf{P}_{11}\mathbf{X}_1^T\}^{-1}$$

It will be shown in the sequel that $\mathbf{P}_{21}(k) = \mathbf{P}_{12}^T(k) = \mathbf{0}$ for all k , under the hardily-limiting assumption that $\mathbf{Q}_{21}(0) = \mathbf{Q}_{12}^T(0) = \mathbf{0}$ and $\mathbf{P}_{21}(0) = \mathbf{P}_{12}^T(0) = \mathbf{0}$. If $\mathbf{P}_{21} = \mathbf{P}_{12}^T = \mathbf{0}$ the above equation can be further simplified to

$$\mathbf{L}(k) = \begin{bmatrix} \mathbf{P}_{11}(k-1)\mathbf{X}_1^T(k)\{\mathbf{R}(k) + \mathbf{X}_1(k)\mathbf{P}_{11}(k-1)\mathbf{X}_1^T(k)\}^{-1} \\ \mathbf{0} \end{bmatrix} \quad (\text{A.9})$$

So the system equations can always be brought in such a form that the unobservable parameters remain just constant at their initial value, due to the zeros in gain matrix $\mathbf{L}(k)$.

To evaluate the discrete time Riccati equation

$$\mathbf{P}(k) = \mathbf{P}(k-1) + \mathbf{Q}(k) - \mathbf{P}(k-1)\mathbf{X}^T(k)\{\mathbf{R}(k) + \mathbf{X}(k)\mathbf{P}(k-1)\mathbf{X}^T(k)\}^{-1}\mathbf{X}(k)\mathbf{P}(k-1)$$

at first matrix partitioning is used to get

$$\mathbf{P}\mathbf{X}^T = \begin{bmatrix} \mathbf{P}_{11} & \mathbf{P}_{12} \\ \mathbf{P}_{21} & \mathbf{P}_{22} \end{bmatrix} \begin{bmatrix} \mathbf{X}_1^T \\ \mathbf{0} \end{bmatrix} = \begin{bmatrix} \mathbf{P}_{11}\mathbf{X}_1^T \\ \mathbf{0} \end{bmatrix} \quad (\text{A.10})$$

and

$$\mathbf{X}\mathbf{P} = \begin{bmatrix} \mathbf{X}_1 & \mathbf{0} \end{bmatrix} \begin{bmatrix} \mathbf{P}_{11} & \mathbf{P}_{12} \\ \mathbf{P}_{21} & \mathbf{P}_{22} \end{bmatrix} = \begin{bmatrix} \mathbf{X}_1\mathbf{P}_{11} & \mathbf{0} \end{bmatrix} \quad (\text{A.11})$$

Hence

$$\mathbf{P}\mathbf{X}^T\{\mathbf{R} + \mathbf{X}\mathbf{P}\mathbf{X}^T\}^{-1}\mathbf{X}\mathbf{P} = \begin{bmatrix} \mathbf{P}_{11}\mathbf{X}_1^T \\ \mathbf{0} \end{bmatrix} \{\mathbf{R} + \mathbf{X}_1\mathbf{P}_{11}\mathbf{X}_1^T\}^{-1} \begin{bmatrix} \mathbf{X}_1\mathbf{P}_{11} & \mathbf{0} \end{bmatrix} = \begin{bmatrix} \mathbf{P}_{11}\mathbf{X}_1^T(\mathbf{R} + \mathbf{X}_1\mathbf{P}_{11}\mathbf{X}_1^T)^{-1}\mathbf{X}_1\mathbf{P}_{11} & \mathbf{0} \\ \mathbf{0} & \mathbf{0} \end{bmatrix} \quad (\text{A.12})$$

Substituting this result in the Riccati equation yields

$$\mathbf{P}(k) = \mathbf{P}(k-1) + \mathbf{Q}(k) - \begin{bmatrix} \mathbf{P}_{11}(k-1)\mathbf{X}_1^T(k)\{\mathbf{R}(k) + \mathbf{X}_1(k)\mathbf{P}_{11}(k-1)\mathbf{X}_1^T(k)\}^{-1}\mathbf{X}_1(k)\mathbf{P}_{11}(k-1) & \mathbf{0} \\ \mathbf{0} & \mathbf{0} \end{bmatrix} \quad (\text{A.13})$$

Conclusion: if $\mathbf{Q}_{21}(0) = \mathbf{Q}_{12}^T(0) = \mathbf{0}$ and $\mathbf{P}_{21}(0) = \mathbf{P}_{12}^T(0) = \mathbf{0}$ then 1) $\mathbf{P}_{21}(k) = \mathbf{P}_{12}^T(k) = \mathbf{0}$ for all k and 2) $\mathbf{P}_{22}(k) = \mathbf{P}_{22}(0) + k\mathbf{Q}_{22}$. Hence, the elements of the block-diagonal matrix \mathbf{P}_{22} in \mathbf{P} associated with the unobservable parameters increase linear in time. In this paper 10 is the maximum value of the diagonal elements of \mathbf{Q}_{22} , hence it takes $10^6/10 = 10^5$ sampling intervals before the largest element of \mathbf{P}_{22} reaches the value 10^6 . In case of sampling interval 5 min this is as long as 1 year.

4 Optimal control of N-removal in ASP's[†]

4.1 Abstract

Optimisation of the operation strategy of N-removing activated sludge processes (ASP's) contributes to improved effluent quality and/or costs savings. This paper deals with the development of an aeration strategy yielding optimal N-removal in continuously mixed, continuously fed ASP's. First, optimal control theory is applied to the generally accepted ASM no.1 model (Henze *et al.*, 1987). This study reveals that, from an N-removal point of view, both alternating nitrification/denitrification and simultaneous nitrification/denitrification at limiting DO-levels might be optimal, depending on the uncertain oxygen half-saturation constants of autotrophic and heterotrophic biomass. Hence, taking into consideration the risk of sludge bulking at limiting DO-levels, an alternating anoxic/aerobic strategy is favoured. A Receding Horizon Optimal Control (RHOC) strategy using NH_4 and NO_3 measurements is developed, enabling feedback control of the alternation between anoxic and aerobic phases with the explicit objective of optimal N-removal. Simple rules are given for straightforward tuning of this controller. The controller successfully passed several tests both in simulation and in application to a pilot plant continuously fed with presettled domestic wastewater.

Keywords: ASM no. 1 model; denitrification; nitrification; receding horizon optimal control; predictive control

4.2 Introduction

Usually aeration tanks in the Netherlands are carrousel with hydraulic characteristics somewhere between continuously mixed and plug flow. Most existing carrousel were designed for COD-removal and nitrification, but are now faced with the legislative demand to reduce the yearly averaged total effluent nitrogen to at most 10 mg/l by the year 1999. Part of the required denitrification capacity can be introduced by the creation of anoxic phases in the aeration tank.

The objective of this paper is to develop an aeration strategy for optimal N-removal in continuously mixed, continuously fed plants. This is regarded as an intermediate step in the development of such control strategies for carrousel. First optimal control theory is applied to the ASM no.1 model (Henze *et al.*, 1987) to study whether alternating nitrification/denitrification is more optimal than simultaneous nitrification/ denitrification. From the results of this simulation study a much simpler on-line implementable receding horizon optimal control (RHOC) strategy is extracted. The merit of RHOC is that it on-line optimises an objective criterion and straightforwardly handles constraints on

[†] published by Lukasse L.J.S., Keesman K.J., Klapwijk A. and Straten G. van in *Wat. Sci. Tech.*, 38(3), 1998, pp. 255-262.

both in- and outputs. By expressing the plant economy in the objective criterion a natural relation between plant control and plant economy emerges. This simple RHOC controller is successfully tested both in simulation and on a continuously mixed pilot plant, continuously fed with presettled municipal wastewater.

4.3 Optimal control of nitrogen removal according to ASM no. 1

According to ASM no.1 (Henze *et al.*, 1987) on a short time scale nitrification/denitrification are mainly affected by the concentrations of S_{NH} , S_{NO} , S_O and S_S (see App. 1 for all symbols in this paper). In this study S_O is treated as control input, in the implementation phase it will be used as set-point for an earlier developed slave S_O -controller (Haarsma and Keesman, 1995). To enable the formulation of an optimal control problem the dynamic mass balances of the three other quantities are required. These can be extracted from ASM no. 1. After some simplifications one gets

$$\frac{dS_{NH}}{dt} = \frac{q_{in}}{V} (f \cdot S_{NH,in} - S_{NH}) - i_{XB} \hat{\mu}_H \frac{S_S}{K_S + S_S} \frac{S_O}{K_{O,H} + S_O} X_{B,H} - i_{XB} \hat{\mu}_H \frac{S_S}{K_S + S_S} \frac{K_{O,H}}{K_{O,H} + S_O} \frac{S_{NO}}{K_{NO} + S_{NO}} \eta_R X_{B,H} \quad (1)$$

$$- (i_{XB} + \frac{1}{Y_A}) \hat{\mu}_A \frac{S_{NH}}{K_{NH} + S_{NH}} \frac{S_O}{K_{O,A} + S_O} X_{B,A}$$

$$\frac{dS_{NO}}{dt} = -\frac{q_{in}}{V} S_{NO} - \frac{1 - Y_H}{2.86 Y_H} \hat{\mu}_H \frac{S_S}{K_S + S_S} \frac{K_{O,H}}{K_{O,H} + S_O} \frac{S_{NO}}{K_{NO} + S_{NO}} \eta_R X_{B,H} \quad (2)$$

$$+ \frac{1}{Y_A} \hat{\mu}_A \frac{S_{NH}}{K_{NH} + S_{NH}} \frac{S_O}{K_{O,A} + S_O} X_{B,A}$$

$$\frac{dS_S}{dt} = \frac{q_{in}}{V} (S_{S,in} - S_S) - \frac{1}{Y_H} \hat{\mu}_H \frac{S_S}{K_S + S_S} \left\{ \frac{S_O}{K_{O,H} + S_O} + \frac{K_{O,H}}{K_{O,H} + S_O} \frac{S_{NO}}{K_{NO} + S_{NO}} \eta_R \right\} X_{B,H} \quad (3)$$

$$+ k_h \frac{X_S / X_{B,H}}{K_X + X_S / X_{B,H}} \left\{ \frac{S_O}{K_{O,H} + S_O} + \frac{K_{O,H}}{K_{O,H} + S_O} \frac{S_{NO}}{K_{NO} + S_{NO}} \eta_h \right\} X_{B,H}$$

In the ASM no. 1 model a wide range of values is given for some of the parameters, in this study the average values were used. Notice that in eqn. 1 $S_{NH,in}$ is multiplied with a factor f . This is based on the knowledge that a certain percentage of influent nitrogen is entrapped in organic components (in this study's pilot plant $\pm 20\%$, hence $f = 1.25$), and the assumption that this is all ammonified. This simplification allows for the omission of a balance for soluble biodegradable organic nitrogen. Also the slower and largely unknown dynamics of X_S , $X_{B,A}$ and $X_{B,H}$ have been neglected by assuming these processes to be in steady state. The remaining three differential equations above describe the major part of the nitrogen dynamics on a time scale of days.

To find the aeration strategy that yields optimal N-removal in continuously mixed aeration tanks whose dynamics are described by eqns. 1-3, the following optimal control problem needs to be solved:

$$\min_{S_O} J(S_O) = \int_{t_0}^{t_f} w \cdot |S_{NH,R} - S_{NH}| + |S_{NO,R} - S_{NO}| dt \quad (4)$$

subject to the system dynamics (eqns. 1-3), the control input constraints

$$0 \leq S_O(t) \leq 3 \quad (\text{g/m}^3) \quad (5)$$

and the input disturbances q_{in} and $S_{NH,in}$.

The control input minimum ($S_O = 0$) is a physical limitation. The control input maximum ($S_O = 3$ mg/l) will allow for oxygen abundance in the reactor, it is generally known that higher S_O will not have any effect. The weight w and the setpoints $S_{NH,R}$ and $S_{NO,R}$ are tuning parameters. In this study $w = 3$ and $S_{NH,R} = S_{NO,R} = 0$. That tuning expresses that a good effluent quality is achieved if both S_{NH} and S_{NO} are low, and that low S_{NH} is more important than low S_{NO} . The case of total-N minimisation can be obtained by selecting $w = 1$ and $S_{NH,R} = S_{NO,R} = 0$. To gain insight in the characteristic optimal control pattern it suffices to use initial time $t_0 = 0$ and final time $t_f = 24$ h, as the dominant disturbance inputs (q_{in} , $S_{NH,in}$) exhibit diurnal cycles.

The solution to this highly non-linear optimal control problem turned out to suffer from (numerically induced) local minima. Moreover, the optimal aeration strategy appeared to be highly dependant on the values of $K_{O,A}$ and $K_{O,H}$. Within the $K_{O,A}$ and $K_{O,H}$ ranges given in the ASM no. 1 model both an aeration strategy aimed at simultaneous and an aeration strategy aimed at alternating nitrification/denitrification may be optimal. E.g. for $K_{O,A} = 1.3$ and $K_{O,H} = 0.1$ mg/l a predominantly alternating aeration strategy is optimal (Fig. 1), while the optimal solution for $K_{O,A} = 1.3$ and $K_{O,H} = 0.2$ mg/l is predominantly aimed at simultaneous nitrification/denitrification at $S_O \approx 0.4$ mg/l (not shown).

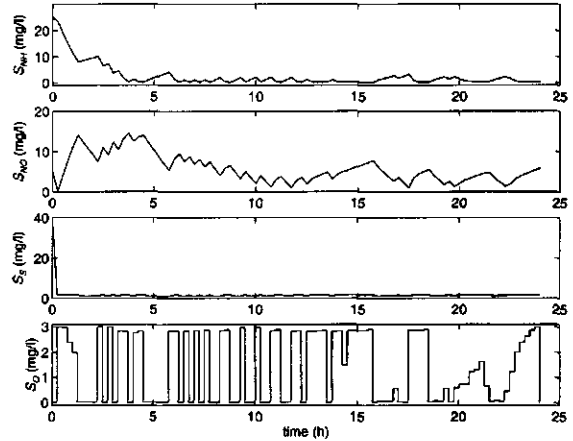


Fig. 1, optimal aeration strategy for ASM no. 1 model with $K_{O,A} = 1.3$ and $K_{O,H} = 0.1$ mg/l.

Although no conclusion can be drawn from the optimal aeration strategies for the ASM no.1 model due to uncertainty in $K_{O,A}$ and $K_{O,H}$, there remains a strong motivation to favour alternating instead of simultaneous nitrification/denitrification: risk of sludge bulking at limiting S_O -levels (van Leeuwen, 1990). Once the choice for alternating nitrification/denitrification has been made, the remaining problem is to make the optimal control strategy suitable for on-line implementation.

4.4 Receding horizon optimal control implementation

The disadvantage of controlling uncertain systems by means of non-linear optimal control theory is that it is an open-loop control strategy. To enable on-line implementation there is a need to introduce feedback, requiring fast computation of the optimal controls. Feedback is introduced by em-

ploying Receding Horizon Optimal Control (RHOC) (Mayne and Michalska, 1990). The basic RHOC approach solves at each sampling instant $k \in \{0, 1, 2, \dots\}$ the optimal control problem with $t_0 = kT$ and $t_f = (k+H)T$ ($H =$ prediction horizon) and implements only $u^*(k)$. At $k+1$ the new output $y(k+1)$, which will deviate from the expected $\hat{y}(k+1|k)$, is measured and the RHOC problem is solved again, with $t_0 = (k+1)T$, $t_f = (k+H+1)T$ and $y(k+1)$ as initial condition. Obviously optimisation over the relatively small time interval $[kT, (k+H)T]$ largely reduces the computational demand. A second reduction in computation time is obtained by imposing the constraint $S_O(k) \in \{0, 3\}$, i.e. requiring alternating aeration.

Finally, a third reduction of computation time is obtained by replacing the complex ASM no.1 model (eqns. 1-3) by a much simpler discrete time model:

$$\begin{bmatrix} S_{NH}(k+1) \\ S_{NO}(k+1) \end{bmatrix} = e^{-\frac{q_{in}T}{V}} \begin{bmatrix} S_{NH}(k) \\ S_{NO}(k) \end{bmatrix} + \frac{e^{-\frac{q_{in}T}{V}} - 1}{-\frac{q_{in}}{V}} \begin{bmatrix} r_{amm} - r_{NH} \\ r_{NH} + r_{NO} \end{bmatrix} u + \begin{bmatrix} \frac{q_{in}}{V} S_{NH,in} \\ -r_{NO} \end{bmatrix} \quad (6)$$

$$r_{NH} = \begin{cases} r_{NH,max} & S_{NH} > 0 \\ \frac{q_{in}}{V} S_{NH,in} + r_{amm} & S_{NH} = 0 \end{cases} \quad (7)$$

$$r_{NO} = \begin{cases} r_{NO,max} & S_{NO} > 0 \\ 0 & S_{NO} = 0 \end{cases} \quad (8)$$

$$\begin{bmatrix} y_1(k) \\ y_2(k) \end{bmatrix} = \begin{bmatrix} S_{NH}(k-\Delta) \\ S_{NO}(k-\Delta) \end{bmatrix} \quad (9)$$

with

$$u \in \{0,1\} \text{ i.e. } \{\text{anoxic } (S_{O,R} = 0), \text{ aerobic } (S_{O,R} = 3 \text{ mg/l})\}$$

$$S_{O,R} \text{ (mg/l)} = \text{dissolved oxygen } (S_O) \text{ setpoint for slave } S_O\text{-controller, control input}$$

This model has been identified in earlier work (Lukasse *et al.*, 1997b). Be aware that the model is only valid for $u \in \{0,1\}$. The value $S_{O,R} = 3$ mg/l ensures total aerobicity during aerated periods. This value itself could be optimised as well, but that is beyond the goal of this paper. Contrary to ASM no. 1 the above model does not contain the unmeasurable S_5 .

Now at time kT the RHOC problem for N-removal is formulated as

$$\min_u J(u) = \sum_{i=1}^H \left\| \begin{bmatrix} w \cdot (S_{NH,R} - S_{NH}(k+i)) \\ S_{NO,R} - S_{NO}(k+i) \end{bmatrix} \right\| \quad (10)$$

subject to the system dynamics (eqns. 6-9), the control input constraints

$$u(k+i-1) \in \{0,1\} \quad i \in [1, H] \quad (11)$$

and the expected input disturbances $q_{in}(k+i-1)$ and $S_{NH,in}(k+i-1)$, $i = 1, \dots, H$. Eqn. 10 is just the ordinary Euler discretisation of

$$\min_u J(u) = \frac{1}{T} \int_{kT}^{(k+H)T} w \cdot |S_{NH,R} - S_{NH}(t)| + |S_{NO,R} - S_{NO}(t)| dt \quad (12)$$

whose integrand is equal to the one used in eqn. 4.

The number of possible control input trajectories over the horizon H is 2^H . The optimal control $u^*(k)$ is determined as the first element of the control trajectory resulting in the lowest objective criterion by just computing the objective criterion value for all 2^H possible control trajectories. The attractive feature of this approach is that a globally optimal solution of eqn. 10 is guaranteed. Moreover the required computation time is known in advance, contrary to e.g. gradient and Gauss-Newton search algorithms. If the computation time is less than the sampling interval the RHOC controller is on-line implementable. It should be stressed here that this has been made possible by largely simplifying the ASM no.1 model and introducing the constraint $u \in \{0, 1\}$.

The RHOC controller has five tuning parameters: T , w , $S_{NH,R}$, $S_{NO,R}$ and H . In this study the sampling interval T is selected equal to the measurement time delay (20 min), as this is roughly the smallest time span at which the aeration in full scale plants is alternated and no roundoff error is introduced when expressing the time delay in whole sampling intervals (Δ in eqn. 9). Obviously, the smaller T the better S_{NH}/S_{NO} may be controlled to their setpoints. However too short sampling intervals make no sense and a lower limit is imposed by the S_O -dynamics.

It is impossible to control both S_{NH} and S_{NO} to their setpoints as their consumption/production are completely coupled (eqn. 6). The positive weight w is a handle to give preference to either S_{NH} or S_{NO} -control. To demonstrate the effect of w on the closed-loop behaviour the fact is invoked that for any pair of 2-dimensional vectors (\mathbf{b}, \mathbf{c})

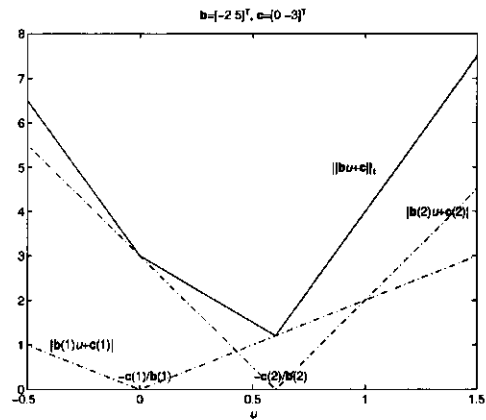


Fig. 2, the 1-norm of $bu+c$ as a function of u .

$$\arg \min_u \|\mathbf{b}u + \mathbf{c}\|_1 \equiv \arg \min_u |\mathbf{b}(i)u + \mathbf{c}(i)| \tag{13}$$

where $\mathbf{b}(i) = \max(|\mathbf{b}|)$. To understand this equality see Fig. 2. Substituting eqn. 6 in the RHOC objective criterion (eqn. 10) with $H = 1$ gives

$$\min_{u(k)} J(u) = \left\| \begin{bmatrix} w \cdot S_{NH,R} \\ S_{NO,R} \end{bmatrix} - e^{-\frac{q_{in}T}{V}} - 1 \begin{bmatrix} w \cdot (r_{amm} - r_{NH}) \\ r_{NH} + r_{NO} \end{bmatrix} u(k) - e^{-\frac{q_{in}T}{V}} - 1 \begin{bmatrix} w \frac{q_{in}}{V} S_{NH,in} \\ -r_{NO} \end{bmatrix} - e^{-\frac{q_{in}T}{V}} \begin{bmatrix} w \cdot S_{NH}(k) \\ S_{NO}(k) \end{bmatrix} \right\|_1$$

in which the \mathbf{b} -vector of eqn. 13 can be recognised as

$$\mathbf{b} = \begin{bmatrix} w \cdot (r_{amm} - r_{NH}) \\ r_{NH} + r_{NO} \end{bmatrix} \tag{14}$$

From eqn. 13 it follows that $S_{NH,R} - S_{NH}$ is minimised if $\mathbf{b}(1) > \mathbf{b}(2)$, and $S_{NO,R} - S_{NO}$ is minimised if $\mathbf{b}(1) < \mathbf{b}(2)$. As r_{NH} and r_{NO} depend on S_{NH} and S_{NO} (eqns. 7-8) there are multiple values of w for which $\mathbf{b}(1)$ equals $\mathbf{b}(2)$. It is easily seen that these are given by

$$w_c = \frac{r_{NH,max} + r_{NO,max}}{|r_{amm} - r_{NH,max}|} \quad S_{NH}, S_{NO} > 0 \tag{15}$$

$$w_l = \frac{r_{NH,max}}{r_{amm} - r_{NH,max}} \quad S_{NH} > 0, S_{NO} = 0 \tag{16}$$

$$w_u = \frac{\frac{q_{in}}{V} S_{NH,in} + r_{amm} + r_{NO,max}}{\frac{q_{in}}{V} S_{NH,in}} \quad S_{NH} = 0, S_{NO} > 0 \tag{17}$$

with usually $w_l < w_c < w_u$. The RHOC behaviour as a function of w is summarised in Table 1. For notational convenience it was chosen to use $H = 1$ in the above analysis. However, it holds for any H as the optimal control solution is independent of H (Fig. 3). Simulations for different combinations of $r_{NO,max}$, $r_{NH,max}$, r_{amm} and q_{in} confirmed correctness of Table 1.

From Table 1 it is seen that if the setpoint for the well-controlled output is zero it should hold that $w_l < w < w_u$, otherwise $S_{O,R}$ remains in one extreme. No plant operator will need the RHOC controller to obtain that situation.

Table 1, effect of weight w on RHOC behaviour.

w	RHOC behaviour
$0 < w < w_c$	S_{NO} well-controlled
$w > w_c$	S_{NH} well-controlled
$0 < w < w_l \wedge S_{NO,R} = 0$	S_{NO} well-controlled, no aeration at all
$w > w_u \wedge S_{NH,R} = 0$	S_{NH} well-controlled, no anoxicity at all

As is shown above either S_{NH} or S_{NO} is controlled to its setpoint, while the other follows as a consequence. Usually one will select both setpoints as 0, as this is every operator's ideal. In most cases one will choose to control S_{NH} to its setpoint by selecting $w > w_c$. One can imagine situations in which it is preferable to select a setpoint larger than zero for the well-controlled state. For example in a reactor with post-aeration and $w > w_c$ a setpoint $S_{NH,R} > 0$ will exchange some nitrification for denitrification in the reactor, while the remaining S_{NH} will be removed during post-aeration.

The last tuning parameter to be set is the prediction horizon H . Generally RHOC yields a suboptimal solution for the full horizon optimal control problem, even when process behaviour and future disturbance inputs are exactly known (Bitmead *et al.*, 1990). In absence of model-plant mismatch it holds that the larger H the closer the RHOC solution approaches the full horizon optimal solution, thus pleading for large H . On the other hand H should be as small as possible because 1) the com-

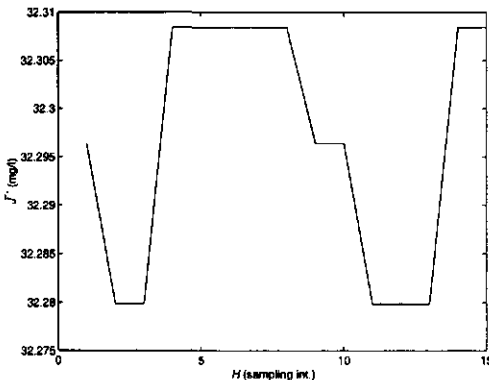


Fig. 3, J^* as a function of H with $S_{NH,in}$ the sine wave of Fig. 4 and q_{in} constant.

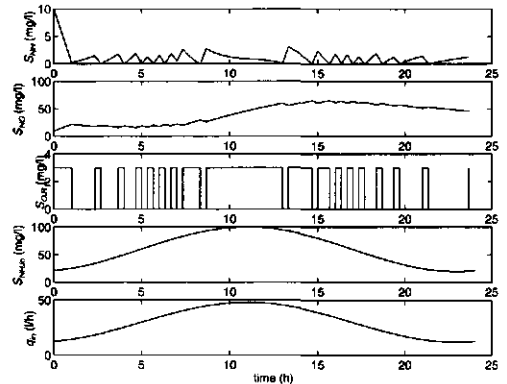


Fig. 4, RHOC in simulation with $S_{NH,R} = S_{NO,R} = 0$ and $w_c < w < w_u$.

putational burden increases exponentially with H and 2) larger H requires inclusion of more-step-ahead predictions and hence more uncertainty. To investigate the effect of H in this specific application the controlled process is simulated for H ranging from 1 to 15 sampling intervals, with the sine wave pattern in Fig. 4 for $S_{NH,in}$. This has been repeated for a whole range of combinations w , $S_{NH,R}$ and $S_{NO,R}$. It turns out that for constant q_{in} RHOC yields the globally optimal solution to the full horizon optimal control problem as local optima are ruled out by solving the RHOC problem by enumeration and reducing H does not increase \bar{J}^* (Fig. 3), where $\bar{J}^* = J^*$ divided by the number of samples. Complementary simulations unravelled that this no longer holds in case of an *a priori* known sine wave pattern for q_{in} . However, knowledge of future q_{in} values is usually poor. Therefore it was decided to stick to the objective criterion in eqn. 10 with $H = 1$, as increasing H only increases the computational burden. A characteristic simulation of the thus controlled process, with sine waves for both $S_{NH,in}$ and q_{in} , is shown in Fig. 4.

4.5 Pilot plant results

The controller has been applied to a pilot scale ASP with continuously mixed aeration tank ($V = 475$ l, $q_{in} = 45$ l/h, MLSS = 3.5 g/l), continuously fed with presettled municipal wastewater. S_{NH} and S_{NO} in the aeration tank are measured using SKALAR auto-analysers type SA 9000. S_O is controlled at a setpoint alternating between 0 and 3 mg/l using the airflow as manipulated variable. Two generated data sets are shown in Fig. 6 and 5 (be aware of the 20 min measurement time delay). The aerated periods with $S_{NH} = 0$ in Fig. 6 are sub-optimal, as aerating while $S_{NH} = 0$ yields $r_{NH} < r_{NH,max}$ and ought to be exchanged for anoxic periods like done in simulation (Fig. 4). It is very likely that these periods are caused by a rather large model-plant discrepancy during that experiment. In the experiment of Fig. 5 the model seems to be better, as no anoxicity appears while $S_{NO} = 0$.

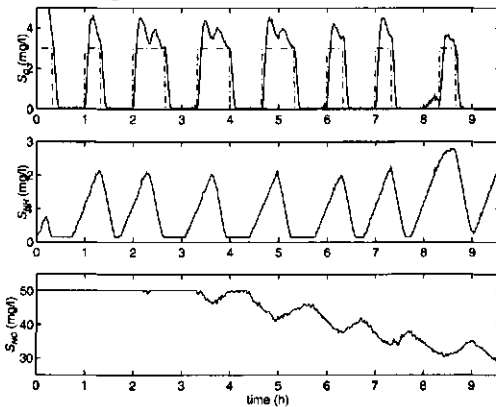


Fig. 6, RHOC applied to pilot plant with $S_{NH,R} = S_{NO,R} = 0$ and $w_c < w < w_u$, S_{NO} out of range for $t < 3.5$.

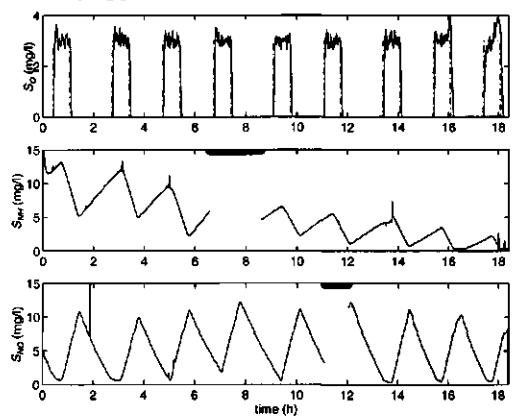


Fig. 5, RHOC applied to pilot plant with $S_{NH,R} = S_{NO,R} = 0$ and $w_l < w < w_c$, fat overbars indicate analyser calibration.

4.6 Discussion

In this RHOC problem there are no limitations to the objective criterion J . Therefore J should just be chosen as close as possible to the truly economical objective of plant operation. This was the aim of selecting J according to eqn. 10. As the currently available knowledge in this field is limited, better alternatives may well emerge in the near future. Even the addition of constraints on S_{NH} and/or S_{NO} is straightforward, these might well appear as a result of authority-imposed limits on the effluent quality. The only drawback of altering the current RHOC formulation is that the nice property of global optimality for $H = 1$ might get lost. Yet this is not too serious as it took only 10.5 min to compute the optimal control $u^*(k)$ with $H = 15$ in Matlab 4.2c running on a 166 MHz PC. This computation time is well within the 20 minutes sampling interval T and only marginally affected by J and possible constraints on S_{NH} and/or S_{NO} .

In simulation it was observed that, if accurate knowledge of future q_{in} variations is available, enlarging H improves controller performance in terms of eqn. 10, as mentioned before. This is probably caused by exploiting moments of high dilution rates as a means to rapidly discard the highest weighted process output. This statement is supported by simulation results that showed the flow-weighted criterion

$$\min_u J(u) = \sum_{i=1}^H q_{in}(k+i) \left\| \begin{array}{c} w \cdot (S_{NH,R} - S_{NH}(k+i)) \\ S_{NO,R} - S_{NO}(k+i) \end{array} \right\| \quad (18)$$

to be much less sensitive for H , in case of known future q_{in} variations. This makes the above objective criterion with large H appealing on precedent that knowledge of future q_{in} values is available. Replacing the objective criterion (eqn. 10) by this flow-weighted one has no further implications for the RHOC controller.

The RHOC success depends on the model accuracy. The model accuracy may be improved by fine-tuning the model to the specific plant under control and accounting for the large system time-variance. This requires recursive identification of the plant. A recursive identification scheme with encouraging results is presented in Lukasse *et al.* (in press b). The successful integration of the developed RHOC and recursive identification method is presented in Lukasse *et al.* (1997a). See Lukasse *et al.* (in press a) for a comparison by means of simulations between the performance of this adaptive RHOC and more traditional controllers.

4.7 Conclusions

A readily implementable aeration control strategy aiming at optimal N-removal in continuously mixed, continuously fed ASP's has been developed. It showed good performance both in simulation and during application to a pilot plant continuously fed with presettled domestic wastewater. Contrary to the general case, this RHOC application yields globally optimal control with a prediction horizon of only one sampling interval. In this paper the objective criterion (eqn. 4) is formulated such that either S_{NH} or S_{NO} is controlled to its setpoint, depending on the weight w . The other follows as a consequence. Analytical expressions for the thresholds of w , determining which one is well controlled, are given in Table 1. Replacement of the current objective criterion (eqn. 4) by any

other functional of q_{in} , S_{O_2} , S_{NH} and S_{NO} and the introduction of constraints on S_{NH} or S_{NO} may demand for a larger prediction horizon H , but does not hamper the applicability of the method. Hence, if better knowledge about the objectives/costs of N-removing plants emerges it can easily be incorporated in the RHOC controller.

With the $K_{O,A}$ and $K_{O,H}$ ranges given in the ASM no.1 model (Henze *et al.*, 1987) both simultaneous and alternating nitrification/denitrification might be optimal in terms of N-removal. It depends on where in the given ranges the true parameters reside.

Acknowledgements: This paper contains work conducted by L.B. Suurmond during his MSc. project. M. Bloemen supported the experimental work. Financial support came from the Dutch Technology Foundation (STW) under grant no. WBI44.3275.

4.8 References

- Bitmead R.R., Gevers M. and Wertz V. (1990). *Adaptive optimal control: the thinking man's GPC*. Prentice Hall, London, U.K.
- Haarsma G.J. and Keesman K.J. (1995). Robust model predictive dissolved oxygen control. *Med. Fac. Landbouww. Univ. Gent, proc. 9th FAB*, 60(4b), Gent, Belgium, 2415-2426.
- Henze M., Grady jr. C.P.L., Gujer W., Marais G.v.R. and Matsuo T. (1987). Activated sludge model no. 1. *IAWQ Scientific and Technical Report no. 1*, IAWQ, London, Great Britain.
- Leeuwen J. van (1990). Review of oxidative control of bulking in activated sludge wastewater treatment to improve sedimentation. *South African journal of chemical engineering*, 2(1), 27-40.
- Lukasse L.J.S., Keesman K.J., Klapwijk A. and Straten G. van (1997a). Adaptive receding horizon optimal control of N-removing activated sludge processes. *Med. Fac. Landbouww. Univ. Gent, proc. 11th FAB*, 62(4b), Gent, Belgium, 1665-1672.
- Lukasse L.J.S., Keesman K.J. and Straten G. van (1997b). Identification for model predictive control of biotechnological processes, case study: nitrogen removal in an activated sludge process. *proc. 11th IFAC symposium on System Identification*, 3, Fukuoka, Japan, 1525-1530.
- Lukasse L.J.S., Keesman K.J., Klapwijk A., Straten G. van (in press a). A comparison of NH_4/NO_x control strategies for N-removing alternating ASP's. *Proc. Application of Models in Water Management (IAWQ)*, submitted to *Wat. Sci. Techn.*
- Lukasse, L.J.S., Keesman, K.J. and Straten, G. van (in press b). Recursive identification of N-removal in alternating activated sludge processes. *Journal of Process Control*.
- Mayne D.Q. and Michalska H. (1990). Receding Horizon Control of Nonlinear Systems. *IEEE Transactions on Automatic Control*, 35(7), 814-824.

4.9 Appendix 1, list of symbols

variable	value [unit]	description
$\hat{\mu}_A$	0.5 [day^{-1}]	maximum specific growth rate of autotrophs
$\hat{\mu}_H$	6.0 [day^{-1}]	maximum specific growth rate of heterotrophs

Δ	1 [sampling intervals]	20 min analysers' time delay in sampling intervals
η_g	0.8 []	correction factor for heterotr. growth under anoxic conditions
η_h	0.4 []	correction factor for hydrolysis under anoxic conditions
i_{XB}	0.086 [g N (g cell COD) ⁻¹]	mass of nitrogen per mass of COD in biomass
k_h	3.0 [g soluble COD (g cell COD) ⁻¹ day ⁻¹]	maximum specific hydrolysis rate
K_{NH}	1.0 [g NH ₄ -N/m ³]	ammonium half-saturation coefficient for autotrophic biomass
K_{NO}	0.5 [g NO ₃ -N/m ³]	nitrate half-saturation coefficient for denitrifying heterotrophs
$K_{O,A}$	0.4-2.0 [g O ₂ /m ³]	oxygen half-saturation coefficient for autotrophic biomass
$K_{O,H}$	0.01-2.0 [g O ₂ /m ³]	oxygen half-saturation coefficient for heterotrophic biomass
K_S	20.0 [g soluble COD/m ³]	RBOS half-saturation coefficient for heterotrophic biomass
K_X	0.03 [g COD (g cell COD) ⁻¹]	hydrolysis saturation ratio
q_{in}	1.0 [m ³ /day]	influent flow rate
r_{amm}	0.03 [mg/l.min]	ammonification rate (ammonium production rate)
$r_{NH,max}, r_{NH}$	0.11, .. [mg/l.min]	(maximum), ammonium consumption rate
$r_{NO,max}, r_{NO}$	0.08, .. [mg/l.min]	(maximum), nitrate consumption rate
$S_{NH,in}, S_{NH,R}, S_{NH}$	60, ..., .. [g NH ₄ -N/m ³]	(influent), (reference), NH ₄ -N concentration
$S_{NO,R}, S_{NO}$.. [g NO ₃ -N/m ³]	(reference), nitrate nitrogen concentration
$S_{O,R}, S_O$.. [g O ₂ /m ³]	(reference), dissolved oxygen concentration
$S_{S,in}, S_S$	125, .. [g soluble COD/m ³]	(influent) RBOS concentration
T	20 [min]	sampling interval
V	0.475 [m ³]	aeration tank volume
$X_{B,A}$	280 [g cell COD/m ³]	autotrophic biomass concentration
$X_{B,H}$	3220 [g cell COD/m ³]	heterotrophic biomass concentration
X_S	30 [g COD/m ³]	SBOS concentration
Y_A	0.24 [g cell COD (g N) ⁻¹]	autotrophic yield coefficient
Y_H	0.6 [g cell COD (g soluble COD) ⁻¹]	heterotrophic yield coefficient

5 Adaptive receding horizon optimal control of N-removing activated sludge processes[†]

5.1 Abstract

In this paper an adaptive Receding Horizon Optimal Controller (RHOC) for optimal N-removal in alternately aerated, continuously mixed, continuously fed activated sludge processes (ASP's) is presented. It is successfully tested both in simulation and pilot plant experiments. The RHOC approach offers an excellent opportunity to link the higher level of plant economy and the lower level of plant control by expressing the plant economy in the RHOC's objective criterion. This is an important novelty in comparison with the existing controllers for this process, which do not explicitly aim at process optimisation. Handling of constraints on both in- and outputs is straightforward. Essential for the performance of RHOC controllers is the availability of accurate predictions of near-future NH_4 and NO_x concentrations. A recursive estimator for the model parameters takes care of this. As with nearly all adaptive controllers (Aström & Wittenmark, 1989) this controller is not globally stable. But throughout many simulations and pilot plant experiments it has been learned how to prevent instability. The step-by-step control algorithm is given in section 4.

5.2 Nomenclature

variable	value [unit]	description
Δ	1 [sampling intervals], 20 [min]	analysers' time delay
$\epsilon(k k-1)$.. [mg/l mg/l]	prediction error at time kT
$\hat{\theta}(k), \theta(k)$.. [mg/l mg/l.min mg/l.min]	(estimated) parameter vector at time kT
$\hat{y}(k), y(k)$.. [mg/l mg/l]	(predicted) [$\text{NH}_4\text{-N}$ $\text{NO}_x\text{-N}$] measurement
H	.. [.]	RHOC prediction horizon
J	.. [mg/l]	RHOC objective criterion
k	.. [.]	index of sampling instants
$P(0)$..	initial parameter covariance P
Q	..	parameter random walk covariance matrix
q_{in}	.. [m^3/day]	influent flow rate
R	..	measurement noise covariance on $y(\cdot)$
$r_{\text{NH,max}}$.. [mg/l.min]	maximum ammonium consumption rate
$r_{\text{NO,max}}$.. [mg/l.min]	maximum $\text{NO}_x\text{-N}$ consumption rate
$S_{\text{NH,in}}, S_{\text{NH,R}}, S_{\text{NH}}$.., .., .. [mg $\text{NH}_4\text{-N/l}$]	(influent), (reference), $\text{NH}_4\text{-N}$ concentration
$S_{\text{NO,R}}, S_{\text{NO}}$.. [mg $\text{NO}_x\text{-N/l}$]	(reference), $\text{NO}_2\text{-N} + \text{NO}_3\text{-N}$ concentration

[†] published by L.J.S. Lukasse, K.J. Keesman, A. Klapwijk and G. van Straten in *Med. Fac. Landbouww. Univ. Gent, proc. 11th FAB*, 62(4b), 1997, Gent, Belgium, pp. 1665-1672.

$S_{O,R}, S_O$.. [mg O ₂ /l]	(reference), dissolved oxygen concentration
T	20 [min]	sampling interval
u^*, u	.. [.]	(optimal) control input at time kT
V	475 [l]	aeration tank volume
w_c, w	.. [.]	(critical) weight in RHOC objective criterion

5.3 Introduction

Usually aeration tanks in the Netherlands are carrousel with hydraulic characteristics somewhere between continuously mixed and plug flow. Most existing carrousel were designed for COD-removal and nitrification, but are now faced with the legislative demand to reduce the yearly averaged total effluent nitrogen to at most 10 mg/l by the year 1999. Part of the required denitrification capacity can be realised by creating anoxic periods in the aeration tank, as it is usually underloaded.

In current practice the alternation between aerobic and anoxic modes in alternatingly aerated ASP's is often based on timers. The currently available feedback controllers for alternatingly aerated ASP's normally employ measurements that are only capable of indicating the depletion of NH₄ and NO_x, e.g. ORP (Ménardiére *et al.*, 1991) or OUR (Surmacz-Gorska *et al.*, 1995). Recently it has been shown that more advanced operation may improve process performance (Zhao *et al.*, 1995).

This paper's objective is to develop an aeration strategy for economically optimal N-removal in continuously mixed, continuously fed plants by means of adaptive receding horizon optimal control (RHOC). This is regarded as an intermediate step in the development of such control strategies for carrousel. The merit of RHOC is that it optimises an objective criterion on-line and straightforwardly handles constraints on both in- and outputs, using model predictions. By expressing the plant economy in the objective criterion a natural relation between plant control and plant economy emerges.

The RHOC success depends strongly on the model quality. To guarantee the availability of an always up to date process model recursive identification of model parameters is required, because the nitrification/denitrification process is subject to strong diurnal and seasonal variations. These variations are due to variations in influent composition, temperature and rainfall (Metcalf & Eddy, 1979). Moreover each individual plant has a unique influent characteristic and microorganism population, to which the model is fine-tuned when using recursive identification. The model parameters are recursively estimated using a Kalman filter. The resulting adaptive RHOC controller is successfully tested both in simulation and on a continuously mixed pilot plant, continuously fed with presettled municipal wastewater.

5.4 RHOC scheme

The basic RHOC approach solves at each sampling instant k an optimal control problem with $t_0 = kT$ and $t_f = (k+H)T$ (T = sampling interval, H = prediction horizon) and implements only $u^*(k)$. At $k+1$ the new output $y(k+1)$, which will deviate from the expected $\hat{y}(k+1|k)$, is measured and the

RHOC problem is solved again, with $t_0 = (k+1)T$, $t_f = (k+H+1)T$ and $y(k+1)$ as initial condition. The RHOC control algorithm for this application is given by

$$\min_u J(u) = \sum_{i=1}^H \left\{ w \cdot |S_{NH,R} - S_{NH}(k+i)| + |S_{NO,R} - S_{NO}(k+i)| \right\} \quad (1)$$

subject to initial condition $[S_{NH}(k) \ S_{NO}(k)]^T$, the control input constraints

$$u(k+i-1) \in \{0,1\} \quad i \in [1, H] \quad (2)$$

the expected input disturbances $q_{in}(k+i-1)$, $S_{NH,in}(k+i-1)$ with $i=1, \dots, H$, and the system dynamics:

$$\begin{bmatrix} S_{NH}(k+1) \\ S_{NO}(k+1) \end{bmatrix} = e^{-\frac{q_{in}T}{V}} \begin{bmatrix} S_{NH}(k) \\ S_{NO}(k) \end{bmatrix} + \frac{e^{-\frac{q_{in}T}{V}} - 1}{-\frac{q_{in}}{V}} \begin{bmatrix} -r_{NH} \\ r_{NH} + r_{NO} \end{bmatrix} u + \begin{bmatrix} \frac{q_{in}}{V} S_{NH,in} \\ -r_{NO} \end{bmatrix} \quad (3)$$

$$r_{NH} = \begin{cases} r_{NH,max} & S_{NH} > 0 \\ \frac{q_{in}}{V} S_{NH,in} & S_{NH} = 0 \end{cases} \quad (4)$$

$$r_{NO} = \begin{cases} r_{NO,max} & S_{NO} > 0 \\ 0 & S_{NO} = 0 \end{cases} \quad (5)$$

$$\begin{bmatrix} y_1(k) \\ y_2(k) \end{bmatrix} = \begin{bmatrix} S_{NH}(k-\Delta) \\ S_{NO}(k-\Delta) \end{bmatrix} \quad (6)$$

with

$$u \in \{0,1\} \text{ i.e. } \{\text{anoxic } (S_{O,R}=0), \text{ aerobic } (S_{O,R}=2 \text{ mg/l})\}$$

$S_{O,R}$ (mg/l) = dissolved oxygen (S_O) setpoint for slave S_O -controller, control input

The dynamic model in eqns. 3-6 is only valid for $S_{O,R} \in \{0,2\}$. It has been identified in earlier work (Lukasse *et al.*, 1997).

The RHOC problem is solved at each sampling instant by enumeration, *i.e.* by just computing the objective criterion value for all 2^H possible control trajectories. The attractive feature of this approach is that a globally optimal solution of eqn. 1 is guaranteed. A detailed study of the RHOC controller's behaviour as a function of the tuning parameters T , w , $S_{NH,R}$, $S_{NO,R}$ and H is presented in Lukasse *et al.* (submitted 2). In summary: the sampling interval T is selected equal to the analysers' time delay Δ (20 min), this may be altered but there is not much to be gained. The weight w acts as a switching function with a threshold

$$w_c = \frac{|r_{NH,max} + r_{NO,max}|}{|r_{NH,max}|} \quad (7)$$

Either S_{NH} or S_{NO} is controlled to its setpoint dependent on w , while the other follows as a consequence. If $0 < w < w_c$ then S_{NO} is well controlled, if $w > w_c$ then S_{NH} is well controlled. Most appealing is to select both setpoints as 0, as this is every operator's ideal. In most cases removal of S_{NH} has priority, so one will choose to control S_{NH} to its setpoint by selecting $w > w_c$. If one wants to stick to a purely economical tuning one will select $S_{NH,R} = S_{NO,R} = 0$ and $w = (\text{costs of effluent } S_{NH} \text{ - aeration costs for } S_{NH} \text{ removal}) / (\text{costs of effluent } S_{NO})$. The prediction horizon H is only one sampling interval, because it was shown in Lukasse *et al.* (submitted 2) that larger H yields no improvement at all, while the computational burden increases exponentially with H .

5.5 Recursive identification scheme

The RHOC controller of the preceding section yields optimal N-removal provided that an accurate dynamic process model is available. Due to the time variance in ASP's an accurate model can only be available when recursively estimating the time varying model parameters:

$$\theta := [S_{NH,in} \quad r_{NH,max} \quad r_{NO,max}]^T$$

The well-known Kalman filter is used to estimate $\theta(k)$:

$$\hat{\theta}(k) = \hat{\theta}(k-1) + L(k)\epsilon(k, \hat{\theta}(k-1))$$

$$L(k) = P(k-1)X^T(k)\{R(k) + X(k)P(k-1)X^T(k)\}^{-1} \quad (8)$$

$$P(k) = P(k-1) + Q(k) - P(k-1)X^T(k)\{R(k) + X(k)P(k-1)X^T(k)\}^{-1}X(k)P(k-1)$$

where the prediction error is given by the two equations below

$$\epsilon(k, \hat{\theta}(k-1)) = y(k) - \hat{y}(k|k-1) \quad (9)$$

$$\hat{y}(k|k-1) = A(k-1)y(k-1) + X(k)\hat{\theta}(k-1) \quad (10)$$

The dynamic model (eqns. 3-6) is brought in the form of eqn. 10 by eliminating the state variables S_{NH} and S_{NO} yielding

$$A(k) = \begin{bmatrix} 1 - T \frac{q^m(k-\Delta)}{V} & 0 \\ 0 & 1 - T \frac{q^m(k-\Delta)}{V} \end{bmatrix} \quad (11)$$

and

$$X(k) = \frac{\partial \hat{y}(k+1|k)}{\partial \theta} = \begin{bmatrix} X_{11} & X_{12} & X_{13} \\ X_{21} & X_{22} & X_{23} \end{bmatrix} \quad (12)$$

with the elements of $X(k)$ defined in Table 1.

Table 1, Jacobian X in all possible operating modes.

	$y(k) > 0$	$\{y_1(k), y_1(k-1)\} = 0$	$\{y_2(k), y_2(k-1)\} = 0$
$X_{11}(k)$	$T \frac{q^m(k-\Delta)}{V}$	0	$T \frac{q^m(k-\Delta)}{V}$
$X_{12}(k)$	$-Tu(k-\Delta)$	0	$-Tu(k-\Delta)$
$X_{13}(k)$	0	0	0
$X_{21}(k)$	0	$T \frac{q^m(k-\Delta)}{V}$	0
$X_{22}(k)$	$Tu(k-\Delta)$	0	0
$X_{23}(k)$	$-T(1-u(k-\Delta))$	$-T(1-u(k-\Delta))$	0

The Kalman filter has three positive definite matrices that need to be initialized: $P(0)$, Q and R . Theoretically Q is the parameter random walk covariance and R the measurement covariance matrix. In practice, however, they are usually treated

as ordinary tuning matrices as the covariances are unknown. Typically $P(0)$, Q and R are diagonal matrices, unless one has prior knowledge about parameter or measurement error correlations. $P(0)$ is usually set at $I \cdot 10^6$, with I the unity matrix, a very large value allowing for fast initial convergence and making an accurate initial guess $\hat{\theta}(0)$ redundant (Young, 1984). A reasonable value for R , the measurement covariance, can be obtained by evaluating the noise on some previous measurement signals. In this study the measurement noise is very small for both outputs, so R is a

diagonal matrix whose diagonal elements get very small values. Most heuristics are involved in setting the \mathbf{Q} -matrix. The tuning of \mathbf{Q} is based on the knowledge that the influent related $S_{NH,in}$ usually exhibits diurnal variations, while $r_{NO,max}$ and $r_{NH,max}$ are sludge related and therefore will show much slower variations. So $\mathbf{Q}(1,1)$ ought to get a much larger value than the two other diagonal elements. By simulating the recursive estimator for different \mathbf{Q} -matrices and evaluating the resulting $\hat{\theta}(k)$ -trajectories an acceptable \mathbf{Q} is determined. Obviously, this choice effects the frequency content of the parameter estimates. The diagonals of the three resulting diagonal matrices are

$$\text{diag}(\mathbf{Q}) = [10 \ 5 \cdot 10^{-7} \ 1 \cdot 10^{-5}], \text{diag}(\mathbf{R}) = [0.1 \ 0.1], \text{diag}(\mathbf{P}(0)) = [1 \ 1 \ 1] \cdot 10^6$$

It has been proven in Lukasse *et al.* (submitted 1) that stability of this recursive estimator is guaranteed provided that the aeration does not remain constant for very long periods (over a year).

5.6 Adaptive RHOC

Adaptive RHOC is just the combination of the preceding RHOC and recursive identification schemes. The overall control algorithm performs at sampling instant k the following steps:

1. check whether $\mathbf{y}(k)$ is reliable, *i.e.* no outliers and analysers not autocalibrating
2. replace each unreliable $y_i(k)$ by $\hat{y}_i(k | k-1, \hat{\theta}(k-1))$
3. determine the correct $\mathbf{X}(k)$ in Table 1 on the basis of $\mathbf{y}(k)$ and $\mathbf{y}(k-1)$
4. estimate $\hat{\mathbf{y}}(k | k-1, \hat{\theta}(k-1))$ according to eqn. 10
5. evolve the Kalman filter (eqn. 8), using $\mathbf{e}(k|k-1)$ and $\mathbf{X}(k)$, to get $\mathbf{P}(k)$ and $\hat{\theta}(k)$
6. reconstruct the state $[S_{NH}(k) \ S_{NO}(k)]^T$ from eqns. 3-6 using $\mathbf{y}(k)$, $\hat{\theta}(k)$, $u(k-\Delta)$, $q_{in}(k-\Delta)$
7. solve the RHOC problem (eqns. 1-6) using $\hat{\theta}(k)$ and initial condition $[\hat{S}_{NH}(k) \ \hat{S}_{NO}(k)]^T$
8. implement the computed optimal control $u^*(k)$

The main difficulty in adaptive control in general is that the controller and the estimator operate together in one closed loop. The overall closed loop behaviour is inherently non-linear in u and $\hat{\theta}$, which makes it generally impossible to get more than a region of stability, *i.e.* local stability results (Aström & Wittenmark, 1989). Moreover, the information in the measured output signal gradually shifts to high frequencies when the process becomes better controlled. When the parameters are estimated on the basis of this ever poorer information the model actually drifts from process model to noise model. Therefore, special precautions need to be taken to preserve sufficient richness of u . The typical solution is to add a little dither signal to the control input or to the setpoint, from which a logical inconsistency emerges: to enable the control improvement by adaptive control it needs to be deteriorated by adding a dither signal.

This paper's application has some features, which make the use of a dither signal redundant. The speciality is that u can only take two values, which guarantees sufficient richness of the measurements provided that u is switched regularly and T is large enough. If T is large enough the shift of measurement information to high frequencies can be excluded. The highest possible input frequency is reached by switching the value of u at each sampling instant. At this frequency, in case $T = 20$ min, there still is sufficient information in the measurement outputs to allow for the estimation of reasonable $\hat{\theta}$ -trajectories. Obviously the smaller T the larger the percentage of time in

which DO is at values between 0 and 2 mg/l. This puts a (not exactly known) lower limit to T , below which the sufficient richness gets lost and $\hat{\theta}$ might drift away indeed. If this behaviour is observed when implementing this paper's adaptive controller, it can be removed by simply increasing T .

The region of stability for this paper's application is defined as all combinations of $y(k)$ and $\hat{\theta}(k)$ for which the closed loop behaviour converges to the optimal cyclic behaviour, *i.e.* alternating $u(k)$ with S_{NH} around its setpoint (if $w > w_c$). One known source of instability is a negative estimate for $r_{NH,max}$, which will erroneously cause the dynamic model (eqns. 3-6) to predict production of S_{NH} under aerobic conditions. So the RHOC controller will not turn on the aeration, no new information to update $\hat{r}_{NH,max}$ is obtained and the deadlock is there. Another source of instability occurs when $S_{NH,R} = 0$, $w > w_c$ and $r_{NO,max}$ is largely underestimated. In that case the RHOC controller will not turn off the aeration, as a consequence no new information to update $\hat{r}_{NO,max}$ is obtained and again the impasse is there. Notice that this last situation will only occur when $S_{NH,R} = 0$. When $S_{NH,R} > 0$ and $w > w_c$ the decision to turn off the aeration will be dominated by the fact $S_{NH} < S_{NH,R}$ and $\hat{r}_{NO,max}$ only plays a minor role.

Both above described instabilities originate from poor estimates $\hat{\theta}(k)$. These may especially occur during start-up when the Kalman filter gain is very high to allow for large steps in $\hat{\theta}(k)$, *i.e.* rapid initial tuning but also the risk of large errors due to poor measurements. This source of instability can simply be excluded by an initial tuning phase: after start-up first switch a few times between aerobic and anoxic phases before the RHOC controller becomes active.

5.7 Simulation results

The adaptive RHOC has been tested in simulation for many different situations. A characteristic simulation is shown in Figs. 1 and 2. The sine wave pattern for the influent related $S_{NH,in}$ and the slower changes in the sludge related $r_{NH,max}$ and $r_{NO,max}$ are believed to be characteristic. Clearly, the

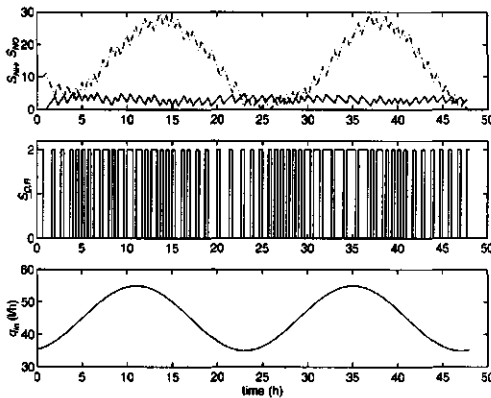


Fig. 2, simulated adaptive RHOC of S_{NH} (-) and S_{NO} (-) with $S_{NH,R} = 2$ mg/l, $S_{NO,R} = 0$ and $w > w_c$.

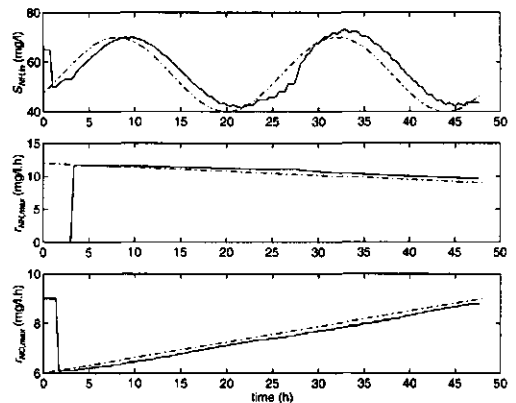


Fig. 1, true (-) and estimated (-) parameters accompanying Fig. 1

recursive estimator is reasonably capable of tracking the variations in θ (Fig. 2). S_{NH} is controlled around its setpoint as a consequence of the choice $w > w_c$. In this simulation the objective criterion value for the adaptive RHOC over the full 48h horizon is 2545 mg/l, while RHOC with constant, average parameter values yields $J^* = 2600$ mg/l. So in this case adaptive RHOC performs slightly better than non-adaptive RHOC. This is the most fortunate comparison for non-adaptive RHOC, as it uses the average θ -values. Hence the observed difference is a lower bound, the worse the θ -values

used by the non-adaptive RHOC the larger the difference will be.

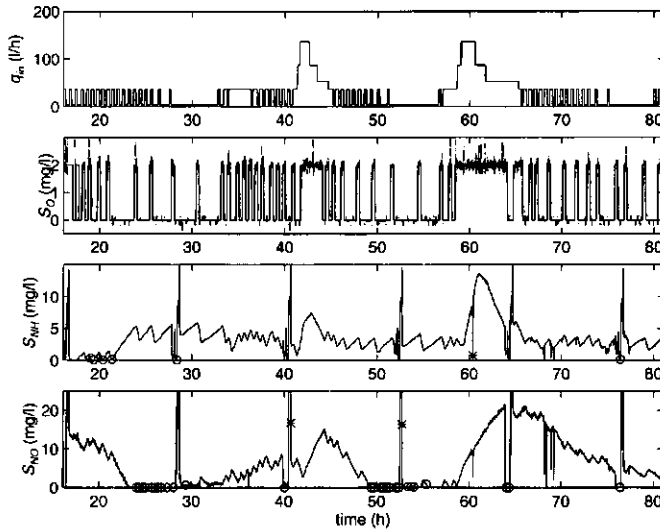


Fig. 3, adaptive RHOC applied to pilot plant with $S_{NH,R}=2$ mg/l, $S_{NO,R}=0$ mg/l and $w > w_c$ (* = outlier, o = depletion)

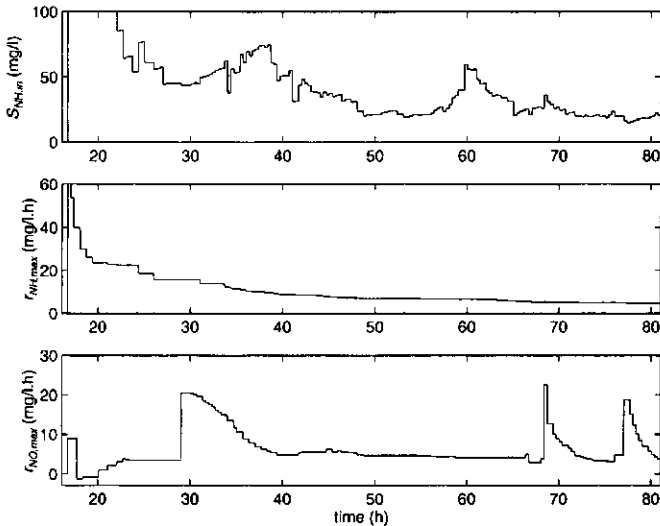


Fig. 4, recursively estimated parameters accompanying Fig. 3

5.8 Pilot plant results

Several experiments have been carried out on a pilot scale ASP with continuously mixed aeration tank ($V = 475$ l, MLSS = 2 g/l), continuously fed with presettled municipal wastewater, preceded by a 40 l anoxic tank for predenitrification. The average sludge load during dry weather conditions is roughly 0.2 kg COD/kg MLSS.day. S_{NH} and S_{NO} in the aeration tank are measured using SKALAR auto-analysers type SA 9000. S_O is tightly controlled at a setpoint alternating between 0 and 2 mg/l by means of an earlier developed robust MPC controller (Haarsma and Keesman, 1995). The q_{in} pattern for the experiments is obtained by monitoring the influent flow of the adjacent full-scale WWTP of the town of Bennekom and downscaling this signal to a reasonable level for the pilot plant. In this way a natural relation between diurnal influent flow and influent pollution variations is guaranteed, moreover real storm events occur in the experiments. One of the resulting data sets and the accompanying estimates of $\theta(k)$ are shown in Figs. 3 and 4.

The sharp peaks of $S_{NH} = 15$ mg/l and $S_{NO} = 25$ mg/l in Fig. 3 are analyser calibrations, due to a software error these were handled by the controller as reliable measurements. As a result the estimates of $\theta(k)$ show some strange oscillations especially in the initial phase of the experiment. Despite this error the controller performance is satisfactory. In low loaded periods the aeration is switched off over longer time spans in order to utilise the possibility of more denitrification without deteriorated effluent S_{NH} . During the two storm events the plant is overloaded, but the controller correctly decides to keep the aerators on.

5.9 Discussion

The controller can be tuned such that it is truly optimal not to alternate, but only nitrify or only denitrify (Lukasse *et al.*, submitted 2). In these situations no information is obtained to update $\hat{r}_{NO,max}$ respectively $\hat{r}_{NH,max}$. Hence these estimates will become ever poorer, and have the potential to lock the controller erroneously in one mode. To enable regular updating of all elements of $\hat{\theta}(k)$ the controller should receive an extra constraint: do not remain in one and the same mode for more than 12 hours. Whether this will work satisfactorily and whether a 12 hours period is suitable remains to be tested.

The denitrification rate is related to the availability of readily biodegradable organic substrates (RBOS) (Henze *et al.*, 1987). In this study no relation between r_{NO} and q_{in} was observable, and therefore in the model $r_{NO} = r_{NO,max}$. The explanation is that no influent RBOS reaches the reactor due to the presence of an anoxic predenitrification tank. In case of the absence of anoxic zones preceding the alternating reactor the model

$$r_{NO} = r_{NO,s} \frac{q_{in}}{V} + r_{NO,end} \quad (13)$$

seems more reasonable. In eqn. 13 $r_{NO,s}$ is related to the influent RBOS concentration, while $r_{NO,end}$ is the endogenous denitrification rate. Whether eqn. 13 holds in absence of anoxic predenitrification remains to be tested.

Reactor pH predominantly is a function of nitrification/denitrification. This can be taken into account in the current controller. For example, during one of the experiments a storm event occurred, causing a period of high influent N-load. The controller was tuned such that S_{NH} was controlled to its setpoint, resulting in a longer than usual period of maximum nitrification. As a consequence the pH temporarily dropped to values around 6.1. During the next day intensive foaming occurred and nearly all sludge disappeared from the reactor. A causal relationship is likely, though not proven yet. As the pH-trajectory predominantly is a function of nitrification/denitrification it is predictable. By adding the simple state equation

$$\frac{d(pH)}{dt} = p_1 \cdot r_{NH} + p_2 \cdot r_{NO} \quad (14)$$

, a pH measurement and a minimum constraint for pH to the RHOC problem in eqns. 1-6 and adding p_1 and p_2 to the recursive estimator repetition of the foaming disaster might be prevented. Obviously installation of an independent pH-controller will remedy the problem as well, but at higher costs.

Monitoring instead of recursively estimating $S_{NH,in}$ is likely to improve controller performance. It is unlikely that the improved controller performance outweighs the extra costs of $S_{NH,in}$ -monitoring, but it may be considered as an option.

Besides a short-term effect, the different operation strategy will have a long-term effect as the sludge composition will adapt to the new operation strategy. In a follow up study this effect will be investigated. There are indications that it might lead to a decreased presence of Nitrobacter in the activated sludge and hence stimulate N-removal via nitrite instead of nitrate (Brouwer, 1997).

5.10 Conclusions

The presented adaptive RHOC controller showed good performance, both in simulation and in pilot plant application. The control algorithm's stability region is not exactly known, but after many simulations and pilot plant experiments it has been learned what the main difficulties are and how to prevent instability. The controller is believed to be of direct practical relevance, because the use of an economy-related objective criterion offers a natural way to bridge the gap between the higher level of plant economy and the lower level of plant control. Moreover the use of a recursive estimator for the RHOC's model parameters will fine-tune the controller to the specific plant under control.

Acknowledgements: We are very grateful to M. Bloemen, who carried out the whole lot of experimental work. This research was financially supported by the Dutch Technology Foundation (STW) under grant no. WBI44.3275.

5.11 References

- Aström KJ, Wittenmark B (1989). Adaptive control. Addison-Wesley Publishing Company, New York, U.S.
- Brouwer H (1997). Sturing actiefslibprocessen op basis van respirometrie in combinatie met een deterministisch model (eindrapport Senter project nr imb 94001) (in Dutch)
- Haarsma GJ, Keesman KJ (1995). Robust model predictive dissolved oxygen control. proc. 9th Forum for Applied Biotechnology, MFLRBER, vol. 60(4b), pp 2415-2426
- Henze M, Grady jr. CPL, Gujer W, Marais GvR, Matsuo T (1987). Activated sludge model no. 1. IAWQ Scientific and Technical Report no. 1, IAWQ, London, Great Britain
- Lukasse LJS, Keesman KJ, Straten G van (1997) Identification for model predictive control of biotechnological processes, case study: nitrogen removal in an activated sludge process. Proc. 11th IFAC symposium on System Identification
- Lukasse LJS, Keesman KJ, Straten G van (submitted 1) Recursive identification of N-removal in alternating activated sludge processes. Journal of process control
- Lukasse LJS, Keesman KJ, Klapwijk A, Straten G van (submitted 2) Optimal control of N-removal in ASP's. IAWQ world congress 1998
- Ménardière M de la, Charpentier J, Vachon A, Martin G (1991) ORP as control parameter in a single sludge biological nitrogen and phosphorus removal activated sludge system. Water SA, vol. 17(2), pp 123-132

- Metcalf & Eddy, Inc. (1979). Wastewater engineering: treatment/disposal/reuse. 2nd edition, McGrawhill, New York
- Surmacz-Gorska J, Gernaey K, Demuynck C, Vanrolleghem P, Verstraete W (1995). Nitrification process control in activated sludge using oxygen uptake rate measurements. *Environmental Technology*, vol. 16, pp 569-577
- Young P (1984). Recursive estimation and time-series analysis, an introduction. Springer-Verlag, Berlin, Germany
- Zhao H, Isaacs SH, Søbereg H, Kümmel M (1995) An analysis of nitrogen removal and control strategies in an alternating activated sludge process. *Water Research*, vol. 29(2), pp 535-544

6 L_1 -Norm optimal control of N-removal in an activated sludge process[†]

6.1 Abstract

This paper presents an L_1 -norm optimal state feedback controller for 2-dimensional linear time invariant (LTI) systems with decoupled dynamics and a single control input. The controller is successfully applied to the problem of N-removal in activated sludge processes, both in simulation and on a pilot plant fed with real municipal wastewater. It optimises the moments at which the plant's aerators are switched on/off. Improvement of operation strategies for the process of N-removal from wastewater is an important topic due to tightening government legislations with the objective to protect the aquatic environment.

Keywords: 1-norm, absolute value, ammonium, nitrate, nitrogen, wastewater treatment

6.2 Introduction

Throughout the last decades many papers have been published in the field of optimal control theory. For a comprehensive overview of the field see *e.g.* Bryson and Ho (1975) or Lewis (1986). Despite the large amount of literature the number of successful applications is relatively small. The major drawback of optimal control in its pure form is its open loop nature, which can only work satisfactory when applied to systems with hardly any uncertainty.

The ideal situation is to derive a state feedback law that realises the optimal control trajectory for the full horizon optimal control problem, as this will automatically compensate for small errors due to system uncertainties. State feedback can be introduced in any optimal control problem by applying receding horizon optimal control (*e.g.* Kwon and Pearson, 1977; Thomas, 1975; Thomas *et al.*, 1977). Unfortunately, in general this can not yield the full horizon optimal trajectory of \mathbf{u} due to the inequality (Bitmead *et al.*, 1990)

$$\min_{\mathbf{u}} \int_{t_0}^{t_f} L(\mathbf{x}, \mathbf{u}, t) dt \leq \min_{\mathbf{u}} \int_{t_0}^{t_1} L(\mathbf{x}, \mathbf{u}, t) dt + \min_{\mathbf{u}} \int_{t_1}^{t_f} L(\mathbf{x}, \mathbf{u}, t) dt \quad \text{with } t_0 < t_1 < t_f \quad (1)$$

The only known exception is the situation in which a quadratic (l_2 -norm) objective criterion is minimised subject to a linear system model. In that case a timevarying static state feedback law exists that yields the full horizon optimal trajectory of \mathbf{u} (Kwakernaak and Sivan, 1972). Due to that attractive property it has been used in many applications.

However, for many controllers the 1-norm is a closer resemblance of the plant's operational objectives than the 2-norm. Yet the use of l_1 -norm objective functionals has been very limited, though

[†] to appear in *Control Engineering Practice* by L.J.S. Lukasse, K.J. Keesman and G. van Straten

some examples are available in the literature (Genceli *et al.*, 1993, Morshedi *et al.*, 1985). In this paper a state feedback law is presented that optimises the full horizon optimal control problem for a 1-norm objective criterion subject to a 2-dimensional linear model with decoupled dynamics and a single control input.

The l_1 -norm optimal state feedback controller has been applied successfully to the process of nitrogen (N) removal in activated sludge processes (ASP's). In most developed countries N-removal from municipal wastewater is enforced by government legislation with the objective to protect the aquatic environment against eutrophication. N is usually biologically removed in ASP's. Biological N-removal requires two processes: nitrification ($\text{NH}_4 \rightarrow \text{NO}_3$) in presence of oxygen and denitrification ($\text{NO}_3 \rightarrow \text{N}_2$ -gas) in absence of oxygen. Application of the denitrification step is relatively new; it is currently being introduced on a large scale in the European Union. Operation strategies for ASP's with both nitrification and denitrification are still evolving (Leeuw and van 't Oever, 1996; Münch *et al.*, 1996). In practice N-removal usually takes place in alternatingly aerated ASP's. In that situation the optimal control problem boils down to the question when to turn the aerators on/off.

6.3 The l_1 -norm optimal state feedback law

In this section an optimal state feedback law will be derived for the digital full-horizon unconstrained l_1 -norm optimal control problem given by

$$\min_{u_0, \dots, u_{n-1}} J(u) = \int_{t_0}^{t_0+nT} \|\mathbf{W}\mathbf{x}(t)\|_1 dt \quad (2)$$

subject to

$$\dot{\mathbf{x}} = \mathbf{A}\mathbf{x} + \mathbf{b}u + \mathbf{d} \quad \mathbf{x}(t_0) = \mathbf{x}_0 \quad (3)$$

with T the control interval, n the number of control intervals, $u \in \mathbb{R}$ the control input, $\mathbf{W} \in \mathbb{R}^{2 \times 2}$ a diagonal weighting matrix and state vector $\mathbf{x} \in \mathbb{R}^2$, disturbance inputs $\mathbf{d} \in \mathbb{R}^2$, $\mathbf{A} \in \mathbb{R}^{2 \times 2}$ and $\mathbf{b} \in \mathbb{R}^2$. In eqn. 2 $\|\mathbf{W}\mathbf{x}(t)\|_1$ is the 1-norm of $\mathbf{W}\mathbf{x}(t)$, which is defined as $\sum_{m=1}^p |\mathbf{W}\mathbf{x}(t)|$ for $\mathbf{x} \in \mathbb{R}^p$. Notice that the use of a setpoint $\mathbf{0}$ for $\mathbf{x}(t)$ in eqn. 2 does not mean any loss of generality.

The state \mathbf{x} at time $t_0+(k+1)T$, \mathbf{x}_{k+1} , as a function of \mathbf{x} , \mathbf{d} and u at time t_0+kT is given by the solution of eqn. 3. When using the assumption that both $u(t)$ and $\mathbf{d}(t)$ are piecewise constant functions, *i.e.* $u(t) = u_k$ and $\mathbf{d}(t) = \mathbf{d}_k$ on the time interval $kT \leq t < kT+T$, this solution is given by:

$$\mathbf{x}_{k+1} = e^{AT} \mathbf{x}_k + (e^{AT} - \mathbf{I})\mathbf{A}^{-1}(\mathbf{b}u_k + \mathbf{d}_k) \quad (4)$$

From this result, \mathbf{x} at time $k+j$ is easily found to be

$$\mathbf{x}_{k+j} = e^{jAT} \mathbf{x}_k + \sum_{i=1}^j (e^{iAT} - e^{(i-1)AT}) \mathbf{A}^{-1}(\mathbf{b}u_{k+j-i} + \mathbf{d}_{k+j-i}) \quad (5)$$

Discretisation of the continuous time objective functional, using the straightforward Euler approximation, yields

$$J(u_0, \dots, u_{n-1}) = \int_{t_0}^{t_f = t_0 + nT} \|\mathbf{W}\mathbf{x}(t)\|_1 dt = \sum_{j=1}^n \int_{t_0 + (j-1)T}^{t_0 + jT} \|\mathbf{W}\mathbf{x}(t)\|_1 dt \approx T \sum_{j=1}^n \|\mathbf{W}\mathbf{x}_j\|_1 \quad (6)$$

Substituting eqn. 5 in eqn. 6 results in

$$\begin{aligned} J(u_0, \dots, u_{n-1}) &\approx T \sum_{j=1}^n \left\| \mathbf{W}e^{jAT} \mathbf{x}_0 + \mathbf{W} \sum_{i=1}^j (e^{iAT} - e^{(i-1)AT}) \mathbf{A}^{-1} (\mathbf{b}u_{j-i} + \mathbf{d}_{j-i}) \right\|_1 \\ &= T \sum_{j=1}^n \left\| \mathbf{W}e^{jAT} \mathbf{x}_0 + \mathbf{W} \sum_{i=1}^j e^{iAT} (\mathbf{I} - e^{-AT}) \mathbf{A}^{-1} (\mathbf{b}u_{j-i} + \mathbf{d}_{j-i}) \right\|_1 \end{aligned}$$

Rewriting this by stacking the n 2-dimensional vector norms yields

$$J(u_0, \dots, u_{n-1}) = \left\| \begin{bmatrix} \mathbf{W}e^{AT} \mathbf{x}_0 \\ \vdots \\ \mathbf{W}e^{nAT} \mathbf{x}_0 \end{bmatrix} + \begin{bmatrix} \mathbf{W}e^{AT} (\mathbf{I} - e^{-AT}) \mathbf{A}^{-1} \mathbf{b} & & \mathbf{0} \\ \vdots & \ddots & \\ \mathbf{W}e^{nAT} (\mathbf{I} - e^{-AT}) \mathbf{A}^{-1} \mathbf{b} & \dots & \mathbf{W}e^{AT} (\mathbf{I} - e^{-AT}) \mathbf{A}^{-1} \mathbf{b} \end{bmatrix} \begin{bmatrix} u_0 \\ \vdots \\ u_{n-1} \end{bmatrix} + \begin{bmatrix} \mathbf{W}e^{AT} (\mathbf{I} - e^{-AT}) \mathbf{A}^{-1} \mathbf{d}_0 \\ \vdots \\ \mathbf{W}e^{nAT} (\mathbf{I} - e^{-AT}) \mathbf{A}^{-1} \mathbf{d}_0 + \dots + \mathbf{W}e^{AT} (\mathbf{I} - e^{-AT}) \mathbf{A}^{-1} \mathbf{d}_{n-1} \end{bmatrix} \right\|_1 \quad (7)$$

An optimal state feedback law exists if and only if u_k^* is independent of u_j^* , $\forall j \in \{k+1, \dots, n-1\}$, i.e. if and only if u_k^* can be computed on the basis of only the first $k+1$ of the n above vector expressions. This only holds for a very limited class of systems. In the sequel it is proven that it holds for linear time-invariant systems with one input, two states and diagonal \mathbf{A} -matrix. To show this the fact needs to be used that

$$\arg \min_u \|\mathbf{b}u + \mathbf{c}\|_1 \equiv \arg \min_u |\mathbf{b}(h)u + \mathbf{c}(h)| \quad (8)$$

where $\mathbf{b} \in \mathbb{R}^2$, $\mathbf{c} \in \mathbb{R}^2$, $u \in \mathbb{R}$ and h is the index of the maximal absolute value in \mathbf{b} , i.e.

$$h = \arg \max_i |\mathbf{b}(i)| \quad (9)$$

The example in Fig. 1 illustrates that the value of u that minimizes $\{|\mathbf{b}(1)u + \mathbf{c}(1)| + |\mathbf{b}(2)u + \mathbf{c}(2)|\}$ is determined by $\max\{|\mathbf{b}(1)|, |\mathbf{b}(2)|\}$, as stated in identity 8. That identity 8 does not automatically hold for systems of order higher than two is shown by a counter example. E.g. if $\mathbf{b} = [-5 \ 2 \ 4]^T$ and $\mathbf{c} = [3 \ 0 \ 0]^T$ then $\|\mathbf{b}u + \mathbf{c}\|_1$ achieves a minimum value of 3 at $u^* \approx 0$, while according to eqn. 9 the minimum value would be 3.6 and $u^* = 0.6$.

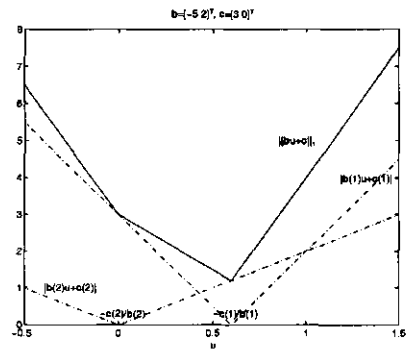


Fig. 1. $\|\mathbf{b}u + \mathbf{c}\|_1$ as a function of u .

Define

$$\mathbf{c} = \begin{bmatrix} \mathbf{c}_1 \\ \vdots \\ \mathbf{c}_n \end{bmatrix} = \begin{bmatrix} \mathbf{W}e^{AT} \mathbf{x}_0 \\ \vdots \\ \mathbf{W}e^{nAT} \mathbf{x}_0 \end{bmatrix} + \begin{bmatrix} \mathbf{W}e^{AT} (\mathbf{I} - e^{-AT}) \mathbf{A}^{-1} \mathbf{d}_0 \\ \vdots \\ \mathbf{W}e^{nAT} (\mathbf{I} - e^{-AT}) \mathbf{A}^{-1} \mathbf{d}_0 + \dots + \mathbf{W}e^{AT} (\mathbf{I} - e^{-AT}) \mathbf{A}^{-1} \mathbf{d}_{n-1} \end{bmatrix} \quad (10)$$

$$\mathbf{D} = \begin{bmatrix} \mathbf{D}_{11} & \dots & \mathbf{D}_{1n} \\ \vdots & & \vdots \\ \mathbf{D}_{n1} & \dots & \mathbf{D}_{nn} \end{bmatrix} = \begin{bmatrix} \mathbf{W}e^{AT}(\mathbf{I} - e^{-AT})\mathbf{A}^{-1}\mathbf{b} & & \mathbf{0} \\ \vdots & \ddots & \\ \mathbf{W}e^{nAT}(\mathbf{I} - e^{-AT})\mathbf{A}^{-1}\mathbf{b} & \dots & \mathbf{W}e^{AT}(\mathbf{I} - e^{-AT})\mathbf{A}^{-1}\mathbf{b} \end{bmatrix} \quad (11)$$

with $\mathbf{c} \in \mathbb{R}^{2n}$ and $\mathbf{D} \in \mathbb{R}^{2n \times 2n}$. After substituting $\mathbf{c}_1 \in \mathbb{R}^2$ and $\mathbf{D}_{11} \in \mathbb{R}^2$ in eqn. 7 it follows from identity 8 that the first of the n vector expressions in eqn. 7 has its optimal solution at

$$\mathbf{D}_{11}(h)u_0 + \mathbf{c}_1(h) = 0 \quad (12)$$

with

$$h = \arg \max_i |\mathbf{D}_{11}(i)| \quad (13)$$

i.e. the optimal control solely depends upon the state that accompanies the largest term in \mathbf{D}_{11} . The control input u_0^* that optimises the first vector expression in eqn. 7 is optimal for the other $n-1$ vector expressions as well if

$$\arg \max_i |\mathbf{D}_{11}(i)| = \arg \max_i |\mathbf{D}_{k1}(i)| \quad \forall k \in \{2, \dots, n\} \quad (14)$$

In that situation, due to identity 8, u_0^*, \dots, u_{n-1}^* are the solution of the set of n equalities

$$\begin{cases} \mathbf{D}_{11}(h)u_0 + \mathbf{c}_1(h) = 0 & (15.1) \\ \vdots & \vdots \\ \mathbf{D}_{n1}(h)u_0 + \dots + \mathbf{D}_{nn}(h)u_{n-1} + \mathbf{c}_n(h) = 0 & (15.n) \end{cases}$$

The usual way to solve the above set of n equalities is to first solve u_0 from the first equality, subsequently u_1 from the second and so on. So if condition 14 is met equalities 15. $k+1$, ..., 15. n pose no limitations on u_0^*, \dots, u_k^* and as a consequence u_k^* can be computed independent of $u_{k+1}^*, \dots, u_{n-1}^*$ (not *vice versa*). Hence, a simple state feedback law exists that minimises objective criterion 2 if condition 14 holds. In appendix 2 it is shown by a counter example that an l_1 -norm optimal state feedback law may not exist if condition 14 is not satisfied.

Theorem 1: The scalar state feedback control law

$$u_k^* = -\frac{e^{A(h,k)T} \mathbf{A}(h,h)}{(e^{A(h,h)T} - 1)\mathbf{b}(h)} x_k(h) \quad (16)$$

is l_1 -norm optimal for single input, 2-dimensional systems with \mathbf{A} diagonal if $\mathbf{A}(h,h) \geq \mathbf{A}(j,j)$ with $j \in \{1, 2\}$ and h given by eqn. 13.

Proof: For diagonal \mathbf{A} -matrices the term $\mathbf{W}e^{kAT}(\mathbf{I} - e^{-AT})\mathbf{A}^{-1}\mathbf{b}$ in the matrix \mathbf{D} (eqn. 11) can be reformulated by using the fact that for any $p \times p$ -matrix \mathbf{A} with p independent eigenvectors

$$e^{AT} = \mathbf{V} \begin{bmatrix} e^{\lambda_1 T} & 0 & 0 \\ 0 & \ddots & 0 \\ 0 & 0 & e^{\lambda_p T} \end{bmatrix} \mathbf{V}^{-1}$$

with \mathbf{V} the matrix of eigenvectors of \mathbf{A} and λ_l the l -th eigenvalue of \mathbf{A} . In case \mathbf{A} is a diagonal matrix $\mathbf{V} = \mathbf{I}$ and the eigenvalues take the value of the diagonal elements of \mathbf{A} . Hence, for the case with $p = 2$

$$\begin{aligned}
 |\mathbf{D}_{k1}| &= \left| \mathbf{W} e^{k\lambda T} (\mathbf{I} - e^{-\lambda T}) \mathbf{A}^{-1} \mathbf{b} \right| = \left| \mathbf{W} \begin{bmatrix} e^{k\lambda_1 T} & 0 \\ 0 & e^{k\lambda_2 T} \end{bmatrix} \begin{bmatrix} 1 - e^{-\lambda_1 T} & 0 \\ 0 & 1 - e^{-\lambda_2 T} \end{bmatrix} \begin{bmatrix} \lambda_1^{-1} & 0 \\ 0 & \lambda_2^{-1} \end{bmatrix} \mathbf{b} \right| \\
 &= \begin{bmatrix} \left| W_{11} e^{k\lambda_1 T} \frac{1 - e^{-\lambda_1 T}}{\lambda_1} b_1 \right| \\ \left| W_{22} e^{k\lambda_2 T} \frac{1 - e^{-\lambda_2 T}}{\lambda_2} b_2 \right| \end{bmatrix} = \begin{bmatrix} \left| W_{11} \frac{1 - e^{-\lambda_1 T}}{\lambda_1} b_1 \right| \cdot |e^{k\lambda_1 T}| \\ \left| W_{22} \frac{1 - e^{-\lambda_2 T}}{\lambda_2} b_2 \right| \cdot |e^{k\lambda_2 T}| \end{bmatrix} \quad (17)
 \end{aligned}$$

According to eqn. 13 h is the index of the maximal absolute element in this vector \mathbf{D}_{k1} for $k = 1$. Condition 14 is met if this index h is invariant to k , which is the case if and only if (eqn. 17)

$$\left| W_{hh} \frac{1 - e^{-\lambda_h T}}{\lambda_h} b_h \right| \cdot |e^{k\lambda_h T}| \geq \left| W_{jj} \frac{1 - e^{-\lambda_j T}}{\lambda_j} b_j \right| \cdot |e^{k\lambda_j T}| \quad \forall k \in \{1, \dots, n\} \quad \text{and} \quad j \in \{1, 2\}$$

Using the fact that $e^{k\lambda_h T}$ and $e^{k\lambda_j T}$ are always positive, the above necessary and sufficient condition can also be written as

$$\lambda_h \geq \lambda_j + \frac{\ln \left(\left| W_{jj} \frac{1 - e^{-\lambda_j T}}{\lambda_j} b_j \right| / \left| W_{hh} \frac{1 - e^{-\lambda_h T}}{\lambda_h} b_h \right| \right)}{kT} \quad \forall k \in \{1, \dots, n\} \quad \text{and} \quad j \in \{1, 2\} \quad (18)$$

Inequality 18 is satisfied for $k = 1$ by the definition of h (eqn. 13). Furthermore, for $k \geq 1$ the second term on the right-hand side is a monotonic function of k . So the remaining conditions for $k \in \{2, \dots, n\}$ are satisfied if and only if inequality 18 holds for $k = n$. In case of infinite horizon control $n = \infty$, while

$$\lim_{n \rightarrow \infty} \frac{\ln \left(\left| W_{jj} \frac{1 - e^{-\lambda_j T}}{\lambda_j} b_j \right| / \left| W_{hh} \frac{1 - e^{-\lambda_h T}}{\lambda_h} b_h \right| \right)}{nT} = 0 \quad (19)$$

So in that case inequality 18 can be simplified to the necessary and sufficient condition $\lambda_h \geq \lambda_j$. In summary, for 2-dimensional single input systems with a diagonal \mathbf{A} -matrix an l_1 -norm optimal state feedback law exists if inequality 18 holds for $k = n$, because a state feedback law exists if condition 14 is met and condition 14 is met if and only if inequality 18 holds for $k = n$. For the case of infinite horizon control $n = \infty$ and inequality 18 for $k = n$ reduces to $\mathbf{A}(h, h) \geq \mathbf{A}(j, j)$ for $j \in \{1, 2\}$ with h given by eqn. 13.

Above it has been shown for which class of problems an l_1 -norm optimal state feedback law exists. Now it remains to be shown that this feedback law is given by eqn. 16. Eqn. 15 illustrates, in conjunction with eqns. 10 and 11, that u_k^* should aim at obtaining $\mathbf{W}(h, h) \mathbf{x}_{k+1}(h) = 0$, while from eqn. 4 it follows that $\mathbf{W} \hat{\mathbf{x}}_{k+1|k}$, the weighted 1-step ahead prediction of \mathbf{x} at time $t_0 + kT$, is given by

$$\mathbf{W} \hat{\mathbf{x}}_{k+1|k} = \mathbf{W} e^{AT} \mathbf{x}_k + \mathbf{W} (e^{AT} - \mathbf{I}) \mathbf{A}^{-1} (\mathbf{b} u_k + \mathbf{d}_k) \quad (20)$$

By setting the h -th row in eqn. 20 to zero ($\mathbf{W} \hat{\mathbf{x}}_{k+1|k}(h) = 0$) and solving for u_k one finds the optimal control law. In case of unknown disturbances, i.e. $\hat{\mathbf{d}}_k = 0$ (control law contains no feedforward component), the optimal control u_k^* is the solution of

$$\mathbf{W}(h, h) e^{A(h, h)T} \mathbf{x}_k(h) + \mathbf{W}(h, h) (e^{A(h, h)T} - \mathbf{I}) \mathbf{A}(h, h)^{-1} \mathbf{b}(h) u_k = 0 \quad (21)$$

and thus the scalar state feedback law in eqn. 16 is optimal. ■

The existence of an l_1 -norm optimal state feedback law has been proven above for a 2-dimensional linear diagonal system with a single control input and an objective functional without weights on the input. Although this is an important class in practice, the question arises to what extent this result can be generalised:

- The effect of (weighted) inputs in the objective functional has not yet been investigated.
- The given proof fails for higher dimensional systems, since identity (8) only holds for single-input-double-outputs systems. Moreover, it is easy to come up with examples of MIMO systems for which an l_1 -norm optimal state feedback law does not exist. Yet, there may be a class of MIMO systems for which an l_1 -norm optimal state feedback controller exists.

6.4 Application to N-removal in activated sludge processes

A schematic representation of the process of N-removal in activated sludge processes (ASP's) is given in Fig. 2. In the pilot plant used in this study the influent is fed to a 40 l anoxic predenitrification reactor, succeeded by a 475 l continuously mixed alternating reactor (Fig. 2). Biomass is controlled at a setpoint of 3.5 g/l ('X-ctrl' in Fig. 2). The pilot plant setup is a prototype of the widely applied alternately aerated carousel with predenitrification reactor. This is a usual layout for plants aiming at both nitrification and denitrification. The alternating reactor to be controlled is the one where the airflow is manipulated by a dissolved oxygen (DO) controller, which receives its alternating setpoint (DO_R) from a higher level N-controller. NH_4 and NO_3 in the reactor are measured using SKALAR auto-analysers type SA 9000. DO is tightly controlled at a setpoint alternating between 0 and 2 mg/l by means of an earlier developed robust model predictive controller (Haarsma and Keesman, 1995).

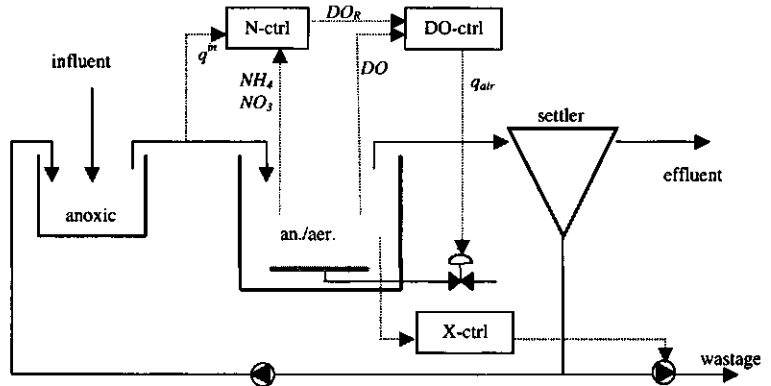


Fig. 2, scheme of ASP pilot plant with cascaded controllers for N and DO.

The optimal control problem of nitrogen removal in continuously mixed, alternately aerated activated sludge reactors can be formulated as

$$\min_{u_0, \dots, u_{n-1}} J(u) = \int_{t_0}^{t_f=t_0+nT} \|W(x(t) - x_R)\|_1 dt \quad (22)$$

subject to

$$\dot{\mathbf{x}} = \begin{bmatrix} -\frac{q^{in}}{V} & 0 \\ 0 & -\frac{q^{in}}{V} \end{bmatrix} \mathbf{x} + \begin{bmatrix} -C_{NH} \\ C_{NH} + C_{NO} \end{bmatrix} u + \begin{bmatrix} \frac{q^{in}}{V} NH_4^{in} \\ -C_{NO} \end{bmatrix} \quad (23)$$

$$C_{NH} = \begin{cases} C_{NH,max} & \text{if } NH_4 > 0 \\ \frac{q^{in}}{V} NH_4^{in} & \text{if } NH_4 = 0 \end{cases} \quad (24)$$

$$C_{NO} = \begin{cases} C_{NO,max} & \text{if } NO_3 > 0 \\ 0 & \text{if } NO_3 = 0 \end{cases} \quad (25)$$

with $\mathbf{W} \in \mathbb{R}^{2 \times 2}$ a diagonal weighting matrix, $n = \infty$, $\mathbf{x} = \begin{bmatrix} NH_4 \\ NO_3 \end{bmatrix} \in \mathbb{R}_+^2$ and $u \in \{0, 1\}$, i.e. $u \in \{\text{anoxic (dissolved oxygen setpoint } DO_R = 0 \text{ mg/l), aerobic (} DO_R = 2 \text{ mg/l)}\}$. This non-linear state space model has been identified in earlier work (Lukasse *et al.*, 1997a and 1997b).

The theoretical result of the preceding section has been derived for LTI-systems with $u_k \in \mathbb{R}$. This application has two complications: 1. it is non-linear, i.e. it switches between different LTI-systems depending on \mathbf{x} (eqns. 24, 25), 2. it has the constraint $u_k \in \{0, 1\}$. In practice the N-controller is tuned such that $h = 1$ in eqn. 13 and $\mathbf{x}_R(1) = NH_{4,R} > 0$. In that situation changes in \mathbf{b} and \mathbf{d} only occur when $\mathbf{x}(2)$ reaches/leaves zero (see eqns. 23-25). This only happens during two small parts of the day: when NO_3 reaches zero during the low-loaded part of the day, late at night, and when NO_3 starts to increase again in the morning, at the start of the high-loaded part of the day (Fig. 4). Therefore the changes in \mathbf{b} and \mathbf{d} are of minor importance and the system behaviour is LTI during the major part of the day, although strictly speaking the system is non-linear.

Due to the other complication, $u \in \{0, 1\}$ instead of $u \in \mathbb{R}$, the existence of an optimal state feedback law like eqn. 16 is no longer guaranteed. This is proven by a counter example. For the simple case of $n = 2$ and $\mathbf{A} = \begin{bmatrix} \lambda & 0 \\ 0 & \lambda \end{bmatrix}$ eqn. 7 is of the form

$$\{u_0, u_1\}^* = \arg \min_{u_0, u_1} \left\| \begin{bmatrix} \mathbf{W} e^{AT} (\mathbf{I} - e^{-AT}) \mathbf{A}^{-1} \mathbf{b} & \mathbf{0} \\ e^{AT} \mathbf{W} e^{AT} (\mathbf{I} - e^{-AT}) \mathbf{A}^{-1} \mathbf{b} & \mathbf{W} e^{AT} (\mathbf{I} - e^{-AT}) \mathbf{A}^{-1} \mathbf{b} \end{bmatrix} \begin{bmatrix} u_0 \\ u_1 \end{bmatrix} + \begin{bmatrix} \mathbf{c}_1 \\ \mathbf{c}_2 \end{bmatrix} \right\| \quad (26)$$

Let $u_k \in \{0, 1\}$, $e^{AT} = 0.9$, $\mathbf{W} e^{AT} (\mathbf{I} - e^{-AT}) \mathbf{A}^{-1} \mathbf{b} = [4.0 \quad 3.0]^T$ and $\mathbf{c}_1 = \mathbf{c}_2 = [-3.4 \quad 2.9]^T$. It is easily checked that sequential optimisation of the two vector expressions in eqn. 26 yields the solution $\{u_0, u_1\} = \{0, 0\}$ with an objective functional value $J(u_0, u_1) = 12.6$. Solving the overall optimisation problem yields $\{u_0, u_1\}^* = \{1, 0\}$ with $J^*(u_0, u_1) = 12.3$. Clearly, the last is a better solution, which cannot be obtained by sequentially optimising the two vector expressions, i.e. an optimal state feedback law does not exist. Hence, this counter example proves that for the class of systems in eqn. 3 with control inputs $u_k \in U$ with U a finite subset in \mathbb{R} , combined with the objective functional in eqn. 2, an optimal state feedback law does not necessarily exist. Be aware that this has nothing to do with the use of 1-norm control, it holds for any norm. Here it suffices to mention that additional conditions on \mathbf{b} can be derived to guarantee the existence of an l_1 -norm optimal state

feedback law for systems with discrete control inputs, but these conditions are too complicated to be reported here.

For the N-removal problem the suboptimality of state feedback has been investigated by simulating the process controlled with a receding horizon optimal controller (RHOC) over two days for prediction horizon H ranging from 1 to 15 control intervals of 20 min. A sine wave pattern for influent ammonium (NH_4^{in}) and constant influent flow (q^{in}) were used. The controller was given perfect knowledge of the process dynamics and only the actual NH_4^{in} (and not its future values). This has been repeated for a whole range of combinations \mathbf{W} and \mathbf{x}_R . It turns out that H does not effect J^* . From this result, and the fact that using enumeration to solve the optimisation problem rules out local optima, it has been concluded that RHOC yields the globally optimal solution to the full horizon optimal control problem. Complementary simulations unravelled that decreasing H slightly deteriorates J^* in case of *a priori* known variations in q^{in} , i.e. in case of *a priori* known time-variations of \mathbf{A} and \mathbf{d} . However, knowledge of future q^{in} values is usually poor. So the best *feasible* result can be obtained by RHOC with $H = 1$. This means that an optimal state feedback law exists, despite the fact that $u \in \{0, 1\}$. Hence, for $H = 1$ the optimal control problem reduces to finding

$$u_k^* = \arg \min_{u_k \in \{0,1\}} \left\| \mathbf{W}(\hat{\mathbf{x}}_{k+1|k} - \mathbf{x}_R) \right\| \quad (27)$$

Using eqn. 20 it follows that

$$u_k^* = \arg \min_{u_k \in \{0,1\}} \left\| \mathbf{W}e^{A^T} \mathbf{x}_k + \mathbf{W}(e^{A^T} - I)\mathbf{A}^{-1}(\mathbf{b}u_k + \mathbf{d}_k) - \mathbf{W}\mathbf{x}_R \right\| \quad (28)$$

For the N-removal process (see eqn. 17)

$$e^{A^T} = e^{\frac{-q^{in}}{V}T} \mathbf{I} \quad (29)$$

and

$$e^{A^T}(\mathbf{I} - e^{-A^T})\mathbf{A}^{-1} = \begin{bmatrix} e^{\frac{-q^{in}}{V}T} & 0 \\ 0 & e^{\frac{-q^{in}}{V}T} \end{bmatrix} \begin{bmatrix} 1 - e^{\frac{q^{in}}{V}T} & 0 \\ 0 & 1 - e^{\frac{q^{in}}{V}T} \end{bmatrix} \begin{bmatrix} \frac{-V}{q^{in}} & 0 \\ 0 & \frac{-V}{q^{in}} \end{bmatrix} = \frac{1 - e^{\frac{-q^{in}}{V}T}}{\frac{q^{in}}{V}} \mathbf{I} \quad (30)$$

Substituting these last two equations in eqn. 28 yields the state feedback law

$$u_k^* = \arg \min_{u_k \in \{0,1\}} \left\| \mathbf{W} \left(e^{\frac{-q^{in}}{V}T} \mathbf{x}_k + \frac{1 - e^{\frac{-q^{in}}{V}T}}{\frac{q^{in}}{V}} (\mathbf{b}u_k + \mathbf{d}_k) - \mathbf{x}_R \right) \right\| \quad (31)$$

The low dimensionality of the above problem makes it possible to compute the objective functional value for both possible solutions and implement the optimal one. A characteristic simulation of the controlled process, using the controller in eqn. 31, is shown in Fig. 3. The trajectories of NH_4^{in} and q^{in} have been measured on a real plant during a dry weather weekday (Spanjers *et al.*, 1997)

Several experiments have been carried out on the pilot scale ASP described at the beginning of this section. The influent flow q^{in} during the experiments is obtained by monitoring the influent flow of the adjacent full-scale wastewater treatment plant of the town of Bennekom and downscaling this signal to a reasonable level for the pilot plant. In this way a natural relation between influent flow

and influent pollutant concentrations is guaranteed. Moreover real rainstorm events occur in the experiments. The pilot plant results in Fig. 4 have been obtained by the previously described RHOC controller extended with a recursive model parameter estimator (Lukasse *et al.*, 1997a). The recursive parameter estimator does not interfere with the control loop as its tuning is such that the dynamics of the parameter estimation loop are much slower than the closed loop dynamics. The sharp peaks of $NH_4 = 15$ mg/l and $NO_3 = 25$ mg/l in Fig. 4 are analyser auto-calibrations. The controller performance is satisfactory. In low loaded periods the aeration is switched off over longer time spans in order to utilise the possibility of more denitrification without deteriorated effluent NH_4 . During the two storm events the plant is overloaded, but the controller correctly decides to keep the aerators on. Summarising, despite the non-linearity and the limitation $u \in \{0, 1\}$ the controller performance is (close to) optimal.

6.5 Conclusions

An l_1 -norm optimal state feedback law has been derived (theorem 1). The theorem holds for 2-dimensional LTI systems with decoupled dynamics, a single input $u \in \mathbb{R}$ and no input weighting in the objective functional.

Straightforward application of the theorem to the control of ammonium and nitrate in an alternating activated sludge process for wastewater treatment is impossible, because the system is only stage-wise linear and $u \in \{0, 1\}$ instead of $u \in \mathbb{R}$. However, application of the l_1 -norm state feedback controller (eqn. 31) to a practical pilot plant yielded very satisfactory and close-to-optimal performance over the full experimental period of more than 3 days (Fig. 4). This successful application to a case with unproven optimality justifies cautious optimism about the method's wider applicability.

Acknowledgements: We are very grateful to M. Bloemen, who carried out the experimental work, and to the Dutch Technology Foundation (STW), that financially supported this research under grant no. WBI44.3275.

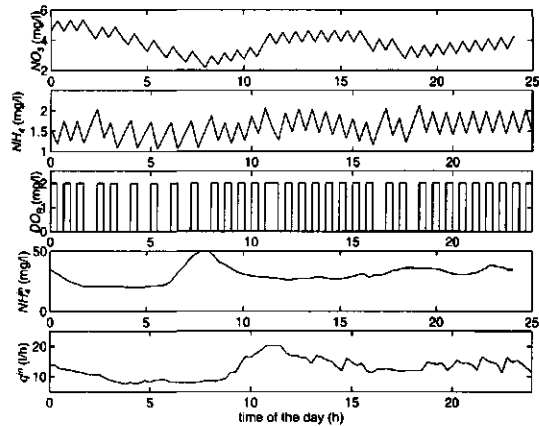


Fig. 3, RHOC in simulation with $x_R = [1.5 \ 0]^T$ and W such that NH_4 is controlled to its setpoint.

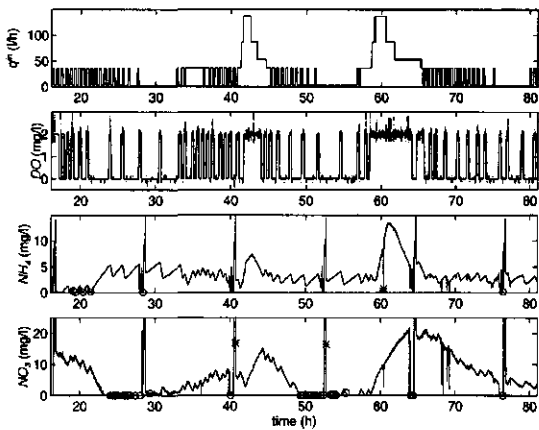


Fig. 4, adaptive RHOC applied to pilot plant with $x_R = [2 \ 0]^T$ mg/l and W such that NH_4 is controlled to its setpoint. (* = outlier, o = $\{NH_4, NO_3 = 0\}$).

6.6 References

- Bitmead, R.R., M. Gevers and V. Wertz (1990). Adaptive optimal control: the thinking man's GPC. London, U.K.: Prentice Hall.
- Bryson jr., A.E. and Y. Ho (1975). Applied optimal control: optimisation, estimation and control. New York: Hemisphere publishing company.
- Genceli, H. and M. Nikolaou (1993). Robust stability analysis of constrained l_1 -norm model predictive control. *AIChE Journal*, **39**(12), 1954-1965.
- Haarsma, G.J. and K.J. Keesman (1995). Robust model predictive dissolved oxygen control. *Med. Fac. Landbouww. Univ. Gent*, **60**(4b), proc. 9th FAB, Gent, Belgium, 2415-2426.
- Kwakernaak, H., and R. Sivan (1972). Linear optimal control systems. New York: John Wiley & Sons.
- Kwon, W.H. and A.E. Pearson (1977). A modified quadratic cost problem and feedback stabilization of a linear system. *IEEE Trans. Aut. Control*, **22**, 838-842.
- Leeuw, E.J. and E. van 't Oever (1996). Process selection, design and operation of the Ede WWTP. *Wat. Sci. Tech.*, **33**(12), 57-63.
- Lewis, F.L. (1986). Optimal control. New York: John Wiley & Sons.
- Lukasse, L.J.S., K.J. Keesman, A. Klapwijk and G. van Straten (1997a). Adaptive receding horizon optimal control of N-removing activated sludge processes. *Med. Fac. Landbouww. Univ. Gent*, **62**(4b), proc. 11th FAB, Gent, Belgium, 1665-1672.
- Lukasse, L.J.S., K.J. Keesman and G. van Straten (1997b). Identification for model predictive control of biotechnological processes, case study: nitrogen removal in an activated sludge process. *Proc. 11th IFAC symposium on System Identification 3*, 1525-1530.
- Morshedi, A.M., C.R. Cutler and T.A. Skovaneck (1985). Optimal solution of dynamic matrix control with linear programming techniques (LDMC). *Proc. Automatic Control Conf., Boston, USA*, 199-207.
- Münch, E.V., P. Lant and J. Keller (1996). Simultaneous nitrification and denitrification in bench-scale sequencing batch reactors. *Water Research*, **30**(2), 277-284.
- Spanjers, H., P. Vanrolleghem, K. Nguyen, H. Vanhooren and G. Patry (1997). Towards a simulation-benchmark for evaluating respirometry-based control strategies. Preprints of 7th int.'l workshop on instrumentation, automation and control of water and wastewater treatment and transport systems. *IAWQ, Brighton, UK*, 101-112.
- Thomas, Y.A. (1975). Linear Quadratic Optimal Estimation and Control with Receding Horizon. *Electron. Lett.*, **11**(1), 19-21.
- Thomas, Y.A., D. Sarlat and L. Shaw (1977). A receding horizon approach to the synthesis of non-linear multivariable regulators. *Electron. Lett.*, **13**(11), 329-331.

6.7 Appendix 1, list of symbols

symbol	value [unit]	description
$\ x\ _1$.. [..]	1-norm of vector x , i.e. $\sum_{i=1}^n x(i) $
$C_{NH,max}$	0.11 [g/m ³ .min]	maximum ammonium consumption rate
$C_{NO,max}$	0.08 [g/m ³ .min]	maximum nitrate consumption rate
q^{in}	1.0 [m ³ /day]	influent flow rate

NH_4^in, NH_4	.. [g NH_4 -N/ m^3]	(influent), ammonium nitrogen concentration
NO_3	.. [g NO_3 -N/ m^3]	nitrate nitrogen concentration
DO_R, DO_{max}, DO	.., 2, .. [g O_2 / m^3]	(ref. for slave controller), (min. nonlimiting), oxygen conc.
T	20 [min]	control interval
V	0.475 [m^3]	reactor volume
W	.. [..]	positive definite weighting matrix
x_R	.. [..]	state vector reference/setpoint

6.8 Appendix 2, counter example

Take the case

$$W = \begin{bmatrix} 0.5 & 0 \\ 0 & 1.0 \end{bmatrix} \quad A = \begin{bmatrix} 0.7 & 0.9 \\ 0.5 & 0.6 \end{bmatrix} \quad b = \begin{bmatrix} 0.8 \\ 0.2 \end{bmatrix} \quad x_0 = \begin{bmatrix} 1 \\ 1 \end{bmatrix} \quad d_0 = d_1 = 0$$

It is easily checked that for this case in eqn. 7

$$D_{11} = \begin{bmatrix} 0.70 \\ 0.62 \end{bmatrix} \quad D_{21} = \begin{bmatrix} 2.32 \\ 2.86 \end{bmatrix}$$

and hence condition 14 is not met. When consecutively solving eqns. 15.1 and 15.2 for respectively u_0 and u_1 , which would happen in case of state feedback, one gets

$$J = \left\| \begin{bmatrix} 0 & 1.38 & 0 & 1.98 \end{bmatrix} \right\|_1 = 3.36 \quad u_0 = -3.07 \quad u_1 = -1.82 \quad (32)$$

When solving the linear programming problem in eqn. 15 jointly, which is impossible in case of state feedback, one gets

$$J^* = \left\| \begin{bmatrix} -1.55 & 0 & 0 & 0.20 \end{bmatrix} \right\|_1 = 1.75 \quad u_0^* = -5.28 \quad u_1^* = 5.44 \quad (33)$$

This result demonstrates that if condition 14 is not satisfied, an l_1 -norm optimal state feedback law may not exist.

7 A comparison of NH_4/NO_3 control strategies for alternating activated sludge processes[†]

7.1 Abstract

Four control strategies for N-removal in alternating activated sludge plants (ASP's) are compared: 1. timer-based, 2. switching the aeration on/off when depletion of nitrate/ammonium is detected, 3. switching the aeration on/off when ammonium crosses an upper/lower-bound, 4. the newly developed adaptive receding horizon optimal controller (ARHOC) as presented in Lukasse *et al.* (1997). The comparison is made by simulating the controllers' application to an alternating continuously-mixed activated sludge reactor preceded by a small anoxic reactor for predenitrification. The biological processes in the reactors are modelled by the activated sludge model no. 1 (Henze *et al.*, 1987). Realistic influent patterns, measured at a full-scale wastewater treatment plant, are used (Spanjers *et al.*, 1997). The results show that three totally different controllers (timer-based, NH_4 -bounds based and ARHOC) can achieve a more or less equal effluent quality, if tuned optimally. The difference mainly occurs in the sensitivity to suboptimal tunings. The timer-based strategy has a higher aeration demand. The sensitivity of the ARHOC controller to sub-optimal tuning, known measurement time delays and changing plant loads is significantly less than that of the other controllers. Also its tuning is more natural and explicit.

Keywords: ammonium; control; nitrate; nitrogen; sensitivity; setpoint

7.2 Introduction

In recent years several types of control strategies for N-removal in continuously mixed ASP's have been developed in response to tightening government legislation with respect to effluent N concentrations. What is missing is a profound comparison of the different control strategies. That is the subject of this paper. The comparison is restricted to N-removal control strategies for *alternating* nitrification under aerobic conditions and denitrification under anoxic conditions.

Three well-known existing alternating control strategies and a newly developed adaptive receding horizon optimal controller (ARHOC) (Lukasse *et al.*, 1997) are compared. The comparison is carried out by *simulating* the application of the controllers to an alternatingly aerated continuously-mixed reactor preceded by a small anoxic reactor for predenitrification. The on/off aeration in the alternating reactor is the only control input to the N-removal control loop. This is a usual layout for plants aiming at both nitrification and denitrification. The use of simulations, rather than experiments, to compare controllers excludes erroneous conclusions due to arbitrary events.

[†] published by by L.J.S. Lukasse, K.J. Keesman, A. Klapwijk and G. van Straten in *proc. application of models in water management (IAWQ)*, 1998, Amsterdam, pp. 215-222 (submitted to *Wat. Sci. Tech.*).

7.3 Methodology

7.3.1 Plant model

The plant is modeled as a 40 l anoxic continuously mixed predenitrification reactor, succeeded by a 475 l continuously mixed alternating reactor (Fig. 1). The biological processes in the two reactors are modeled by the generally accepted activated sludge model no. 1 (ASM no.1) (Henze *et al.*, 1987) with default kinetic/stoichiometric parameters at 20 °C. For computational reasons the settler model is highly idealised: it has no volume, the sum of the two outflows equals the settler influent flow, while there are exclusively soluble components in the effluent. The sludge concentration in the reactors is controlled at 3.5 g/l. The simulations have been carried out in SIMBA™.

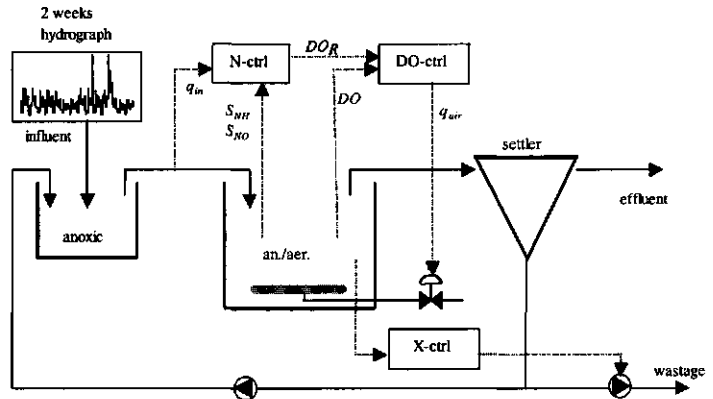


Fig. 1, simulated ASP with 2 weeks influent hydrograph and cascaded controllers for N and DO.

The output of the N-controllers is the DO setpoint DO_R , which alternates between 0 and 2 mg/l. A lower level DO controller realises DO_R more or less instantaneously. The DO controller saves aeration costs by adjusting the airflow to the DO consumption rate.

The output of the N-controllers is the DO setpoint DO_R , which alternates between 0 and 2 mg/l. A lower level DO controller realises DO_R more or less instantaneously. The DO controller saves aeration costs by adjusting the airflow to the DO consumption rate.

7.3.2 Influent scenario

Input for the simulations are the influent data over a period of 14 days, proposed as a benchmark by Spanjers *et al.* (1997). These influent data contain most naturally occurring influent scenario's (Fig. 2): dry weather working days, dry weather weekends, a storm event and a second storm event two days later.

The influent flow is scaled such that the average effluent S_{NH} and S_{NO} concentrations reach usual values. This turns out to occur at an average dry weather influent flow of 12.5 l/h, resulting in an average sludge load of

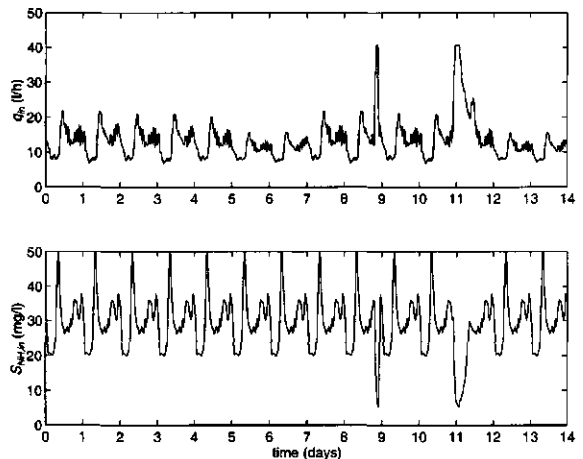


Fig. 2, influent flow and S_{NH} pattern used in simulation.

$$B_x = \frac{\frac{1}{14} \int_0^{14 \text{ days}} q_m \cdot \text{COD}_{in} dt}{V \cdot \text{MLSS}} = \frac{1647/14}{(40+475) \cdot 3.5} = 0.065 \left(\frac{\text{kg COD}}{\text{kg COD} \cdot \text{day}} \right) \quad (1)$$

7.3.3 Evaluation criteria

The most important criterion for comparison is the effluent quality, which is quantified as

$$J(u) = \frac{1}{14} \int_0^{14 \text{ days}} 3 \cdot S_{\text{NH}}(t) + S_{\text{NO}}(t) dt \quad (2)$$

The above integral expresses that a good effluent quality is achieved if both S_{NH} (ammonium) and S_{NO} (nitrate) are low, and that low S_{NH} is more important than low S_{NO} .

The lowest feasible values of objective criterion $J(u)$, J^* , for the four controllers are compared. Moreover, the sensitivity of J^* to suboptimal tuning, to measurement time delays and to load changes is determined. Before computing J^* the $X_{B,A}:X_{B,H}$ -ratio is brought in its steady state for each individual controller by simulating the controlled process over 112 days, with the influent being the repeated 14 days data set of Spanjers *et al.* (1997). Another important evaluation criterion is the average airflow \bar{q}_{air} which is needed to achieve J^* , as \bar{q}_{air} directly reflects the aeration costs.

7.4 Controllers to be compared

The most basic controller to be evaluated is the timer-based on/off controller. This open-loop controller has only two tuning parameters: the duration of aerobic (t_{aerobic}) and anoxic periods (t_{anoxic}). It easily causes time wasting: sometimes the aeration is on while $\text{NH}_4 = 0$ mg/l, or it is off while $\text{NO}_3 = 0$ mg/l. Controller 1:

$$u(t) = \begin{cases} 1 & \text{for } kT_c < t \leq kT_c + t_{\text{aerobic}} \\ 0 & \text{for } (k+1)T_c - t_{\text{anoxic}} < t \leq (k+1)T_c \end{cases} \quad (3)$$

where $T_c = t_{\text{aerobic}} + t_{\text{anoxic}}$, $k = \{0, 1, 2, \dots\}$ and $u \in \{0, 1\}$, i.e. $\text{DO}_R \in \{0, 2\}$ mg/l, {anoxic, aerobic}

A more advanced control scheme is one that switches the aeration off/on when serious limitation of the (de)nitrification rates due to low NH_4/NO_3 , i.e. depletion, occurs. In reality it uses measurements of quantities directly related to the process rates. The most usual is ORP (e.g. de la Ménardière, 1991), but pH and OUR may be used as well (Al-Ghusain *et al.*, 1994; Surmacz-Gorska *et al.*, 1995; Klapwijk *et al.*, in press). In these simulations it is assumed that depletion is detected as soon as NO_3/NH_4 fall below the controller parameters $S_{\text{NO},\text{min}}/S_{\text{NH},\text{min}}$. This prevents the difficulty of modelling the measurement devices (controller 2):

$$u(kT) = \begin{cases} 0 & \text{if } S_{\text{NH}}(kT) < S_{\text{NH},\text{min}} \\ 1 & \text{if } S_{\text{NO}}(kT) < S_{\text{NO},\text{min}} \\ u((k-1)T) & \text{if } (S_{\text{NH}}(kT) > S_{\text{NH},\text{min}}) \wedge (S_{\text{NO}}(kT) > S_{\text{NO},\text{min}}) \end{cases} \quad (4)$$

where $T =$ sampling interval (1 min), $k = \{0, 1, 2, \dots\}$, $S_{\text{NH},\text{min}} = \text{NH}_4$ lower-bound and $S_{\text{NO},\text{min}} = \text{NO}_3$ lower-bound

Another approach that is sometimes used in practice is the measurement of NH_4 and controlling it between two bounds. Time wasting occurs when NH_4 is kept between its bounds while NO_3 hits zero. Controller 3:

$$u(kT) = \begin{cases} 0 & \text{if } S_{NH}(kT) \leq S_{NH,\min} \\ 1 & \text{if } S_{NH}(kT) \geq S_{NH,\max} \\ u((k-1)T) & \text{if } S_{NH,\min} < S_{NH}(kT) < S_{NH,\max} \end{cases} \quad (5)$$

where T = sampling interval (1 min), $k = \{0, 1, 2, \dots\}$ and $S_{NH,\min}/S_{NH,\max}$ = NH_4 lower/upper-bound (tuning parameters)

The last controller is the newly developed adaptive receding horizon controller (ARHOC) for N-removal (Lukasse *et al.*, 1997), it needs measurements of NH_4 , NO_3 and influent flow q_{in} . An earlier version of the ARHOC controller has been tested successfully in pilot scale experiments. It is given by (controller 4):

$$\min_u J(u) = \int_{kT}^{(k+H)T} 3 \cdot S_{NH}(t) + S_{NO}(t) + \lambda \cdot \max \left(\begin{bmatrix} 0 \\ 0 \end{bmatrix}, \begin{bmatrix} S_{NH,\min} - S_{NH}(t) \\ S_{NO,\min} - S_{NO}(t) \end{bmatrix} \right) dt \quad (6)$$

subject to initial conditions $[S_{NH}(kT) \ S_{NO}(kT)]^T$, control input constraint $u \in \{0,1\}$, expected disturbances:

$$\begin{aligned} \hat{q}_{in}((k+i-1)T) &= q_{in}(kT) & \text{for } i = 1, \dots, H \\ \hat{S}_{NH,in}((k+i-1)T) &= S_{NH,in}(kT) & \text{for } i = 1, \dots, H \end{aligned}$$

and the model predictions:

$$\begin{bmatrix} S_{NH}((k+1)T) \\ S_{NO}((k+1)T) \end{bmatrix} = e^{-\frac{q_{in}T}{V}} \begin{bmatrix} S_{NH}(kT) \\ S_{NO}(kT) \end{bmatrix} + \frac{e^{-\frac{q_{in}T}{V}} - 1}{-\frac{q_{in}}{V}} \begin{bmatrix} -r_{NH} \\ r_{NH} + r_{NO} \end{bmatrix} u + \begin{bmatrix} \frac{q_{in}}{V} S_{NH,in} \\ -r_{NO} \end{bmatrix} \quad (7)$$

$$r_{NH} = \begin{cases} r_{NH,\max} & S_{NH} > 0 \\ \frac{q_{in}}{V} S_{NH,in} & S_{NH} = 0 \end{cases} \quad (8)$$

$$r_{NO} = \begin{cases} r_{NO,\max} & S_{NO} > 0 \\ 0 & S_{NO} = 0 \end{cases} \quad (9)$$

$$\begin{bmatrix} y_1(kT) \\ y_2(kT) \end{bmatrix} = \begin{bmatrix} S_{NH}(kT - t_d) \\ S_{NO}(kT - t_d) \end{bmatrix} \quad (10)$$

with λ = weighting parameter, H = prediction horizon (in sampling intervals), $r_{NH,\max}$ = maximum nitrification rate (mg/l.min), $r_{NO,\max}$ = maximum denitrification rate (mg/l.min), $S_{NH,in}$ = NH_4 concentration in influent (mg/l), $S_{NH,\min}$ = NH_4 lower-bound (mg/l), $S_{NO,\min}$ = NO_3 lower-bound (mg/l) and T = sampling interval (min)

The ARHOC's adaptive part exists of a recursive estimator for the time-varying model parameters $S_{NH,in}$, $r_{NH,\max}$ and $r_{NO,\max}$, based on the well-known Kalman filter (Lukasse *et al.*, submitted). The dynamic model in eqns. 7-10 is only valid for $u \in \{0, 1\}$. The good fit of the model outputs to measured S_{NH} and S_{NO} concentrations observed in Lukasse *et al.* (1997) demonstrates that the model suf-

fices for short term predictions of NH_4 and NO_3 . The major simplifications with respect to the ASM no.1 enable the on-line solution of the optimisation problem above.

The ARHOC objective criterion (eqn. 6) contains three tuning parameters: weight λ , and the NH_4/NO_3 lower-bounds $S_{\text{NH},\text{min}}$ and $S_{\text{NO},\text{min}}$. The weight λ should just be very large such that the last term in eqn. 6, a so-called soft constraint, prevails over the first two terms, therefore λ is set to 100. $S_{\text{NH},\text{min}}$ and $S_{\text{NO},\text{min}}$ will be optimised. The soft constraint ensures that S_{NH} and S_{NO} stay out of the region of substrate limited process rates as long as possible. Use of this soft constraint is necessary because of the large difference between the kinetics in ASM no.1 and in the ARHOC's internal model. In the default ASM no.1 the (de)nitrification rates are substrate limited by Monod kinetics with $k_{\text{NH}}=1.0$ and $k_{\text{NO}}=0.5$ mg/l. However, in the model identification experiments much smaller half saturation constants have been observed (Lukasse *et al.*, 1997), which justified the replacement of the Monod kinetic terms by the switching functions in eqns. 8 and 9.

The remaining tuning parameters are prediction horizon H and sampling interval T . They are set to $H=1$ and $T=20$ min. In Lukasse *et al.* (in press) it is shown that using $H>1$ yields no improvement at all. The sampling interval T has a not exactly known lower-bound: the point where too fast switching occurs, it is expected that this is not far below 20 min; at least faster switching does not occur in practice. Summarising, the ARHOC tuning in this study is $H=1$, $T=20$ min and $\lambda=100$. $S_{\text{NH},\text{min}}$ and $S_{\text{NO},\text{min}}$ will be optimised.

7.5 Best feasible results

In this section the most favourable results for all controllers are compared. The tuning of controller 1 that minimises $J(u)$ turns out to be $t_{\text{aerobic}} = 20$ min and $t_{\text{anoxic}} = 24.9$ min. In the optimisation the constraint was used that each phase should last at least 20 min, the adopted sampling interval of controller 4. Controller 1 realises a more or less constant S_{NO} , while the influent cycle occurs in S_{NH} (Fig. 3). This was to be expected: if both the (de)nitrification rates and the ratio $t_{\text{aerobic}}:t_{\text{anoxic}}$ are constant then the average S_{NO} is constant.

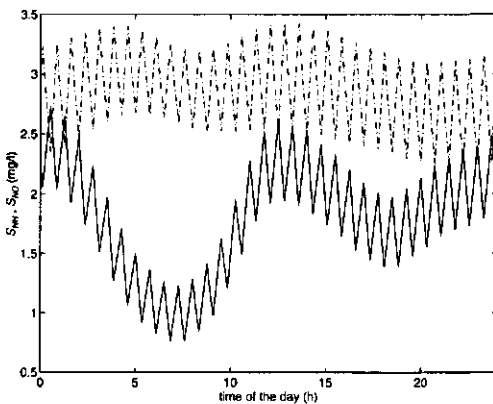


Fig. 3, simulated S_{NH} (-) and S_{NO} (-.) for controller 1 during a dry weather weekday.

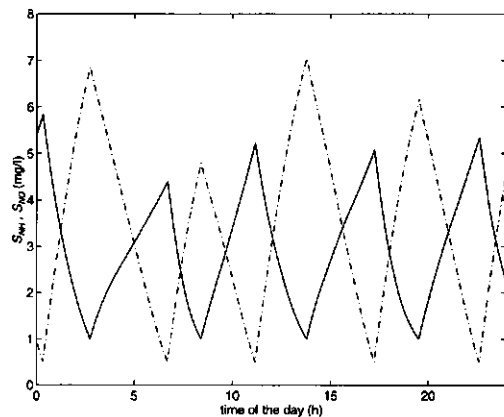


Fig. 4, simulated S_{NH} (-) and S_{NO} (-.) for controller 2 during a dry weather weekday.

$S_{NH,min}$ and $S_{NO,min}$ for controller 2 are tuned to respectively 1.0 (k_{NH}) and 0.5 (k_{NO}) mg/l, i.e. substrate limitation is detected when the process rate has dropped to 50% of the maximum rate. Optimising $S_{NH,min}$ and $S_{NO,min}$ results in switching the aeration on/off at about 10-20% process rate limitation, but such an early detection is impossible in practice. Controller 2 establishes a compromise between control of S_{NH} and S_{NO} , while the switching frequency is very low (Fig. 4).

For controller 4 only the lower-bounds $S_{NH,min}$ and $S_{NO,min}$ need to be optimised. It is enforced that $S_{NH,min} = 2 S_{NO,min}$, because $k_{NH} = 2 k_{NO}$. The optimal tuning turns out to be $S_{NH,min} = 1.4$ and $S_{NO,min} = 0.7$ mg/l. Clearly controller 4 tightly controls S_{NH} , while the influent cycle occurs in S_{NO} (Fig. 5). The bounds $S_{NH,min}$ and $S_{NH,max}$ in controller 3 are tuned at resp. 1.3 and 1.9 mg/l, the average S_{NH} -levels at which the *optimally tuned* controller 4 turns the aeration on/off. With this tuning controller 3 performs close-to-optimal, as it closely mimics the close-to-optimal controller 4 (Fig. 5). Controller 3 achieves more constant upper and lower limits on the S_{NH} cycles than controller 4, because the restriction to aerate for multiples of 20 min is lacking.

The quantitative performance measures of the four controllers with optimal tuning are listed in Table 1. All numbers in Table 1 are 14 days averages. From the J^* -values in Table 1 it is immediately clear that the effluent quality achieved with controller 2 is the worst, while the aeration costs are about equal to those of controllers 3 and 4. The J^* and \bar{q}_{air} achieved by controllers 3 and 4 are nearly equal, as their behaviour is nearly equal. The optimally tuned open-loop controller 1 slightly outperforms controllers 3 and 4 in terms of the criterion J^* , but this is achieved at the expense of 12% higher aeration costs (\bar{q}_{air}). By applying more denitrification during the high loaded part of the day (the period with relatively high S_S , and thus high $r_{NO,max}$), controller 1 better exploits the increased denitrification capacity than controllers 3 and 4 do.

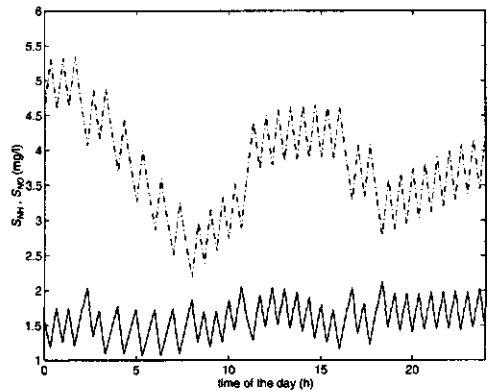


Fig. 5, simulated S_{NH} (-) and S_{NO} (-) for controller 4 during a dry weather weekday.

Strong rainfall occurs at the end of day 8 and during the first half of day 12 (see Fig. 2). The first

Table 1, controller performance at $\bar{q}_{in} = 12.5$ l/h.

controller	1 timers	2 depletion	3 S_{NH} bounds	4 ARHOC
J^* (mg/l)	8.23	12.0	8.27	8.31
\bar{q}_{air} (m ³ /day)	12.3	11.1	11.0	10.9
\bar{S}_{NH} (mg/l)	1.8	2.9	1.6	1.6
\bar{S}_{NO} (mg/l)	3.0	3.4	3.5	3.6
sensors	-	ORP, pH or OUR	NH ₄	NH ₄ and NO ₃
no. settings	2	0	2	3

rain event flushes the sewerage, causing high RBOS concentrations in the reactors, and hence high denitrification rates. In the simula-

tions this positive effect exceeds the negative effect of temporarily increased loading. At the start of the second rain event the sewerage had just been flushed, therefore the denitrification rate increase is much less and the negative effect of high loading dominates. Due to the use of an idealised settler model the most important rain effect does not occur in the simulations: sludge being pushed into the settler or effluent. Hence, these simulations are inconclusive with respect to the controllers' responses to rain events.

7.6 Sensitivity analysis

Besides the best feasible performance it is of interest to study the controllers' sensitivities to less ideal circumstances. Therefore in this section the sensitivity of $J(u)$ to tuning parameters, measurement time delays and influent load is investigated. Fig. 6 presents the sensitivity of controller 1 with respect to its tuning parameters $t_{aerobic}$ and t_{anoxic} (eqn. 3). It nicely illustrates that controller 1 is much more sensitive to the ratio $t_{aerobic}:t_{anoxic}$ than to their actual values.

For controller 2 it is important at which S_{NO}/S_{NH} values substrate limitation can be detected with how much time delay t_d . To reduce the dimensionality of the sensitivity analysis the ratio $S_{NH,min}:S_{NO,min}$ (eqn. 4) is kept equal to $k_{NH}:k_{NO}$. It turns out that J^* is much more sensitive to $S_{NO,min}$ and $S_{NH,min}$ than to t_d (Fig. 7), because reduction of S_{NH} from e.g. 0.5 to 0.4 mg/l takes more time than a 10 min measurement time delay in detection of $S_{NH} = 0.5$ mg/l. This time could be spent much more efficiently for denitrification.

Controller 3 has two tuning parameters $S_{NH,min}$ and $S_{NH,max}$ (eqn. 5). The sensitivity is presented in Fig. 8. The interesting phenomenon occurs that an increasing $S_{NH,max}$ causes an increase in $J(u)$ at high $S_{NH,min}$, but a decrease in $J(u)$ at low $S_{NH,min}$. The reason is that S_{NH} -limitation is no issue at high $S_{NH,min}$, and therefore an increased $S_{NH,max}$ just causes an increase in \bar{S}_{NH} and hence in $J(u)$. However, at low $S_{NH,min}$ increasing $S_{NH,max}$ reduces the part of the cycle in the S_{NH} -limiting range and hence a slight increase in \bar{S}_{NH} is compensated by a large decrease in \bar{S}_{NO} and as a result a reduced $J(u)$. In practice the exceeding of the bounds is detected with a time delay t_d . It turns out that $J(u)$, at

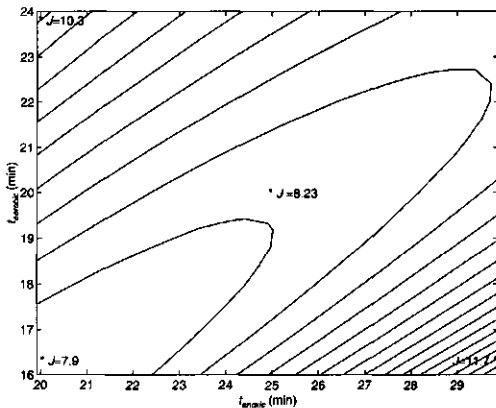


Fig. 6, sensitivity of controller 1 with respect to $t_{aerobic}$ and t_{anoxic} .

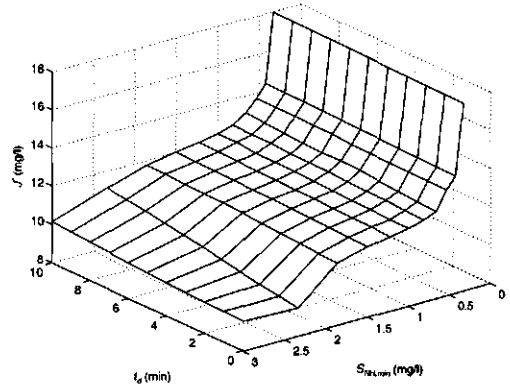


Fig. 7, sensitivity of controller 2 with respect to t_d and $S_{NH,min}$, with $S_{NH,min} = 2 S_{NO,min}$.

nominally tuned $S_{NH,min}$ and $S_{NH,max}$, increases nearly linear with t_d from $J^*=8.27$ at $t_d=0$ till $J^*=9.45$ mg/l at $t_d=10$ min. The larger t_d the larger the amplitude of the S_{NH}/S_{NO} -cycles and hence the larger the part of the cycles that is located in the substrate-limiting range.

The only tuning parameters of controller 4 for which a sensitivity analysis makes sense are $S_{NO,min}$ and $S_{NH,min}$ (eqn. 6), because it is hard to say what their optimal tuning is. Like in the sensitivity analysis for controller 2, the ratio $S_{NH,min}:S_{NO,min}$ is fixed at 2 and the analysis is combined with the effect of the measurement time delay t_d (Fig. 9). Fig. 9 shows that $J(u)$ is especially sensitive for too small $S_{NH,min}$ and that the larger t_d the larger the optimal $S_{NH,min}$. The larger $S_{NH,min}$ counteracts the fact that S_{NH} drops below $S_{NH,min}$ due to its delayed measurement. Moreover, t_d has a worse effect at low $S_{NH,min}$ than at high $S_{NH,min}$: delayed detection of the exceeding of a low $S_{NH,min}$ keeps the S_{NH} -cycle in the S_{NH} -limiting range for a larger percentage of time than delayed detection of the exceeding of a high $S_{NH,min}$.

To investigate the effect of the constraint on the minimum switching frequency of u , the sensitivity of $J(u)$ to the sampling interval T in controller 4 is evaluated. $J(u)$ is computed for T ranging from 4 to 30 min, resulting in a $J(u)$ increasing close-to-linearly from 7.52 till 8.95 mg/l. A smaller T clearly results in a smaller $J(u)$, due to the reduced amplitude of the S_{NH} -cycle at constant $S_{NH,min}$ and hence a reduction of \bar{S}_{NH} .

The sensitivity of $J(u)$ with respect to \bar{q}_m , the plant load, has been analysed for all controllers (Fig. 10). It turns out that the performance of controller 1 largely deteriorates at high plant loads due to

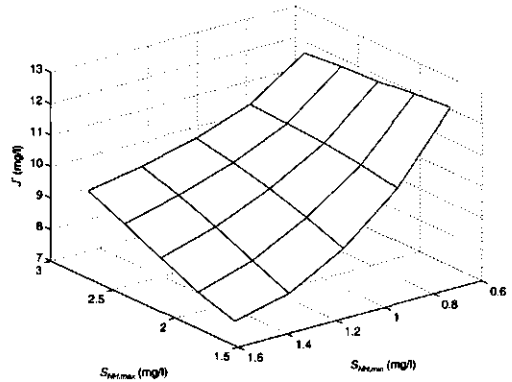


Fig. 8, sensitivity of controller 3 with respect to $S_{NH,max}$ and $S_{NH,min}$.

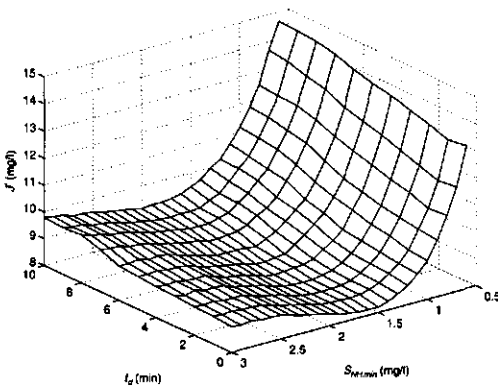


Fig. 9, sensitivity of controller 4 with respect to t_d and $S_{NH,min}$.

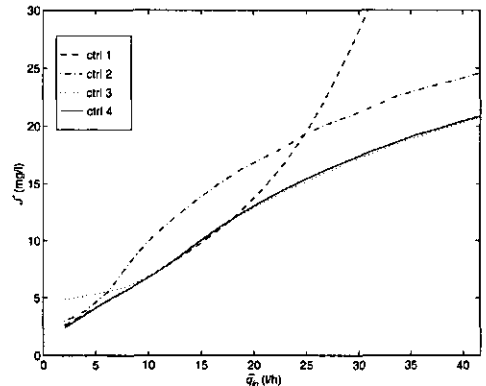


Fig. 10, J^* for controllers 1-4 as a function of \bar{q}_m .

high \bar{S}_{NH} . Controller 2 is significantly worse than all others are, except for the low loaded region, but in that region detection of nitrification/denitrification endpoints becomes more difficult and the simulation may well give a too positive impression. Only during low process loads controller 4 outperforms controller 3 by reducing both S_{NH} and S_{NO} below their lower-bounds, while controller 3 just controls S_{NH} between its bounds.

7.7 Discussion

Although controller 4 is an adaptive receding horizon *optimal* controller, its performance is not truly optimal in terms of $J(u)$ in eqn. 2; this is demonstrated by the slightly lower J^* -values achieved by controllers 1 and 3 (Table 1). The suboptimality of controller 4 has two reasons. First, controller 4 turns the aeration on/off for multiples of 20 min sampling interval. This is a theory-driven constraint, the process only poses the constraint that the switching interval should be at least 20 min. At the moment work is going on to change the fixed sampling interval into a minimal sampling interval T . The second reason for suboptimality of controller 4 is that its internal model is a major simplification of the ASM no.1. This discrepancy introduces errors in the predicted NH_4 and NO_3 concentrations, but it makes the simulations more realistic.

To reduce the negative effect of *known* measurement time-delays one can use state estimators, requiring the availability of a process model. In contrast to controllers 1-3 the ARHOC controller uses a process model anyway. Good results have been obtained for the ARHOC with state estimator in pilot scale experiments with known 20 min measurement delays in both S_{NH} and S_{NO} (Lukasse *et al.*, 1997)

7.8 Conclusions

The existing N-control strategies and a newly developed adaptive receding horizon optimal controller (ARHOC) (Lukasse *et al.*, 1997) for N-removal in alternating activated sludge processes have been compared by means of simulation. The comparison is restricted to the usual plant layout of a small continuously mixed anoxic predenitrification reactor, succeeded by a continuously mixed alternating reactor where the on/off aeration is the only manipulated input variable to the N-removal control loop (Fig. 1).

The difference in the best achievable effluent quality of the four controllers is insufficient to conclude that one of them is indisputably the best. The cheap timer-based controller (controller 1) is able to perform very well, but due to its open-loop nature it is very sensitive to suboptimal tuning, load variations and changing process rates. Controller 2 (switching the aeration on/off when depletion of nitrate/ammonium is detected) requires relatively simple measurements and only little tuning, but it performs significantly worse than all others do. Controller 3 (switching the aeration on/off when ammonium crosses an upper/lower-bound) mimics the close-to-optimal behaviour of controller 4 (adaptive receding horizon optimal control) as long as nearly complete nitrification and denitrification during the low loaded part of the day is infeasible.

Summarising, ARHOC requires more complex sensors than the other controllers, while the achievable effluent quality is nearly equal for ARHOC, timer-based and NH_4 -measurement based control.

The superiority of ARHOC comes in terms of its low sensitivity to suboptimal tuning and load changes, and in terms of the little retuning that is required. Moreover, the ARHOC controller yields estimates of $r_{NH,max}$, $r_{NO,max}$ and $S_{NH,in}$ as additional outputs. The enhanced process knowledge can improve e.g. the detection of toxic effects or could be used in optimising the sludge concentration setpoint.

Acknowledgements: We are very grateful to M. Bloemen for his contribution to the software programming and to H. Spanjers for providing us with the influent data set and his useful comments. We thank the Dutch Technology Foundation (STW) for financially supporting this research under grant no. WBI44.3275.

7.9 References

- Al-Ghusain I.A., Huang J., Hao O.J. and Lim, B.S. (1994) Using pH as a real-time control parameter for waste water treatment and sludge digestion processes. *Wat. Sci. Tech.* **30**(4), 159-168.
- Henze M., Grady jr. C.P.L., Gujer W., Marais G.v.R. and Matsuo T. (1987) Activated sludge model no. 1. *IAWQ Scientific and Technical Report no. 1*, IAWQ, London, Great Britain.
- Klapwijk A., Brouwer H. Vrolijk E. and Kujawa K. (1998). Control of intermittently aerated nitrogen removal plants by detection endpoints of nitrification and denitrification using respirometry only. *Wat. Res.*, **32**(5), 1700-1703.
- Lukasse L.J.S., Keesman K.J., Klapwijk A. and Straten G. van (1997) Adaptive receding horizon optimal control of N-removing activated sludge processes. *Med. Fac. Landbouww. Univ. Gent, proc. 11th FAB*, **62**(4b), Gent, Belgium, 1665-1672.
- Lukasse L.J.S., Keesman K.J., Klapwijk A. and Straten G. van (in press) Optimal control of N-removal in ASP's. *IAWQ world congress 1998*.
- Lukasse L.J.S., Keesman K.J. and Straten G. van (submitted) Recursive identification of N-removal in alternating activated sludge processes. *Journal of Process Control*.
- Ménardière M. de la, Charpentier J., Vachon A. and Martin G. (1991) ORP as control parameter in a single sludge biological nitrogen and phosphorus removal activated sludge system. *Water SA* **17**(2), 123-132.
- Spanjers H., Vanrolleghem P., Nguyen K., Vanhooren H. and Patry G. (1998) Towards a simulation-benchmark for evaluating respirometry-based control strategies. *Wat. Sci. Tech.*, **37**(12), pp. 219-226
- Surmacz-Gorska J., Gernaey K., Demuyne C., Vanrolleghem P. and Verstraete W. (1995) Nitrification process control in activated sludge using oxygen uptake rate measurements. *Environmental Technology* **16**, 569-577.

8 Optimised operation and design of alternating activated sludge processes for N-removal[†]

8.1 Abstract

This paper presents a simulation study with the scope to optimise the plant design and operation strategy of 2-reactors alternating activated sludge processes with only flow schedule and aeration on/off as control inputs. The methodology is to simulate the application of Receding Horizon Optimal Control (RHOC) to a range of different plant designs within this class of systems, and select the combination of design and operation strategy with the best performance. Subsequently a simple feedback controller is designed that closely imitates the optimal operation strategy. Starting-point is the plant layout with maximal degree of freedom within the above-mentioned class (Fig. 1), which is commercially available under the name BIODENITRO™. The simulation results indicate that in the optimal combination of plant design and operation strategy the performance in terms of nitrogen removal improves significantly as compared to current practice, especially if a shorter cycle length is used. In the optimal process design the two reactors are placed in series, the first reactor is about four times as large as the second one. The possibilities to feed influent to reactor 2 and to withdraw effluent from reactor 1 are redundant. A conceptually simple feedback controller (OSCAR, Operating a Series Connection of two Alternating Reactors) is presented that straightforwardly implements the improved operation strategy.

Keywords: BIODENITRO™; process design; OSCAR; nitrogen; process operation; optimal control

8.2 Introduction

In recent years several approaches to biological N-removal from wastewater in activated sludge processes (ASP's) have been developed in response to tightening government legislation with respect to effluent N concentrations. Biological N-removal requires aerobic conditions for nitrification (ammonium → nitrate) and anoxic conditions for denitrification (nitrate → nitrogen gas). One implementation used in practice is the operation of two hydraulically connected, alternatingly aerated, continuously mixed reactors.

This paper aims at optimisation of the operation strategy of this type of ASP (Fig. 1) in interaction with the plant design. Starting point is a plant design with two equally large reactors and the largest possible degree of freedom within the class of 2-reactors alternating processes with only flow schedule and aeration on/off as control inputs. Influent can be fed to either of the two reactors, effluent can be withdrawn from either reactor, there can be a flow between the two reactors in either

[†] to appear in *Water Research* by L.J.S. Lukasse and K.J. Keesman

direction, and each reactor can be either aerobic or anoxic. This type of plant is commercially available under the name BIODENTRO™.

Although a lot of attention has been paid to the operation of this type of process, the (sub)optimality of the combination of process design and operation strategy has never been studied. To investigate this (sub)optimality the application of Receding Horizon Optimal Control (RHOC) to the 2-reactors process will be simulated in SIMBA™. The following research questions are formulated:

1. Is the current practice of running the two reactors in counter phase at approximately equal ammonium and nitrate concentrations optimal?
2. Should the two reactors have equal volumes and is it useful to equip the plant hydraulics with all possible degrees of freedom?
3. Could a simply implementable feedback control strategy be formulated, which closely imitates the optimal operation strategy?

The use of simulations, rather than experiments, to *compare* combinations of plant design and operation strategy excludes erroneous conclusions due to arbitrary events. Moreover it would be practically impossible to make a fair experimental comparison between all the combinations of design and operation, which are compared in these simulations. Drawback of simulations is that the dynamics of the process need to be modelled and even the best model of the ASP is just a poor resemblance of the real process. Therefore at the end of the day full-scale experiments are required to verify/falsify the main conclusions.

8.3 Currently available operation strategies

All published controllers for the BIODENTRO™ process (Fig. 1) aim at operating the two reactors in counter phase (equal loading). Most of the time, one reactor is aerated while the other is anoxic. The influent is usually fed into the anoxic reactor, in order to maximally utilise its organic carbon content for denitrification. The role of the two reactors is toggled as soon as the nitrate concentration (S_{NO}) in the anoxic reactor reaches a preset value close to 0 or if the process cycle length t_c is exceeded. Several reports are available on manipulating t_c with the objective to reduce effluent total-N (Isaacs, 1997; Zhao *et al.*, 1994). Usually nitrification is faster than denitrification. If the ammonium concentration (S_{NH}) in a reactor reaches a preset value close to 0 before S_{NO} in the other reactor does, the aeration in the nitrifying reactor is switched off already. Effluent is always withdrawn from the reactor with lowest S_{NH} . In that way the buffering of S_{NH} in the reactors is increased to avoid idle time during the low loaded part of the day, *i.e.* the process runs with more S_{NH} to nitrify/denitrify in storage. All published controllers share the disadvantage that setting the large number

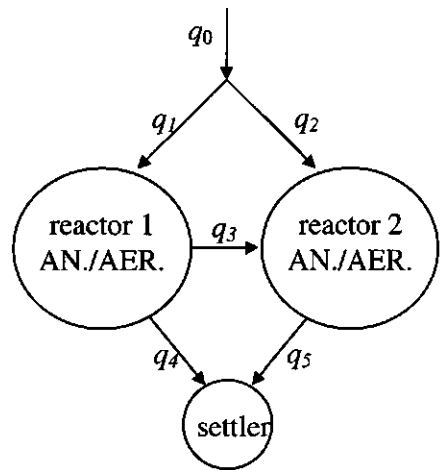


Fig. 1, scheme of the 2-reactors alternating system.

of tuning parameters really is a specialist's task, because of their indirect relation to the operational objectives of the process. For more details see *e.g.* Thornberg *et al.* (1993), Zhao *et al.* (1995), Isaacs (1996), Isaacs and Thornberg (1998) or Thomsen *et al.* (1998).

In principle the currently available control strategies have about 10 tuning parameters: the eight phase lengths (a phase is defined as a possible combination of aeration on/off and influent feed location in the two reactors in Fig. 1) and some additional tuning parameters (*e.g.* lower bound on S_{NH} and upper bound on length of aerated periods) that incidentally overrule the phase lengths. To reduce the controller's complexity at least two, and often even four, of the possible phases are discarded, at the expense of a deterioration of the controller's best feasible performance. The complexity of the control algorithm and the indirect relation between costs and effluent quality on the one hand and tuning parameters on the other hand do not invite the optimisation of tuning parameters in practice. As a consequence it is unknown to what extent the current combination of process design and operation strategy approaches the optimal case. In this study the application of receding horizon optimal control to a range of process designs is simulated in order to find the close-to-optimal combination of design and operation strategy.

8.4 Simulation methodology

8.4.1 The 2-reactors alternating process model

The plant is modelled as two 800 l continuously mixed alternating reactors (Fig. 1). The control inputs are the flows q_1 and q_2 , and the dissolved oxygen (DO) setpoints in reactor 1 (DO_1) and in reactor 2 (DO_2). The biological processes in the reactors are modelled by the generally accepted activated sludge model no. 1 (ASM no.1) (Henze *et al.*, 1987) with default kinetic/stoichiometric parameters at 20 °C. For computational reasons it is assumed that lower level DO controllers realise their setpoints instantaneously, *i.e.* the DO-balance is omitted. Also for computational reasons the settler model is highly idealised: it has no volume, the sum of the two outflows equals the settler influent flow, while there are exclusively soluble components in the effluent. The sludge concentration in the reactors is controlled at 4 g/l by means of the waste flow. The recirculation flow (q_r) is manipulated such that $q_r/q_{in} = 1$ (with q_{in} the influent flow rate in l/h), according to the common concept of recycle ratio control (Metcalf and Eddy, 1979). This plant model equals the one used in Isaacs and Thornberg (1998) to test their controller, except for the assumed steady state of the DO balance.

8.4.2 Influent scenario

Input for the simulations are the influent data over a period of 14 days, proposed as a benchmark by Spanjers *et al.* (1998). These influent data contain most naturally occurring influent scenario's (Fig. 2): dry weather working days, dry weather weekends, a storm event and a second storm event two days later.

The influent flow q_{in} is scaled such that the average dry weather influent flow is 90 l/h, the value used in Isaacs and Thornberg (1998). The resulting average sludge load B_X is

$$B_x = \frac{\frac{1}{14} \int_0^{14 \text{ days}} q_{in} \cdot COD_{in} dt}{(V_1 + V_2) \cdot MLSS} = 0.132 \left(\frac{\text{kg COD}}{\text{kg COD} \cdot \text{day}} \right) \quad (1)$$

where COD_{in} = influent Chemical Oxygen Demand (kg COD/l), V_1 = volume of reactor 1 (l), V_2 = volume of reactor 2 (l) and $MLSS$ = sludge concentration (kg COD/l).

8.4.3 Evaluation criteria

The most important evaluation criterion for a combination of plant design and operation strategy is the effluent quality, which is quantified as

$$J(\mathbf{u}) = \frac{\int_0^{14 \text{ days}} 3 \cdot (q_4(t) \cdot S_{NH,1}(t) + q_5(t) \cdot S_{NH,2}(t)) + q_4(t) \cdot S_{NO,1}(t) + q_5(t) \cdot S_{NO,2}(t) dt}{\int_0^{14 \text{ days}} (q_4(t) + q_5(t)) dt} \quad (\text{mg/l}) \quad (2)$$

where $S_{NH,1}$ and $S_{NH,2}$ (respectively $S_{NO,1}$ and $S_{NO,2}$) are ammonium (respectively nitrate) in reactors 1 and 2, and q_4 and q_5 are flow rates as defined in Fig. 1. $J(\mathbf{u})$ is the flow-weighted average of ($3S_{NH} + S_{NO}$) in the plant's effluent. This objective functional expresses that a good effluent quality is achieved if both S_{NH} and S_{NO} are low, and that low S_{NH} is more important than low S_{NO} . Additional evaluation criteria are average effluent S_{NH} and S_{NO} , sludge production and effluent COD.

Before computing $J(\mathbf{u})$ for a specific combination of process design and operation strategy the ratio of autotrophic ($X_{B,A}$) and heterotrophic ($X_{B,H}$) organisms is brought in its steady state by simulating the controlled process over 112 days, with the influent being the repeated 14 days data set of Spanjers *et al.* (1998).

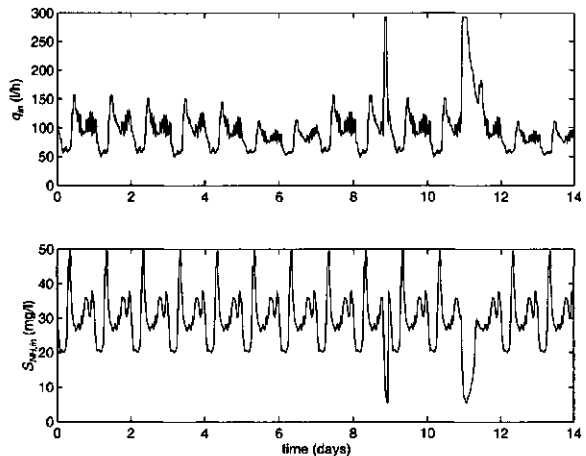


Fig. 2, influent flow and S_{NH} pattern used in simulation.

8.5 Receding horizon optimal control of the alternating process

In principle the theory of optimal control (Lewis, 1986) is the most suitable tool to compute the optimal control strategy for a given plant design. In practice however it has some major drawbacks: large computational demand, not implementable on-line, and the risk of getting stuck at local minima. The first two drawbacks are not shared by RHOC (Receding Horizon Optimal Control) (e.g. Mayne and Michalska, 1990). The third drawback can be avoided by using the enumeration algorithm to solve the optimization problem, in eqn. 3 it will become clear that this algorithm is only

practical in the RHOC context. For these reasons RHOC is favoured in this study, accepting the RHOC's drawback that its limited prediction horizon disables the exact solution of the full-horizon optimal control problem (Bitmead *et al.*, 1990).

In simulating the application of RHOC to the problem of N-removal in the above described 2-reactors system there are four control input trajectories to be optimised over each process cycle, being q_1 , q_4 , DO_1 and DO_2 . The control input constraints are

$$q_1, q_4 \in \{0, q_0\} \text{ (l/h)}$$

$$DO_1, DO_2 \in \{0, 2\} \text{ (mg/l)}$$

Altogether this gives $2^4 = 16$ possible combinations of control inputs. Notice that once q_1 and q_4 are known, the other flows q_2 , q_3 and q_5 follow as a consequence (Fig. 1). Flow q_4 is decoupled from the other controls by adopting the current strategy to withdraw the effluent from the reactor with lowest S_{NH} (work queuing). The remaining three controls are parametrised according to Fig. 3, where u_1 , u_2 and u_3 are multiples of the control interval T . T is a multiple of half the cycle length t_c , i.e. $t_c/T = n$ with n even. By limiting the controls u_1 , u_2 and u_3 to be multiples of the control interval T the number of possible combinations of control input trajectories over the RHOC prediction horizon H is reduced from infinite to

$$m = \left(\frac{t_c}{2T} + 1 \right)^{3H} \quad (3)$$

The RHOC controller solves at each start of half a process cycle (kt_c with $k \in \{0, 1/2, 1, 1.5, 2, \dots\}$) the non-linear optimisation problem in eqns. 4-8 by just computing $G(\mathbf{u})$ for all m possible combinations of control input trajectories, and selecting the one that minimises $G(\mathbf{u})$. The attractive feature of this so-called enumeration algorithm is its guaranteed globally optimal solution of the RHOC's optimisation problem within fixed time. Drawback is the computational inefficiency of the enumeration algorithm. Only the first half cycle of the computed optimal combination of control input trajectories is implemented, i.e. applied to the earlier described process model (section Simulation Methodology). After this half cycle the optimisation problem is solved again with q_1 , DO_1 and DO_2 in Fig. 3 flipped upside down and the state at time $(k + 1/2)t_c$ as initial condition. Solving at each half cycle, instead of each whole cycle, increases the feedback from the process and hence reduces the negative effect of prediction errors by the RHOC's internal model (eqn. 7). The RHOC optimisation problem is given by

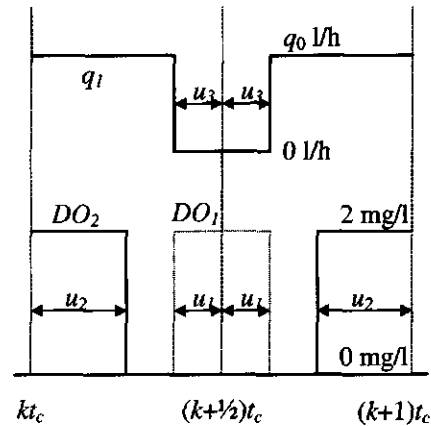


Fig. 3, control inputs parametrization over one process cycle.

$$\begin{aligned}
 \mathbf{u} = [u_1 \quad u_2 \quad u_3] \quad \min_{\mathbf{u}} \quad G(\mathbf{u}) = & \int_{kt_c}^{(k+H)kt_c} w_1 (q_4 S_{NH,1} + q_5 S_{NH,2}) + (q_4 S_{NO,1} + q_5 S_{NO,2}) \\
 & + w_2 ((\bar{S}_{NH,1} - \bar{S}_{NH,2})^2 + (\bar{S}_{NO,1} - \bar{S}_{NO,2})^2) + w_3 \left(\frac{q_1}{q_0} DO_1 + \frac{q_2}{q_0} DO_2 \right) \quad (4) \\
 & + w_4 \sum \max \left(\begin{bmatrix} 0 \\ 0 \\ 0 \\ 0 \end{bmatrix}, \begin{bmatrix} (S_{NH,\min} - S_{NH,1}) DO_1 \\ (S_{NO,\min} - S_{NO,1})(2 - DO_1) \\ (S_{NH,\min} - S_{NH,2}) DO_2 \\ (S_{NO,\min} - S_{NO,2})(2 - DO_2) \end{bmatrix} \right) dt
 \end{aligned}$$

subject to initial conditions $[S_{NH,1}(kt_c) \quad S_{NO,1}(kt_c) \quad S_{NH,2}(kt_c) \quad S_{NO,2}(kt_c)]^T$, expected disturbances:

$$\hat{q}_0(kt_c + iT) = 2 \cdot q_{in}(kt_c) \quad \text{for} \quad i = 0, \dots, nH \quad (5)$$

$$\hat{S}_{NH,0}(kt_c + iT) = 0.5 \cdot S_{NH,in}(kt_c) \quad \text{for} \quad i = 0, \dots, nH \quad (6)$$

and subject to the model predictions:

$$\begin{aligned}
 \begin{bmatrix} S_{NH,1}(kt_c + (i+1)T) \\ S_{NO,1}(kt_c + (i+1)T) \\ S_{NH,2}(kt_c + (i+1)T) \\ S_{NO,2}(kt_c + (i+1)T) \end{bmatrix} = & \begin{bmatrix} e^{-D_1 T} & 0 & -\frac{\min(0, q_3) 1 - e^{-D_1 T}}{V_1} & 0 \\ 0 & e^{-D_1 T} & 0 & -\frac{\min(0, q_3) 1 - e^{-D_1 T}}{V_1} \\ \frac{\max(0, q_3) 1 - e^{-D_2 T}}{V_2} & 0 & e^{-D_2 T} & 0 \\ 0 & \frac{\max(0, q_3) 1 - e^{-D_2 T}}{V_2} & 0 & e^{-D_2 T} \end{bmatrix} \begin{bmatrix} S_{NH,1}(kt_c + iT) \\ S_{NO,1}(kt_c + iT) \\ S_{NH,2}(kt_c + iT) \\ S_{NO,2}(kt_c + iT) \end{bmatrix} \quad (7) \\
 + & \begin{bmatrix} \frac{1 - e^{-D_1 T}}{D_1} \left[\frac{q_1}{V_1} - \frac{1}{2} DO_1 \right] & 0 \\ \frac{1 - e^{-D_2 T}}{D_2} \left[\frac{q_2}{V_2} - \frac{1}{2} DO_2 \right] & 0 \end{bmatrix} \begin{bmatrix} S_{NH,0} \\ r_{NH,max} \\ r_{NO,max} \end{bmatrix}
 \end{aligned}$$

where

$$D_1 = \frac{q_4 + \max(0, q_3)}{V_1} \quad \text{and} \quad D_2 = \frac{q_5 - \min(0, q_3)}{V_2} \quad (8)$$

The vector of control inputs \mathbf{u} is related to q_1 , DO_1 and DO_2 according to Fig. 3. By taking the initial conditions equal to the current state of the process perfect non-time-delayed measurements are assumed. This choice is unrealistic for a practical implementation, but yields better insight in the optimal performance of the process. The incoming q_0 and $S_{NH,0}$ are the total reactors' inflow (effect of influent and return flow!). As the return flow is adjusted such that $q_r = q_{in}$ (ratio-control), the resulting flow q_0 is double the influent flow q_{in} (eqn. 5). S_{NH} in the return flow is much lower than $S_{NH,in}$ and hence neglected, resulting in eqn. 6. The RHOC's internal dynamic model (eqn. 7) is just the equivalent discrete time system (Lewis, 1986) of simple continuous time mass balances for S_{NH} and S_{NO} over the two reactors. The possibility of a flow q_3 in both directions necessitates the use of the terms $\max(0, q_3)$ and $\min(0, q_3)$ in eqn. 7, a flow from reactor 1 to reactor 2 is defined as positive. The good fit of the same type of model for a 1-reactor alternating system to measured S_{NH} and S_{NO} concentrations observed in Lukasse *et al.* (1997) demonstrates that the model suffices for short term predictions of S_{NH} and S_{NO} in alternating reactors. The model is only valid for $[DO_1, DO_2] \in \{0, DO^*\}$ (mg/l), with DO^* a non-limiting DO-concentration, say $DO^* > 1.5$ mg/l. The model parameters $r_{NH,max}$ (max. nitrification rate) and $r_{NO,max}$ (max. denitrification rate) are estimated from simu-

lated process trajectories. The major simplifications with respect to the ASM no.1 model (Henze *et al.*, 1987) enable the fast simulation of the model over the prediction horizon H .

The RHOC's tuning parameters and their values are listed in Table 1. The first two terms in $G(\mathbf{u})$ represent the numerator of the evaluation criterion (eqn. 2), reflecting the desired effluent quality. In Lukasse *et al.* (1998) it is shown that weight $w_1 = 3$ is a suitable value, much lower w_1 will make low S_{NO} more important than low S_{NH} , while much higher values will make S_{NO} totally irrelevant. The weight w_2 can be used to enforce equal

Table 1. RHOC's tuning parameters

parameter	description	value
w_1	weight	3
w_2	weight	0
w_3	weight	1300
w_4	weight	$5 \cdot 10^3$
$S_{NH,min}$ (mg/l)	S_{NH} min. bound	0.3
$S_{NO,min}$ (mg/l)	S_{NO} min. bound	3.1
t_c (min)	cycle length	120
T (min)	control interval	$t_c/12$
H	prediction hor.	1

loading of the two reactors, it penalizes differences between the *average* ammonium $(\bar{S}_{NH,1} - \bar{S}_{NH,2})^2$ and nitrate $(\bar{S}_{NO,1} - \bar{S}_{NO,2})^2$ concentrations in the two reactors during a cycle. The default value of w_2 is 0, a value of 350 was found to be sufficient for obtaining reasonably equal loading. Weight w_3 penalises feeding influent to an aerobic reactor. This penalty term is an effort to compensate for the absence of the known positive effect of q_0 on $r_{NO,max}$ in the controller's internal model. A value $w_3 = 1300$ appears to suffice for preventing the feeding of influent to the aerobic reactor. Finally weight $w_4 = 5 \cdot 10^3$, this is just a very high value which forces the process to stay out of the region of substrate limited process rates as long as $S_{NH} > S_{NH,min}$ or $S_{NO} > S_{NO,min}$ (Table 1). This penalty term justifies the absence of substrate limitation terms in the controller's internal model. The tuning parameters w_3 , $S_{NH,min}$ and $S_{NO,min}$ have been tuned iteratively such that $J(\mathbf{u})$ in eqn. 2 is minimised.

The cycle length t_c is initially set equal to 120 min, the value used in the controller to which Isaacs and Thornberg (1998) compared. The control interval T is set to $t_c/12$ (in case $t_c = 120$ min, this yields $T = 10$ min). It was found that smaller T only yields a minor improvement at the expense of a rapidly increasing computational demand (eqn. 3).

8.6 RHOC results

For RHOC in general it holds that, in absence of model-plant mismatch, the larger H and the more prior knowledge about future disturbance inputs, the better the controller performance (Bitmead *et al.*, 1990). Therefore the effect of H was tested by computing $J(\mathbf{u})$ for $H = 1$ and $H = 2$ cycle lengths, both with and without prior knowledge about q_0 and $S_{NH,0}$ in eqns. 5-6. The differences in $J(\mathbf{u})$ occurred to be less than one percent, while the computation time increases sharply with H (eqn. 3). So it is justified to set $H = 1$. Fig. 4 depicts the state trajectories for the default case.

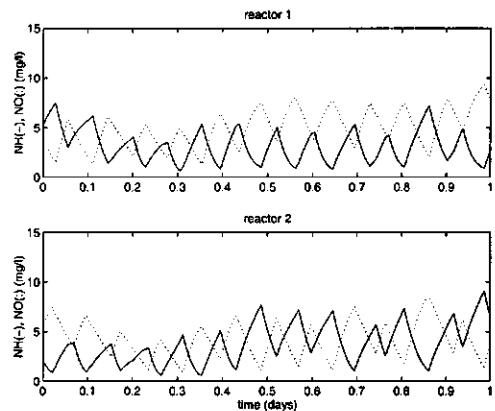


Fig. 4. dry weather weekday state trajectories of the plant in Fig. 1 with RHOC, $t_c = 120$ min.

Now the first research question (Is it optimal to run the two reactors in counter phase?) is addressed by investigating the effect of enforcing equal loading of the two reactors as a function of cycle length t_c . Both the default RHOC controller (Table 1), the RHOC with enforced equal loading ($w_2 = 350$) and the rule-based controller to which Isaacs and Thornberg (1998) compared their controllers are simulated over the characteristic 14 days period, for different t_c -values. The results are presented in Fig. 5. It turns out that the explicitly optimising RHOC controller without the equal loading constraint outperforms the other controllers. Especially at short cycle lengths RHOC is superior, and hence running in counter phase is suboptimal. This can be understood by observing that the shorter t_c the smaller the amplitudes in the S_{NH}/S_{NO} cycles. Hence the shorter t_c the more eminent concentration differences between the two reactors can be realised, *i.e.* the larger the possible advantage of non-equal loading of the two reactors. RHOC exploits the possibility to create larger concentration differences between the two reactors: In the predominantly denitrifying reactor 1 the fluctuations in $S_{NH,in}$ are attenuated and S_{NO} is kept low (Fig. 6), while the effluent is withdrawn from the predominantly nitrifying reactor 2, where S_{NH} is low. Influent is fed to reactor 1 except when reactor 1 is aerobic while reactor 2 is anoxic. All effluent is withdrawn from reactor 2.

As the role of the reactors is no longer the same in case of RHOC, it is no longer obvious that the volumes should be equal (research question 2). To investigate the effect of non-equal volumes RHOC is applied to a plant design with volume V_1 ranging from 400 to 1450 l, while the total volume remains fixed, *i.e.* $V_1 + V_2 = 1600$ l. This simulation is done for RHOC with $t_c = 40$ min and with $t_c = 120$ min, to see whether the effects of t_c and V_1 interact. It turns out that in the optimal design of the RHOC controlled plant V_1 and V_2 are approximately equal, regardless of t_c (Fig. 7). The optimality for $V_1 = V_2$ looks very coincidental in the light of the two opposite effects of changing V_1 : I. The larger V_1 the better the influent cycle is dampened in reactor 1, and II. The smaller V_1 the higher the concentration readily biodegradable organic substrate (S_S) and hence the higher $r_{NO,max}$ in the predominantly denitrifying reactor 1.

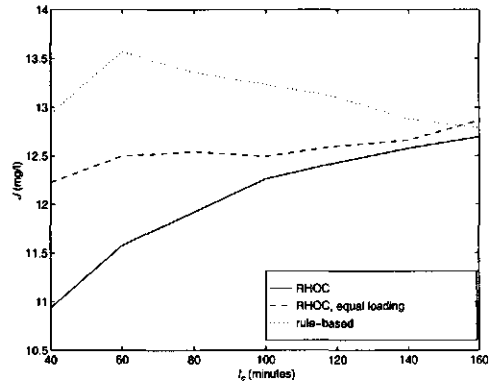


Fig. 5. $J(u)$ as a function of t_c for different controllers.

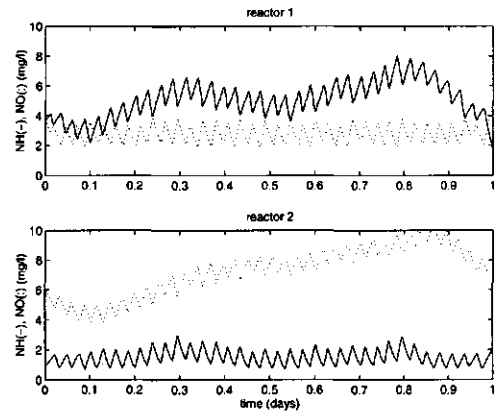


Fig. 6. dry weather weekday state trajectories of the plant in Fig. 1 with RHOC, $t_c = 40$ min.

The results of this RHOC study show that the optimal operation strategy uses short cycles and keeps S_{NO} low in reactor 1 and S_{NH} low in reactor 2 (Fig. 6). Influent is fed to reactor 1, except when reactor 1 is aerobic while reactor 2 is anoxic. All effluent is withdrawn from reactor 2. Hence, running the two reactors in counter phase is suboptimal (research question 1). With respect to the process design (research question 2) the RHOC simulation results show that the possibility to withdraw effluent from reactor 1 is redundant and that the optimal volume distribution is $V_1 = V_2$ (Figs. 6, 7).

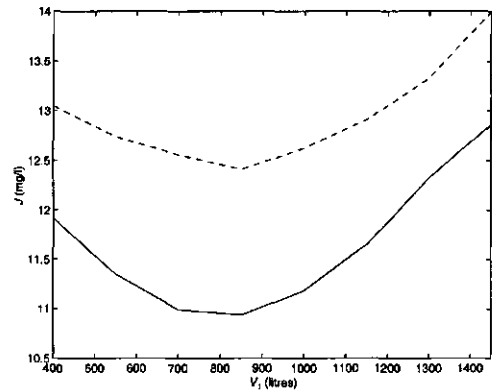


Fig. 7. $J(u)$ as a function of V_1 for $t_c = 40$ min (-) and $t_c = 120$ min (--) in case of RHOC with default tuning.

8.7 Simple controllers imitating RHOC

Implementing RHOC on-line is possible (Lukasse *et al.*, 1998), but rather complex. However, the observed optimal behaviour can be cast in some easily implemented rules (research question 3), which will closely mimic the optimal RHOC's behaviour (Fig. 6). The rules are:

1. Always withdraw the effluent from reactor 2.
2. Control S_{NO} in reactor 1 between a lower and upper bound:

$$DO_1(kT) = \begin{cases} 0 & \text{if } S_{NO,1} > S_{NO,max} \\ DO_1((k-1)T) & \text{if } S_{NO,min} < S_{NO,1} < S_{NO,max} \\ 2 & \text{if } S_{NO,1} < S_{NO,min} \end{cases} \quad (9)$$

where T is control interval (1 min), $S_{NO,max}$ is nitrate upper bound (3.6 mg/l) and $S_{NO,min}$ is nitrate lower bound (2.0 mg/l)

3. Control S_{NH} in reactor 2 between a lower and upper bound:

$$DO_2(kT) = \begin{cases} 0 & \text{if } S_{NH,2} < S_{NH,min} \\ DO_2((k-1)T) & \text{if } S_{NH,min} < S_{NH,2} < S_{NH,max} \\ 2 & \text{if } S_{NH,2} > S_{NH,max} \end{cases} \quad (10)$$

where $S_{NH,max}$ is ammonium upper bound (1.8 mg/l) and $S_{NH,min}$ is ammonium lower bound (0.8 mg/l)

4. Always feed the influent to reactor 1, except when reactor 1 is aerated and reactor 2 unaerated.

The tuning of upper/lower bounds in the algorithm above is such that these rules mimic the optimal RHOC behaviour with $t_c = 40$ min and $V_1 = V_2 = 800$ l (Fig. 6) as close as possible. In the sequel this controller will be referred to as 'stepfeeding', as not using the possibility to withdraw effluent from reactor 1 reduces the BIODENITRO™-design to a system of 2-reactors in series with stepfeeding (Stehfest, 1985). As expected, implementing this new rule-based controller yields state trajectories very much like those for RHOC with $t_c = 40$ min in Fig. 6 (not shown). Evaluating the ob-

jective functional value $J(\mathbf{u})$ for V_1 ranging from 400 till 1450 l yields the dashed line (--) in Fig. 8. Especially for $V_1 > V_2$ stepfeeding largely outperforms RHOC. While RHOC performs optimally at $V_1 = V_2$, the stepfeeding controller achieves its optimal performance at V_1 about 1300 l ($V_1 \approx 4 V_2$).

In the simulations it was observed that the stepfeeding algorithm above hardly uses the possibility to feed influent to reactor 2. Therefore the stepfeeding control algorithm is further simplified by modifying rule 4 into

4. Always feed the influent to reactor 1.

This new algorithm is referred to as 'OSCAR' (Operating a Series Connection of Alternating Reactors). It can be implemented in a plant design of just two alternately aerated reactors in series. Simulating the OSCAR-algorithm for V_1 ranging from 400 till 1450 l yields the solid line in Fig. 8. It turns out that OSCAR even slightly outperforms the stepfeeding algorithm when $V_1 > 700$ l. Characteristic state trajectories for OSCAR control with $V_1 = 1300$ l are shown in Fig. 9.

The fact that OSCAR outperforms the stepfeeding algorithm can be explained by looking at the two effects of feeding influent to reactor 2:

- I. Increased denitrification in reactor 2 due to increased soluble organic substrate.
- II. Deteriorated effluent due to temporarily overloading of reactor 2.

Effect I becomes weaker when V_1 increases, while effect II becomes stronger when V_1 increases. The superior performance of OSCAR for $V_1 > 700$ l shows that the first, positive, effect no longer outweighs the second, negative, effect when $V_1 > 700$ l.

8.8 Discussion

The value of $J(\mathbf{u})$ for the simulated BIODENTRO™ plant model with RHOC control and equal loading (operating in counter phase) at a 120 min cycle length is about 12.6 mg/l (Fig. 5, RHOC, equal loading at $t_c = 120$ min). Applying OSCAR at approximately 40 min cycle length for the same plant model yields $J(\mathbf{u}) = 10.4$ mg/l (Fig. 8, OSCAR at $V_1 = 800$ l). Hence replacing the current practice of operating in counter phase by OSCAR control yields an improvement of about 17%. In

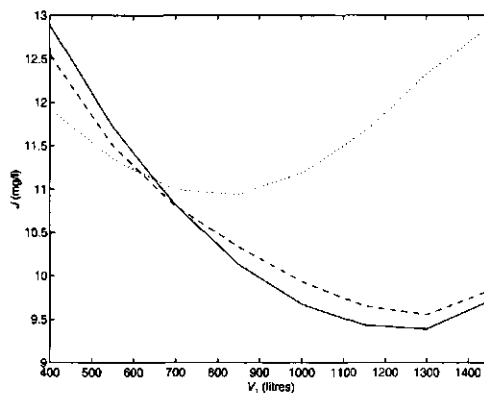


Fig. 8. $J(\mathbf{u})$ as a function of V_1 for stepfeeding (--), OSCAR (-) and RHOC with $t_c = 40$ min (·).

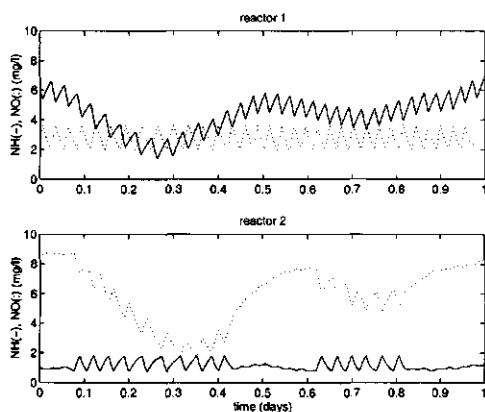


Fig. 9. dry weather weekday state trajectories achieved with OSCAR in case $V_1 = 1300$ l.

the simulations an additional 10% performance improvement ($J(\mathbf{u}) = 9.4$ mg/l) was achieved by using OSCAR control and modifying the plant design from $V_1 = V_2$ into $V_1 = 4V_2$, while keeping $V_1 + V_2$ unchanged (Fig. 8, OSCAR at $V_1 = 1300$ l).

Up to here the results have only been evaluated in light of the objective criterion $J(\mathbf{u})$, a flow-weighted sum of effluent S_{NH} and S_{NO} . Obviously, it is interesting to know the average flow-weighted effluent concentrations of S_{NH} and S_{NO} itself as well. Other additional criteria are sludge production, effluent COD and aeration costs. These complementary quantities are presented in Table 2 for the most interesting combinations of control and design only. The averages in Table 2 are flow-weighted.

Table 2, additional performance measures for most interesting cases.

controller/plant design	$\bar{S}_{NH,ef}$ (mg/l)	$\bar{S}_{NO,ef}$ (mg/l)	sludge prod. (g COD/day)	\overline{COD}_d (mg COD/l)
RHOC, equal loading, $t_c = 120$ min	2.0	6.7	294.1	31.1
RHOC, $t_c = 120$ min	2.18	5.8	294.4	31.1
RHOC, $t_c = 40$ min	1.48	6.5	295.4	31.0
OSCAR, $V_1 = 800$ l	1.25	6.5	289.1	30.5
OSCAR, $V_1 = 1300$ l	1.25	5.6	288.1	31.1

In the preceding section it was already observed that OSCAR is superior in terms of $J(\mathbf{u})$. From table 2 it appears that OSCAR is superior both in terms of effluent S_{NH} , effluent S_{NO} and, though marginally, sludge production. The effect of the controller/plant design combination on effluent COD is marginal. Unfortunately the aeration costs are not explicitly available from the simulations, as they were run without the oxygen balance in ASM no.1. A qualitative indication is the process knowledge that lower $\bar{S}_{NO,ef}$ at equal \overline{COD}_d is only possible by replacing some of the DO as electron-donor with S_{NO} . Hence it is unlikely that OSCAR causes increased aeration costs (Table 2).

Adding penalty terms to objective functionals in RHOC and optimal control problems is a usual way to remediate known model shortcomings (e.g. Tap *et al.*, 1996). Sometimes this is the best one can do, but these simulation results nicely illustrate the risk of doing so. As mentioned before, the

penalty term $w_3 \left(\frac{q_1}{q_{in}} S_{O,1} + \frac{q_2}{q_{in}} S_{O,2} \right)$ in the RHOC objective functional (eqn. 4) is used to replace the

absence of the known positive effect of influent soluble organic substrate on $r_{NO,max}$ in the RHOC's internal model. The fact that OSCAR and stepfeeding largely outperform RHOC at $V_1 > V_2$ illustrates that the penalty term indeed enforces the feeding of influent to reactor 2, but that the negative effect of overloading reactor 2 outweighs the positive effect of increased $r_{NO,max}$. The negative effect especially occurs when V_2 is small. Clearly, in that case the penalty term fails to replace the model shortcoming in a satisfactory way.

In practice the 'best' t_c is unknown, because besides $J(\mathbf{u})$ other factors play a role as well. One of these is the sluggish response of the hydraulics in the BIODENITRO™ plant design when the flow direction between the two reactors is reversed. In the currently available operation strategies this moment usually coincides with the toggling of anoxicity/aerobicity in the two reactors. The result-

ing undesired flow from the aerobic to the anoxic reactor advocates the use of a long cycle length. In case of OSCAR control this argument no longer holds as the flow direction is never reversed.

Further refinement of the OSCAR rules, and fine-tuning to the specific plant under control, can probably further improve the OSCAR performance. The first thing to look at would be the optimisation of tuning parameters $S_{NO,max}$, $S_{NO,min}$, $S_{NH,max}$ and $S_{NH,min}$. It is good to be aware that the cycle lengths in reactors 1 and 2 increase approximately linear with increasing $S_{NO,max} - S_{NO,min}$ and $S_{NH,max} - S_{NH,min}$ respectively.

In the OSCAR-algorithm aerobicity/anoxicity in a reactor is independent of the other reactor's state. It will be interesting to investigate the effect of some kind of synchronisation between the reactors. Especially because reactor 2 can never be fully anoxic when it is fed from an aerobic reactor 1. This effect was not incorporated in the current simulations due to the omission of the dissolved oxygen balance from the ASM no. 1 model. The effect of this assumption on the simulation results is likely to be small, as reactor 2 mainly serves for nitrification. However, if it appears to be significant then synchronisation will be useful. Another argument in favour of synchronisation is that aerobicity in reactor 2 requires less aeration in case its inflow from reactor 1 is aerobic (possibility to reduce operational costs).

8.9 Conclusions

Running the two equally large reactors of a BIODENITRO™ plant in counter phase does not fully exploit the plants capability to attenuate varying influent concentrations. From the simulations it appeared favourable to attenuate variations in influent ammonium and keep nitrate low in reactor 1, while withdrawing effluent from reactor 2, where ammonium is low (Fig. 6). This can be achieved effectively by a straightforwardly implementable rule-based controller (OSCAR), which is conceptually very simple. The OSCAR strategy works best at short cycle lengths. Additional advantage of this new type of operation is that it can achieve this superior result in a simplified plant design with just two reactors in series.

Operating the simulated BIODENITRO™ plant model by OSCAR control at a 40 min cycle length yields a performance improvement of 17% in terms of the evaluation criterion in eqn. 2 as compared to the current practice of operating in counter phase at a 120 min cycle length. An additional 10% performance improvement was achieved by using OSCAR control and modifying the plant design from $V_1 = V_2$ into $V_1 \approx 4V_2$, while keeping $V_1 + V_2$ unchanged (Fig. 8). The simulated performance improved both in terms of ammonium, nitrate and sludge production (Table 2).

With respect to the methodology it is important to conclude that in this application it has been very successful. A significant performance improvement has been achieved in simulation, and new insight was gained, by the methodology of successively building a dynamic model of the system, simulating the application of receding horizon optimal control to different plant designs, and deriving a simple controller imitating the optimal behaviour.

Acknowledgements: We are very grateful to the Dutch Technology Foundation (STW), which financially supported this research under grant no. WBI44.3275.

8.10 References

- Bitmead, R.R., Gevers, M. and Wertz, V. (1990) *Adaptive optimal control: the thinking man's GPC*. Prentice Hall, London, U.K.
- Henze, M., Grady jr., C.P.L., Gujer, W., Marais, G.v.R. and Matsuo, T. (1987) Activated sludge model no. 1. *IAWQ Scientific and Technical Report no. 1*, IAWQ, London, Great Britain.
- Isaacs, S. (1996) Short horizon control strategies for an alternating activated sludge process. *Water Science and Technology* **34** (1-2), pp. 203-212.
- Isaacs, S. (1997) Automatic adjustment of cycle length and aeration time for improved nitrogen removal in an alternating activated sludge process. *Water Science and Technology* **35** (1), pp. 225-232.
- Isaacs, S. and Thornberg, D. (1998) A comparison between model and rule based control of a periodic activated sludge process. *Water Science and Technology* **37** (12), pp. 343-352.
- Lewis, F.L (1986) *Optimal Control*. John Wiley & Sons, New York, pp. 64.
- Lukasse, L.J.S., Keesman, K.J., Klapwijk, A. and Straten, G. van (1998) Optimal control of N-removal in ASP's. *Preprints of IAWQ 19th Biennial International Conference 2*, IAWQ, Vancouver, pp. 388-395, (to appear in *Water Science and Technology* **38** (3)).
- Lukasse, L.J.S., Keesman, K.J. and Straten, G. van (1997) Identification for model predictive control of biotechnological processes, case study: nitrogen removal in an activated sludge process. Proc. 11th IFAC symposium on System Identification **3**, pp. 1525-1530.
- Mayne D.Q. and Michalska H. (1990) Receding horizon control of nonlinear systems. *IEEE Transactions on Automatic Control* **35**(7), pp. 814-824.
- Metcalf and Eddy, Inc. (1979). *Wastewater engineering: treatment/disposal/reuse*. 2nd edition, McGrawhill, New York.
- Spanjers, H., Vanrolleghem, P., Nguyen, K., Vanhooren, H. and Patry, G. (1998) Towards a simulation-benchmark for evaluating respirometry-based control strategies. *Water Science and Technology* **37** (12), pp. 227-236.
- Stehfest, H. (1985) Optimal periodic control of a steep-feed activated sludge plant. *Environmental Technology Letters* **6**, pp. 556-565.
- Tap, R.F., Willigenburg, L.G. van, Straten, G. van (1996) Experimental results of receding horizon optimal control of greenhouse climate. *Acta Horticulturae* **406**, pp. 229-238.
- Thomsen, H.A., Nielsen, M.K., Nielsen, E.H. and Hansen, N.P. (1998) Load dependent control of BNR-WWTP by dynamic changes of aeration volumes. *Water Science and Technology* **37** (12), pp. 157-164.
- Thornberg, D.E., Nielsen, M.K. and Andersen, K.L. (1993) Nutrient removal: on-line measurements and control strategies. *Water Science and Technology* **28** (11-12), pp. 549-560.
- Zhao, H., Isaacs, S.H., Sørensen, H. and Kümmel, M. (1994) Nonlinear optimal control of an alternating activated sludge process. *Journal of Process Control* **4** (1), pp. 33-43.
- Zhao, H., Isaacs, S.H., Sørensen, H. and Kümmel, M. (1995) An analysis of nitrogen removal and control strategies in an alternating activate sludge process. *Water Research* **29** (2), pp. 535-544.

***PART II, identification on the basis of DO-measurements
and respirometry***

9 Grey-box identification of dissolved oxygen dynamics in activated sludge processes[†]

9.1 Abstract

In this paper a grey-box modelling approach for the identification of nonlinear, time-varying dissolved oxygen dynamics in an activated sludge wastewater treatment process (ASP) is presented. Herein, singular value decomposition of the locally available Jacobian matrix, or equivalently eigenvalue decomposition of the parameter covariance matrix, as well as parameter transformation are essential tools to arrive at a model suitable for adaptive, long-range prediction. The use of on-line respiration rate measurements circumvents the need to model substrate dynamics, and thus greatly simplifies the modelling procedure.

Keywords: system identification, modelling, eigenvalue decomposition, dissolved oxygen, activated sludge process

9.2 Introduction

Many biotechnological systems show a nonlinear and time-varying behaviour (Bastin and Dochain, 1990). Relevant for this study is that the system output is nonlinear in the parameters. When dealing with identification of this type of systems the class of candidate model structures is very large, thus frustrating the choice of a suitable model structure when no first principles are used. Black-box (data-based) modelling techniques based on neural nets or wavelets, for instance, limit the class of candidate model structures, but in general they lead to models not appealing to engineers in the field of application. Moreover, such black-box model structures are only valid on a limited prediction range. Since long-range prediction of the dissolved oxygen (DO) concentration within a Model-Based Predictive Control (MBPC) strategy is the ultimate goal, it is chosen to start from a mechanistic-based point of view.

Naturally, time-varying parameters are identified by using recursive parameter estimation techniques. For the sake of convergence rate it is desirable to reduce parameter correlations and thus overparametrization as much as possible (Ljung and Söderström, 1983; Young, 1984). This requirement as well as the utilization of first principles put constraints on the feasible model structures. Hence, the problem is to find a model with corresponding parameters for the non-linear, time-varying dissolved oxygen process, that is suited for our intended use of adaptive long-range prediction, using both prior system knowledge and measured data.

[†] published by L.J.S. Lukasse, K.J. Keesman and G. van Straten in *proc. 13th IFAC World Congress*, 1996, vol. N, San Francisco, pp. 485-490.

This paper demonstrates the application of a modelling approach which starts from a nonlinear first principle model structure and iteratively adjusts the number of unknown parameters in the prior structure on the basis of available data, without sacrificing too much of the model's whiteness. In this approach eigenvalue decomposition of the locally available covariance matrix as well as parameter transformation play a crucial role.

9.3 Modelling approach

9.3.1 Prior knowledge and preassumptions

The prior knowledge of continuously mixed biotechnological systems is available in the form of a dynamic model for the states (x) of the process,

$$\frac{dx}{dt} = \frac{q_{in}}{V} \cdot x_{in} - \frac{q_{out}}{V} \cdot x + prod - cons \quad (1)$$

where q_{in} and q_{out} are flow rates, V the volume and x_{in} the concentration of x in the inflow.

In addition to the state equation the following sampled-data measurement equation relates the states to the measured outputs:

$$y(t_k) = g(x(t_k), u(t_k), t_k; \theta) + e(t_k) \quad (2)$$

in which $e(\cdot)$ is the so-called "output-error", $u(\cdot)$ the input and $\theta \in \mathbb{R}^p$ the vector of model parameters. It is assumed that eqn. 1 is exact and the measurement noise is white.

9.3.2 Identification of model structure and parameters

The next step is the design of an identification experiment using the prior knowledge expressed in the preliminary model. The main issues in this design are the choice of sampling interval, excitation of input signals, length of the experiment and variables to be measured. After preprocessing the experimental data (see e.g. Ljung, 1987) the parameter vector θ is usually estimated in a (constrained) least-squares sense, which for the single-output case gives

$$\hat{\theta}_N = \arg \min_{\theta \in D} \sum_{k=1}^N \varepsilon(t_k | \theta)^2 \quad (3)$$

where $\varepsilon(\cdot | \theta) = y(\cdot) - g(\cdot, \cdot, \cdot; \theta)$ is the output residual error and D is the prior parameter domain. If the residuals are nonlinear in the parameters, the estimation problem is usually solved by static optimization tools (see e.g. Fletcher, 1987).

The result of the first stage is a first principles model and an estimated parameter vector $\hat{\theta}_N$. The procedure could stop here, but often the prior model turns out to be overparametrized or may give unsatisfactory residuals. So, subsequently the phase of iteratively modifying the model structure within the conceivable model class M and estimating new parameter vectors starts.

In making a choice between candidate model structures one essentially has to trade-off misfit against complexity. Here, the misfit is expressed in terms of the residual error variance,

$$\sigma_\epsilon^2 = \frac{1}{N-p} \sum_{k=1}^N \epsilon(t_k | \theta)^2 \quad (4)$$

Unlike the linear case, a universal complexity measure for nonlinear model structures is not available. In our approach overparametrization is avoided by evaluating the dominant directions in the uncertainty region of the estimates. The procedure is to first make the residual error variance as small as possible, and subsequently to reduce both the number of unknown (freely selectable) parameters and their correlations as much as possible, if necessary by modifying the model structure within the class of candidate model structures M .

Local parameter uncertainties around the estimate $\hat{\theta}_N$ are given by the covariance matrix of the estimates, defined by

$$\text{Cov } \hat{\theta}_N = \sigma_\epsilon^2 (\mathbf{X}^T \mathbf{X})^{-1} \quad (5)$$

where \mathbf{X} is the Jacobian matrix $\frac{d\epsilon(t_k | \theta)}{d\theta_j}$ with $k=1, \dots, N$ and $j=1, \dots, p$. Dominant parameter directions

can be found from an eigenvalue decomposition of the covariance matrix, that is

$$\mathbf{V}^T \text{Cov } \hat{\theta}_N \mathbf{V} = \Lambda \quad (6)$$

where \mathbf{V} is an orthogonal matrix of eigenvectors and Λ is a diagonal matrix with eigenvalues. A large value of the j -th diagonal element in Λ , as compared to other elements indicates a relatively large uncertainty in the direction spanned by the j th column of \mathbf{V} ; a formal significance test of differences between eigenvalues can be found in Kendall (1980). If, for instance, element $V_{i,j}$ is large (almost equal to one) as compared to other elements in this column, parameter estimate $\hat{\theta}_{N,i}$ contains relatively large uncertainty and would hardly affect the sum of squares. Hence, such a parameter is a candidate to be fixed during further analysis, thus reducing the remaining parameter uncertainties. So in the parameter reduction procedure an increase in the sum of squares is outweighed against a decrease in the parameter estimates uncertainty.

After having selected and estimated the dominant parameters, the assumptions with respect to the whiteness of the output error, and hence with respect to the exactness of the system dynamics representation, are checked by evaluating the autocorrelation function of the output residuals. Furthermore, it is checked whether there still remains information in the residual sequence with respect to observed inputs. Dependence between u and e is usually tested by computing the sample cross-correlation function. If one of these correlation functions shows significant correlation at a specific time lag, either the model structure of eqn. 1 needs modification or a system noise term must be added in eqn. 1 to represent the unmodelled system dynamics.

9.4 Application

The procedure is applied to the modelling of the dissolved oxygen (DO) concentration in the completely mixed aerator of an activated sludge pilot plant. A novelty in the present application is the availability of a direct measurement of the non-DO-limited oxygen uptake rate, or actual respiration rate, r_{act} , by means of the commercially available RA1000 (Manotherm B.V., Holland) (Spanjers, 1993). The use of respirometry avoids identifiability problems associated with direct estimation

from DO-measurements (Holmberg, 1982; Holmberg *et al.*, 1989; Bocken *et al.*, 1989), as well as the need of modelling the substrate kinetics.

9.4.1 Prior knowledge

The *a priori* knowledge of the DO-dynamics is contained in the following model:

$$\frac{dC}{dt} = -f(C)r_{act} + k_L a(q_{air}) \cdot (C_S - C) - \frac{q_{in} + q_r}{V} C \quad (7)$$

$$k_L a(q_{air}) = \alpha \cdot q_{air}(t) + \gamma \quad (8)$$

$$f(C) = \frac{C}{C + k_C} \quad (9)$$

$$y(t) = C(t) + e(t) \quad (10)$$

where $q_{in} = q_r = 0.8$ l/min and $V = 475$ l. From previous experiments it was roughly known that $C_S = 9.23$ mg/l, $\alpha = 3.34 \cdot 10^{-3}$ l⁻¹, $\gamma = 5.90 \cdot 10^{-2}$ min⁻¹, and $k_C = 0.3$ mg/l (see list of symbols). The oxygen mass balance (eqn. 7) consists of an oxygen uptake term, a term to describe air supply and a transport term. The initial model (eqns. 7 - 9) is a collection of knowledge from first principles, literature and previous experiments. Uncertainties in the model structure are mainly found in the relation between $k_L a$ and q_{air} . This relationship is usually assumed to be linear, either with or without an off-set γ (Marsili-Libelli, 1989; Holmberg, 1982; Dochain and Perrier, 1992; Tanuma *et al.*, 1985), although it is likely that the slope of the curve decreases with increasing q_{air} (Carlsson and Wigren, 1990). Also the oxygen uptake limitation term $f(C)$, here taken as the well-known Monod kinetics, is uncertain.

9.4.2 Experiment design

The inputs to eqn. 7 are $q_{air}(t)$ and $r_{act}(t)$. A random binary sequence (RBS) superimposed on a triangular-like signal was put on the air-flow (Fig. 1a), covering its relevant operating range. The only way to excitate r_{act} is by manipulating the substrate concentration in the aerator by means of the influent. Due to technical limitations it was only possible to switch between real waste water and tap water. An RBS was designed to switch between these two (Fig. 1b). The pilot plant data are sampled every minute, which is considered fast enough in view of the dominant time constant of the DO process of several minutes.

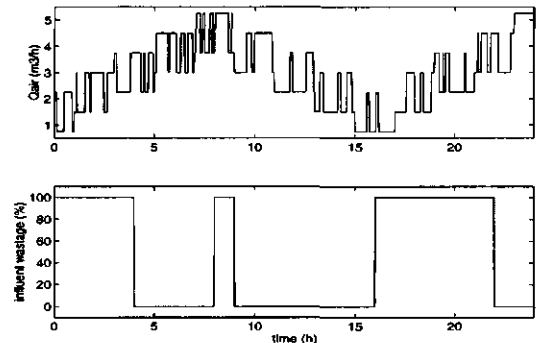


Fig. 1. Designed experimental inputs.

9.4.3 Identification of model structure and parameters

The resulting observations over the first 11 hours are shown in Fig. 2. In periods where the plant only receives tap water, the DO exceeds the normal operating range. Therefore, initially, the identi-

fication was restricted to the data of the first couple of hours, leaving out the noisy period around $t = 3$ hours, where there were temporary difficulties with the r_{act} measurements.

The fit of the model consisting of eqns. 7 - 10 with optimised parameters k_C , α , γ , and C_S appeared to be unsatisfactory, so the model structure needed to be modified. Firstly, in view of the discussion in section 3.1 it was decided to extend eqn. 8 with a term proportional to the square root of q_{air} . Secondly, based on cross-correlation analysis a dead time (Δ) was introduced for q_{air} . Physically, this is justified due to the delay between putting the airflow setpoint on the outport of the process computer and the actual occurrence of a new column of bubbles in the aerator. Thirdly, a scaling factor (f_{max}) to r_{act} was introduced in order to trace a possible systematic error in this signal. In these three steps eqns. 8 and 9 are transformed into

$$k_L a(q_{air}) = \alpha \cdot q_{air}(t - \Delta) + \beta \cdot \sqrt{q_{air}(t - \Delta)} + \gamma \tag{11}$$

$$f(C) = f_{max} \cdot \frac{C}{C + k_C} \tag{12}$$

The model consisting of eqns. 7, 10 - 12 contains seven unknown parameters, to be estimated from the data. The result for $t \in [0, 150]$ min. is presented in Table 1 (column 2) and Fig. 3, showing that the model output satisfactory fits the data.

Now, the number of estimated parameters needs to be reduced as far as possible. The estimated value of f_{max} close to one confirms the correctness of the measured r_{act} , so for the time being f_{max} is fixed at one. In a later stage its recursive estimation might be reintroduced as an alarm for failures of the respiration meter. As stated before the time lag Δ is caused in the electro-mechanical part of the system, and so will be largely time-invariant, therefore it is fixed at 0.5 min. The optimal estimates for the remaining five parameters are presented in Table 1 (column 3). As can be seen the error variance σ_e is hardly increased by fixing f_{max} and Δ .

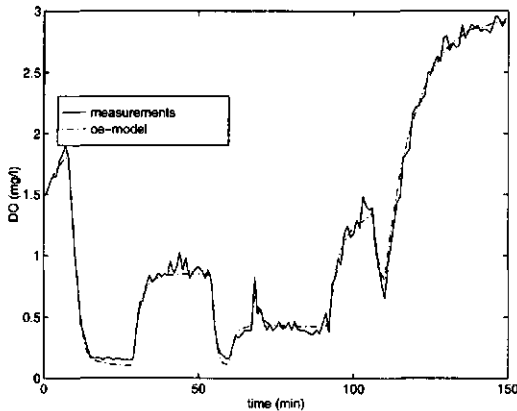


Fig. 3, Best fitting model.

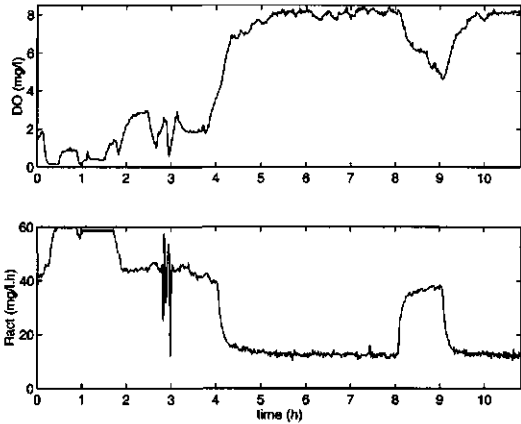


Fig. 2, Measured DO and r_{act} during the experiment.

Successive reductions in the number of free parameters were made on the basis of analysis of dominant direction in parameter space. As an illustration of the procedure consider App. 1.

The largest eigenvalue of the covariance matrix is about 15 times the second largest, indicating

an insensitive direction in the parameter space. The accompanying eigenvector that spans this insensitive direction is dominated by the fourth parameter, being C_S . This means that the errors in the estimate of C_S have only minor influences on the sum of squares of the residuals.

The estimated C_S -value of 17.4 for $t \in [0, 150]$ is much larger than the physically expected values which should be in the range of 8 - 10 mg/l. In view of the uncertainty in C_S it was decided to estimate both C_S and the parameters determining $k_L a$ from the measurements at high DO concentration, i.e. for $t \in [300, 450]$ (Fig. 2).

Table 1

parameter	estimated value				exp.
Δ (min)	0.5				
f_{max}	1.04				
α (l^{-1})	-0.82	-0.80	-1.29		10^{-3}
β ($l^{1/2} \text{ min}^{1/2}$)	1.88	1.85	3.60	2.13	10^{-2}
γ (min^{-1})	-4.71	-4.67	-8.33	-4.51	10^{-2}
k_C (mg l^{-1})	0.54	0.54	0.29	3.16	
C_S (mg l^{-1})	17.5	17.4			
σ_ϵ (mg l^{-1})	6.8	6.8	9.4	9.6	10^{-2}

From these data it was found that $C_S = 9.12$ mg/l.

In the following analyses C_S was fixed at this value. This slightly deteriorates the results for the lower DO concentrations, but it makes the model much more acceptable to engineers in the field of application. The result of optimising the remaining four parameters, again for $t \in [0, 150]$, is found in Table 1 (column 4). As before the estimates of α , β and γ turned out to be heavily correlated (not shown), indicating that one may expect convergence difficulties during on-line recursive estimation. In view of the fact that the absolute value of α is small it was decided to set its value equal to zero, thus further reducing model complexity (Table 1, column 5).

As expected the correlation between β and γ is still very large (not shown). Moreover, from the small values of the remaining eigenvalues (not shown) it is concluded that further parameter reduction is no longer justified. The remaining large correlation between β and γ may well become a stumbling block during recursive estimation, and therefore this is not very satisfying as final result.

A possible way out is to reformulate the model, such that the parameters are less correlated. Most correlation in eqn. 7 is caused by the products of β and γ with C_S . This correlation is removed by substituting eqn. 11 with $\alpha = 0$ into eqn. 7 and defining a new set of parameters. This transformation is purely a parameter transformation, offering some model whiteness, resulting in

$$\frac{dC}{dt} = -f(C) \cdot r_{act} + \alpha' \cdot \sqrt{q_{air}(t-\Delta)} + \beta' \cdot \sqrt{q_{air}(t-\Delta)} \cdot C + \gamma' \cdot C + \delta' - \frac{q_{in} + q_r}{V} \cdot C \quad (13)$$

with $\alpha' = \beta \cdot C_S$, $\beta' = -\beta$, $\gamma' = -\gamma$ and $\delta' = \gamma \cdot C_S$.

The estimated parameters are presented in Table 2 (column 2). Analysis of the covariance matrix shows that γ' is insignificant, so it should be possible to fix γ' at zero without introducing a large error (Table 2, column 3).

In accordance with our expectation, quitting γ' only causes a minor increase in the sum of squares. From the correlation matrix (not shown) there appears to be a quite strong correlation between β' and k_C , although it is much less profound than that between β and γ in the model consisting of eqns. 7, 10 - 12. The eigenvector associated with the largest eigenvalue is dominated by a combination of β' and k_C . Therefore it is not straightforward to fix another parameter. The resulting model fit with $\sigma_\epsilon = 7.4 \cdot 10^{-2}$ instead of $6.8 \cdot 10^{-2}$ mg/l is visually hardly distinguishable from that of Fig. 3.

Table 2

parameter	estimated value	
α' ($\text{mg l}^{-1.5} \text{ min}^{-1/2}$)	0.1656	0.1608
β' ($\text{l}^{-1/2} \text{ min}^{-1/2}$)	$-1.3213 \cdot 10^{-2}$	$-6.2162 \cdot 10^{-3}$
γ' (min^{-1})	$5.2014 \cdot 10^{-2}$	
δ' ($\text{mg l}^{-1} \text{ min}^{-1}$)	-0.4285	-0.3831
k_C (mg l^{-1})	0.6266	0.6023
σ_ε (mg l^{-1})	$7.3 \cdot 10^{-2}$	$7.4 \cdot 10^{-2}$

To test the noise assumptions of the model the autocorrelation of the residuals and the cross correlation of the residuals with the inputs are shown in Fig. 4. While the latter are well within the 95% confidence interval around zero, there is still a significant autocorrelation, indicating the presence of system noise, and hence violation of the assumption that the system dynamics are represented exactly. Consequently, in further analyses the state eqn. 7 is extended with an additional white noise term.

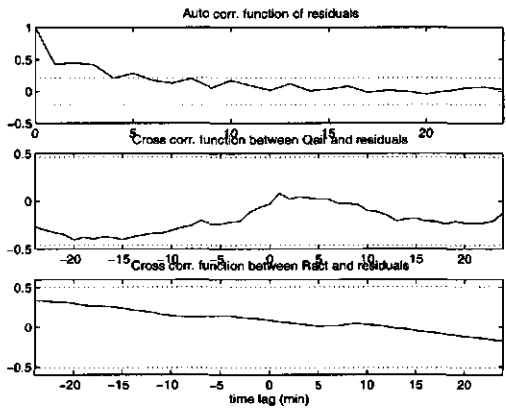


Fig. 4, Correlation functions.

Because of the relatively low parameter correlation the model consisting of eqns. 9, 10 and 13 is preferred above that of eqns. 7 - 10 as a starting point for recursive identification.

An extended Kalman filter (see e.g. Young, 1984), has been applied to the model consisting of eqns. 9, 10 and 13 over the complete data set. Over the application relevant operation range of the first three hours the parameter estimates are reasonably constant. However, when the system is forced to a radically different operation range, the resulting parameter trajectories (Fig. 5) do not converge to a constant value as expected. This demonstrates the need for an adaptive modelling approach resulting in different parameter values for each output range. If, for instance, the operation range is extended to higher DO concentrations, the saturation concentration C_S will become more and k_C less significant

9.5 Conclusions

A nonlinear modelling approach, starting from a first principles model and using eigenvalue decomposition analysis to indicate superfluous parameters, has been presented. Essentially, the approach allows for a well-balanced decision between preserving model-whiteness and good identification properties in a recursive estimation context.

The method has been illustrated to work well on the identification of the DO-dynamics in an

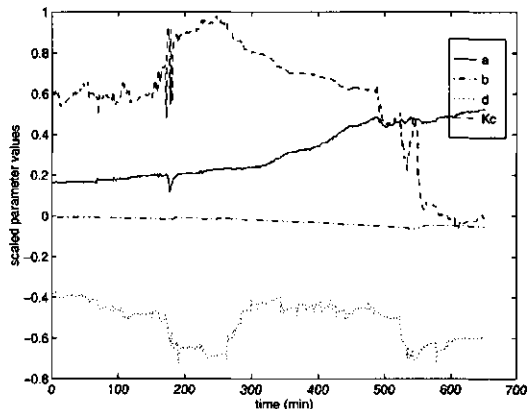


Fig. 5, Recursively estimated parameter values.

activated sludge process. In this example it proved to be possible to arrive at a well identifiable model, while largely respecting the prior knowledge of the nonlinear system dynamics.

Acknowledgments: This research is supported by the Technological Foundation (STW) under grant no. WBI44.3275. The authors thank Dr. Bram Klapwijk of the Environmental Engineering Department for his helpful comments.

9.6 References

- Bastin, G. and D. Dochain (1990). *On-line Estimation and Adaptive Control of Bioreactors*. Elsevier, Amsterdam.
- Bocken, S.M., M. Braae and P.L. Dold (1989). Dissolved oxygen control and oxygen utilization rate estimation: extension of the Holmberg/Olsson method. *Water Sci. Techn.*, **21**, 1197-1208.
- Carlsson, B. and T. Wigren (1993). On-line identification of the dissolved oxygen dynamics in an activated sludge process. *Proc. 12th IFAC World Congress*, **7**, 421-426.
- Dochain, D. and M. Perrier (1992). Adaptive linearizing control of the activated sludge process. *Mededel. Fac. Landbouwwet. University of Gent*, **57(4b)**, 2239-2248.
- Godfrey, K. (1993). *Perturbation Signals for System Identification*. Prentice Hall, New Jersey.
- Holmberg, A. (1982). A microprocessor-based estimation and control system for the activated sludge process. *Proc. 1st IFAC Workshop on Modelling and Control of Biotechn. Processes*, Pergamon, Oxford, pp. 111-119.
- Holmberg, U., G. Olsson and A. Bengt (1989). Simultaneous DO control and respiration estimation. *Water Sci. Techn.*, **21**, 1185-1195.
- Kendall, M. (1980). *Multivariate Analysis*. Charles Griffin & Co, High Wycombe, Bucks, UK.
- Ljung, L. and T. Söderström (1983). *Theory and Practice of Recursive Identification*. MIT Press, Cambridge, Mass.
- Ljung, L. (1987). *System Identification: Theory for the User*. Prentice Hall, New Jersey.
- Spanjers, H. (1993). *Respirometry in Activated Sludge*. PhD-thesis, Wageningen Agricultural University, The Netherlands.
- Tanuma, R., K. Sasaki and I. Matsunaga (1985). Gain maximizing dissolved oxygen control in the activated sludge process. *Proc. 4th. IAWPRC Workshop on Instrum. Control Water Wastewater Treat. Transp. Syst.*, Pergamon, New York, 481-488.
- Young, P.C. (1984). *Recursive Estimation and Time Series Analysis*. Springer Verlag, Berlin.

9.7 Appendix 1, list of symbols

C	= DO-concentration (mg/l)
C_S	= DO-saturation constant (mg/l)
q_{in}	= influent flow (l/min)
q_r	= return sludge flow (l/min)
V	= aerator volume (l)
r_{act}	= actually measured respiration rate (mg/l.min)
$k_L a(q_{air})$	= oxygen transfer coefficient (min^{-1})
q_{air}	= air flow (l/min)

α	= oxygen transfer parameter (l^{-1})
β	= oxygen transfer parameter ($l^{-1/2} \text{ min}^{-1/2}$)
γ	= oxygen transfer coefficient at zero q_{air} (min^{-1})
$f(C)$	= oxygen limitation term
k_C	= Monod constant in DO-limitation term (mg/l)

9.8 Appendix 2, parameter uncertainties in eqns. 7, 10 - 12

$$\hat{\theta}_N = [\alpha \beta \gamma C_S k_C] = [-0.80 \quad 1.85 \quad -4.67 \quad 17.4 \quad 5.41] \text{ (exponents omitted)}$$

Cov $\hat{\theta}_N$:

0.0320	-0.0463	0.1146	0.1543	0.0514
-0.0463	0.0759	-0.1852	-0.3647	-0.0969
0.1146	-0.1852	0.4595	0.8408	0.2176
0.1543	-0.3647	0.8408	2.9952	0.6295
0.0514	-0.0969	0.2176	0.6295	0.1833

Correlation matrix:

1.0000	-0.9379	0.9445	0.4982	0.6711
-0.9379	1.0000	-0.9913	-0.7649	-0.8215
0.9445	-0.9913	1.0000	0.7166	0.7498
0.4982	-0.7649	0.7166	1.0000	0.8495
0.6711	-0.8215	0.7498	0.8495	1.0000

V:

-0.0562	-0.2839	0.7719	-0.0682	0.5619
0.1225	0.3065	-0.4710	0.0276	0.8176
-0.2852	-0.8309	-0.3921	0.2450	0.1201
-0.9271	0.3424	0.0470	0.1411	0.0329
-0.2023	-0.1332	-0.1621	-0.9564	0.0192

diag(Λ):

3.4487	0.2554	0.0007	0.0412	0.0000
--------	--------	--------	--------	--------

10 Estimation of BOD_{st} , respiration rate and kinetics of activated sludge[†]

10.1 Abstract

Tight control of Activated Sludge Processes (ASP) is hampered by the lack of reliable information about important process characteristics. Some of those important characteristics are sludge kinetics, short-term biochemical oxygen demand (BOD_{st}) and respiration rate in the aeration tank. Spanjers *et al.* (1994) developed a technique to estimate those characteristics from data collected from a continuously fed respirometer with a specially developed operation strategy. Essential in their estimation technique is the instable backward integration of a forwardly stable differential equation.

In this paper an improved on-line implementable estimation methodology is presented. The estimation problem is formulated as a non-linear optimization problem, avoiding backward integration and estimating the respirometer flow. This novel methodology has been applied to the data set of Spanjers *et al.* (1994). The resulting estimates turn out to be comparable to those obtained by Spanjers *et al.* (1994). But, contrary to expectation, the estimates still suffer from unacceptable inaccuracy due to large parameter correlation.

However, a slight modification in the measurement strategy is proposed which will eliminate the problem of parameter correlation to a large extent and so enable more accurate estimation. The new measurement strategy is only advantageous when combined with the novel estimation methodology presented in this paper.

Keywords: estimation, identification, respirometry, short term biochemical oxygen demand, sludge kinetics, uncertainty analysis

10.2 Nomenclature

BOD_{st}	= short term biochemical oxygen demand
C_{in}, C	= dissolved oxygen concentration in influent and effluent (mg/l)
DO	= dissolved oxygen
e	= measurement noise, assumed to be white
k_S	= kinetic constant (min^{-1})
q	= flow through the respiration chamber (l/min)
r_{act}	= actual total respiration rate in aeration tank (mg/l.min)
r_e	= endogenous respiration rate, being the sum of truly endogenous respiration rate and the respiration of possible hydrolysis products (mg/l.min)

[†] published by L.J.S. Lukasse, K.J. Keesman and G. van Straten in *Water Research*, 31, 1997, pp. 2278-2286.

r_S	= substrate respiration rate (mg/l.min)
$r_{S,max}$	= maximum substrate respiration rate (mg/l.min)
$R_{\hat{\theta}}$	= correlation matrix of $\hat{\theta}$
S, S_{in}, S_{AT}	= substrate concentration in respirometer, respirometer influent and aeration tank (mg BOD _{st} /l)
t_0, t_f	= initial and final time of measurement in a mode (min)
t_k	= k-th sampling instant in a mode (min)
V	= respiration chamber volume = 0.731 l
y	= measured dissolved oxygen concentration (mg/l)
Δ	= time shift in switching point between two successive modes (min)
ϵ	= model mismatch, i.e. measured DO - estimated DO (mg/l).
σ_{ϵ}^2	= residual variance (mg ² /l ²)
$\Sigma_{\hat{\theta}}$	= covariance matrix of $\hat{\theta}$
θ	= p -dimensional parameter vector
v^e	= variable v in e-mode, where v can be any variable.
v^l	= variable v in l-mode, where v can be any variable.
\bar{v}	= steady state value of v , where v can be any variable.
\hat{v}	= estimated value of v , where v can be any variable.

10.3 Introduction

In the past few years it has been recognized that respirometry, involving the reconstruction of the oxygen uptake rate from DO measurements under specific conditions, has great potentials (Shamas and Englande, 1992; Spanjers, 1993; Vanrolleghem, 1994). However, the on-line estimation of wastewater and sludge characteristics using respirometric data has not yet been fully explored. This paper is an attempt to further explore this area from an identification point of view. But, let us first mention a number of control-relevant estimation items related to respirometry.

In the DO control loop the actual respiration rate (r_{act}) is the main disturbance. Haarsma and Keesman (1995) showed that explicit use of its on-line measured value can largely improve the performance of a DO controller. The currently available measurement technique requires the addition of a small continuous flow of influent to the respirometer proportional to the varying influent flow of the aeration tank (Klapwijk *et al.*, 1992). This small flow is vulnerable to errors due to congestion of the thin hose required to maintain the small flow. So there is a need for an easier way to monitor r_{act} .

Active control with the objective to meet effluent BOD₅ norms is impossible because of the 5-days time delay inherent to the measurement. Yet, effluent BOD₅ is effected by many control inputs, like length of anaerobic/anoxic/aerobic phases, feedpoints, intensity of aeration and (internal) recycle flows. BOD_{st} is defined as the sum of oxygen demand for oxidation of all sorts of readily biodegradable organic compounds and NH₄. When reliable estimates of BOD_{st} are available these may be used explicitly in feedback control loops, as BOD_{st} reflects the controllable part of BOD₅. In the currently available respirogram-based measurement technique, like applied by Vanrolleghem and

Van Daele (1994), the measured BOD_{st} always has a time lag of at least half an hour, which is unfavorable for control purposes. Hence, a faster method of measuring BOD_{st} is required.

Sludge kinetics will vary due to *e.g.* changing temperature, concentration and composition of both substrate and sludge. Therefore their on-line identification has received considerable interest in recent years (Vanrolleghem & Verstraete, 1993; Vanrolleghem & Coen, 1995; Carstensen *et al.*, 1995). It is believed that subsequent adaptation of setpoints of controllers for substrate concentration and respiration rates may be a useful tool in optimizing process operation.

The estimation methodology used by Spanjers *et al.* (1994) uses the *backward integration* of the substrate balance, being a differential equation stable in forward time. The inherent exponentially growing integration error is reduced by *shifting the integration starting point*, thus violating the initial conditions. This boils down to a hard choice between variance and bias of the estimates and is formally incorrect. Furthermore the methodology assumes the flow through the respiration meter to be known from measurements. In practice this assumption is often violated, as the flow slowly changes due to wearing and fouling.

The main objective of this paper is to present an estimation procedure of some relevant characteristics in an ASP using a nonlinear optimization problem formulation. Herein, the flow through the respirometer is included in the vector of parameters to be estimated and all differential equations are integrated *forward* in time. By applying the new methodology to the *same data set* as used by Spanjers *et al.* (1994) the estimates can be compared.

The outline of the paper is such that first Spanjers' measurement strategy is shortly summarized. Then the estimation problem is formulated as a nonlinear optimization problem and results are presented. Next the estimation of the actual respiration rate in the aeration tank is addressed. Subsequently the estimation results are discussed, from which proposals for improved experimental design emerge. Finally the paper ends with some conclusions.

10.4 Measurement strategy

The measurement strategy, as applied by Spanjers *et al.* (1994), is based on the repeated excitation of the dynamics in the respiration chamber of an RA-1000 respirometer. Basically, this respirometer consists of a peristaltic pump maintaining a flow of activated sludge through a small intensively stirred respiration chamber of 0.75 l. At the exit of the respiration chamber a DO-probe measures the dissolved oxygen concentration. Every 30 seconds the flow direction through the respiration chamber is changed, and so every 30 seconds a measurement of alternately effluent and influent DO is obtained (Fig. 1, Fig. 6a). Excitation is obtained by alternately loading the respirometer with loaded sludge from an aeration tank, fed with presettled domestic waste water, in the so-called *l-mode* and endogenous sludge, produced in a bypass tank (1 h detention time), in the so-called *e-mode*, each mode lasting 15 minutes (Fig. 1). A constant flow of 0.3575 l/min has been used. For a more detailed description of the experimental conditions we refer to Spanjers *et al.* (1994).

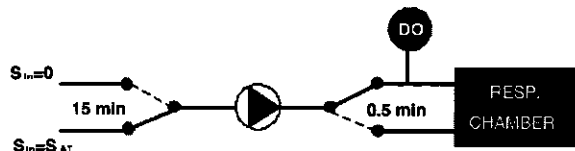


Fig. 1, schematic operation of respirometer.

The oxygen measurement data set consists of 90 l- and e-mode cycles. Every sixth l-mode is replaced by an a-mode measuring the actual respiration rate r_{act} in the aeration tank (Fig. 2). This will be used to compare the estimated r_{act} with. To measure r_{act} an additional small influent flow is fed to the respiration chamber s.t. in steady state $S = S_{AT}$, while in l-mode steady state $S_{in} = S_{AT}$ and so $S < S_{AT}$ and the measured $r_{tot} \leq r_{act}$.

10.5 Respirometer model

Under the reasonable assumption of constant biomass concentration, the respirometer is completely described by the DO and substrate balances, given by

$$\frac{dC}{dt} = \frac{q}{V} \cdot (C_{in}(t) - C(t)) - r_e - r_s(t) \quad (1)$$

and

$$\frac{dS}{dt} = \frac{q}{V} \cdot (S_{in}(t) - S(t)) - r_s(t) \quad (2)$$

where

$$S_{in}(t) = \begin{cases} S_{AT}(t) & \text{l-mode} \\ 0 & \text{e-mode} \end{cases}$$

In these balances the only measurable quantities are $C(t)$ and $C_{in}(t)$. In the sequel the notation C^l , S^l and C^e , S^e denote DO and substrate (mg BOD_{st}/l) in the respirometer during respectively the l-mode and e-mode.

The influent flow switches immediately after the last sample $C(t_f)$ of a mode, being the first sample $C(t_0)$ of the next mode. The exact switching moment of $C_{in}(t)$ is slightly later but unknown due to a time delay in the supply hose. This uncertainty is dealt with by introducing a time shift Δ . Let $C_{in}(t_{-1})$ denote the last measured influent DO concentration before switching time t_0 and accordingly $C_{in}(t_2)$ the first after t_0 . Then on the interval $[t_{-1}, t_2]$ $C_{in}(t)$ is interpolated as:

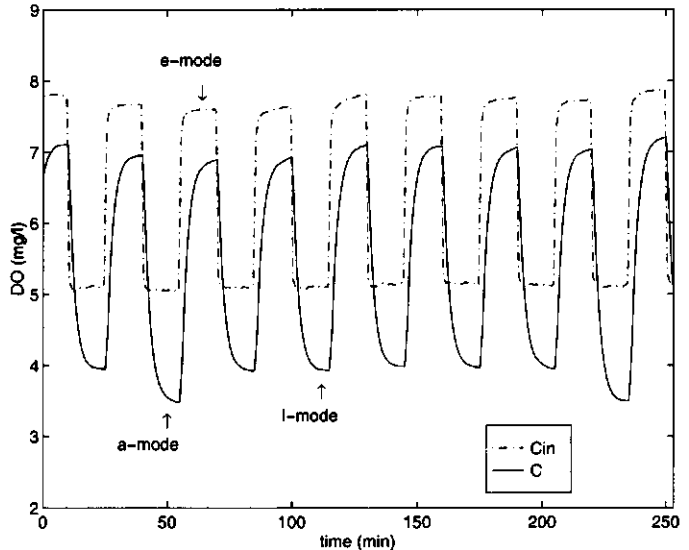


Fig. 2, characteristically measured DO concentrations in a-, e- and l-mode.

$$C_{in}(t) = \begin{cases} C_{in}(t_{-\frac{1}{2}}) & t_{-\frac{1}{2}} < t < t_0 + \Delta \\ C_{in}(t_{\frac{1}{2}}) - \frac{t_{\frac{1}{2}} - t}{t_{\frac{1}{2}} - t_{-\frac{1}{2}}} (C_{in}(t_{\frac{1}{2}}) - C_{in}(t_{-\frac{1}{2}})) & t_0 + \Delta < t < t_{\frac{1}{2}} \end{cases}$$

Exactly the same interpolation is applied to $S_{in}(t)$.

Under normal conditions the endogenous respiration rate r_e is rather constant, as it mainly depends on the hardly varying biomass concentration. Its value may be determined by observing that in the *steady state* at the end of the e-mode $\frac{dC(t)}{dt} = 0$ and $r_s(t) = 0$, so from eqn. 1 it follows that:

$$r_e(t) = \frac{q}{V} (\bar{C}_m^e - \bar{C}^e) \quad (3)$$

where the overbar denotes steady state values. Once r_e is known the substrate respiration rate r_s may be determined from eqn. 1:

$$r_s(t) = \frac{q}{V} (C_{in}(t) - C(t)) - r_e(t) - \frac{dC(t)}{dt} \quad (4)$$

As the DO concentration is non-limiting and the biomass concentration is constant, r_s solely depends upon the substrate concentration. In literature a number of models have been proposed to describe this kinetic relationship. In this paper the Blackman (1/0) model is used:

$$r_s(S, t) = \begin{cases} k_s \cdot S(t) & S(t) < r_{s,max} / k_s \\ r_{s,max} & S(t) \geq r_{s,max} / k_s \end{cases} \quad (5)$$

During the experiment the measured r_{act} at the end of a-modes was significantly higher than the measured r_{tot} at the end of l-modes (Fig. 2), so $r_s(t) < r_{s,max}$. Under this condition eqn. 5 is a bijective mapping and so it may be inverted to give:

$$S(t) = \frac{r_s(t)}{k_s} \quad S(t) < r_{s,max} / k_s \quad (6)$$

Once $r_s(t)$ is known from eqn. 4, $S(t)$ for known k_s follows from eqn. 6 and finally the influent substrate concentration in the l-mode, which is equal to S_{AT} , follows from the *steady state* of the substrate balance (eqn. 2) at the end of the l-mode:

$$S_{AT}(t) = \bar{S}^l + \frac{\bar{r}_s^l}{q} \quad (7)$$

By reformulating eqn. 4 for the l-mode *steady state* and substituting eqns. 3, 4 and 6 in eqn. 7 the following expression for S_{AT} is found:

$$S_{AT}(t) = (\{\bar{C}_{in}^l - \bar{C}^l\} - \{\bar{C}_{in}^e - \bar{C}^e\}) \cdot (1 + \frac{q}{k_s V}) \quad (8)$$

Once r_e , k_s and S_{AT} are known the actual respiration rate r_{act} in the aeration tank may be reconstructed as the sum of r_e and $r_{s,AT}$, where $r_{s,AT}$ is found by substituting S_{AT} and k_s into the kinetic model (eqn. 5):

$$r_{act}(t) = r_e(t) + k_s S_{AT}(t) \quad (9)$$

and by substituting eqn. 3 and 8 in eqn. 9:

$$r_{act}(t) = (k_s + \frac{q}{V})(\bar{C}_m^l - \bar{C}^l) - k_s(\bar{C}_m^e - \bar{C}^e) \quad (10)$$

10.6 Estimation procedure

From the equations and measurements discussed in the preceding section the parameters k_s , Δ and q are estimated. Though measurable, the flow q is estimated. Its estimation is unlikely to become a problem, as it is dominantly present in the system.

On the basis of the reasonable assumption that the endogenous respiration rate is constant during one cycle of e- and l-mode, it can be estimated from the *steady state* of the DO balance at the end of the e-mode. Furthermore, by assuming that the substrate concentration S_{AT} in the aeration tank is constant during one l-mode, it may be estimated from the steady state of the substrate balance at the end of the l-mode. This might introduce small errors in case of fast changing plant load, as van Straten *et al.* (1993) derived that typical values for the time constant of the substrate balance in the aeration tank are in the range of 20 - 30 min.

Initially one overall estimation problem was formulated. However the correlation between the three parameter estimates turned out to be very large, causing large computation times. Therefore the estimation problem is split up in two parts, by utilizing both eqns. 4 and 5 to estimate $r_s(t)$. Decomposition cannot remove parameter correlation, but it is a way to circumvent its slowing effect on the estimation process. The two steps of the estimation problem are outlined below.

10.6.1 step 1 Estimation of q and Δ

The first problem is the estimation of q and Δ , estimating the trajectory $r_s(t)$ directly from the DO data. The optimization problem is stated as

$$\min_{\theta_1 = [q \ \Delta]} J(\theta_1) = \sum_{k=1}^N \varepsilon(t_k; \theta_1)^2 \quad (11)$$

subject to

$$\varepsilon(t_k; \theta_1) = y(t_k) - \hat{C}(t_k; \theta_1)$$

$$y(t_k) = C(t_k) + e(t_k)$$

$$\frac{d\hat{C}(t)}{dt} = \frac{q}{V} \cdot (C_m(t) - \hat{C}(t)) - r_e - r_s(t) \quad , \quad \hat{C}(t_0) = y(t_0)$$

$$r_e = \frac{q}{V}(\bar{C}_m^e - \bar{C}^e)$$

$$r_s(t) = \frac{q}{V}(C_m(t) - \hat{C}(t, \theta_1)) - r_e - \frac{dy(t)}{dt}$$

$$\frac{dy(t)}{dt} = \frac{y(t_k) - y(t_{k-1})}{t_k - t_{k-1}} \quad t_{k-1} < t \leq t_k \quad k = 1, \dots, N$$

$$C_m(t) = \begin{cases} C_m(t_{-\frac{1}{2}}) & t_0 < t < t_0 + \Delta \\ C_m(t_{\frac{1}{2}}) + \frac{t_{\frac{1}{2}} - t}{t_{\frac{1}{2}} - t_{-\frac{1}{2}}} (C_m(t_{-\frac{1}{2}}) - C_m(t_{\frac{1}{2}})) & t_0 + \Delta < t < t_{\frac{1}{2}} \end{cases}$$

where N is the number of measurement points in one mode ($= 15$), and $y(t_k)$, $C(t_k)$, $\hat{C}(t_k)$ are the measured, true and estimated DO concentration at sampling instant t_k in a mode. From this estimation problem an estimate of the substrate respiration rate $r_s(t_k)$ at the 15 measurement points in a cycle is obtained. These estimates are used in the next step.

10.6.2 step 2 Estimation of k_s

In this step the kinetic constant k_s is estimated by fitting the estimates $r_s(S, t)$ from the kinetic model (eqn. 5) to the estimates from step 1, denoted by $\hat{r}_s(t_k; \theta_1)$. The optimization problem is formulated as

$$\min_{\theta_2 = k_s} J(\theta_2) = \sum_{k=1}^N \{ \hat{r}_s(t_k; \theta_1) - r_s(S, t_k; \theta_2) \}^2 \quad (12)$$

subject to

$$\begin{aligned} \frac{dS(t)}{dt} &= \frac{q}{V} \cdot (S_{in} - S(t)) - r_s(S, t; \theta_2) \quad , \quad S(t_0) = \hat{r}_s(t_0; \theta_1) / k_s \\ r_s(S, t; \theta_2) &= k_s S(t) \\ S_{in} &= \begin{cases} S_{\lambda r} = \{ (\bar{C}_{in}^l - \bar{C}^l) - (\bar{C}_{in}^e - \bar{C}^e) \} \cdot (1 + \frac{q}{k_s V}) & \text{l-mode, } t > t_{\frac{1}{2}} \\ 0 & \text{e-mode, } t > t_{\frac{1}{2}} \end{cases} \\ S_m(t) &= \begin{cases} S_m(t_{-\frac{1}{2}}) & t_0 < t < t_0 + \Delta \\ S_m(t_{\frac{1}{2}}) + \frac{t_{\frac{1}{2}} - t}{t_{\frac{1}{2}} - t_{-\frac{1}{2}}} (S_m(t_{-\frac{1}{2}}) - S_m(t_{\frac{1}{2}})) & t_0 + \Delta < t < t_{\frac{1}{2}} \end{cases} \end{aligned}$$

In addition to the parameter estimates obtained from the optimization problem, the uncertainty in the estimate $\hat{\theta}$ is evaluated, like done by Lukasse *et al.* (1996), Schneider & Munack (1995) and Vanrolleghem *et al.* (1995). A measure of the uncertainty resulting from each individual step in the estimation procedure is provided by the covariance matrix associated with $\hat{\theta}$, which is given by

$$\Sigma_{\hat{\theta}} = \sigma_{\epsilon}^2 (\mathbf{X}^T \mathbf{X})^{-1} \quad (13)$$

where \mathbf{X} is the locally available Jacobian matrix with the elements

$$\mathbf{X}(k, j) = \frac{d\epsilon(t_k | \hat{\theta})}{d\hat{\theta}_j} \quad k = 1, \dots, N \quad \text{and} \quad j = 1, \dots, p \quad (14)$$

and σ_{ϵ}^2 is the residuals variance, defined by

$$\sigma_{\epsilon}^2 = \frac{1}{N - p} \sum_{k=1}^N \epsilon(t_k | \hat{\theta})^2 \quad (15)$$

with N the number of data points in one mode. Another measure closely related to the covariance matrix is the correlation matrix of $\hat{\theta}$,

$$R_{\hat{\theta}}(k, j) = \frac{\Sigma_{\hat{\theta}}(k, j)}{\sqrt{\Sigma_{\hat{\theta}}(k, k) \cdot \Sigma_{\hat{\theta}}(j, j)}} \quad (16)$$

The correlation matrix indicates dependencies between parameter estimates.

An extra source of uncertainty in the two step procedure of this section is the propagation of uncertainty from the estimates of step 1 into the estimates of step 2. The easiest way to evaluate this effect is by laying a grid over the 2σ -bounded uncertainty region of $\hat{\theta}_1$ and estimating θ_2 and Σ_{θ_2} for each individual grid point. From this a 2σ -region for $\hat{\theta}_2$ can be constructed, based on the combined effects of Σ_{θ_2} and propagation from Σ_{θ_1} .

10.7 Results

The presented results are limited to the model fitted in the l-mode, as this mode contains the most information in the range of $S(t)$, which is of interest for a control system design. Generally speaking, the e-mode results were smoother, but less significant. The estimation procedure has also been applied using Monod (containing an extra parameter) and Blackman ($1/2$) kinetic models, but with worse results. Hence, there is focused on results using a Blackman ($1/0$) kinetic model and data obtained in l-mode under non-saturating substrate concentrations.

Despite the high signal-to-noise ratio of the oxygen measurements (Fig. 6a) the simultaneous estimation of q and Δ in step 1 of the estimation procedure appeared to be nearly impracticable due to huge parameter correlation. Fig. 3a shows a set of $\{q, \Delta\}$ pairs equally distributed within the 2σ -

bounded region of $[\hat{q}, \hat{\Delta}]$, approximated from its covariance matrix. Clearly the correlation between \hat{q} and $\hat{\Delta}$ is large. By solving the second step in the estimation procedure for all pairs $\{q, \Delta\}$ in Fig. 3a the uncertainty propagation to \hat{k}_S is found. In Fig. 3b and c the resulting estimates of k_S (without individual uncertainty regions) are plotted versus q and Δ . It turns out that \hat{k}_S is insignificant and the estimated S_{AT} can take any value (Fig. 3d), because \hat{S}_{AT} has a vertical asymptot at $k_S = 0$ (eqn. 8).

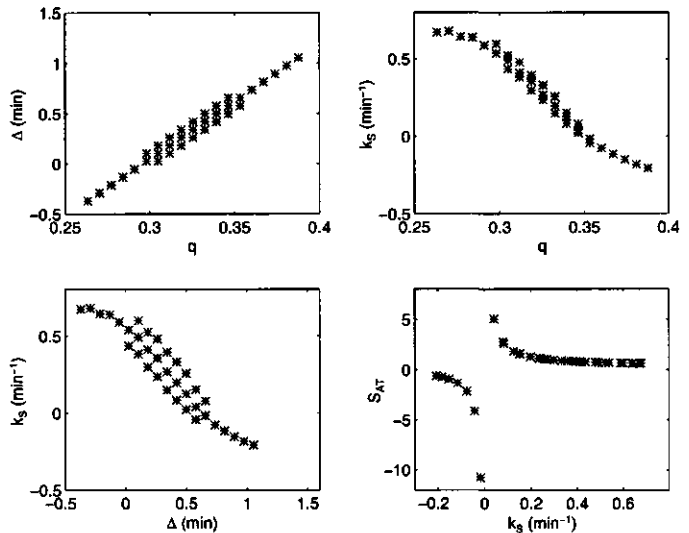


Fig. 3, characteristic 2σ uncertainty regions in l-mode.

To investigate the potential of estimating q for known Δ , it is fixed at a reasonable value and only q is estimated. A proper choice of a value for Δ in l-mode is found to be 0.07 minutes. Obviously a wrong value for Δ will result in biased estimates, but for an evaluation of the potential of the estimation procedure this is acceptable. As can be seen from Fig. 4 the estimates of q for known Δ are accurate, confirming the correctness of the choice for its on-line estimation.

The uncertainty in \hat{q} propagates into \hat{k}_s , which itself has a relatively large variance as well, resulting in mainly insignificant estimates \hat{k}_s , and so insignificant approximations of S_{AT} . Fig. 4 contains the nominal estimates and their 2σ -bounds for all available l-modes.

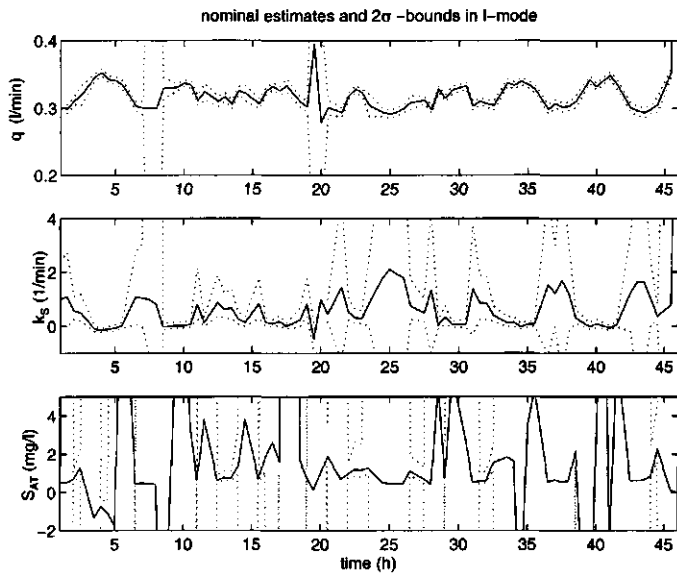


Fig. 4, estimation results from l-mode with significant estimates of S_{AT} stressed by fat underbar.

Summarizing, the parameter correlations inherent to the current combination of model structure and data set are unacceptably large. Only the resulting numerical problem has been solved by splitting the estimation procedure in two steps. It is expected that the parameter correlations themselves can be largely reduced by optimizing the measurement strategy for the estimation procedure of this paper, as will be demonstrated in the sequel.

10.8 Estimation of the actual respiration rate in the aeration tank

Using the outcomes of the estimation problem in the preceding section $r_{act}(t)$ may be estimated from eqn. 10, in analogy with Spanjers *et al.* (1994). This method has been applied to the l-mode estimation results of the preceding section. It appeared that the order of magnitude of the estimates $\hat{r}_{act}(t)$ corresponds with that of the measured $r_{act}(t)$ (Fig. 5). Yet the estimates are unsatisfactory both because of the too large 2σ -interval and because of the unrealistic spikiness of the nominal estimates.

10.9 Proposals for improved measurement strategy

The main difficulty in the estimation procedure is the large correlation between time delay Δ and flow q in combination with the poor identifiability of Δ . The uncertainty in parameter Δ only exists because of a lack of samples of $C_{in}(t)$ around time t_0 . An obvious way to overcome this problem is

high frequent sampling of $C_{in}(t)$ around t_0 , making estimation of Δ redundant. This will largely reduce the uncertainty in \hat{q} and \hat{k}_s , to see this compare the current uncertainty regions of \hat{q} and \hat{k}_s with those for one given Δ (Fig. 3a, c).

The observations justify linear interpolation of $C_{in}(t)$ between $C_{in}(t_{\downarrow})$ and $C_{in}(t_{\uparrow})$ (Fig. 2), allowing for high frequent sampling of $C(t)$ during the intermediate time span, without losing information on $C_{in}(t)$. This will increase the information content of the data set and so further reduce the uncertainty in \hat{q} and \hat{k}_s . Moreover, if the new data are sufficiently rich, estimation of $r_{S,max}$ may be possible. This greatly enhances the applicability of the method, as it is no longer required that $r_S < r_{S,max}$. Moreover in that case the choice for Blackman (1/0) kinetics instead of the generally used Monod kinetics needs to be re-considered.

So far sensor dynamics have been neglected in this work. In non-steady-state, inherent to the employed operation strategy, this introduces a systematic deviation between the true and measured DO concentration. The DO sensor itself is known to exhibit first order dynamics (Spanjers & Olsson, 1992; Lindberg & Carlsson, 1996):

$$y(k+1) = p_1 y(k) + p_2 C(k) + e(k) \tag{17}$$

The unknown parameters p_1 and p_2 can be estimated from the transients measured at the end of a mode (Fig. 6b) using ordinary least squares estimation. Now, the true DO concentration at the membrane during the whole mode can be reconstructed from:

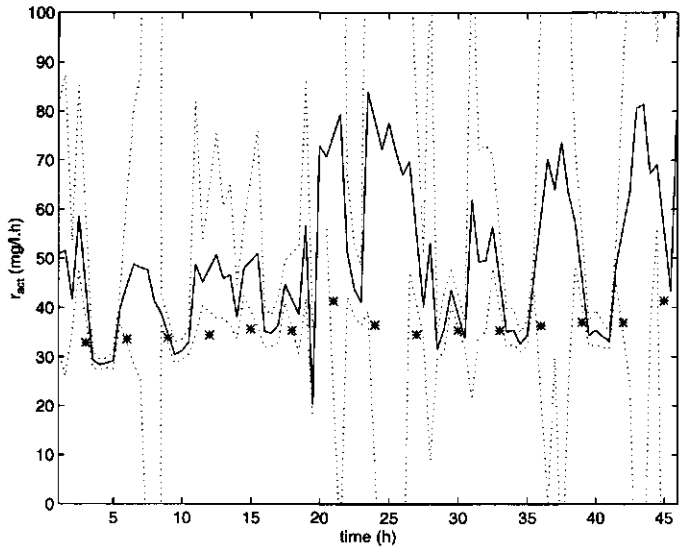


Fig. 5, measured (*) and estimated (-) r_{act} with 2σ -bounds (:)

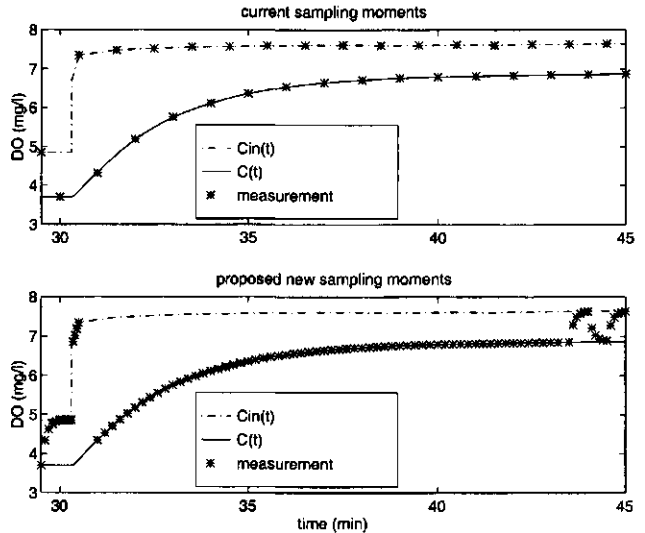


Fig. 6, current and proposed new measurement strategy.

$$\hat{C}(k) = \frac{y(k+1) - p_1 y(k)}{p_2} \quad (18)$$

In Fig. 6 the proposed new sampling strategy is visualized.

With respect to the reconstruction of S_{AT} (eqn. 8) the following is noticed. The uncertain part in this relation is $\frac{\hat{q}}{\hat{k}_s V}$. Hence, the contribution of this term to S_{AT} can be reduced by reducing q , and as a result of that the term $(\bar{C}_{in}^i - \bar{C}^i) - (\bar{C}_m^e - \bar{C}^e)$ in eqn. 8 increases. Consequently, by reducing q part of the contribution of the uncertain estimates to S_{AT} is exchanged for a contribution by reliably measured DO concentrations. A lower limit for q is given by the constraint that DO measurements in the respirometer must be obtained under non-limiting oxygen concentrations. The cost for this reduction of q is that a longer cycle period is needed to reach steady state, thus reducing the sampling rate of S_{AT} .

For \hat{r}_{act} the situation is less obvious. Reducing q will reduce \bar{S}^i and so \hat{k}_s is estimated from lower substrate concentrations. As a result the identified kinetic model will be further extrapolated in the computation of r_{act} (eqn. 9), and so structural errors in the kinetic model will become more serious.

10.10 Conclusions

The presented *methodology*, which starts from a system identification point of view, enables the estimation of both BOD_{st} , actual respiration rate and sludge kinetics in the aeration tank of an activated sludge plant without facing the numerical problems encountered in Spanjers' approach. Moreover the flow through the respiration chamber is accurately estimated from the measured in- and effluent DO concentrations of the respiration chamber, which is very useful as a tool to monitor the well-functioning of the respirometer. As with any estimate of process kinetics from in-sensor experiments, it remains to be seen to what extent the estimates reflect the true kinetics in the aeration tank.

Essential in this paper is the formal identification approach, which also allows for a direct evaluation of the uncertainty in the estimates. This uncertainty evaluation clearly reveals the main problem of large correlations between the parameter estimates, making the 95% confidence interval of \hat{S}_{AT} unacceptably large. A two-step estimation procedure has been used to overcome the numerical problems resulting from these correlations. Finally, a new measurement strategy has been suggested, enabling a reduction of both the size of the parameter vector and the uncertainty of the remaining parameters.

Acknowledgments: The authors indebt very much to Dr. H. Spanjers and Dr. A. Klapwijk of the Environmental Engineering Department in our university for their collaboration and putting their experimental data available to us. The authors thank the referees for their useful and constructive comments. This research is supported by the Dutch Technological Foundation (STW) under grant no. WBI44.3275.

10.11 References

- Carstensen J., Harremoës P. and Madsen H. (1995) Statistical identification of Monod-kinetic parameters from on-line measurements. *Wat. Sci. Tech.*, **31(2)**, 125-133.
- Haarsma G.J. and Keesman K.J. (1995) Robust model predictive dissolved oxygen control. *proc. 9th Forum for Applied Biotechnology, part II*, Gent, 2415-2425.
- Henze M., Grady C.P.L. jr., Gujer W., Marais G.v.R. and Matsuo T. (1986) Activated sludge model no. 1. (IAWQ task group on mathematical modeling for design and operation of biological wastewater treatment).
- Klapwijk A., Spanjers H. and Temmink H. (1992) Control of activated sludge plants based on measurement of respiration rates. *Journal A* **33(3)**, 33-37.
- Lindberg C.F., Carlsson B. (1996) Estimation of the respiration rate and oxygen transfer function utilizing a slow DO sensor. *Wat. Sci. Tech.*, **33(1)**, 325-333.
- Lukasse L.J.S., Keesman K.J. and Straten G. van (1996) Grey-box identification of dissolved oxygen dynamics in activated sludge processes. *proc. 13th IFAC World Congress*, San Francisco.
- Schneider R. and Munack A. (1995) Improvements in the on-line parameter identification of bioprocesses. *proc. 6th Int. Conf. on Computer Applications in Biotechnology*, Garmisch-Partenkirchen, Germany.
- Shamas J.Y. and Englande A.J. (1992) Use of the immediate maximum specific oxygen uptake rate as an activated sludge process control parameter. *Wat. Sci. Tech.*, **25(1)**, 123-132.
- Spanjers H. (1993) *Respirometry in Activated Sludge*. Ph.D. thesis, Dept. of Environmental Engineering, Wageningen Agricultural University, Wageningen, the Netherlands.
- Spanjers H. and Olsson G. (1992) Modeling of the dissolved oxygen probe response in the improvement of the performance of a continuous respiration meter. *Wat. Res.*, **26**, 945-954.
- Spanjers H., Olsson G. and Klapwijk A. (1994) Determining short-term biochemical oxygen demand and respiration rate in an aeration tank by using respirometry and estimation. *Wat. Res.*, **28**, 1571-1583.
- Straten G. van, Keesman K.J. and Klapwijk A. (1993) Basic analysis of activated sludge process dynamics and control. *proc. 7th Forum for Applied Biotechnology*, Gent.
- Vanrolleghem P.A. (1994) *On-line Modeling of Activated Sludge Processes: Development of an Adaptive Sensor*. Ph.D. thesis, Dept. of Agricultural and Applied Biological Sciences, University of Gent, Gent, Belgium.
- Vanrolleghem P.A. and Coen F. (1995) Optimal design of in-sensor-experiments for on-line modeling of nitrogen removal processes. *Wat. Sci. Tech.*, **31(2)**, 149-160.
- Vanrolleghem P.A. and Van Daele M. (1994) Optimal experimental design for structure characterization of biodegradation models: on-line implementation in a respirographic biosensor. *Wat. Sci. Tech.*, **30(4)**, 243-253.
- Vanrolleghem P.A. and Verstraete W. (1993) Simultaneous biokinetic characterization of heterotrophic and nitrifying populations of activated sludge with an on-line respirographic biosensor. *Wat. Sci. Tech.*, **28(11-12)**, 377-387.
- Vanrolleghem P.A., Van Daele M. van and Dochain D. (1995) Practical identifiability of a biokinetic model of activated sludge respiration. *Wat. Res.*, **29(11)**, 2561-2570.

11 Diagnosis and identification by excitation of the dynamics in continuous flow respirometers[†]

11.1 Abstract

This paper deals with excitation of the respiration chamber dynamics in a continuous flow respirometer with the objective to extract additional information from its dissolved oxygen (DO) sensor readings. A measurement strategy is proposed from which it is theoretically possible to identify the respiration chamber's dilution rate, the DO-sensor dynamics, the sludge kinetics and the BOD_{st} concentration in the inflow of the respirometer. In experiments with activated sludge, fed with municipal wastewater, the method proved successful in identifying the respiration chamber's dilution rate and the DO-sensor dynamics. Experimental results over a longer period nicely illustrate the point in doing so. Finally, the results convincingly discourage further efforts to identify sludge kinetics and BOD_{st} from this type of experiments, despite the theoretical feasibility.

Keywords: autocalibration, dilution rate, fault detection, kinetics, respirometry, sensor dynamics

11.2 Introduction

A respirometer is a device to measure the respiration rate in a sample of activated sludge, *i.e.* the amount of DO used per unit of time per unit of volume by this specific sample. Despite the large and ongoing attention for respirometry in control of Activated Sludge Processes (ASP's) on a scientific level, its practical implementations are still scarce. This is partially due to the lack of robustness of the available measurement devices, resulting in too large a need for maintenance. For a comprehensive overview of literature, possible applications and available measurement principles see Spanjers *et al.* (1998).

While the respiration rate depends on substrate and sludge, BOD_5 and BOD_{st} are sludge independent measures for the load of Biochemical Oxygen Demand on the receiving surface water. Effluent BOD_5 is a measure of the total amount of DO required to oxidize all available carbonaceous substrate and NH_4 in the receiving surface water. Active control with the objective to meet effluent BOD_5 standards is impossible because of the 5-days time delay inherent to its measurement. BOD_{st} is the rapidly degradable part of BOD_5 . When reliable estimates of BOD_{st} are available these may be used explicitly in feedback control loops, as BOD_{st} reflects the controllable part of BOD_5 .

This study focuses on methods for diagnosis and identification from the excited dynamics of a continuous flow respirometer with a DO-sensor at only one entry and a reversible flow direction (Fig. 1). Obviously the methods are applicable to designs with DO-sensors at both entries as well if the

[†] submitted to *Water Environment Research* by Leo Lukasse, Karel Keesman, Henri Spanjers and Michiel Bloemen.

facility is there to reverse the flow direction (e.g. Vanrolleghem & Spanjers, 1998). Three separate methods, unified in one framework, are investigated. All three are experimentally tested on large new datasets. The concrete aims of the separate methods are

1. Estimation of the respiration chamber's dilution rate D from the DO-sensor readings.
2. Identification of the DO-sensor dynamics from its step response.
3. Identification of sludge kinetics and BOD_{st} using known D and known DO-sensor dynamics.

The first method, estimation of the respiration chamber's dilution rate D from the DO-sensor readings, takes away the main difficulty in the operation of continuous flow respirometers: The measurement of the respiration chamber's dilution rate D (flow/volume, i.e. q/V), which is required for calculating the respiration rate. Errors made in the manual determination of q and V result in a systematic error in the computed respiration rate. Moreover q is subject to gradual changes due to changing pump characteristics, wearing and clogging. Automatic flow measurement devices are expensive. Hence a method for estimation of D from the DO-sensor readings will be useful as an auto-calibration method. No such method has been reported in the literature, although the theoretical feasibility has been recognized by Vanrolleghem & Spanjers (1998).

The second method, identification of the DO-sensor dynamics from its step response, is a slight modification on the method presented in Spanjers & Olsson (1992). Incorporating this method in the standard operation of a continuous flow respirometer is attractive for two reasons. Firstly it enables on-line diagnosing of the DO-sensor; observation of too slow dynamics means that the sensor fouling is getting too serious and hence it is time for maintenance. Secondly during transient modes the measured DO lags behind the true DO; when the DO-sensor dynamics are known the true DO can be reconstructed from the measured DO (see e.g. Suescun *et al.*, 1998).

The main differences with Spanjers & Olsson (1992) are the detection of natural sensor fouling in the experiments whereas they introduced artificial fouling in their experiments, and the use of a non-iterative estimation procedure for the model parameters whereas their procedure is iterative. The non-iterative nature of the modified algorithm makes its on-line implementation a lot easier. Iterative estimation algorithms in general are not very suitable for on-line implementation, because that requires guarantees with respect to the speed of convergence and larger on-line computation power.

The third method, identification of sludge kinetics and BOD_{st} , is a continuation of Lukasse *et al.* (1997), which itself already was a continuation of Spanjers *et al.* (1994). The method aims at identification of the sludge kinetics and BOD_{st} in the respirometer inflow from DO transients induced by alternately feeding the respirometer with endogenous and loaded sludge. The major incentive for this measuring strategy is that it allows for more frequent sampling than the existing respirogram-based approach (Brouwer *et al.*, 1998; Vanrolleghem and Van Daele, 1994). If accurate estimation appears possible then this method can be used to monitor BOD_{st} in an ASP reactor at a relatively high sampling rate. This would enable the application of BOD_{st} -controllers.

Lukasse *et al.* (1997) presented an effort to identify the kinetic relationship between substrate respiration rate r_S and BOD_{st} from the data used in Spanjers *et al.* (1994) and to estimate the incoming BOD_{st} concentration by inverting that relationship, but failed to achieve accurate estimates. In Lukasse *et al.* (1997) a new experimental design was proposed through which it could be possible to overcome the inaccuracy problem. These experiments and their results are reported in this paper.

11.3 Dynamic respirometer model

The continuous flow respirometer with a DO-sensor at only one entry and a reversible flow direction (Fig. 1) is commercially available as the Manotherm RA-1000™ respirometer. Basically, this respirometer consists of a peristaltic pump maintaining a flow of activated sludge through a small intensively stirred respiration chamber. The flow direction through the respiration chamber is reversible by either opening valves (v_1, v_2) and closing (v_3, v_4) or closing (v_1, v_2) and opening (v_3, v_4). The flow reversion enables alternating measurement of in- and outflowing DO with only one DO-sensor. The major part of the dynamics of the continuously mixed respiration chamber and the DO sensor measuring the DO concentration in its in- and outflow are described by

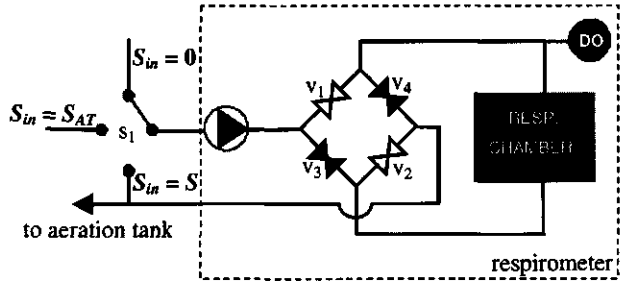


Fig. 1, scheme of respirometer setup.

by either opening valves (v_1, v_2) and closing (v_3, v_4) or closing (v_1, v_2) and opening (v_3, v_4). The flow reversion enables alternating measurement of in- and outflowing DO with only one DO-sensor. The major part of the dynamics of the continuously mixed respiration chamber and the DO sensor measuring the DO concentration in its in- and outflow are described by

$$\begin{bmatrix} \dot{C} \\ \dot{S} \\ \tau \dot{C}_M \end{bmatrix} = \begin{bmatrix} -D & 0 & 0 \\ 0 & -D & 0 \\ 0 & 0 & -1 \end{bmatrix} \begin{bmatrix} C \\ S \\ C_M \end{bmatrix} + \begin{bmatrix} DC_{in}(t) - r_e - r_S(t) \\ DS_{in}(t) - r_S(t) \\ u(t - \Delta) \end{bmatrix} \quad \begin{matrix} (1.1) \\ (1.2) \\ (1.3) \end{matrix}$$

$$y(k) = C_M(k) + e(k)$$

See the section 'nomenclature' for the meaning of all symbols in this paper. In the sequel the three balances above will be referred to as DO-balance (eqn. 1.1), S-balance (eqn. 1.2) and sensor-dynamics (eqn. 1.3). All diagnosis/identification methods below are based on the on-purpose excitation of the dynamics in eqn. 1 and estimation of model parameters from the resulting $y(k)$ -trajectories. In the next section it will be shown how all model parameters (D, r_e, τ and Δ) in eqn. 1 can be identified from the measurements $y(k)$ when exciting the respirometer dynamics in an appropriate way.

11.4 Identification of respirometer model parameters D, r_e, τ and Δ

In principle the respirometer dynamics (eqn. 1.1-1.3) can be excited by manipulating q (i.e. D), C_{in} and S_{in} , and by reversing the flow direction (i.e. switching u between C and C_{in}). Treating the endogenous respiration rate r_e as a (time-varying) model parameter is justified, because it mainly depends on the hardly varying biomass concentration, and hence it changes only slowly.

The first step in identifying the model parameters is bringing the system in eqns. 1.1-1.3 in steady state such that $y(k) = u(k) = C_{in}(k)$ and subsequently switching to $y(k) = u(k) = C(k)$, while keeping $r_e + r_S(t)$ constant. This measurement sequence is conducted by positioning s_1 in Fig. 1 such that $S_{in} = S_{AT}$ or $S_{in} = 0$, and first opening valves (v_1, v_2) and closing valves (v_3, v_4) such that $u(t) = C_{in}(t)$, and subsequently closing (v_1, v_2) and opening (v_3, v_4) such that $u(t) = C(t)$. If in that situation s_1 is switched into the position $S_{in} = S$, then effectively there is no dilution in the respiration chamber ($D = 0$), while yet maintaining the flow along the DO-sensor and hence:

$$\dot{C} = -r_e - r_s(t) \quad (2)$$

The more obvious case of switching off the pump would accomplish $D = 0$ as well, but the flow along the DO-sensor would disappear causing erroneous DO measurements ($u(t) \neq C(t)$).

Using Laplace transform and final value theorem (Stephanopolous, 1984) it is easily verified that after an initial startup phenomenon $\dot{C}_M = \dot{C}$, if \dot{C} is constant. As a result the measurement sequence $y(k)$ exhibits a linearly descending trajectory if the assumption is satisfied that $r_e + r_s$ is constant, i.e. if there is no, or constant, C- and S-limitation. The ordinary least squares (o.l.s.) estimate (see e.g. Ljung, 1987) of the constant $r_e + r_s$ is obtained from the $y(k)$ -trajectory by

$$\hat{r}_e + \hat{r}_s = (\mathbf{x}^T \mathbf{x})^{-1} \mathbf{x}^T \mathbf{y} \quad (3)$$

where

$$\mathbf{x} = \begin{bmatrix} -T \\ \vdots \\ -T \end{bmatrix}, \quad \mathbf{y} = \begin{bmatrix} y(2) - y(1) \\ \vdots \\ y(n) - y(n-1) \end{bmatrix}$$

Under the reasonable assumption that during the whole above described measurement sequence $r_e + r_s(t)$ and $C_{in}(t)$ remain constant the dilution rate D may now be solved from the steady state of eqn 1.1:

$$D(C_{in} - C) - r_e - r_s(t) = 0 \quad (4)$$

Once D is known the usual continuous flow method for estimating $r_e + r_s(t)$ can be used to determine r_e . It can be solved from eqn. 4 by alternating between the respirometer steady states with $y(k) = u(k) = C_{in}(k)$ and $y(k) = u(k) = \bar{C}(k)$, while keeping $r_s(t) = 0$ by feeding endogenous sludge to the respirometer (s_1 in Fig. 1 such that $S_{in} = 0$). The underlying assumption is that C_{in} and \bar{C} are constant on a small timescale.

The last two parameters to be identified (τ and Δ) concern the sensor dynamics. Suitability of the first order linear model structure has been demonstrated in Spanjers and Olsson (1992). The parameters τ and Δ can be identified by reversing the flow direction (switching u from C to C_{in} or vice versa) when the system is in steady state, resulting in a first order step response of the measurement sequence $y(k)$. From this step response τ and Δ can be identified using the exact discretization of the first order linear sensor model (eqn. 1.3):

$$C_M(k+1) = aC_M(k) + (1-a)u(k-d) \quad (5)$$

with $a = e^{-T/\tau}$ and $d = \Delta$ rounded off at whole sampling intervals. The o.l.s. estimate of a is given by

$$\hat{a} = (\mathbf{x}^T \mathbf{x})^{-1} \mathbf{x}^T \mathbf{y} \quad (6)$$

with

$$\mathbf{x} = \begin{bmatrix} C_M(d) - u(0) \\ \vdots \\ C_M(n-1) - u(n-d-1) \end{bmatrix}, \quad \mathbf{y} = \begin{bmatrix} C_M(d+1) - u(0) \\ \vdots \\ C_M(n) - u(n-d-1) \end{bmatrix}$$

The assumption is used that $u(k) = y(n) = C_M(n)$ for $k \in \{0, \dots, n-d-1\}$, i.e. it is assumed that the sensor-dynamics are in steady state at the end of the measurement sequence. Characteristically the sen-

sor reaches its new steady state in about 20 s. Hence in a measurement sequence of only 30 s the assumption is normally satisfied.

Once a has been estimated the sensor time constant τ can be reconstructed from \hat{a} by

$$\hat{\tau} = -T/\ln(\hat{a}) \quad (7)$$

The sum of squared one-step-ahead prediction errors is given by

$$sse = (\mathbf{y} - \mathbf{x}\mathbf{a})^T (\mathbf{y} - \mathbf{x}\mathbf{a}) \quad (8)$$

The pair (a, d) may be estimated by computing a for several positive values of d and accepting the pair (\hat{a}, \hat{d}) yielding the smallest sse .

The main difference between this estimation procedure for τ and Δ and the procedure in Spanjers and Olsson (1992) is its non-iterative nature, as already mentioned in the introduction. Spanjers and Olsson (1992) used $u(k) = \alpha$, with α a constant, and as a consequence needed an iterative estimation procedure for estimation of τ and α . Replacing the estimation of α by the assumption $u(k) = y(n) = C_M(n)$ for $k \in \{0, \dots, n-d-1\}$ enables the use of the non-iterative o.l.s. estimation procedure, probably at the expense of a somewhat higher sse .

11.5 Identification of sludge kinetics and S_{in}

What is missing in the respirometer model in eqn. 1 is the kinetic relationship between S and r_S . This section presents a method to identify both the sludge kinetics and S_{in} from the DO-measurements in the respirometer, based on excitation of the S -balance (eqn. 1.2). This excitation can be obtained by alternately loading the respirometer with endogenous sludge in the so-called e-mode, and loaded sludge in the so-called l-mode. This is realized by toggling switch s_1 (Fig. 1) between $S_{in} = 0$ (e-mode) and $S_{in} = S_{AT}$ (l-mode).

Obviously periodic excitation of the S -balance induces a periodic behavior of $r_S(t)$ as well. If during the transients $u(k) = C(k)$ then the $r_S(t)$ -trajectory can be reconstructed from the DO-balance (eqn 1.1) and the sensor dynamics (eqn 1.3) in two steps. The first step is to reconstruct the trajectory of $u(k)$, i.e. $C(k)$, from the $y(k)$ -trajectory by solving eqn. 5 for $u(k)$, assuming $y(k) = C_M(k)$, i.e. $e(k) = 0$. This yields

$$u(k) = C(k) = \frac{y(k+d+1) - ay(k+d)}{1-a} \quad (9)$$

The second step is to reconstruct $r_S^c(k)$ from the DO-balance:

$$r_S^c(k) = D(C_{in}(k) - C(k)) - r_e - \dot{C}(k) \quad (10)$$

where $\dot{C}(k)$ is approximated by

$$\dot{C}(k) = \frac{C(k+1) - C(k-1)}{2T} \quad (11)$$

Drawback of this two steps procedure is that both eqn. 9 and 11 are differentiating filters, which are notorious amplifiers of the measurement noise $e(k)$. Therefore, in order to achieve a reasonable signal-to-noise ratio in the reconstructed $r_S^c(k)$ -trajectory, the measurement noise of the DO-sensor must be very low and the use of a low-pass noise filter may be necessary.

By simulating the S -balance a simulated $r_s^s(k)$ -trajectory is obtained. Under the reasonable assumptions of constant biomass concentration and no DO limitation, r_s solely depends upon the substrate concentration:

$$r_s^s(k) = f(S(k)) \quad (12)$$

The inflowing substrate concentration during a mode relates to r_s according to (eqn. 1.2):

$$S_{in} = \bar{S}(n) + \frac{\bar{r}_s^c(n)}{D} \quad (13)$$

with the overbar denoting steady state values and according to eqn. 12

$$\bar{S}(n) = f^{-1}(\bar{r}_s^c(n)) \quad (14)$$

assuming S in the region where $f(S)$ is invertible. Integrating the substrate balance (eqn. 1.2) for an estimated $f(S)$ with the above-calculated S_{in} and $S(0) = f^{-1}(\bar{r}_s^c(0))$ yields both an $S(k)$ -trajectory and a simulated $r_s^s(k)$ -trajectory. In the ideal case this simulated $r_s^s(k)$ -trajectory coincides with the $r_s^c(k)$ -trajectory reconstructed from the DO measurements (eqn. 10). Hence the kinetic model $f(S)$ can be identified by fitting the $r_s^s(k)$ -trajectory to the $r_s^c(k)$ -trajectory, *i.e.* by iteratively solving the non-linear optimization problem

$$\min_{f(S)} J(f(S)) = \sum_{k=1}^n (r_s^c(k) - r_s^s(k))^2 \quad (15)$$

subject to eqns. 1.2, 12, 13, 14 and $S(0) = f^{-1}(\bar{r}_s^c(0))$. Inherently S_{in} follows from eqn. 13.

Spanjers *et al.* (1994) already tried to reconstruct S_{in} and the sludge kinetics from this type of experiments, using a totally deviant estimation procedure. Essential in their estimation procedure is the unstable backward integration of the S -balance (eqn 1.2). Hence the inaccuracy of their results is inherent to the method. The only difference between the above estimation procedure for k_s and the one used in Lukasse *et al.* (1997) is that the low frequent sampling in their dataset forced them to neglect the DO-sensor dynamics in reconstructing the $r_s^c(k)$ -trajectory, *i.e.* they assumed $u(k) = y(k+d)$ ($a = 0$ in eqn. 9). The new measurement strategy necessary to support the new estimation procedure is discussed in the next section.

11.6 Measurement strategy

In principle all measurements required for the identification procedures of the two preceding sections could be combined in one measurement procedure. Yet the measurements are split in two separate experiments for practical reasons. Experiment 1 is designed to estimate D . The design of experiment 2 aims at the identification of τ , Δ , sludge kinetics and S_{in} , for known D .

Experiment 1 consists of a series of 1586 identical measurement cycles, Fig. 2 shows only one of them. In the design of experiment 1 a measurement cycle is composed of four phases:

- I. Switch s_1 (Fig. 1) such that $S_{in} = S_{AT}$. (v_1, v_2) closed and (v_3, v_4) opened such that $u(t) = C(t)$. Lasts 720 s.
- II. Reverse flow direction ($u(t) = C_{in}(t)$). Lasts 120 s.
- III. Reverse flow direction again ($u(t) = C(t)$). Lasts 60 s.

IV. Switch s_1 (Fig. 1) such that $S_{in} = S$. Lasts 300 s.

In phase I $y(t)$ converges to \bar{C} , then the flow direction is changed in phase II and $y(t)$ converges to the approximately constant $C_{in}(t)$. After changing the flow direction again $y(t)$ rapidly converges to \bar{C} again in phase III, as a preparation to phase IV. Finally in phase IV $D = 0$, while yet maintaining a constant flow along the DO-sensor membrane, and $y(t)$ becomes a linearly decreasing sequence with the slope $-r_e - r_S(t)$.

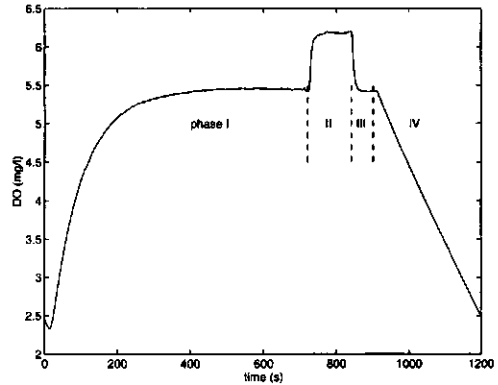


Fig. 2, characteristic measurement cycle for estimation of D (real data).

Identification of the sludge kinetics in experiment 2 requires the alternation between l- and e-modes as already mentioned in the preceding section. The endogenous sludge, required for the e-mode, is produced in a bypass tank with 3 h retention time. The loaded sludge is taken from an aerobic reactor continuously fed with presettled domestic wastewater. One measurement cycle in experiment 2 consists of an l- and an e-mode. Each mode lasts 15 minutes and can be subdivided in 3 phases:

- I. Valves (v_1, v_2) closed and (v_3, v_4) opened such that $u(t) = C(t)$. Lasts 780 s.
- II. Reverse flow direction ($u(t) = C_{in}(t)$). Lasts 60 s.
- III. Reverse flow direction again ($u(t) = C(t)$). Lasts 60 s.

In total 542 measurement cycles are collected. One characteristic measurement cycle is shown in Fig. 3. Sensor parameters τ and Δ can be identified from phases II and III of both modes. The sludge kinetics and S_{in} can be identified from phase I in each mode, after reconstruction of the $r_S^C(k)$ -trajectory.

11.7 Experimental results

The estimation results for experiment 1 are presented in Fig. 4. In the 12 days data set gradual changes in \hat{D} are clearly observable. Moreover the difference between the manually measured D at time $t = 0$ (horizontal line in Fig. 4) and the estimates during the first day is about 15%, despite accurate manual measurement of q and V . Fig. 5 depicts estimates of $r_e + r_S$ obtained both from the continuous flow method (eqn. 4) using phases II and III of a measurement cycle and from the batch method (eqn. 3) using phase IV of a measurement cycle. In the estimation of $r_e + r_S$ from phase IV the initial startup phenomenon is skipped by discarding the data for which DO is less than 0.2 mg/l below the last measured DO in phase III. From

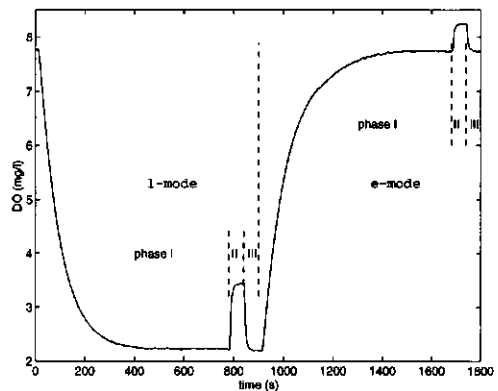


Fig. 3, measurement cycle for estimation of τ , Δ , sludge kinetics and S_{in} (real data).

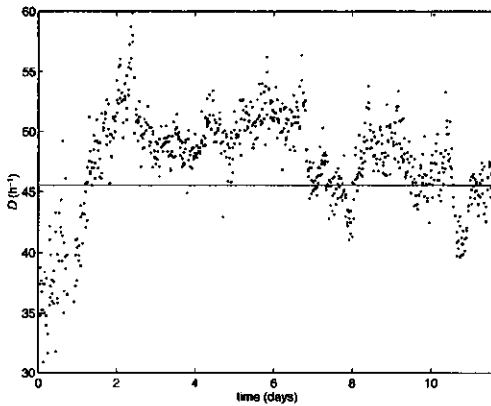


Fig. 4, estimated (·) and measured (—) dilution rate.

Fig. 2 it is clear that a margin of 0.2 mg/l suffices. The assumption of no, or constant, C -limitation is satisfied by ensuring high C_{in} and using only the first 60 datapoints for which DO is 0.2 mg/l below the last measured DO of phase III. The usage of only this first minute of reliable data also prevents serious violation of the assumption of no, or constant S -limitation, as S hardly changes on this timescale.

In experiment 2 each measurement cycle contains four DO sensor step responses (phases II and III in l- and e-mode) from which τ and Δ for the DO sensor (manufacturer WTW, meter model OXY-191 with sensor model EO90) can be estimated by means of eqns. 6-8. Fig. 6 depicts 12 days of τ -estimates from the step responses in phase III. In a first run sse was minimized with respect to the pair (τ, Δ) for each mode, according to the method discussed in eqns. 5-8. In most cases the optimal Δ -value occurred to be 3. In the second run only τ was estimated with Δ fixed at 3 s, as a result the graph in Fig. 6 is not blurred by correlation between τ and Δ . A slight gradual change of τ is visible over the whole time span. A large sudden increase in τ occurs around $t = 6$ days due to fouling of the sensor membrane by a flake of dried sludge, which has visually been observed. After thoroughly cleaning the sensor's membrane at $t = 7.8$ days τ approximately returns at its old level (Fig. 6). This observation nicely illustrates the use of identifying the DO-sensor dynamics: It is a straightforward tool for automatic detection of membrane fouling.

The last method is the reconstruction of the $r_s^c(k)$ -trajectory from phase I in the l- and e-mode, and the subsequent identification of sludge kinetics and S_{in} . First the $C(k)$ -trajectories are reconstructed by filtering the $y(k)$ -trajectory through the inverse sensor model (eqn. 9).

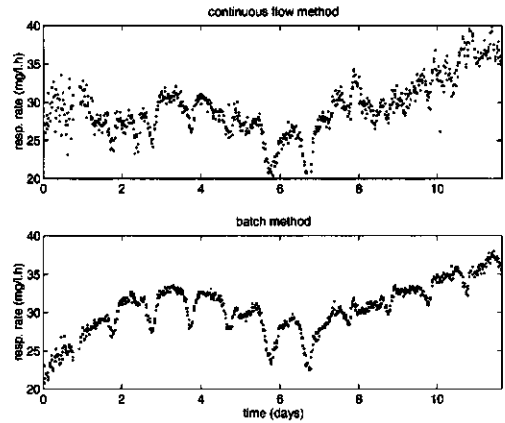


Fig. 5, r_e+r_S determined by continuous flow and batch method.

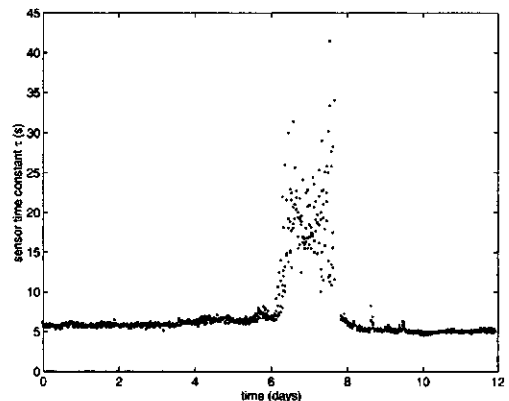


Fig. 6, τ -estimates from phase 3 with $\Delta = 3$ s.

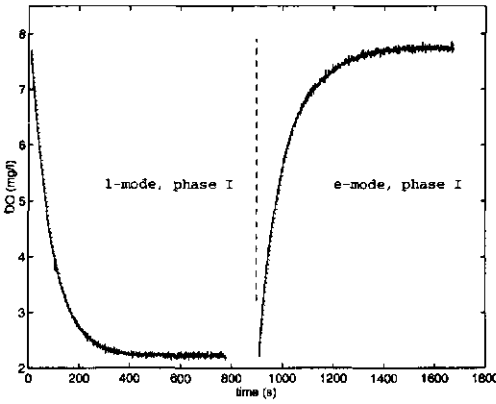


Fig. 7, trajectories of $y(k)$ (dotted) and $\hat{C}(k)$ (solid) during the l- and e-mode in Fig. 3.

Clearly the $\hat{C}(k)$ -trajectories (Fig. 7) are disrupted by a significant high-frequent noise. The next step, reconstructing the $r_5^C(k)$ -trajectory from the $\hat{C}(k)$ -trajectory by means of eqn. 10 results in a very poor signal-to-noise ratio (Fig. 8). The noise needs to be reduced by applying a low-pass filter to either of the sequences $y(k)$, $\hat{C}(k)$ or $\hat{r}_5^C(k)$. It was chosen to filter the $\hat{C}(k)$ -trajectory, as this is the first sequence in which a significant noise is observable.

Any measurement sequence consists of a signal and a noise part. Low-pass filtering reduces the high-frequent noise part at the risk of signal distortion. The cut-off frequency of the filter is the main design handle to make the trade-off between noise reduction and signal distortion. To enable a balanced trade-off the frequency content of the $\hat{C}(k)$ -trajectory is determined, using the fast Fourier transform. Through analyzing the frequency content it was learned that the main part of the *signal* in

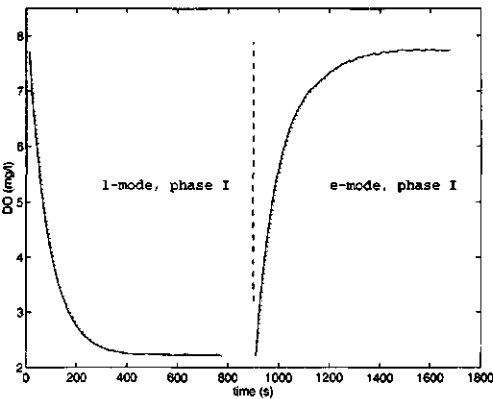


Fig. 9, trajectories of $y(k)$ (dotted) and filtered $\hat{C}(k)$ (solid) for the l- and e-mode in Fig. 3.

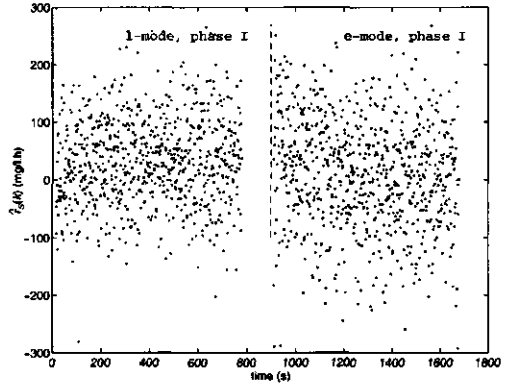


Fig. 8, $\hat{r}_5^C(k)$ according to eqn. 10 from unfiltered $\hat{C}(k)$ -trajectories in Fig. 7.

the $\hat{C}(k)$ -trajectory resides below 0.08 Hz. A fourth order low-pass Butterworth filter with cut-off frequency 0.08 Hz is designed to filter the data. The $\hat{C}(k)$ -trajectory is filtered forward and backward to prevent the introduction of a phase shift. Visual observation of the results confirms the successful noise reduction in absence of a significant signal distortion (compare Figs. 7 and 9).

Reconstruction of the $r_5^C(k)$ -trajectory from this filtered $\hat{C}(k)$ -trajectory by means of eqn. 10 results in a reasonable signal-to-noise ratio (Fig. 10). The significant startup phenomenon in $\hat{r}_5^C(k)$

at the start of both modes demonstrates a systematic error in $\hat{r}_s^C(k)$. This phenomenon is not an incident, it has been observed in all 542 evaluated measurement cycles. The most likely explanations are structural errors in the assumed DO- and sensor-dynamics (eqns. 1.1, 1.3) (e.g. the first order linear approximation of the sensor dynamics is insufficient or the respiration chamber mixing is imperfect).

Despite the observed systematic error, an effort was made to fit a kinetic model to the reconstructed $\hat{r}_s^C(k)$ -trajectory. Blackman ($1/2/0$) kinetics are assumed:

$$\hat{r}_s^S = f(S) = k_s \sqrt{S} \quad (16)$$

Rapid convergence of the non-linear optimization problem (eqn. 15) for k_s in the equation above occurred. But as expected, the resulting systematic data-model mismatch during the transients is unacceptable (Fig. 10).

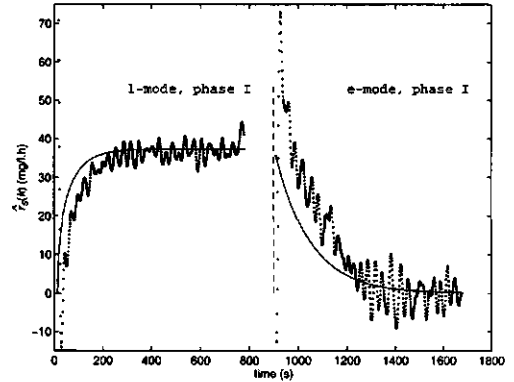


Fig. 10, $\hat{r}_s^C(k)$ according to eqn. 10 (-) and $\hat{r}_s^S(k)$ from $f(S)$ in eqn. 12 (-).

11.8 Discussion

With respect to the estimation of D (Fig. 4) the key question is: What comes closer to reality, the manually measured D or the estimates of \hat{D} ? As the true dilution rate is unknown the answer has to be sought by comparing the likelihood of errors in the manually measured D and the estimates of \hat{D} . Recall that \hat{D} is the solution of eqn. 4 with $\hat{r}_e + \hat{r}_s(t)$ estimated from \hat{C} in phase IV (eqn. 3) of the measurement cycle, and C_{in} and C measured in phases II and III (Fig. 2). Errors in \hat{D} are the consequence of errors in $\hat{r}_e + \hat{r}_s(t)$ and $C_{in} - C$. Possible sources of errors in $\hat{r}_e + \hat{r}_s(t)$ are:

1. The assumption of no DO-limiting measurements is violated, and hence $\hat{r}_e + \hat{r}_s(t) < r_e + r_s(t)$.
2. $\hat{C}_m \neq \hat{C}$ in phase IV.
3. S decreases significantly and r_s is S -limited during phase IV, and hence $\hat{r}_e + \hat{r}_s(t) < r_e + r_s(t)$.
4. Systematic measurement errors due to errors in the linear DO-sensor calibration curve

$$DO = c_1 \cdot \text{amperage} + c_2:$$

4.1 Errors in slope c_1 .

4.2 Errors in offset c_2 .

4.3 Non-linearity of the calibration curve.

Sources of errors in $C_{in} - C$, besides the above mentioned calibration errors, are hard to imagine. Moreover if $C_{in} - C$ is overestimated by a factor f then it will cause an underestimation of D by a factor $1/f$ (eqn. 4). This underestimation is advantageous as in the continuous flow method for estimating $\hat{r}_e + \hat{r}_s(t)$ the two errors will cancel against each other.

Error possibility 1 is excluded because the lowest DO-measurement in the whole dataset used to estimate $\hat{r}_e + \hat{r}_s(t)$ is as high as $y(k) = 4.4$ mg/l. Possibility 2, $\hat{C}_M \neq \dot{C}$, only occurs during the initial startup phenomenon. In the preceding section it was shown that this phenomenon is not present in the data from which $r_e + r_s(t)$ is estimated. Possibility 3, S decreases significantly during phase IV, may be the explanation for the observed little increase of \dot{C} in Fig. 2 during phase IV. As mentioned before in the one minute of data used to estimate $\hat{r}_e + \hat{r}_s(t)$ the S -decrease could only be very small. Moreover decreased S would yield $\hat{r}_e + \hat{r}_s(t) < r_e + r_s(t)$, that contradicts with the observation that the batch method yields higher estimates than the continuous flow method in the main part of the data (Fig. 5). Possibility 4, errors in the DO-sensor calibration curve, is very unlikely to cause errors in \hat{D} . The WTW DO-sensor EO90 was calibrated at the start of the experiment and automatically corrects for temperature changes. Moreover an error in the slope c_1 (4.1) would effect $\hat{r}_e + \hat{r}_s(t)$ and $C_{in} - C$ in the same way and hence would not effect \hat{D} (eqn. 4). An error in the constant offset c_2 (4.2) would effect neither $\hat{r}_e + \hat{r}_s(t)$ nor $C_{in} - C$. A non-linearity (4.3) could explain a systematic error in \hat{D} , but not the observed variations in Fig. 4. Moreover it is very unlikely for a well-established device like this, as any manufacturer does his utmost best to prevent that.

By now it is very likely that both $\hat{r}_e + \hat{r}_s(t)$ and $C_{in} - C$ contain only minor errors, while in the introduction several possible error sources are given for the manually measured D . So there is good reason to believe that \hat{D} comes closer to reality than the measured D does. Hence both the observed gradual changes in \hat{D} and the large initial difference between the measured and the estimated D strongly advocate the on-line estimation of D on regular intervals as an autocalibration method for continuous flow respirometers.

With respect to identification of the DO-sensor dynamics there remains one thing to be investigated. If the DO-sensor dynamics become more sluggish the assumed steady state at the end of phases II and III in experiment 2 (Fig. 3) is not reached, and hence using the assumption $u(k) = y(n) = C_M(n)$ for $k \in \{0, \dots, n-d-1\}$ yields an underestimated input $u(k)$ for $k \in \{0, \dots, n-d-1\}$. Could the modified method fail to detect DO-sensor fouling due to this newly introduced assumption? To answer this question stepresponses of the DO-sensor model in eqn. 1.3 are simulated over 60 seconds and stored at 1 s intervals, like in experiment 2, for $\Delta = 0$ and τ ranging from 6 till 100 s. Subsequently $\hat{\tau}$ is estimated from the simulated data according to the procedure in eqns. 6-7. The results are shown in Fig. 11. Clearly no scenario exists in which τ gets very large, while $\hat{\tau}$ still resides in the acceptable range.

In the preceding section the estimation of sludge kinetics and BOD_{st} from dynamic respirometer experiments failed. The collected measurements in experiment 2 are excellent and, though the true system dynamics are unknown, one would expect

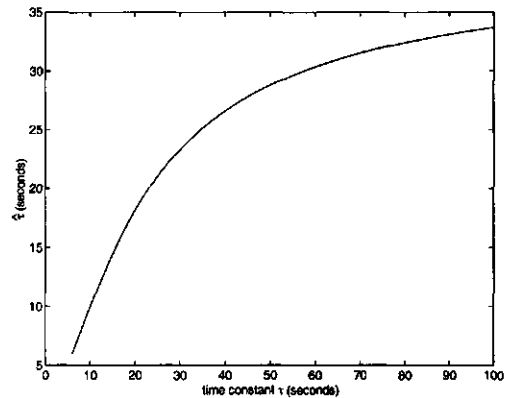


Fig. 11, $\hat{\tau}$ as a function of true DO-sensor τ for $\Delta = 0$.

the major part of the system dynamics to be contained in the dynamic model (eqn. 1). Yet the quality of the measurements and the dynamic model appeared insufficient to estimate the sludge kinetics and BOD_{st} . The measurement noise problem was tackled by using a rather heuristically designed low-pass filter. This filtering procedure can definitely be improved upon by using a more fundamental approach. The quality of the dynamic model may be improved by adding a black box model describing higher order system dynamics. An overview of relevant software and books is available at <http://www.mathworks.com/products/sysid/> and <http://www.mathworks.com/products/signal/>.

If one would succeed to come up with seemingly reliable estimates of sludge kinetics and BOD_{st} , then there still are the questions whether a static kinetic relationship suffices in the dynamic experimental conditions (Baltes *et al.*, 1994) and what exactly is the meaning of a quantity called BOD_{st} . Moreover the objective is to use the BOD_{st} -estimates in BOD_{st} -controllers. Hence the final estimation procedure should be sufficiently fast for on-line implementation and come to satisfactory estimates of BOD_{st} without manual intervention. Especially this last requirement will be hard to meet.

The encountered difficulties, together with the expected difficulties ahead, convincingly discourage the further development of the proposed method for estimation of sludge kinetics and BOD_{st} . Yet, the authors will be happy to put the data available to anybody who wants to give it a try.

11.9 Conclusions

A method to automatically estimate the dilution rate in a continuous flow respirometer proved successful. In the experiments (Fig. 4) gradual changes in the dilution rate are clearly observed, moreover a significant systematic difference between the manually measured and the estimated dilution rate occurs. It has been argued that the estimates of D come closer to reality than the manually measured D does. Therefore it is worthwhile to consider accommodation of the method in an auto-calibration procedure, as that will allow for the generation of more accurate measurements by continuous flow respirometers.

The method of Spanjers and Olsson (1992) to identify the DO-sensor dynamics has been modified. The modification simplifies the on-line implementation of the method. The modified method is well suited to auto-monitor the DO-sensor quality in continuous flow respirometers and generate warning messages when the DO-sensor deteriorates. Fig. 6 nicely illustrates how the DO-sensor dynamics may change if sudden membrane fouling occurs.

Reliable estimates for sludge kinetics and BOD_{st} from dynamic respirometer experiments have not been achieved. The proposed method makes a too high demand on the quality of the measurements and the dynamic model. Though possible ways out are indicated the resulting method will probably be very complex, if feasible at all. The encountered difficulties, together with the expected difficulties ahead, convincingly discourage the further development of the proposed method for estimation of sludge kinetics and BOD_{st} .

Acknowledgments: This research was financially supported by the Dutch Technological Foundation (STW) under grant no. WBI44.3275.

11.10 Nomenclature

variable	unit [value]	description
\bar{C}	mg/l	steady state DO in respiration chamber
τ	s	DO sensor time constant
Δ	s	time delay in DO sensor dynamics
$r_s^C(k), r_s^S(k)$	mg/l	r_s at time kT estimated from DO-balance, - from S-balance
a	sampling intervals	discrete time DO sensor model coefficient ($e^{-T/a}$)
BOD_{st}	mg/l	short term biochemical oxygen demand
C_{in}, C, C_M	mg/l	DO in resp. influent, effluent and in sensor
D	h^{-1}	dilution rate q/V
d	sampling intervals	Δ rounded off at whole sampling intervals
e	mg/l	measurement noise, assumed to be white
k	-	k -th sampling instant in a mode
n	-	no. of data points for o.l.s. parameter estimation
n_c	-	no. of sampl. interv. used to approximate \dot{C}
q	l/h	flow through the respiration chamber
r_e	mg/l.h	endogenous respiration rate
r_S	mg/l.h	substrate respiration rate
S, S_{in}, S_{AT}	mg/l	BOD_{st} in respirometer, its influent, aeration tank
sse	mg^2/l^2	Sum of Squared one-step-ahead prediction Errors
t	s	time
T	s [1]	sampling interval
t_0, t_f	h	initial and final time of a mode
$u(t)$	mg/l	DO at sensor membrane (either C or C_{in})
V	l [0.480]	respiration chamber volume
y	mg/l	measured dissolved oxygen concentration

11.11 References

- Baltes M., Schneider R., Sturm C., Reuss M. (1994) Optimal experimental design for parameter estimation in unstructured growth models. *Biotechnological Progress*, 10, pp. 480-488.
- Brouwer H., Klapwijk A., Keesman K.J. (1998) Identification of activated sludge and wastewater characteristics using respirometric batch-experiments. *Water Research*, 32(4), pp. 1240-1254.
- Ljung, L. (1987). *System Identification: Theory for the User*. Prentice Hall, New Jersey.
- Lukasse L.J.S., Keesman K.J., Straten G. van (1997) Estimation of BOD_{st} , respiration rate and kinetics of activated sludge. *Water Research*, 31, pp. 2278-2286.
- Spanjers H. and Olsson G. (1992) Modeling of the dissolved oxygen probe response in the improvement of the performance of a continuous respiration meter. *Wat. Res.*, 26, 945-954.
- Spanjers H., Olsson G. and Klapwijk A. (1994) Determining short-term biochemical oxygen demand and respiration rate in an aeration tank by using respirometry and estimation. *Wat. Res.*, 28, 1571-1583.
- Spanjers H., Vanrolleghem P.A., Olsson G., Dold P.L. (1998) *Respirometry in control of the activated sludge process: principles*. IAWQ Scientific and Technical Report no. 7.

- Stephanopoulos, G. (1984). Chemical process control: an introduction to theory and practice. Prentice Hall, New Jersey.
- Suescun J., Irizar I., Ostolaza X. and Ayesa E. (1998) Dissolved oxygen control and simultaneous estimation of oxygen uptake rate in activated-sludge plants. *Wat. Env. Res.*, 70(3), pp. 316-322.
- Vanrolleghem P.A. and Spanjers H. (1998) A hybrid respirometric method for more reliable assessment of activated sludge model parameters. *Wat. Sci. Tech.*, 37(12), pp. 237-246.
- Vanrolleghem P.A. and Van Daele M. (1994) Optimal experimental design for structure characterization of biodegradation models: on-line implementation in a respirographic biosensor. *Wat. Sci. Tech.*, 30(4), pp. 243-253.

12 Conclusions and suggestions

In chapter 1 the research objectives have been listed (section 1.6). The related conclusions are summarised in the section below, although all conclusions can be found in the individual chapters as well. Especially the conclusions, which are most important from a practitioner's point of view, are highlighted. Moreover some remaining ideas with respect to the problem of total-N removal are given as suggestions in this chapter. In chapter 1 the new problem of total-N removal has been discussed and the large research efforts related to that were coarsely reviewed. After building up four years of experience in the field my impression is that there still exist several unexplored lacunas offering good possibilities for costs savings and/or effluent quality improvement. Some ideas concern those lacunas, but came too late to study them myself. Those ideas, which I believe are novel and likely to be successful, are expounded in the last sections of this chapter.

12.1 Conclusions for the practitioner

In chapters 2 and 3 a simple model for the ammonium (S_{NH}) and nitrate (S_{NO}) dynamics in alternating reactors is developed. The simplicity is achieved by capturing the slower process dynamics in time-varying model parameters. Therefore in chapter 3 a recursive identification algorithm for those parameters is presented. Two of those parameters represent the actual rates of nitrification and denitrification under aerobic and anoxic conditions respectively. The scope of the recursively identified model is its use in the adaptive receding horizon optimal controller (RHOC) of chapter 5, but it can be used independent of the N-controller. A practically relevant spin-off is the on-line monitoring of the rates of nitrification and denitrification from S_{NH} and S_{NO} measurements. These estimates contain information with respect to the product of concentration and activity of both nitrifiers and denitrifiers. This information is currently not on-line available in practice, and least of all closely monitored. From this enhanced process knowledge it can be deduced to what extent the process is over/underloaded, and hence whether the sludge concentration should be increased/decreased. Another application is the detection of toxic effects when the rates of nitrification/denitrification drop too low.

The combination of recursive identification with RHOC, adaptive RHOC, has been tested extensively in both simulation and pilot scale experiments (chapter 5). On-line implementation proofed very well possible, but the algorithm is complex and it requires the measurement of both S_{NH} and S_{NO} . From chapters 4, 5 and 6 it is concluded that its performance is close-to-optimal in terms of the evaluation criterion formulated in chapter 7. This evaluation criterion expresses the wish for low total-N, and especially low S_{NH} .

In chapter 7 four different control strategies for total-N removal in alternating reactors are compared by means of simulations: 1. timer-based, 2. switching the aeration on/off when depletion of nitrate/ammonium is detected, 3. switching the aeration on/off when S_{NH} crosses an upper/lower-bound, 4. the newly developed adaptive RHOC. It appears that timers, S_{NH} -bounds based, and adaptive RHOC can do an approximately equally good job, although adaptive RHOC is least sensi-

tive to suboptimal tuning. Especially the good performance of the open-loop timer-based operation is surprising. The potential of optimally tuned timers, together with the observed sensitivity to sub-optimal tuning, has led to a suggestion in the sequel of this chapter how to auto-tune the timers on-line.

Although in this application the simple timer-based operation is just as good as adaptive RHOC in terms of the evaluation criterion in chapter 7, there may well be situations in ASP control in which adaptive RHOC is superior. This situation may already occur if a more complete evaluation criterion is used, in which *e.g.* aeration costs, sludge production costs, effluent COD, sludge settleability etc. are taken into account. The principle advantage of RHOC remains unaffected by the results of chapter 7 it is a *feedback* controller that directly aims at minimisation of an *objective criterion*. By formulating the objective criterion such that it resembles the plant *economy* the higher level economic objectives are naturally linked to the lower level control objectives.

Application of the RHOC algorithm to the 2-reactors alternating process in simulation has resulted in a performance improvement by using an operation strategy which is totally deviant from current operation strategies for that process. By applying the RHOC algorithm to a range of plant designs within the class of 2-reactors alternating processes the combination of process design and operation is optimised. A conceptually simple, straightforwardly implementable control algorithm successfully imitates the new operation strategy of the RHOC algorithm. It should be stressed that the performance improvement has only been achieved in simulation, and has not yet been confirmed by full-scale experiments (chapter 8).

In chapters 10 and 11 an effort was made to bring the respirometry-based estimation procedure for BOD_{st} in Spanjers *et al.* (1994) to perfection. The disappointing conclusion is that it is unlikely that the procedure will ever work (chapter 11). Therefore it is strongly discouraged to spend time on efforts to estimate BOD_{st} from the kind of dynamic respirometer experiments first proposed in Spanjers *et al.* (1994) (also discussed in chapter 10).

Positive are the conclusions in chapter 11 with respect to monitoring of the respirometer's DO-sensor dynamics and respiration chamber dilution rate. Both of them serve to increase the reliability of respiration rate measurements and are easily implementable in the every day operation of continuous flow respirometers. Their practical relevance is illustrated by the experimental results in chapter 11. Especially the new procedure for estimation of the dilution rate is useful. It will reduce the bias in estimates of respiration rates. The indication in chapter 11 is that this bias may easily be 15%. Therefore it is worthwhile to consider accommodation of the method in an autocalibration procedure for continuous flow respirometers.

12.2 Increased NH_4 concentration to meet total-N standards

Many plants have difficulties in meeting the effluent total-N standards, while their effluent NH_4 concentration (S_{NH}) is close to zero. These plants could easily improve their effluent total-N by exchanging some nitrification for denitrification, as only denitrification reduces effluent *total-N*. However, increasing effluent S_{NH} increases the risk of nitrifiers washout. Nitrifier washout occurs if the *aerobic* sludge age is lower than $1/(\mu_{max,A}-b_A)$, where $(\mu_{max,A}-b_A)$ is the net maximum specific

growth rate of autotrophs. A typical value for the minimum required aerobic sludge age is 5 days (e.g. Andrews *et al.*, 1980; Potter *et al.*, 1998).

The need to comply with a *total-N* norm motivated Potter *et al.* (1998) and Tseng *et al.* (1998) to modify the design of an ASP plant in order to enable operation at elevated S_{NH} without nitrifier washout. Positive side effects are the reduced aeration costs and a reduced amount of sludge needed in the system. They stated that in the usual plant designs instability due to washout is unavoidable if elevated effluent S_{NH} is permitted.

In my opinion Potter *et al.* (1998) chose a promising approach in solving the problem of total-N removal, but they are wrong in stating that the approach of elevated S_{NH} cannot work in the usual plant designs. This generally accepted point of view has blocked any research towards the possibility to permit elevated S_{NH} in ordinary plant designs. However the risk of nitrifiers washout only exists in case no feedback control of S_{NH} is applied, but the concentration of nitrifiers will be stabilised by S_{NH} -feedback controllers. If S_{NH} exceeds its setpoint then an S_{NH} -feedback controller will automatically increase the hydraulic residence time in aerobic phases, and hence inherently increase the aerobic sludge age. Hence control engineers should start to explore the path of permitting elevated S_{NH} in ordinary plant designs using S_{NH} -feedback control for the aerobic phase. If desired, the risk of gross failures can be further reduced by using a surplus sludge storage facility (e.g. Yuan *et al.*, 1997). Extra safety comes from the fact that the total-N standards concern yearly averages. So there are eleven months left to cancel the negative effect of a washout incident in January.

12.3 Control in view of time-averaged effluent standards

Up to now no reports are available on how to relate the every day plant control to *time-averaged* effluent standards. Yet the E.U. effluent standards for phosphate (P) and total-N are expressed as integrals over time, weekly averages apply for P and yearly averages for total-N. Important costs savings may be possible by explicitly exploiting this time-averaged nature of the effluent standards.

The problem of yearly-averaged total-N control has a long time-scale. Because the sludge dynamics are slow, the sludge concentration setpoint $MLSS_{ref}$ in the reactor seems a suitable control input for controlling the yearly-averaged total-N (sludge = Mixed Liquor Suspended Solids, MLSS). In current practice $MLSS_{ref}$ is based on heuristics and MLSS is controlled manually by manipulating waste flow rate q_w . Reducing MLSS to the minimum concentration required for meeting effluent total-N standards offers several advantages:

- Reduced aeration costs due to reduced nitrification and lower endogenous respiration (inherently increasing the sludge production!).
- Higher percentage of biomass in the sludge, due to less inert solids (Yuan *et al.*, 1997).
- Less sludge in the plant and hence less risk of solids loss in the effluent due to settler overloading.
- Reduced risk of sludge settling problems due to lower sludge age (Seviour *et al.*, 1994).

Let the maximally permitted yearly averaged effluent total-N concentration for the controlled plant be \bar{N}_{ef} . Then a possible higher level control objective aiming at just complying with the integral constraint is:

$$\min_{MLSS_{ref}} x = \int_0^{365 \text{ days}} (0.9 \cdot \bar{N}_{ef} - S_{NH} - S_{NO}) dt \tag{1}$$

Multiplication of \bar{N}_{ef} in the above integral with a factor 0.9 introduces a 10% safety margin. A possible way to implement a controller aiming at minimising the integral x in eqn. 1 is depicted in Fig. 1, where $N_{ref} = 0.9 \cdot \bar{N}_{ef}$. The existing controllers C_2 for $MLSS$ (usually the operator himself) and C_3 for S_{NH} and S_{NO} can remain unmodified. C_3 manipulates u , which may contain variables like the size of aerated phases, external carbon dosage rate and the internal recirculation flow rate in case of the anoxic zones approach. For example all controllers simulated in chapter 7 would be represented by C_3 . The algorithm for yearly-averaged total-N control will be

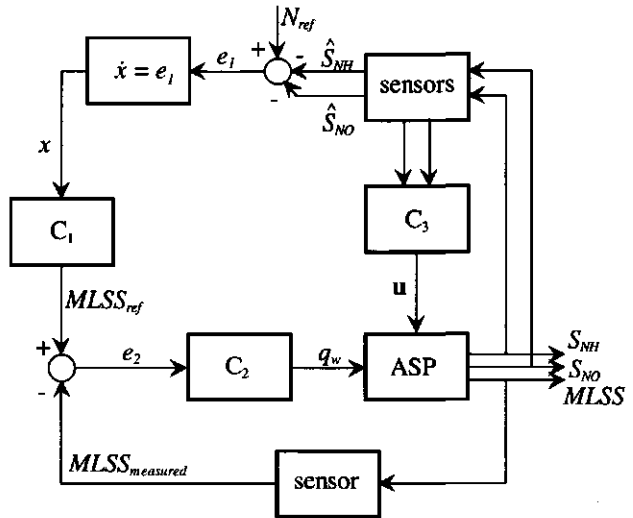


Fig. 1, possible feedback control loop for yearly-averaged total-N control.

placed in block C_1 . It is expected that a sluggish PID-controller with anti-integral windup ($0 < MLSS_{ref} < \text{settler constraint}$) (see e.g. Peng *et al.*, 1996) for C_1 will suffice to control x (Fig. 1) to zero. In case one has objections against the proposed manipulation of $MLSS_{ref}$ one could think of a setup in which C_1 dictates S_{NH} and S_{NO} setpoints for C_3 instead of $MLSS_{ref}$ for C_2 . In either implementation care should be taken to prevent oscillatory behaviour due to interaction of the different control loops. The most obvious approach is to use the principle of time scale decoupling: design C_1 such that $MLSS_{ref}$ varies only slowly, and C_2 such that $MLSS$ tracks $MLSS_{ref}$ sufficiently fast.

If the above suggested control strategy proves worthwhile, then a valuable next step is to compute the optimal N_{ref} -trajectory throughout the year in order to account for the reduced process rates and the improved oxygen transfer during winter. This is possible by formulating an optimal control problem for the whole year with N_{ref} treated as control input and the system being the controlled ASP-plant, i.e. plant + C_1 + C_2 + C_3 (Fig. 1). The availability of a simple model is required to enable solution of the problem in reasonable time. A first step could be time scale decomposition of ASM no. 1 (Henze *et al.*, 1987), i.e. neglecting the dynamics of the faster subprocesses. Furthermore, assumptions need to be made about the average yearly temperature cycle in the reactor and the influent disturbance. Solving this optimal control problem yields the optimal trajectory for N_{ref} , but also for $MLSS_{ref}$, q_w and q_{air} . Obviously in the implementation phase one should only feed the optimal N_{ref} -trajectory to the system, the others being computed on-line by the feedback controllers C_1 , C_2 and C_3 . In this way the feedback from the uncertain process is maximised and hence the risk of not meeting the \bar{N}_{ef} -standard is minimised.

12.4 pH-based auto-tuning of timers for N-removal

Open loop timer-based operation of alternating aeration in reactors is attractive, because timers are cheap, simple and have a little risk of failures. From the simulation study in chapter 7 it appeared that this operation strategy even performs close-to-optimal, provided that the tuning is optimal. However the sensitivity to suboptimal tuning appeared to be large as well, which is a consequence of the timer's open-loop nature. Hence the bottleneck in using timers is how to maintain the optimal tuning.

The main problem in tuning timers is setting the percentage of aerobic time p_{air} in a cycle of aerobic + anoxic period, after the length of the whole cycle has been determined. Suppose that it is known what the optimal daily averaged S_{NH} and S_{NO} in the reactor are. Then $p_{air} \in [0, 1]$ can be solved from the steady state of the S_{NH} and S_{NO} balances:

$$\dot{S}_{NH} = \frac{q}{V}(S_{NH,in} - S_{NH}) - r_{NH,max} \cdot p_{air} = 0 \quad (2)$$

$$\dot{S}_{NO} = -\frac{q}{V}S_{NO} + r_{NH,max} \cdot p_{air} - r_{NO,max} \cdot (1 - p_{air}) = 0 \quad (3)$$

The above model structure has already been introduced in chapter 3. The first term in both eqn. 2 and 3 describes the dilution effect. $S_{NH,in}$ is the NH_4 concentration in the inflow of the reactor, which is not necessarily equal to the NH_4 concentration in the treatment plant's influent. The maximum rates of nitrification ($r_{NH,max}$) and denitrification ($r_{NO,max}$) are assumed to be limited by aerobicity/anoxicity (p_{air}) only. Limitation by low S_{NH} or low S_{NO} is neglected, as this will hardly occur in case of good control.

The optimal tuning p_{air}^* is a trade-off between the one following from the desired \bar{S}_{NH} (solve from eqn. 2)

$$p_{air}^* = \frac{\frac{\bar{q}}{V}(\bar{S}_{NH,in} - \bar{S}_{NH})}{r_{NH,max}} \quad (4)$$

and the one following from the desired \bar{S}_{NO} (solve from eqn. 3)

$$p_{air}^* = \frac{\frac{\bar{q}}{V}\bar{S}_{NO} + r_{NO,max}}{r_{NH,max} + r_{NO,max}} \quad (5)$$

In eqns. 4 and 5 the overbars mean daily averages.

Hence the tuning of timers requires knowledge of \bar{q} , $\bar{S}_{NH,in}$, $r_{NH,max}$ and $r_{NO,max}$. Feedback from the process is required because \bar{q} , $\bar{S}_{NH,in}$ and especially $r_{NH,max}$ and $r_{NO,max}$ are subject to gradual changes. Usually reasonable knowledge exists with respect to \bar{q} and $\bar{S}_{NH,in}$, but $r_{NH,max}$ and $r_{NO,max}$ are largely unknown. Hence the following question comes to mind: could a device be developed that estimates $r_{NH,max}$ and $r_{NO,max}$ on regular intervals (once a day suffices)?

The answer is: yes, probably. Both nitrification and denitrification effect pH: H^+ -ions are released during nitrification, while they are consumed during denitrification. Hence pH-measurements have the potential to yield information about both processes. In in-sensor batch experiments Gernaey *et*

al. (1998) regulated pH in a 4 l continuously mixed vessel filled with nitrifying sludge on a constant value by *base* addition. From the required *base* dosage they were able to reconstruct $r_{NH,max}$ and $S_{NH}(t_0)$. In a very similar device (DECADOS) Bogaert *et al.* (1997) regulated pH in a vessel filled with denitrifying sludge on a constant value by *acid* addition. The purpose of their experiments is determination of the optimal carbon-dosage flow rate in the denitrification phase of a full-scale plant. From the required *acid* dosage during their experiments they were able to reconstruct $S_{NO}(t_0)$, required carbon dosage and denitrification capacity (mg/l.h). If it is possible to measure denitrification capacity, then it should be possible to modify the measurements such that $r_{NO,max}$ in the reactor is measured as well. Integration of the two automatic measurement strategies in one device is straightforward. The required sampling rate for timer auto-tuning is low. Hence a device for auto-tuning of timers is within arm's reach.

A constant pH in the vessel (Gernaey *et al.*, 1998; Bogaert *et al.*, 1997) is maintained to make the measurement independent of the wastewater's buffer capacity. In my opinion a possible alternative is the periodic determination of the wastewater's buffer capacity by in-sensor experiments and use this knowledge to deduce $r_{NH,max}$ and $r_{NO,max}$ from pH-profiles in alternating reactors.

It is interesting to observe that the device used by Gernaey *et al.* (1998) and Bogaert *et al.* (1997) looks very much like a respirometer, except for the DO-sensor, which has been replaced by a pH-sensor. In the past there was no drive to replace the DO-oriented respirometer by a pH-based respirometer-like device, as only aerobic phases occurred in ASP's. Nowadays ASP's contain aerobic, anoxic, and increasingly anaerobic zones. The principle advantage of the change from DO- to pH-sensors is that the pH-sensor has the potential to yield information about biological processes in all three phases. This explains the growing interest in manipulating control inputs in ASP's on the basis of pH measurements (Al-Ghusain *et al.*, 1994; Carucci *et al.*, 1997; Wett *et al.*, 1997)

12.5 Dynamic simulations: the future

In chapters 7 and 8 we conducted simulation studies to compare the performance of different operation strategies. In chapter 8 receding horizon optimal control was used to search for the optimal combination of plant design and operation. In my opinion this kind of simulation studies is very useful and should be applied to many more cases. It is the only practically feasible way to quantify the differences between different combinations of operation and design. Especially the combination of these simulations with optimal control is powerful. They are complex to carry out, but can come up with simple unexpected solutions, as occurred both in chapters 7 and 8. In many cases the optimal combination of operation and design is unknown. In chapters 7 and 8 the above-described type of simulation studies proved very helpful in collecting knowledge with respect to this important topic.

This call for optimal control simulation studies puts no blame on past generations, who did not or hardly use them. It is the evolution of technique which enables far more comprehensive simulations now than only ten years ago. For successful simulations of complex systems three things are required: powerful computers, user-friendly simulation packages and good models. Especially the progress in the fields of computers and simulation packages has been tremendous over the last decade(s).

Two possible topics for simulation studies related to activated sludge processes are:

- Compare the optimal operation of a one tanks system with that of a 2, 3, 4, 5, ..., n tanks system to learn about the marginal value of adding extra tanks. This relates to the discussion of plug flow vs. continuously mixed hydraulics (Jenkins and Garrison, 1968). After all, plug flow reactors can be approximated as a series connection of continuously mixed reactors.
- Compare the optimal operation of an alternating two tanks system (anoxic periods approach) with that of the equally large optimally operated 2-tanks system with internal recirculation (anoxic zones approach).

This list contains only two suggestions for simulation studies, but undoubtedly there remain many more questions in the field of ASP-design and operation which could be (partly) answered by means of optimal control simulation studies.

12.6 References

- Al-Ghusain I.A., Huang J., Hao O.J. and Lim, B.S. (1994) Using pH as a real-time control parameter for waste water treatment and sludge digestion processes. *Wat. Sci. Tech.* **30**(4), 159-168.
- Andrews J.F., Sørensen P.E. and Garrett M.T. (1980). Control of nitrification in the oxygen activated sludge process. *Prog. Wat. Tech.*, **12**(5), pp. 497-519.
- Bogaert H., Vanderhasselt A., Gernay K., Yuan Z., Thoeye C. and Verstraete W. (1997). New sensor based on pH effect of denitrification process. *Journal of Environmental Engineering*, **123**, pp. 884- 891.
- Carucci A., Rolle E. and Smurra P. (1997) Experiences of on-line control at a wastewater treatment plant for nitrogen removal. *Preprints of 7th int.'l workshop on instrumentation, automation and control of water and wastewater treatment and transport systems*. IAWQ, Brighton, 459-465. (to appear in *Wat. Sci. Techn.*, 1998)
- Gernaey, K.; Vanrolleghem, P. and W. Verstraete. (1998) On-line estimation of nitrosomonas kinetic parameters in activated sludge samples using titration in-sensor-experiments. *Wat. Res.*, **32**(1), pp. 71-80.
- Henze M., Grady jr. C.P.L., Gujer W., Marais G.v.R. and Matsuo T. (1987). Activated sludge model no. 1. *IAWQ Scientific and Technical Report no. 1*, IAWQ, London, U.K.
- Jenkins D. and Garrison W.E. (1968). Control of activated sludge by mean cell residence time. *J. of Water Pollution Control Federation*, **40**(11), part 1.
- Peng Y., Vrancic D., Hanus R. (1996). Anti-windup, bumpless, and conditioned transfer techniques for PID-controllers, *IEEE Control systems*, **8**, pp. 48-57.
- Potter T.G., Tseng C. Koopman B. (1998). Nitrogen removal in a partial nitrification/ complete denitrification process. *Water Environment Research*, **70**(3), pp. 334-342.
- Seviour E.M., Williams C., DeGrey B. Soddell J.A., Seviour R.J. and Lindrea K.C. (1994). Studies of filamentous bacteria from Australian activated sludge plants. *Wat. Res.*, **28**(11), pp. 2335-2342.
- Spanjers H., Olsson G. and Klapwijk A. (1994). Determining short-term biochemical oxygen demand and respiration rate in an aeration tank by using respirometry and estimation. *Water Research*, **28**, pp. 1571-1583.

- Tseng C.C., Potter T.G. and Koopman B. (1998). Effect of influent chemical oxygen demand to nitrogen ratio on a partial nitrification complete denitrification process. *Water Research*, 32(1), pp. 165-173.
- Wett B., Rostek R., Rauch W. and Ingerle K. (1998). pH-controlled reject-water-treatment. *Wat. Sci. Techn.*, 37(12), pp. 165-172.
- Yuan Z., Bogaert H., Vansteenkiste G. and Verstraete W. (1998) Sludge storage for countering nitrogen shock loads and toxicity incidents. *Wat. Sci. Techn.*, 37(12), pp. 173-180.

Summary

This thesis is about control and identification in activated sludge processes (ASP's). The chapters in this thesis are divided in two parts. Part I deals with the development of the best feasible, close-to-optimal adaptive receding horizon optimal controller (RHOC) for N-removal in a continuously mixed alternating activated sludge process reactor. Subsequently this controller and the most common existing controllers are mutually compared by means of simulations. In addition the application of the close-to-optimal RHOC controller to a system of two hydraulically connected alternating reactors is simulated for a range of plant designs within this class. In this way the combination of design and operation is optimized. Part II concerns identification on the basis of DO-measurements and respirometry. First the DO-dynamics in a continuously mixed ASP reactor are identified, including the non-linear relation between $k_L a$ and q_{air} . Subsequently the dynamics of a (DO-sensor based) continuous flow respirometer are identified by exciting its dynamics.

In chapter 1 the principles of the N-removing ASP are shortly explained. The new problem of total-N removal is discussed. The general features of the ASP control problem are listed: disturbance attenuation, storm events, process uncertainty and variation, multiple time-scales. Special attention is paid to the potential of RHOC. The literature with respect to operational aspects of N-removal as well as the use of DO-sensors and respirometers in ASP operation is coarsely reviewed. It is argued that the anoxic *periods* approach for N-removal offers two principle advantages over the anoxic *zones* approach: excitation of dynamics and no need for internal recirculation. Some problems in the field are indicated. With respect to DO-sensors it is illustrated that the challenges today are in the field of extracting not only DO but also additional information from its readings. All experiments in this thesis have been carried out at a pilot scale ASP. A description of this pilot plant is given in chapter 1. The chapter ends with the formulation of research objectives and the thesis outline.

Chapters 2 till 5 present the design procedure for the adaptive RHOC for control of NH_4 and NO_x , though not exactly chronologically. The first step is presented in chapter 4, it concerns application of optimal control to the N-removal part of the generally accepted Activated Sludge Model no. 1. From this optimal control study it occurs that alternating nitrification/denitrification, as opposed to simultaneous nitrification/denitrification, may be optimal indeed. This, together with the risk of sludge bulking at limiting DO-values, justifies the limitation to alternating process operation. To implement an optimal control strategy on-line the receding horizon principle is needed, leading to RHOC. RHOC uses an internal process model for short term predictions. Hence a computationally efficient process model is required. Such a model is developed in chapter 2 by capturing the slower process dynamics in time-varying model parameters. It is taken into account that the model structure must be suited for recursive identification of the time-varying model parameters from the measurements.

RHOC, like any model predictive controller, computes the current controls on the basis of model predictions upto horizon H . Hence the sum of squared 1, 2, ..., H -step ahead prediction errors is a natural identification criterion. In chapter 2 this idea is postulated and applied to NH_4/NO_x measurements collected from the pilot scale ASP described in chapter 1. H appears to affect the

parameter estimates significantly, supporting the idea that use of this new identification criterion will improve MPC performance in general.

In chapter 4 RHOC with this simple model is applied to the pilot plant's alternating reactor. The controller successfully passed several tests, but it also appeared that the performance of this controller is suboptimal due to inaccurate model predictions. This was to be expected, as the simplicity of the N-removal model in chapter 2 has been achieved by capturing the slower process dynamics in the model parameters, while in this stage they are not recursively estimated.

The results of chapter 4 illustrate that recursive identification of (some of the) model parameters is required to keep the model uptodate. Chapter 3 presents the algorithm for recursive identification of those model parameters. The Kalman filter is used, because it has the attractive feature that the filter gain accompanying non-identifiable parameters (e.g. the nitrification rate during anoxic periods) increases linearly in time. It is proven that this increase of the filter gain will not cause instability during normal process operation. The method performs excellently on real data.

Chapter 5 concerns adaptive RHOC of N-removal in alternating ASP reactors, being the combination of the recursively identified model in chapter 3 and the RHOC controller in chapter 4. Although stability of the nonlinear RHOC feedback controller has not been proven, not to mention its combination with recursive identification, only one source of instability was encountered in many experiments. This is the scenario in which NH_4 dominates the objective functional, its setpoint is zero and the estimated rate of nitrification has become negative for whatever reason. In that case the controller will keep aeration off to prevent the predicted *production* of NH_4 , as a consequence no new information to update the estimated nitrification rate is obtained and the deadlock is there. Obviously this scenario is easy to prevent and does not occur under normal operating conditions.

In chapter 4 the unusual observation is done that the RHOC performance is nearly invariant to its prediction horizon. This triggered a study on the cause of this phenomena and an effort to generalize the results as far as possible, the results are presented in chapter 6. It has led to the derivation of an l_1 -norm optimal state feedback controller for 2-dimensional linear time invariant systems with decoupled dynamics and a single control input.

In chapter 7 the close-to-optimal adaptive RHOC of chapter 5 and three existing control strategies (timers, NH_4 -bounds based and ORP, Oxidation Reduction Potential, based) for N-removal in continuously mixed alternating reactors are compared by means of simulation. The simulations are carried out in SIMBA™, a commercially available application within the MATLAB/SIMULINK™ environment, based on the Activated Sludge Model no. 1. Drawback of simulations is that the dynamics of both the sensors and the process need to be modelled. And even the best model of the ASP is nothing but a poor resemblance of the real process. However, a fair experimental *comparison* of multiple controllers is impossible, not only for financial reasons. Simultaneous experimental testing would require the availability of multiple identical plants in parallel. Sequential testing on one plant would disrupt the results by changes in process conditions and influent, disabling a mutual comparison. Hence simulation is the best way to compare different control-schemes. It appears that three totally different controllers (timers, NH_4 -bounds based and adaptive RHOC) can achieve a more or less equal performance, if tuned optimally. Adaptive RHOC

turns out to be superior in terms of sensitivity to suboptimal tunings. The timers approach is attractive for its simplicity, but very sensitive to suboptimal tuning.

Chapter 8 describes a simulation study with the scope to optimise the plant design and operation strategy of alternating activated sludge processes for N-removal with two hydraulically connected reactors. The methodology is to simulate the application of RHOC to a range of different plant designs within this class of systems. The RHOC algorithm is obtained by reformulating the controller of chapter 4 for a 2-reactors system. It appears that in the optimal process design the two reactors are placed in series, the first reactor is about four times as large as the second one. A conceptually simple feedback controller straightforwardly implements the improved operation strategy. The results of this chapter strongly advocate the simulation of optimal control applied to complex process models. The results are unexpected and indicate a significant outperformance of the current operation strategy. This kind of simulation studies at least serves as an ideas generator.

Chapter 9 presents a grey-box modelling approach for the identification of the nonlinear DO dynamics. Herein, singular value decomposition of the locally available Jacobian matrix, or equivalently eigenvalue decomposition of the parameter covariance matrix, as well as parameter transformation are essential techniques. The use of respiration rate measurements greatly simplifies the modelling procedure. The approach is amongst others capable of identifying the non-linear function $k_{LA}(q_{air})$, i.e. the relationship between k_{LA} and the aeration input signal q_{air} . This is especially valuable in experimental identification of the relationship between $k_{LA}(q_{air})$ and the design of (newly developed) aeration equipment, the use of specific carrier materials in aerated reactors, or the presence of certain detergents. After all a higher k_{LA} at a given q_{air} results in a higher efficiency of energy usage for aeration, and hence identification of $k_{LA}(q_{air})$ for newly developed equipment can yield important sales arguments.

Chapters 10 and 11 both deal with excitation of the respiration chamber dynamics in a continuous flow respirometer with the objective to extract additional information from its dissolved oxygen (DO) sensor readings. Chapter 10 is an effort to improve the accuracy of the BOD_{st} -estimation technique developed by Spanjers *et al.* (1994). Contrary to expectation, the estimates still suffer from unacceptable inaccuracy due to large parameter correlation. However, a slight modification in the measurement strategy is proposed which is expected to enable more accurate estimation. The results of experiments with this modified measurement strategy are reported in chapter 11. The estimation results convincingly discourage further efforts to identify sludge kinetics and BOD_{st} from this type of experiments.

The two other objectives of chapter 11 are the identification of the DO-sensor dynamics and the dilution rate in a continuous flow respirometer by excitation of the respiration chamber dynamics. Two separate simple procedures are presented. Both procedures consist of on-purpose in-sensor experiments succeeded by an ordinary least squares estimation step. The feasibility of both procedures is verified in experiments with activated sludge, fed with municipal wastewater. Large experimental data sets are presented, which strongly advocate the on-line incorporation of both procedures in the everyday operation of the respirometer.

In chapter 12 those conclusions drawn in the individual chapters which are of direct relevance to practitioners are summarized. Moreover some remaining ideas, which I believe are novel and likely to be successful, are shortly expounded in chapter 12 as well. The ideas concern: 1) Meeting N-total

effluent standards by permitting elevated effluent NH_4 ; 2) Control explicitly aiming at meeting *yearly averaged* effluent standards; 3) The use of pH-measurements for continuous on-line tuning of timers in a timer-based operation strategy for alternating N-removal in a continuously mixed ASP reactor.

Samenvatting

Het thema van dit proefschrift is de regeling en identificatie in actief-slib processen (ASP's). De hoofdstukken zijn onderverdeeld in twee delen. Deel I gaat over de ontwikkeling van de best haalbare, nagenoeg-optimale adaptieve optimale regelaar met voortschrijdende horizon (RHOC) voor N-verwijdering in een continu gemengde alternerende actief-slib reactor. Vervolgens worden deze regelaar en de meest gebruikelijke bestaande regelaars onderling vergeleken door middel van simulaties. Daarnaast wordt de toepassing van de nagenoeg-optimale RHOC regelaar op een systeem met twee hydraulisch verbonden reactors gesimuleerd voor een reeks procesontwerpen binnen die klasse. Op die manier wordt de combinatie van ontwerp en besturing geoptimaliseerd. Deel II betreft identificatie op basis van zuurstofmetingen en respirometrie. Eerst wordt de zuurstofdynamica in een continu gemengde ASP reactor geïdentificeerd, inclusief de niet-lineaire relatie tussen $k_L a$ en q_{air} . Vervolgens wordt de dynamica van een (op een zuurstofsensoren gebaseerde) continu doorstroomde respirometer geïdentificeerd door excitatie van de dynamica.

In hoofdstuk 1 worden het principe van het N-verwijderende ASP kort uitgelegd en het nieuwe probleem van totaal-N verwijdering uitgelegd. Ook de algemene kenmerken van ASP regeling worden kort besproken: verstoringsonderdrukking, regenbuien, proces onzekerheid en - variatie en meerdere tijdschalen. Extra aandacht gaat uit naar de potentie van RHOC. Ook bevat dit hoofdstuk een kort overzicht van de literatuur met betrekking tot de operationele aspecten van zowel N-verwijdering als het gebruik van zuurstofsensoren en respirometrie in ASP besturing. Twee principiële voordelen van de anoxische perioden aanpak voor N-verwijdering (in plaats van de anoxische zones aanpak) zijn: excitatie van de dynamica en de afwezigheid van interne recirculatie. Een aantal actuele problemen met betrekking tot N-verwijdering worden aangegeven. Een kort overzicht maakt duidelijk dat de hedendaagse uitdagingen met betrekking tot het gebruik van zuurstofsensoren liggen op het gebied van het verkrijgen van meer informatie uit de metingen dan enkel de zuurstofconcentratie. Alle experimenten in dit proefschrift zijn uitgevoerd op een ASP proefopstelling, die wordt beschreven in hoofdstuk 1. Het hoofdstuk eindigt met een beschrijving van de onderzoeksdoelen en een kort overzicht van de inhoud van het proefschrift.

Hoofdstuk 2 tot 5 presenteren de ontwerpprocedure voor de adaptieve RHOC voor regeling van NH_4 and NO_x , hoewel niet helemaal chronologisch. De eerste stap, applicatie van optimal control op het N-verwijderings deel van Aktief-Slib Model no. 1, wordt omschreven in hfst. 4. Hieruit blijkt dat alternerende nitrificatie/denitrificatie optimaal kan zijn. Dit resultaat, samen met het bekende risico van licht slib bij limiterende zuurstofconcentraties, rechtvaardigt de beperking tot alternerende procesvoering. Om de optimale regelstrategie on-line te implementeren is het voortschrijdende horizon principe nodig, wat leidt tot RHOC. RHOC gebruikt een intern proces model voor korte termijn voorspellingen, dus is een rekenkundig efficiënt model vereist. Zo'n model wordt ontwikkeld in hfst. 2, de tragere procesdynamica wordt daarbij met tijdsvariante modelparameters beschreven. Er wordt in deze fase al rekening mee gehouden dat de modelstructuur geschikt moet zijn voor recursieve identificatie van de tijdsvariante parameters.

RHOC, zoals iedere modelvoorspellende regelaar, berekent de huidige sturingen op basis van model voorspellingen tot een horizon H . Daarom is de som van gekwadrateerde 1, 2, ..., H -staps vooruit voorspellingen een logisch identificatie criterium. In hfst. 2 wordt dit idee toegepast op NH_4/NO_x -metingen, die zijn verricht aan de in hfst. 1 beschreven proefopstelling. H blijkt een belangrijk effect te hebben op de parameterschattingen, daarmee het idee ondersteunend dat dit nieuwe identificatiecriterium zal leiden tot verbetering van de prestatie van modelvoorspellende regelaars in het algemeen.

In hfst. 4 wordt RHOC met dit simpele model toegepast op de alternerende reactor van de proefopstelling. De regelaar heeft meerdere tests met succes doorstaan, wel bleek de prestatie suboptimaal als gevolg van onnauwkeurige model voorspellingen. Dit was te verwachten, want de eenvoud van het N-verwijderings model in hfst. 2 is bereikt door de tragere dynamica te beschrijven middels model parameters, die in dit stadium nog niet recursief geschat worden.

De resultaten van hfst. 4 tonen aan dat recursieve identificatie van (een deel van) de modelparameters nodig is om het model actueel te houden. Hfst. 3 presenteert het algoritme voor recursieve identificatie van die modelparameters. Het Kalman filter is gebruikt, omdat dat de aantrekkelijke eigenschap heeft dat de versterkingsfactor van het filter behorend bij niet-identificeerbare parameters (bijv. de nitrificatiesnelheid tijdens anoxische perioden) lineair toeneemt in de tijd. Het wordt bewezen dat deze toename van de versterkingsfactor bij normale procesvoering niet zal leiden tot instabiliteit. De methode blijkt prima te werken op echte data.

Hfst. 5 behandelt de adaptieve RHOC voor N-verwijdering in alternerende ASP reactors. Dit is de combinatie van recursieve identificatie in hfst. 3 en de RHOC regelaar in hfst. 4. Hoewel stabiliteit van de niet-lineaire RHOC feedback regelaar niet kan worden bewezen, om maar niet te spreken van de combinatie met recursieve identificatie, is er maar één bron van instabiliteit ontdekt in een hele reeks experimenten. Dit is het scenario waarin NH_4 de doelfunctie domineert, het NH_4 -setpoint nul is en de geschatte nitrificatiesnelheid, om welke reden dan ook, negatief is geworden. In dat geval zal de regelaar de beluchting niet aanschakelen om *productie* van NH_4 te voorkomen, dientengevolge komt geen nieuwe informatie beschikbaar om de geschatte nitrificatiesnelheid bij te stellen en dus zit de regelaar in een impasse. Uiteraard is dit scenario eenvoudig te voorkomen en bovendien zal het niet optreden onder normale omstandigheden.

In hfst. 4 wordt de ongebruikelijke waarneming gedaan dat de RHOC prestatie vrijwel onafhankelijk is van de voorspelhorizon. Dit is aanleiding geweest voor een studie naar de oorzaak van dit ongebruikelijke fenomeen en een poging om de resultaten zover mogelijk te generaliseren. De resultaten worden gepresenteerd in hfst. 6. Deze studie heeft geleid tot de afleiding van een l_1 -norm optimale toestandsteruggekoppelde regelaar voor 2-dimensionale lineair tijdsinvariante systemen met ontkoppelde dynamica en een enkele sturingang.

In hfst. 7 worden de nagenoeg-optimale adaptieve RHOC uit hfst. 5 en de drie bestaande regelstrategieën (tijdsklokken, NH_4 -grenzen en redox-gebaseerd) voor N-verwijdering in continue gemengde alternerende reactors vergeleken middels simulaties. Deze simulaties zijn uitgevoerd in SIMBA™, een commercieel beschikbare toepassing binnen de MATLAB/SIMULINK™ omgeving, gebaseerd op het Aktief-Slib Model no. 1. Nadeel van simulaties is dat de dynamica van zowel sensoren als het proces gemodelleerd moeten worden, en zelfs het beste model van een ASP is niet meer dan een slechte weergave van het werkelijke proces. Máár een eerlijke experimentele

vergelijking van meerdere regelaars is onmogelijk, niet enkel om financiële redenen. Gelijktijdig experimenteel testen vereist de beschikbaarheid van meerdere identieke installaties. Sequentieel testen op één installatie zou de resultaten vertekenen door veranderingen in procesomstandigheden en influent. Dus simulatie is de beste manier om verschillende regelschema's onderling te vergelijken. Het blijkt dat drie totaal verschillende regelaars (tjidsklokken, NH_4 -grenzen en adaptieve RHOC) een min of meer gelijke prestatie kunnen leveren, mits optimaal ingesteld. Adaptieve RHOC blijkt superieur in termen van gevoeligheid voor sub-optimale instellingen. De tjidsklokken aanpak is aantrekkelijk vanwege haar eenvoud, maar erg gevoelig voor sub-optimale instellingen.

Hfst. 8 beschrijft een simulatiestudie met als doel de optimalisatie van procesontwerp in samenhang met de procesbesturing voor alternerend actief-slib processen voor N-verwijdering met twee hydraulisch verbonden reactoren. De methode is gebaseerd op simulatie van de toepassing van RHOC op een reeks verschillende procesontwerpen binnen die klasse van systemen. Het RHOC algoritme wordt verkregen door de regelaar uit hfst. 4 te herformuleren voor een 2-reactoren systeem. In het optimale procesontwerp blijken de twee reactoren in serie geschakeld te worden, waarbij de eerste reactor ongeveer viermaal zo groot is als de tweede. Een conceptueel simpele teruggekoppelde regelaar implementeert de verbeterde besturingsstrategie rechttoe rechtaan. De resultaten van dit hoofdstuk pleiten sterk voor de simulatie van optimal control toegepast op complexe procesmodellen. Dit soort simulatiestudies doet immers op z'n minst dienst als ideeën generator.

Hfst. 9 presenteert een grey-box modelleringsaanpak voor identificatie van de niet-lineaire zuurstofdynamica. Essentiële technieken hierin zijn singuliere waarden decompositie van de lokaal beschikbare Jacobiaan matrix, ofwel eigenwaarden decompositie van de parameter covariantie matrix, en parameter transformatie. Het gebruik van respiratiesnelheidsmetingen brengt een belangrijke vereenvoudiging van de modelleringsprocedure met zich mee. De procedure is o.a. in staat om de niet-lineaire functie $k_{LA}(q_{air})$ te identificeren, *i.e.* de relatie tussen k_{LA} en het beluchtingsingangssignaal q_{air} . Dit is in het bijzonder waardevol voor de experimentele identificatie van de relatie tussen $k_{LA}(q_{air})$ en het ontwerp van (nieuw ontwikkelde) beluchtingsapparatuur, het gebruik van bepaalde dragermaterialen in beluchte reactoren, of de aanwezigheid van bepaalde wasmiddelen. Een hogere k_{LA} bij een bepaalde q_{air} resulteert immers in een betere benutting van de beluchtingsenergie. Dus kan identificatie van $k_{LA}(q_{air})$ voor nieuw ontwikkelde apparatuur een belangrijk verkoopargument opleveren.

Hfst. 10 en 11 behandelen beiden de excitatie van de respiratiekamer dynamica in een continu doorstroomde respirometer met het doel om extra informatie te verkrijgen uit de zuurstofmetingen in de respirometer. Hfst. 10 is een poging tot verbetering van de nauwkeurigheid van de BZV_{kt} -schattingstechniek ontwikkeld door Spanjers *et al.* (1994). In tegenstelling tot de verwachting bevatten de schattingen nog steeds een onacceptabele onnauwkeurigheid als gevolg van parametercorrelatie. Er wordt echter een kleine wijziging in de meetstrategie voorgesteld, waarvan wordt verwacht dat het nauwkeurigere schattingen mogelijk maakt. De resultaten van experimenten met deze gewijzigde meetstrategie worden gerapporteerd in hfst. 11. De schattingresultaten ontmoedigen verdere pogingen ter identificatie van de slibkinetiek en BZV_{kt} uit dit soort experimenten overtuigend.

De twee andere doelen van hfst. 11 zijn identificatie van de zuurstofsensordynamica en de verdunningssnelheid in een continu doorstroomde respirometer door excitatie van de respiratiekamer dynamica. Twee gescheiden procedures worden gepresenteerd. Beide procedures bestaan uit doelge-

richte in-sensor experimenten gevolgd door een gewone kleinste kwadraten schatting. De haalbaarheid van beide procedures is geverifieerd in experimenten met actief-slib, gevoed met huishoudelijk afvalwater. Grote experimentele data-sets worden gepresenteerd, die het on-line gebruik van beide procedures in de alledaagse besturing van de respirometer bepleiten.

In hfst. 12 worden de praktisch relevante conclusies, die in de individuele hoofdstukken al getrokken zijn, nog een keer samengevat. Bovendien bevat hfst. 12 ook nog een korte uiteenzetting van een aantal resterende ideeën, waarvan ik geloof dat ze nieuw en kansrijk zijn. Deze ideeën betreffen: 1) Het voldoen aan N-totaal effluent normen door een hoger effluent NH_4 toe te staan; 2) Regeling met als expliciet doel het voldoen aan *jaarlijks-gemiddelde* effluent normen; 3) Het gebruik van pH-metingen voor continue on-line tuning van tijd klokken in een op tijd klokken gebaseerde besturingsstrategie voor alternerende N-verwijdering in een continu gemengde ASP reactor.

Curriculum vitae

Leo Lukasse werd geboren op 11 September 1971 te Middelhamis. In 1989 behaalde hij het VWO diploma aan het Ichthus College te Veenendaal. Aansluitend begon hij de studie Landbouwtechniek aan de Landbouwwuniversiteit Wageningen. Binnen deze studie volgde hij het meet- en regeltechnische profiel. In 1993 liep hij stage bij Silsoe Research Institute in Engeland. Onderwerp van de stage was 'A study of Neighbouring Optimal Control Theory'. Zijn eerste afstudeervak ('Modellering van een gesloten NFT-teeltsysteem') deed hij op het IMAG-DLO. Het tweede afstudeervak ('Optimal control of lucerne drying, using solar energy') deed hij bij de Systems and Control group aan de LUW.

Na het behalen van het doktoraaldiploma in 1994 begon hij zijn promotie-onderzoek, als onderzoeker in opleiding, in de Systems and Control group aan de LUW, gefinancierd door NWO-STW. De resultaten van dit onderzoek hebben tot dit proefschrift geleid. Tijdens zijn promotie werden 3-weekse werkbezoeken afgelegd aan Lund Institute of Technology (Zweden) en Danish Technical University (Kopenhagen, Denemarken). Sinds 1 januari 1999 is hij als wetenschappelijk onderzoeker in dienst van ATO-DLO, alwaar hij zich bezighoudt met procesbeheersingsvraagstukken bij de verwerking en opslag van agrarische (afval)produkten.